Studies of Creaming, Flocculation and Crystallisation in Emulsions : Computer Modelling and Analysis of Ultrasound Propagation

by

Valerie Jane Pinfield

Submitted in accordance with the requirements for the degree of
Doctor of Philosophy

The University of Leeds
Procter Department of Food Science

February, 1996

The candidate confirms that the work submitted is her own and that appropriate credit has been given where reference has been made to the work of others.

Abstract

The processes of creaming, flocculation and crystallisation are important factors in the stability and properties of food emulsions. Measurements of the ultrasound velocity and attenuation in an emulsion are used as a non-destructive probe of emulsion behaviour. The present work aims to increase the understanding of the destabilisation processes themselves and to improve the techniques for interpretation of ultrasound measurements on such systems. These aims were addressed through the computer modelling of creaming, flocculation and crystallisation behaviour, and through the investigation of theories for interpreting ultrasound measurements.

Two computer models have been developed of creaming in emulsions, both with and without flocculation. One takes a phenomenological approach, and is able to predict macroscopic concentration profiles of emulsions. The other is a small-scale simulation at the level of individual particles. The results of the phenomenological model are in qualitative agreement with experimental results in the absence of particle interactions. The effects of flocculation on creaming behaviour were not, however, reproduced by the model. The small-scale simulation demonstrated that a simplified model of flocculation and creaming could result in features in the concentration profiles which are comparable with those observed experimentally. However, some aspects of creaming behaviour were not reproduced by either model.

The investigation of theories of ultrasound propagation in emulsions concluded that multiple scattering theory is appropriate for the typical emulsions studied. The complex calculations required by the application of the theory are simplified in some special limits, which are presented. Alternative, practical, techniques are presented for the interpretation of ultrasound measurements. These are based on scattering theory but utilise experimental determination of the scattering properties of the emulsion, so avoiding the difficulties associated with multiple scattering theory calculations. The methods which have been developed are particularly relevant to creaming and crystallisation studies. The effects of particle size variation in emulsions can influence the interpretation of ultrasound measurements, and restrictions are therefore placed on the application of the methods.

Contents

Figures

Tables

Acknowledgements

Thanks are due to my supervisors, Professor Eric Dickinson and Dr. Malcolm Povey for their guidance throughout the project, and for many stimulating discussions. I would also like to thank my colleagues in the colloid group, in particular Jian Guo Ma, Matt Golding and Martin Whittle. I am grateful to Jian Guo Ma for permission to use his experimental creaming data in the ultrasound analysis. The assistance of the staff of the University Library and the University Computing Service is gratefully acknowledged.

My thanks are also due to the members of my family, who have always been a great source of strength. Finally, I would particularly like to thank my husband, Stephen, for his unfailing support and encouragement, and, in addition, for his assistance in proof-reading.

Chapter 1 : Introduction

Many foods are dispersed systems, consisting of a quantity of oil or fat (or both) dispersed as tiny droplets in a continuous aqueous phase, or as water droplets in an oil dispersion medium. The term emulsion should, perhaps, strictly be applied only to those systems where the particles are in the colloidal size range (1 nm-1 μm) and the two constituent phases are liquid. However, the term is in practice commonly used also for the many food systems which include some particles larger than 1 μm, or a partially crystallised phase (either the dispersed phase or the continuous phase). Dispersed systems in which one of the phases exists as a gel may also be referred to as emulsions. This wider scope of the term emulsion is applied to the systems studied in the present work. Familiar examples of food emulsions are milk and mayonnaise (oil in water emulsions), margarine and butter (water in oil emulsions with some solid fat in the continuous phase), and ice-cream (a combination of an oil in water emulsion and a foam; both ice crystals and solid fat are also present).

Emulsions are thermodynamically unstable; that is, their free energy is greater than if the two phases existed separately. Exceptions to this are microemulsions and solutions of some macromolecules. Energy must be supplied in order to form an emulsion, through the homogenisation or mixing process. In the absence of stabilisation of the emulsion by physical or chemical means, the emulsion would be "broken", separating into homogeneous regions of its constituent phases, which is the thermodynamically stable state. Prevention of the immediate rejoining of dispersed phase particles is achieved by the use of an emulsifier, usually a protein in food systems. The protein (acting as a surfactant) forms a protective layer around the surfaces of the droplets, causing an energy barrier which must be overcome for particles to join together.

In the longer term, the thermodynamic instability of the emulsion manifests itself through a number of destabilisation mechanisms: creaming, flocculation, coalescence, Ostwald ripening, and phase inversion. Creaming occurs when the dispersed phase has a lower density than the continuous phase, and the dispersed particles rise to the top of the emulsion. Flocculation refers to the tendency of particles to stick together, although retaining their individual identity. In contrast, coalescence is the merging of two or more

dispersed phase droplets into a single, larger droplet. Ostwald ripening causes larger droplets to grow at the expense of smaller droplets. This effect is produced by the mass transport of dispersed phase material between droplets because of a degree of solubility in the continuous phase. In most food emulsions, Ostwald ripening is usually negligible because of the very low solubility of triglycerides in water. Phase inversion, in which an oil in water emulsion becomes a water in oil emulsion, or vice versa, is only significant at high concentrations. A more detailed description of each of these destabilisation mechanisms can be found in works such as Dickinson (1992a).

Although thermodynamically unstable, a large degree of kinetic stability can be attained for emulsions, by physical or chemical means. An emulsion may be considered to be stable if it remains apparently unchanged over a specified time interval. Some food emulsions need only to be stable for a short period, such as a salad dressing which can be shaken before use. Others must remain apparently unaltered over a period of several years (e.g. cream liqueurs). Creaming is one of the principal destabilisation processes in food emulsions, and is considered to be a major determinant of shelf-life (Fillery-Travis et al., 1990). The formation of a cream on top of the emulsion is unsightly, and can in some cases be considered a spoiling of the product, for example in infant formula (Fligner et al., 1991). In contrast, a cream liqueur is expected to have a lifetime of several years, but a small amount of cream development may be acceptable over that period, since it is dispersed on pouring.

Although creaming itself is reversible by shaking, coalescence or strong flocculation may occur in the concentrated cream region after some time. The formation of an oily layer as the result of coalescence in the cream is irreversible and is definitely unacceptable to consumers. Flocculation and coalescence in the bulk of an emulsion are also important factors in food stability, not only because of their effects on food taste and texture, but also through their influence on the creaming rate. Coalescence of oil droplets leads to an increase in the creaming rate. Flocculation can also cause a considerable increase in creaming speed, at relatively low oil concentrations. At higher concentrations, an emulsion may be stabilised against creaming by the flocculation of particles into a networked structure. The kinetic stability of emulsions, particularly in regard to creaming, is therefore of great significance to the food industry.

In some foods, such as ice-cream and margarine, the presence of a solid phase in the emulsion is of vital importance. The crystalline substance may be present in the aqueous or oil phase, and is often a critical component of the food structure (Darling and Birkett, 1987, Walstra, 1987a, 1987b). For example, the air bubbles in ice-cream are to some extent stabilised by partially coalesced globules containing fat crystals, and ice crystals form a networked structure in the aqueous phase of the emulsion. The apparently solid nature of a margarine is in part due fat crystals, which may be present in relatively small quantities. The solid components of chocolate are also significant in attributing a 'hard' structure, and a pleasing, shiny finish to the product. The melting and crystallisation properties of food fats are also key components in the taste and texture of food products. Several common food fats have melting ranges around body temperature, causing a melt-in-the-mouth characteristic. This is the case in margarines and in chocolate. The undesirable melting and recrystallisation of one of the morphological forms of cocoa butter can cause the unsightly 'blooming' of the chocolate. In other foods a degree of crystallisation is essential for the control of a desirable destabilisation process such as in the whipping of cream. The relevant properties of the common food fats can be found in The Lipid Handbook (Gunstone et al., 1994). The crystallisation and melting behaviour of foods must be considered to be an important subject in the 'freezer-to-microwave' culture.

1.1 Stability of emulsions

1.1.1 Creaming

Gravitational destabilisation occurs when the two phases of the emulsion are of different densities. The dispersed phase tends to float to the top of the emulsion (creaming) if it is less dense than the continuous phase, and to sink to the bottom (sedimentation) if it is more dense. Since the present work was concerned primarily with oil in water emulsions, this process is usually called creaming. In the absence of particle interactions and any flocculation or coalescence of particles, the rate at which creaming occurs can be reduced by the control of a number of adjustable physical quantities. The driving force for creaming is the difference between a particle's weight, and the buoyancy force (which is equal to the weight of surrounding fluid displaced by the

particle). Hence the difference in density between the two phases is a determining factor in the creaming rate. In many food emulsions, the continuous phase is water or an aqueous solution, and the density difference between water and many food oils (such as sunflower oil) is approximately 50 kg m^{-3}. This relatively small difference (compared with a low molecular weight alkane in water system, for example) allows some food emulsions to be stabilised against creaming for several years. Some food systems have in the past been modified by the addition of substances such as brominated vegetable oils (in soft drinks) in order to reduce the density difference. However, the use of these oils has now been prohibited. The densities of the component phases are not readily modified, and greater creaming stability is usually achieved through the control of other physical factors.

Particle size is one of the major determinants of creaming rate. In a very dilute emulsion, the creaming speed of a particle is proportional to the square of its diameter. In a polydisperse emulsion, different sizes of particle cream at different rates, the largest creaming more rapidly than the smallest. The existence in the emulsion of only a small number of significantly larger droplets can cause the formation of an undesirable oil film on the top of the emulsion. This is due to the rapid development of a cream of the largest particles, which can then coalesce into an oil layer. Homogenisation of an emulsion can be used to obtain a small particle size distribution, in order to control the creaming rate. This is noticeable in homogenised milk which is apparently much more stable to creaming than the natural version. Smaller particles not only cream more slowly, but they are also more diffusive and so resist the changes in concentration associated with creaming. Creaming is therefore essentially undetectable when particles are below a certain size.

The final key parameter in the control of emulsion stability against creaming is the viscosity of the continuous phase. This is a more readily controllable parameter which is affected by the temperature, the presence of polymer in the continuous phase etc. The study of the viscous (or viscoelastic) properties of materials is a significant research area, which is given the term *rheology*. An increase in viscosity of the continuous phase reduces the mobility of the dispersed phase particles and hence slows down the creaming process. Since it is particle mobility which is affected, other dynamic processes, such as flocculation, are similarly reduced, since they depend on the rate of collisions between

particles. In foods, modification of the viscosity of the continuous phase must be balanced by consideration of the textural properties of the product. A simple thickening of the continuous phase by the addition of some substance has a direct effect on the apparent properties of the food. However, the shear stress dependence of the viscosity of some solutions can be put to advantage in this application. The stress induced by particle movement under gravity is much smaller than the stresses encountered at the macroscopic level, associated with pouring, spreading etc. At these very low shear stresses, some hydrocolloid solutions have a very high viscosity, exhibiting pseudo-plastic behaviour (Dickinson, 1992a). In the extreme case, control of particle mobility can be achieved through a gel structure in the continuous phase, which prevents any macroscopic movement of particles at the stresses involved in the creaming process. For example, at sufficiently high concentrations, the polysaccharide xanthan produces a gel in the continuous phase which stabilises the emulsion (Dickinson et al., 1994). Modification of viscosity is one of the most important methods of enhancing emulsion stability against creaming.

The concentration of the dispersed phase also has an influence on creaming rate. At higher concentrations, particle mobility is reduced due to hydrodynamic interactions. In addition to the direct obstruction of particle movement by other particles, the reverse flow of the continuous phase fluid also reduces the net creaming speed. Hence, an increase in concentration can lead to stabilisation of the emulsion. However, the dispersed phase volume fraction is not a parameter which is readily adjustable to improve stability, because of its effects on flavour, appearance, cost, texture and calorific value.

1.1.2 Flocculation

Flocculation occurs when a minimum exists in the interparticle energy at some separation (usually small). The potential minimum represents a favourable energy state for particles to remain close together. Particles retain their individual identity, rather than coalescing to form a single, larger droplet. The depth of the potential minimum determines the reversibility of flocculation, which is the tendency of the floc to break up again. This may take place if the particles have sufficient thermal energy to escape from the potential well and to move apart. In order for flocculation to occur, particles must first approach each other to within a small interparticle separation. This close approach of particles is caused by some form of

relative particle motion, for example Brownian motion (leading to perikinetic flocculation) or a shearing motion (leading to orthokinetic flocculation). The shear processes include low shear motion, such as relative creaming rates of different sized particles in a polydisperse sample, and high-shear action, caused by shaking or stirring.

The numbers of close encounters or collisions between pairs of particles (the binary collision rates) can be derived from the dynamic properties of the particles, and their effective collision cross-sections. The collision rate due to Brownian motion in a monodisperse emulsion was derived by Smoluchowski (1913). The combination of the diffusivity of a particle and its collision area produce a collision rate which is independent of particle size in this case. The rate is reduced by an increase in the continuous phase viscosity, or a decrease in temperature. Since a binary collision process is at work, the collision rate in a dilute emulsion is proportional to the square of the number density of particles.

In a polydisperse emulsion, the Brownian collision rate is increased, because of interactions between small and large particles. The greater mobility of the smaller particles combines with the greater collision cross sections of larger particles to produce a higher effective collision rate. A second source of relative particle motion in a polydisperse emulsion is caused by the different creaming speeds of particles of different sizes. Larger particles which are moving more rapidly collide with smaller, more slowly moving particles. The factors affecting particle creaming rates have similar influences on the gravitational flocculation rate. The range of particle sizes in the emulsion (or the degree of polydispersity) is an additional determining factor. Hence the polydisperse nature of emulsions has an influence on the flocculation rate through both Brownian and gravitational processes.

The collision rate is a measure of the frequency of events in which particles are sufficiently close together to allow flocculation. However, the form of the interparticle potential determines whether or not flocculation occurs following such an encounter. If the only interparticle interactions are van der Waals forces, the interparticle potential is attractive over all length scales. No energy barrier exists to flocculation, and the potential minimum is infinitely deep. Thus, every collision event results in flocculation, which is irreversible. In most emulsions, however, flocculation is modified both by the existence of an energy barrier which reduces flocculation rate, and by the finite depth of the

potential minimum, which causes some degree of reversibility in the flocculation. If an energy barrier exists in the interparticle potential, there is only a finite probability that two colliding particles have sufficient energy to overcome the barrier and thereby flocculate in the potential minimum. The existence of an energy barrier is therefore a stabilising effect on the emulsion. Enhanced stability of an emulsion against flocculation can be achieved by physico-chemical means to produce such an energy barrier, which prevents the close approach of particles.

There are two main stabilisation mechanisms for preventing flocculation through the existence of an energy barrier in the interparticle potential. These are electrostatic and steric stabilisation (Dickinson, 1992a). Electrostatic stabilisation results from a repulsive force between colloidal particles, caused by the charged polar groups on the adsorbed molecules. The dispersed phase particles carry the same (in sign) electrical charge, and as they approach each other, ions in solution with the opposite charge become more concentrated in the interparticle region. The resulting excess osmotic pressure in the space between the particles drives them apart, preventing them from flocculating. This is known as the double layer repulsion. The combination of this electrostatic repulsion and the van der Waals attraction results in the classical Derjaguin-Landau-Verwey-Overbeek (DLVO) potential, which is often used to describe particle interactions in colloidal systems. The potential includes an energy barrier due to the electrostatic repulsion, which slows down the flocculation rate. The strength of the barrier is also influenced by other conditions such as the pH and ionic strength.

Steric stabilisation is effected by the resistance of the adsorbed layer of polymer to close approach of the particles. At small interparticle separations, the protruding segments of the adsorbed polymer layers must either be compressed or interpenetrate. Compression of the layers is always associated with a free energy increase. Interpenetration may or may not be energetically favourable, depending on the quality of the continuous phase as a solvent for the protruding polymer segments. A free energy increase results from interpenetration if the continuous phase is a good solvent for the polymer, so that the two polymer layers prefer to exist separately in the solvent. Hence, steric stabilisation is achieved using heterogeneous polymers which have parts which adsorb strongly to the surface, but other regions which favour existence in the continuous phase. Under these conditions, an energy barrier exists in the interparticle

potential due to these two entropic factors which are unfavourable to particle approach. Therefore, flocculation is to some extent prevented by this mechanism.

Having considered the factors which enhance emulsion stability against flocculation, it is necessary also to understand the circumstances under which flocculation is promoted. The same chemical species which produce emulsion stability can, under different conditions, destabilise the emulsion. There are two principal flocculation mechanisms in this category: bridging flocculation and depletion flocculation. Bridging flocculation occurs when there is insufficient adsorbing polymer present to achieve full surface coverage of the emulsion particles. When particles approach each other, a favourable energy state is achieved by 'sharing' a single polymer molecule between the surfaces of both particles. Thus, the polymer acts as a bridge between droplets. A sufficient quantity of adsorbing polymer must therefore be included in the emulsion in order to avoid the bridging phenomenon. In some cases, the flocs formed by this process tend to be rather weak, and are easily disrupted by stirring. However, strong bridging flocculation is effectively irreversible. The mechanism has been demonstrated by computer simulation (Dickinson and Euston, 1992).

In contrast, depletion flocculation occurs when an excess of adsorbing polymer is present in the continuous phase. If the interparticle separation becomes smaller than the radius of gyration of the polymer, polymer is excluded from the region between the droplets. An osmotic pressure gradient then exists between the interparticle region (which is deficient in polymer) and the surrounding polymer solution. It is, therefore, energetically more favourable for the particles to come together, causing flocculation (Asakura and Oosawa, 1954, 1958). This reversible process is called depletion flocculation, since it is driven by the absence, or depletion, of polymer in the interparticle region. Flocculation can be caused by non-adsorbing macromolecules or surfactant micelles by the same mechanism. An investigation of the influence of various system characteristics on depletion flocculation rate was carried out by Liang et al. (1993). In practice, it can be difficult to distinguish between weak bridging and depletion mechanisms of flocculation in a sample.

The adsorbing polymer species which promote steric stabilisation may, therefore, *cause* flocculation in certain conditions. Too little polymer can lead to bridging flocculation, whereas too much polymer may cause depletion flocculation. In addition, a

reduction in the solvent quality for the sterically stabilising polymer may induce flocculation, since it is then more favourable for the polymer layers to overlap. Just as stability or instability can be caused by the same species in these cases, a non-adsorbing polysaccharide in the aqueous phase may be used as a stabiliser in sufficient concentration, since it increases the effective viscosity. However, at lower concentrations the presence of the macromolecule can induce depletion flocculation (Dickinson et al., 1994). The overall effect on emulsion stability is the net result of the competitive processes of depletion flocculation and the stabilising effect of increased viscosity.

1.1.3 Crystallisation

Although crystallisation is not in itself a mode of instability, both the existence of solid fat in an emulsion, and the crystallisation of liquid oil can influence the destabilisation processes. The mechanism of crystallisation of oil droplets in an oil in water emulsion is not the subject of this study. Rather, it is the effect of solid fat and the crystallisation process, particularly on creaming behaviour, which is of interest. There are several possible mechanisms for crystallisation in an oil in water emulsion containing a mixture of solid and liquid droplets (see studies by Bennema et al., 1992, Bennema, 1993, Simoneau et al., 1993, Ozilgen et al., 1993, Boode et al., 1991). One suggested mechanism of heterogeneous crystallisation involves binary collisions between solid and liquid droplets (McClements et al., 1993). A finite proportion of such collisions results in the nucleation of crystal growth in the liquid droplet, and thereafter its rapid solidification.

The binary collision process is one of the principal controls on the flocculation rate. In this heterogeneous crystallisation mechanism, collisions must occur between solid and liquid droplets in order to be effective, but essentially the collision process is identical. Hence, the factors which influence the flocculation rate in an emulsion (which were discussed in the preceding sections) are also effective in the crystallisation rate, if such a heterogeneous mechanism is valid. In addition, the stabilisation mechanisms which are effective in the case of flocculation, may produce similar reductions in the crystallisation rate. The thickness of the adsorbed layer is thought to be particularly important in preventing the nucleation of crystal growth when particles collide.

1.1.4 Interrelationships between creaming, flocculation and crystallisation

The destabilisation processes of creaming and flocculation, and the crystallisation process have been considered independently in the preceding sections. However, they may occur simultaneously in an emulsion, and the interaction between them may be significant. Some of the physical factors which stabilise an emulsion against flocculation also reduce the creaming and crystallisation rate. For example, an increase in viscosity of the continuous phase impedes the mobility of particles, and therefore reduces the rate of all dynamic processes which depend on particle movement. Therefore, the effects of these processes should now be considered together.

Flocculation in an emulsion is often difficult to determine directly, especially if the flocs are held together only weakly. Attempts to measure the effective particle size distribution, and so to observe floc formation, are undermined by the need to dilute and stir the emulsion. The shear forces applied, and the change in environment, may be sufficient to break up the flocs, so that an increase in effective particle size may not be apparent in the size distribution measurement. If the flocs are strong enough, an increase in mean particle size will be detected. Rheological examination of flocculated emulsions may also be thwarted if the application of a shear stress causes the flocs to be disrupted. However, the presence of flocs can often be inferred through the modification in the creaming behaviour of an emulsion.

Flocculation may increase or decrease the creaming rate (see for example Dickinson et al., 1994). A discussion of the role of the adsorbed polymer layer in emulsion stability against flocculation, and thereby also its affect on creaming was presented by Dickinson (1992b). In a dilute system, a compact floc would be expected to move under gravity more quickly than its constituent particles. The net buoyancy of the floc is the sum of the buoyancy of the particles, but the viscous drag on the floc is less than the sum of the drag on the individual particles. Therefore, the floc can move more rapidly, and in these dilute conditions the formation of flocs can produce a noticeable increase in creaming rate. In a more concentrated emulsion, the increased obstruction experienced by flocs due to their larger collision cross-section can cause a reduction in the creaming rate when flocculation becomes extensive. In the extreme case, the linkage of individual flocs to each other can develop a particle network which spans the whole sample, and essentially prevents further movement. Some compression of the network

under gravity may be observed, but creaming in the classical sense is no longer possible. Although such a network stabilises the emulsion against creaming, it may be undesirable as far as the food product is concerned, for reasons of texture etc.

The formation of flocs can therefore have a significant impact on the creaming behaviour of an emulsion, either to increase the creaming rate or to stabilise the emulsion. It is also true that the creaming motion of particles increases the flocculation rate in a polydisperse emulsion. The difference in creaming speeds between small and large particles leads to a higher rate of collisions between particles, so increasing the opportunity for flocculation. The same is true in principle of the crystallisation rate, if it is propagated heterogeneously by collisions between solid and liquid particles.

Crystallisation of emulsion droplets can also have an impact on the stability of an emulsion (Mulder and Walstra, 1974, Boode et al., 1991, van Boekel and Walstra, 1981). The density of solid fat is usually higher than that for the liquid oil. In most food systems, therefore, the density difference between the dispersed and continuous phases is less for the solid fat than for the liquid oil. Hence, the creaming rate for solid particles is often significantly lower than when the dispersed phase is liquid. Thus, crystallisation may improve the emulsion stability against creaming. However, the needle-like crystals which occur in some food fats can stabilise or destabilise the emulsion (Coupland et al., 1993, Boode et al., 1991). The crystallisation rate may increase since a collision with a liquid droplet is more likely to nucleate crystal growth because of the penetration of the needle-like crystal. The formation of protruding crystals removes the effectiveness of the adsorbed layers in preventing flocculation and coalescence. A particle collision involving a protruding crystal may lead to the particles sticking together, as the needle penetrates the adsorbed layers. In dairy emulsions, droplets which include both solid fat crystals and liquid oil can be formed, which may undergo partial coalescence due to the same interpenetration mechanism (Walstra, 1987a, 1987b, Boode et al., 1991). The continued development of such needles may lead to a complete interconnecting network sustained by crystal 'bridges'. Creaming would in this situation be reduced. Alternatively, coalescence of particles by the breakage of the adsorbed layers causes increased creaming because larger particles are formed.

The processes of creaming, flocculation and crystallisation are therefore interdependent. Experimental observation of creaming is one method of indirectly

determining the influence of the other interactions in the system, which have some effect on creaming behaviour.

1.2 Experimental studies of creaming

Real food systems tend to be rather complex in their composition and therefore also in their physical and chemical interactions. For example, milk is a familiar oil in water emulsion, which undergoes creaming, but which has a number of complicating features. Some oil may be crystallised, and a degree of flocculation may also be present, due to the dispersed protein in the aqueous phase. Studies of such food systems are practically useful and sometimes informative, but it is often difficult to obtain reliable information on the fundamental processes occurring in the system, due to the number of contributing interactions. Hence, many studies of emulsions are carried out using model systems, in which the number of components is limited, and the composition can be carefully controlled. Some studies have used monodisperse silica particles in an aqueous dispersion medium (van Duijneveldt et al., 1993). Others use food-grade materials such as sunflower oil in water emulsions (Ma, 1995). Alternatively, low molecular weight alkane oil in water emulsions have been studied (Gouldby et al., 1991, McClements et al., 1993). The choice of model system depends on the emulsion properties and the type of behaviour under consideration. Components which are commonly present in foods are often added in a controlled manner to the model system in order to assess their effect on emulsion stability.

A substantial number of studies of creaming in emulsions have been published. These studies are intended both to assess the effects of various food components on the stability of emulsions, and also to attempt to understand the mechanisms underlying these effects. The influence of flocculation on creaming behaviour is a particular aspect of recent investigations. Some non-adsorbing polymers, such as the polysaccharide xanthan, are used to stabilise food oil in water emulsions. This stabilisation occurs, above a critical polymer concentration, due to the formation of a weak gel in the continuous phase, which prevents particle movement. However, it has been observed that at polymer concentrations below a critical value the emulsion is destabilised (Luyten et al., 1993). It is thought that this effect is due to depletion flocculation. The very marked increase in creaming rate under some conditions indicates that the flocs are able to move much more

quickly than the single particles. The result has been confirmed in many later studies, under a variety of emulsion conditions, for example Dickinson et al. (1994) and Fillery-Travis et al. (1993). Both of these works also refer to the influence of oil volume fraction on the flocculation effect.

Some investigations of the effect of flocculation on creaming rate as a result of added polymer have considered the influence of food-like conditions on the system. For example, the type of surfactant was shown to influence the stabilising or destabilising effect of polymer in a recent study by Dickinson et al. (1995). This was demonstrated by the alteration in creaming rate for the different surfactants, and was attributed to interactions between the surfactant and the biopolymer added to the continuous phase. An earlier study by Cao et al. (1991) inferred a degree of complexation between the sodium caseinate emulsifier and carboxymethylcellulose (a nonadsorbing polymer present in the continuous phase). The interaction apparently caused an increase in the flocculation rate, due to bridging. This occurred in addition to the depletion flocculation which had been seen to increase the creaming rate with a number of other polymers. In view of the presence of salt in many food systems, Dickinson et al. (1994) have studied the influence of ionic strength on creaming stability in systems which are thought to include depletion flocculation. Salt was added to mineral oil in water emulsions which included the polysaccharide xanthan. The addition of salt did have an effect on the creaming behaviour, and this was interpreted in terms of a possible change in the structure of xanthan molecules with a change in ionic strength. Ionic strength is also thought to affect the strength and range of the depletion interaction between particles.

Experimental investigations of crystallisation in oil in water emulsions are often concerned with the mechanism of the crystallisation process. Crystallisation in emulsions of mixed solid and liquid droplets is the subject of much debate. Both food-grade and non-food emulsions have been studied. The fats commonly occurring in foods can manifest needle-like crystal growth, which may affect emulsion stability through increased coalescence, or through the formation of a stabilising network of the crystals. A study of crystallisation in alkane in water emulsions with solid and liquid droplets was carried out by McClements et al. (1993). The kinetics were found to be consistent with a binary collision process. However, recent results on emulsions in the presence of xanthan, which is thought to induce depletion flocculation, have appeared to show

inconsistencies with this interpretation (Ma, 1995, Dickinson et al., 1996). The interacting effects of flocculation and crystallisation are not therefore properly understood. The work of Ma (1995) proceeded to examine the creaming behaviour of the crystallising emulsions. This is not an area which has been widely studied. The preliminary results suggest that the crystallisation processes did not in this instance have a significant impact on the creaming of the emulsion. The interactions between creaming, flocculation and crystallisation have not yet been fully explored.

The preceding discussion demonstrates that the investigation of creaming behaviour, and its connection with the other processes of flocculation and crystallisation is an active research area. Many of these studies of creaming are not only concerned with emulsion stability, but also on increasing the understanding of the fundamental processes taking place in the emulsion. However, much work has also been carried out on the prediction of emulsion stability. Food systems are often expected to exhibit long term stability (perhaps months or years), particularly against creaming, and therefore direct tests of this stability are difficult and time-consuming. A correlation between some property of the fresh emulsion and its long-term stability would be of great benefit in assessing food emulsions. Alternatively, a quantifiable measure of the short-term behaviour of the emulsion which demonstrated the onset of creaming at a very early stage would be equally beneficial.

A comparison of various tests for predicting emulsion stability was carried out by Fligner et al. (1991). The bench mark of stability was taken to be the measured cream thickness in the emulsion after a specified time, when left to cream naturally under gravity. Other 'predictive' tests were the degree of creaming by centrifugation, emulsion viscosity, the amount of adsorbed protein (although this is somewhat specific to the systems used), and a measure of fat globule size determined from light scattering measurements. Measurements were made on the fresh emulsion, and a correlation was made with the natural creaming stability over a period of 10-18 weeks. It was found that the best predictors of stability were the centrifugation measurements and the emulsion viscosity. The particle size (of fat globules) was found to be a very poor indicator of stability, in spite of it being widely used as such (Fligner et al., 1991). The effects of fat globule size, concentration and polydispersity on creaming and centrifugation rates were

also investigated by Walstra and Oortwijn (1975), relating to predictions of emulsion stability.

The conditions present during centrifugation (particularly the shear forces) are very different from those in a naturally settling emulsion. In addition, the dynamic processes of flocculation and creaming do not scale in the same way with the applied acceleration. A prediction of emulsion stability on the basis of centrifugation may therefore not be applicable in emulsions where flocculation is significant. However, the study of a mineral oil in water emulsion in the presence of rhamsan (Dickinson et al., 1993a) similarly illustrated a connection between creaming stability and the rheological behaviour of the emulsion. Previous investigations had attempted to relate the creaming stability to the rheology of the continuous phase of the emulsion, but this was found not to be a reliable indicator. Flocculation of the particles contributes to the apparent emulsion viscosity provided the flocs are sufficiently strong.

The assessment of such methods for measuring stability illustrates the need for techniques which can detect the early onset of instability, particularly creaming. In addition, studies of creaming behaviour have indicated the wealth of fundamental information which can be extracted from creaming results. The interacting processes of flocculation and crystallisation can be examined through their influence on creaming. In the past, creaming experiments have used a visual technique to measure the height of the serum and cream regions. In some cases, these regions are clearly defined, and such measurements are simple. In other conditions, the serum layer may remain significantly turbid, with a very poorly defined interface, making a meaningful measurement difficult. The cream may also be difficult to detect in an opaque emulsion. The onset of creaming could in principle be detected at an earlier stage than is possible with visual creaming methods if a small change in concentration could be measured at the top or bottom of the emulsion. In addition, detailed vertical profiles of concentration variation within the sample offer a significant probe of the creaming, flocculation and crystallisation processes. A number of experimental methods have been developed to attempt to obtain more detailed information on the variation of dispersed phase concentration within the sample. One such technique is magnetic resonance imaging, which has been used both to obtain qualitative images of the emulsion, and to produce quantitative measures of the concentration variation (Pilhofer et al., 1993, Kauten et al., 1991). An alternative method

of measuring the oil concentration in emulsions is the use of low power ultrasound, and it is this technique which is discussed in the following sections.

1.3 The ultrasound method

Ultrasound is the term applied to sound waves which are of a higher frequency than is audible by the human ear (approximately 16 kHz). High power, continuous operation ultrasound methods are used in food applications for cleaning purposes, for emulsification or for breaking up aggregates. However, the application of ultrasound to the measurement of emulsion properties involves the use of very low power acoustic fields (<100 mW). The power levels are not sufficient to cause any disruption of the particles or to modify the emulsion, and it therefore constitutes a non-destructive technique. Typically, these low power applications of ultrasound are operated in pulsed mode so that only a short burst of sound is passed through the emulsion.

The technique involves measurement of the properties of ultrasound propagation in the emulsion. Usually, the parameter which is measured is either the velocity or attenuation of the sound wave in the emulsion. Alternatively, a determination of the wavelength of the sound wave (which is closely related to the velocity) may be used. Although there are a number of practical ways of measuring the velocity and attenuation, the principles are the same in most cases (Povey and McClements, 1989). A pulse of ultrasound is passed through the emulsion, and is either reflected off a hard surface (pulse-echo) and received at the transmitter, or passes right through the emulsion and is received at the other side. The velocity in the emulsion can be calculated from the time taken for the pulse to pass through the emulsion, and the attenuation from the reduction in signal amplitude.

The application of the ultrasound technique to creaming experiments involves the measurement of ultrasound velocity in the emulsion as a function of position and time. From these data, concentration profiles can be determined, which demonstrate the progression of creaming in the emulsion. A schematic diagram of the equipment used for such creaming experiments is shown in Figure 1.1. A similar technique has been used by other workers with some variations (Fillery-Travis et al., 1993, Dickinson et al., 1993a). The sample is contained in a square-section glass cell which is placed in a water bath to maintain a constant temperature and to achieve ultrasound coupling. The emulsion

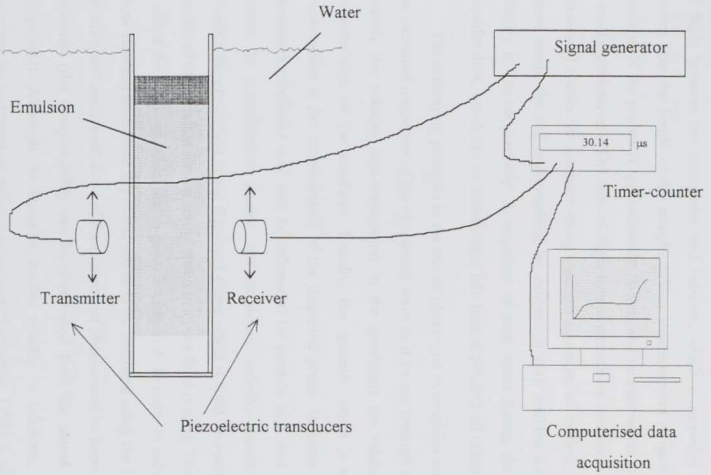

Figure 1.1 Schematic diagram of the ultrasound scanner used to obtain concentration profiles in creaming emulsions.

sample has dimensions of approximately 250 mm × 35 mm × 35 mm. Use of such a large sample enables features to be seen which would be insignificant in a small sample. The thickness of cream formed depends on the volume of oil in the sample, and so a taller sample produces a thicker cream layer.

The piezoelectric transducers act as a transmitter and receiver of a pulse of low power ultrasound which is passed through the cell. A timer-counter determines the time of flight between the transmitter and receiver, which is recorded by computer. The probes scan the height of the sample, taking measurements at specified intervals. The diameter of the probes is approximately 10 mm, and measurements are typically made at 5 mm height intervals. The time-of-flight measurements are converted into the velocity of ultrasound within the emulsion using standard equations of motion. The path length of sound inside the cell is determined by calibration with distilled water, for which the velocity is known precisely. A sequence of such scans during the creaming process provides data, which can be transformed into time dependent oil concentration profiles.

The underlying principle in the use of ultrasound in emulsion measurements is that the measured properties of the ultrasound wave as it passes through an emulsion sample (usually the velocity and attenuation in the emulsion) are related to the physical characteristics of the emulsion. Usually, the quantity which is obtained from the measurement is the concentration of the dispersed phase. In some circumstances, the ultrasound properties may also be influenced by particle size, and other contributory factors. In crystallisation studies, the ultrasound velocity measurement is used to calculate the proportion of the dispersed phase which is solid. In many cases, a modified version of the equation for the sound speed in a pure fluid is used. The modified equation is called the Urick equation, and is given in chapter 4. In order to calculate the dispersed phase concentration from the sound speed in an emulsion using the Urick equation, the densities and compressibilities of the component phases must be known. These are easily measured (the compressibility can be determined from the sound speed in the bulk component). Although the equation applies reliably to solutions, and is used as a technique for investigating solution properties (Sarvazyan, 1991), it is not always valid in emulsions. In some cases where discrepancies have been detected in the use of the Urick equation, the sound speed/ concentration relationship has been determined experimentally by using a series of uniform emulsions of known concentration.

Several studies of creaming behaviour using the ultrasound technique have been published in recent years. An example of the results which can be obtained is shown in chapter 2 (figure 2.24, Ma, 1995) for a sunflower oil in water emulsion containing xanthan. This figure, and other published results, illustrate the greater detail available from the method when compared to visual creaming experiments. The technique therefore allows more fully the study of the interaction between flocculation, crystallisation and creaming. Many studies of depletion flocculation present the contrasting concentration profiles obtained with or without added polymer. For example, the addition of xanthan was found to increase the creaming rate very significantly (Cao et al., 1991) and to produce a sharp serum interface which moves steadily up the system. In the absence of xanthan, creaming is much slower, and the serum is less clearly defined. At a much higher oil concentration (50 wt.%), the same study (Cao et al., 1991) demonstrated that the addition of xanthan caused a serum region to develop. However, the concentration in the rest of the emulsion remained mostly uniform, showing only a gradual increase with time. A clear cream layer was not observed. The result indicated the gradual compression and rearrangement of the flocculated structure, 'squeezing' out the continuous phase to form a serum. This behaviour would not be detectable by visual creaming experiments.

Emulsions containing polymer have been shown to exhibit very complex creaming behaviour (Gouldby et al., 1991). Concentration profiles were obtained using the ultrasound technique, in the absence of polymer, and with a range of polymer concentrations. The concentration of polymer influenced the shape of the concentration profiles in a variety of ways. In some cases, the flocculated emulsion exhibited monodisperse creaming behaviour. The serum interface was sharp and moved steadily up the sample. In a sample with a lower polymer concentration, the concentration profiles indicated that creaming was proceeding as if two separate species were present – a rapidly-creaming flocculated species, and unflocculated particles which creamed much more slowly. The flocs creamed rapidly, leaving a low concentration in the emulsion which then creamed like an unflocculated emulsion. This result was also seen in a later study (Fillery-Travis et al., 1993). The measurements were also able to detect a change in concentration in the cream region between samples of different polymer concentration. This is an indication of the sparse nature of the flocs formed and the efficiency with which they can pack together in the cream. In addition, in some flocculated samples, the

concentration in the cream was found to be fairly uniform but became more concentrated with time, as the cream was compressed into a more densely packed arrangement. It was particularly noted in one case that the creaming was not visible by eye until it was well-advanced, although the concentration profiles showed that considerable changes had occurred.

The development of a serum layer with a sharp interface has been seen in several studies of flocculated emulsions. In some cases, the position of the serum interface does not move with time, as seen in the studies discussed above. Instead, the interface develops rapidly, but the creaming rate is then reduced and can continue in a variety of ways (Dickinson et al., 1993a, Dickinson et al., 1994). The addition of rhamsan to a mineral oil in water emulsion with Tween20 emulsifier was found to cause creaming to cease after a serum layer had developed (Dickinson et al., 1993a). The system was sufficiently concentrated (30 wt.% oil) and flocculated to prevent further movement. In contrast, the concentration profiles in mineral oil in water emulsions in the presence of xanthan showed substantial changes with no corresponding change in serum interface position (Dickinson et al., 1994). In some cases no cream development was observed. At a higher xanthan concentration, a serum interface was formed and remained in the same position. However, cream continued to develop and the concentration in the bulk of the emulsion decreased with time.

The development of a serum, with a sharply defined interface appears to be a characteristic feature at low xanthan concentrations. At higher concentrations of xanthan, creaming behaviour appears to be dominated by the cream development, and the concentration profiles show a gradual increase throughout the rest of the emulsion. The addition of salt to the mineral oil in water emulsions was found to influence the concentration profiles in the presence of xanthan (Dickinson et al., 1994). At low xanthan concentrations, less serum development was observed, but at higher xanthan concentrations, the emulsions appeared to be less stable when salt was added. The differences in concentration profiles under the different conditions hold information on the processes occurring in the emulsion, for example the extent of flocculation, the apparent floc size, etc. (see, for example, the analysis of Fillery-Travis et al., 1993).

The preceding sections have shown that the processes of creaming, flocculation and crystallisation interact. The use of an ultrasound technique enables detailed

information on the creaming behaviour to be obtained. The objective of the present work was to understand more fully the physico-chemical factors behind the experimental observations of creaming, flocculation and crystallisation made using the ultrasound scanner. There are two main aspects to the study: firstly, computer modelling of the creaming process and the contributory effects of flocculation and crystallisation, and, secondly, the investigation of methods of interpretation of ultrasound measurements. Computer modelling of creaming is intended to help understand the contributions of various physical processes to the creaming behaviour which is observed. The study of methods of interpreting ultrasound measurements aims to improve the ways in which useful information can be extracted from ultrasound measurements on dynamic emulsion systems, to observe creaming, flocculation and crystallisation behaviour quantitatively. The various theories of ultrasound interpretation can also be tested using the computer model, which provides fully-characterised data of concentration and particle size variation.

1.4 Computer modelling

The computer modelling of creaming behaviour in emulsions is intended to increase the understanding of the influences of the various contributory physical processes. This can be achieved by constructing a model of the emulsion including a limited number of phenomena and interactions, to observe the individual effects of the different factors. Initially creaming alone was modelled. Later, the effects of crystallisation and flocculation on creaming behaviour were considered in a limited way. The models have been designed for oil in water emulsions, and initially the model was tailored to the experimental technique of the ultrasound scanner. Thus, the modelling results could be directly compared with the observations of real emulsions. As will be argued later, the size of the samples involved leads to a phenomenological approach to the problem, rather than a model of particulate dynamics.

Previous modelling of the phenomenon of creaming has mostly been concerned with the inverse problem of sedimentation (in which the dispersed phase is more dense than the continuous phase). The related field of fluidisation (in which an upward flow of fluid is used to 'suspend' particulate matter) has been the subject of analysis in other cases. A number of different approaches have been adopted by previous workers. The

early work of Kynch (1952) was concerned with the rate of fall of the supernatant interface in a monodisperse suspension as sedimentation proceeded. He proposed a solution of the continuity equations by the method of characteristics. The mass balance of particles could then be used to relate the interface position to the dependence of particle velocity on local concentration. The principles of this solution have been used by many other later workers.

The same approach was applied to a polydisperse system by Stamatakis and Chi Tien (1988). The suspension is assumed to comprise a number of zones of constant concentration. The interfaces between the zones represent the upper limit of particles of each size fraction. The rate at which those interfaces fall is determined by the local concentration, according to an assumed relationship between particle creaming velocity and concentration. This relationship is obtained from previous analytical and empirical studies. A solution for the concentration in each zone and the speed of fall of the zone interfaces can be determined using the mass balance of particles between the zones. Special care is taken at the interface with the sediment, which grows with time, and changes composition as the zone interfaces meet the sediment. This is a relatively simple and efficient process. However, it does require assumptions, such as constant concentration in the sediment, with no compression. It is also difficult to see how diffusion, or other forces on the particles, could be included.

An alternative method of solution, used by the same authors (Stamatakis and Chi Tien, 1988, 1992), is to solve the continuity equations for the local volume fraction of dispersed phase. The velocity of the particles is determined by the local concentration, again using a previously obtained correlation for creaming speed. The solution of the continuity equation is achieved by a finite difference technique on a one-dimensional grid. The compressive stress in the sediment can be included in this formulation, assuming empirically determined relationships for the dependence of the stress on parameters such as permeability. The model is applicable to polydisperse suspensions, although only monodisperse and bidisperse systems were analysed.

The finite difference approach was also employed by Shih et al. (1986, 1987), but these workers solved the continuity and conservation of momentum equations for the system. The techniques previously described assume that the inertial effects and the particle acceleration can be neglected. The motion of particles can therefore simply be

described by the creaming speed, which is obtained from the local concentration. The solution of the equations of motion (continuity and momentum equations) is more general, and includes inertial and acceleration effects. However, a number of constitutive relationships are still required, for example for the dependence of the drag force on a particle with concentration. Thus, it does not avoid the need to use previously obtained analytical or empirical relationships. Other forces can, however, be easily included in this scheme, through the momentum equation. An applied electric field, for example, exerts a force on charged particles.

Shih et al. (1986) used the method of characteristics to obtain the characteristic solutions to the equations of motion. These were then solved using a finite difference method. The computational expense of the numerical analysis led them to modify their model and neglect the inertial and acceleration terms in the equation of motion. The equations then reduce to a continuity equation and a force balance equation, which is essentially the same formulation as used in the other methods (Kynch, 1952, Stamatakis and Chi Tien, 1988, 1992). The method of characteristics and a finite difference technique were used to obtain the solution. The model was also extended to polydisperse systems (Shih, et al., 1987).

The general consensus in these analyses is to neglect inertial and acceleration terms in the equations of motion. The critical components of a phenomenological creaming model are therefore the mass balance of particles (continuity equation) and some relationship for the rate of particle movement. This may be determined through a creaming speed, or through a force balance equation, if other forces are to be included. The creaming speed or drag force is related to the local concentration of particles. These components were present in the model of Zimmels (1988, 1992). Instead of solving the equations of motion, however, the changes in concentration were modelled by the cumulative displacement of thin layers of particles. The layers have a constant thickness and concentration. The overlap of layers for different sizes of particles results in the overall concentration profile in the system. Alternatively, Williams and Amarasinghe (1989, 1991) calculate the displacement of particles of each size fraction in order to determine the change in local concentration. In both of these models, the system is defined as a set of horizontal layers, within each of which the concentration is uniform. Techniques such as these, in which the effects of particle movement on local

concentration are calculated directly, are an alternative to solving the equations of motion.

The models of creaming which have been discussed in the preceding paragraphs are appropriate for a phenomenological description of the process. Such an approach enables direct comparison with the experimental results obtained from the ultrasound scanner, for example. However, some microscopic processes are difficult to simulate in a phenomenological manner. The influence of these processes can sometimes best be understood by a simulation at the level of the individual particles. The incorporation of greater complexity and detail into a simulation must inevitably be associated with a reduction in the size of system which can be analysed, due to the limitations of computational resources. Thus, a particulate model can not reproduce the concentration profiles obtained experimentally, but can only be used to indicate the anticipated effects of various processes on creaming profiles. This approach was applied in a later section of the present work to understand the effects of flocculation on creaming behaviour. A number of different approaches to particulate modelling are discussed in the following paragraphs.

The statistical mechanical characteristics of fluids have been studied for a number of years using the well established technique of molecular dynamics. The molecules in the fluid are treated as if they exist in a vacuum, with their motion determined by the intermolecular forces. The definitive reference work in this area is by Allen and Tildesley (1989). On colloidal length scales, where the particle sizes are of the order of 10^3 times larger than molecular dimensions, a molecular simulation is impractical. At this level, continuum descriptions can be applied to the component fluids. In particular, when the Reynolds number is small (as is the case for most emulsions at rest), the continuous phase fluid obeys the Navier-Stokes equations of motion. An important simulation technique which is designed for these conditions is Stokesian dynamics, or Brownian dynamics. Useful reviews of the technique are presented by Brady (1992) and Dickinson (1985). The intermolecular forces are replaced by effective forces between the dispersed particles, and hydrodynamic forces which are mediated by the continuous phase fluid. The effect of collisions by continuous phase fluid molecules on the dispersed particles is exhibited in an additional random (stochastic) motion of those particles. This is commonly called Brownian motion, and is simulated by applying a stochastic force to the particles.

The Brownian dynamics approach has been applied to the simulation of many processes at the colloidal level, particularly to obtain rheological and diffusional properties. References to many recent studies are given by Davis (1993). The formation of gels and aggregates is an important area of Brownian dynamics simulation, in which an interaction energy is applied between particles to cause them to stick together. For example, a recent study by Bijsterbosch et al. (1995) examined the effect of interparticle interactions on particle gel structure. A simulation of sedimentation was carried out by Ansell and Dickinson (1986), in which particles were added to the system one at a time to observe the growth of a sediment. A simulation of many-body sedimentation by this method would require considerably more resources. Brownian dynamics is therefore in principle applicable to creaming and flocculation in an emulsion, but the calculation of pairwise hydrodynamic interactions in a many-body system is very computationally demanding, and a simplified approach may be more appropriate.

An alternative technique for including hydrodynamic interactions in colloidal simulations is by the lattice-gas and lattice-Boltzmann models. The lattice-gas simulation applies a lattice to the continuous phase fluid. Each node of the lattice acts as a site which can be occupied (or not) by a fluid 'particle', with a given velocity. These fluid particles move between adjacent sites and collide with other particles according to predefined rules to conserve momentum and energy. The colloidal, dispersed phase particles are introduced by defining boundaries, at which the lattice-gas particles interact. The interaction may be through a non-slip condition, for example, resulting in forces on the colloidal particles. The considerable statistical fluctuations in the model require spatial averaging to obtain meaningful results. Although the standard method is time-consuming for dispersed systems, the more recent modification to the technique (lattice-Boltzmann) improves its efficiency considerably. In this method, the earlier single-'particle' occupation of lattice nodes is replaced by the real-valued average number of particles at the node with a given velocity. The collision rules are obtained from the corresponding lattice gas rules, but including the probability of such a collision occurring, based on the local populations. Thus, the lattice-Boltzmann method implicitly conducts the ensemble averaging process which is necessary with the lattice-gas approach. The application of the lattice-Boltzmann technique to colloidal dispersions is relatively recent (see for example, McNamara and Alder, 1993, Ladd, 1993, Yuan et al., 1993) but may be a suitable method of simulation for creaming and flocculation.

A simplified approach to the dynamics of particle motion is to neglect the hydrodynamic interactions altogether. In addition, the system can be discretised spatially, so that only a finite number of particle locations are permitted. Particle movement is therefore reduced to movement between the allowed sites. Such techniques are usually called lattice simulations since a lattice is applied to the system to define the permitted particle locations. This term should not be confused with the lattice-gas and lattice-Boltzmann techniques in which the lattice refers to the continuous phase molecular properties, not to the locations of the colloidal particles. Movement is specified through the diffusional (and creaming) properties of the particles. The benefit of such simulations is that relatively large systems can be investigated. Although many physical interactions are ignored in this description, the influence of bonding energy between particles on aggregate structure, for example, can successfully be modelled (Haw et al., 1995). Lattice models have been applied to the sedimentation problem (van der Knaap et al., 1994, Huang and Somasundaran, 1988), and are therefore appropriate for the study of flocculation and creaming required in the present work.

1.5 Ultrasound theory

The use of the ultrasound technique as a probe of emulsion behaviour was discussed briefly in a previous section. In particular, ultrasound has been used to determine the detailed creaming characteristics of emulsions, sometimes in the presence of flocculation or crystallisation. The technique has also been applied to studies of the kinetics of crystallisation and the detection of phase transitions in emulsions. A crucial element of the method is the determination of the dispersed phase volume fraction or the solid fat content from the measurement of ultrasound velocity. Measurements of attenuation have been found to suffer from difficulties caused by diffraction and other effects, whereas velocity measurements have been found to be more reliable.

In colloidal systems, such ultrasound methods often operate in the long wavelength region; that is, the wavelength of the sound wave is much larger than the particle size. In this case, Urick (1947) suggested that the Wood equation for the speed of sound in a homogeneous fluid, could be modified to apply to dispersed systems (see chapter 4). The density and compressibility are replaced by the volume averages of these quantities for the dispersion. Thus, the sound speed is related to the concentration of the dispersed

phase. Although this formulation has been adopted by many workers, significant deviations have been observed experimentally. Several other approaches have been applied to the problem of sound wave propagation in dispersed systems. These range from complex analytical treatments of the scattering problem to proposed empirical relationships between velocity and concentration with little physical basis. Since it is the long wavelength limit which is of interest here, some of these studies can be neglected, such as the ray-tracing formulations of Pal (1994) and Bonnet and Tavlarides (1987).

The two major approaches to the problem seem to be multiphase hydrodynamic methods, and scattering theories. The multiphase continuum theories are based on the equations of motion for fluid flow in the dispersion, such as the multiphase continuity and momentum equations. The properties of the dispersion are treated as local volume averages which therefore relates them to the local concentration of the dispersed phase. Additional properties are supplied through constitutive equations to include effects such as heat flow between the phases, stress relationships and the effects of viscous drag. One such approach is described in the review by Harker and Temple (1988), with reference to the work of Ahuja (1972, 1973). A more recent study on similar lines is that presented by Margulies and Schwarz (1994). This last study is formulated only for very dilute systems, due largely to the assumptions of dilute limits for the hydrodynamic expressions in the viscosity, for example.

The scattering theory formulation is based on the analysis of the modification of a sound wave by a single particle, and the cumulative effects of a dispersion of many such particles. A sound wave which is incident on a particle initiates scattered waves inside and outside that particle, which interfere with the incident wave and modify its phase and intensity. Studies of the scattering characteristics of single particles are numerous, and are discussed in chapter 4. The effect of many such particles in a dispersed medium is a more difficult problem. One method, adopted by Gaunaurd and Überall (1982, 1983) and Gaunaurd and Wertman (1989) is the effective medium approach. The scattering properties of a spherical volume of the effective medium are defined to be equivalent to the sum of the scattering characteristics of all the individual particles within that volume. Multiple scattering of sound waves is omitted. There is some discussion over the validity of the effective medium approach and its relationship to multiple scattering theories (Anson and Chivers, 1989, McClements et al., 1990b, Gaunaurd and Wertman, 1990).

The multiple scattering approach is based on the determination of the acoustic field which results from the scattering and rescattering of the incident wave by the dispersed particles. The result is usually expressed as an infinite series in the different scattering modes (representing the different angular dependencies of the scattering fields). However, the formalism is most appropriate for the long wavelength regime, in which the series can be truncated after only a few terms (corresponding to monopole and dipole scattering). The major analytical studies are by Waterman and Truell (1961), Fikioris and Waterman (1964), Lloyd and Berry (1967), Ma et al. (1984, 1990).

It is the multiple scattering theory solutions which are most widely used, and therefore the present work is based on this formulation of the ultrasound interpretation issue. Experimental evidence (McClements and Povey, 1989) suggests that, at least in some systems, multiple scattering theory accurately relates ultrasound velocity to concentration. However, other studies have found different relationships to be of greater accuracy in other experimental systems. It is apparent that confidence is not high that existing scattering theories can be directly applied to determine dispersed phase concentration from ultrasound velocity measurements. In addition, the calculations are rather complicated and not easy to implement for an experimental system. The approach taken in the present work, therefore, is to adopt the established theoretical basis of multiple scattering theory, but to develop techniques by which it can be accurately applied in experimental systems.

1.6 Objectives and preview

The study of creaming, flocculation and crystallisation in emulsions has been conducted through the two aspects of computer modelling and the investigation of techniques for the interpretation of ultrasound measurements. The development of a computer model of creaming in emulsions was intended to demonstrate the effects of the contributory physical processes on creaming behaviour. Having modelled the behaviour of an emulsion in the absence of particle interactions, the influence of flocculation and crystallisation on creaming was also to be investigated. In particular, the model was intended to reproduce the concentration profiles observed experimentally. Such a correlation would indicate that the model of the physical processes used in the computer simulation was a valid description of the experimentally observed creaming behaviour.

Initially, a phenomenological approach to the modelling of creaming was adopted, so that comparison could be made with experimental studies. The overview of simulation techniques presented in section 1.4 illustrated that a particulate description of emulsions on the scales used in experiments is not possible at the current level of computational resources. Hence a phenomenological description was used, and the model which has been developed in the current work is presented in chapter 2. Although this model produced a good representation of creaming behaviour in emulsions with no flocculation, it was unable to reproduce the concentration profiles observed in flocculating systems. Hence, a second model was developed on a microscopic scale to examine the creaming and flocculation behaviour at the level of individual particles. This model is presented in chapter 3.

Only with accurate and reliable techniques of interpretation can ultrasound be applied as a valuable non-destructive probe of emulsion behaviour. A number of theories currently exist, and it was intended to establish which of these was the most appropriate method for interpreting ultrasound measurements, and under what circumstances it should be used. In addition, the practical complications and difficulties associated with the experimental application of multiple scattering theory, for example, needed to be overcome. The theoretical principles of multiple scattering theory are considered to be the most appropriate basis for the work, and the main results of the theory are presented in chapter 4. In this chapter, the relationship between multiple scattering theory and other, simpler formulae (such as the Urick equation) is also established. The range of conditions under which the different theoretical results can be applied is illustrated both in the theoretical investigation (chapter 4), and through the results of the phenomenological creaming model (chapter 2). The model was used to predict the ultrasound velocity profiles anticipated by a number of ultrasound theories.

Following a study of the ultrasound theories currently available, an attempt has been made to develop methods which may be readily applied to a range of experimental systems. The techniques which have been developed are based on the theoretical principles of multiple scattering theory. However, it was intended to circumvent some of the difficulties of complexity and uncertainty associated with the established methods which are outlined in chapter 4. The alternative methods which have been developed for the interpretation of ultrasound measurements are presented in chapter 5.

Chapter 2 : Phenomenological Modelling of Creaming

In chapter 1, the study of creaming in emulsions was presented as a means of investigating emulsion stability and the effects of flocculation and other processes. The objective of the phenomenological computer modelling was initially to develop a model of creaming behaviour in an ideal oil in water emulsion (in the absence of particle interactions) which would reproduce the concentration profiles observed in practice. Such a model allows the contributions of the different physical processes to be investigated. The effects of crystallisation and flocculation on creaming behaviour were to be later included in the model. It was intended to establish whether simple models of flocculation and crystallisation could explain the deviations from ideal creaming behaviour which have been observed experimentally. In addition to the study of the creaming process, the computer model was designed also to assist in the investigation of appropriate theories of ultrasound propagation. The data produced by such a model are fully characterised (in terms of concentration and particle size variation), and representative of real emulsions. This allows the different methods of interpretation of ultrasound measurements in creaming emulsions to be compared.

Several widely differing approaches to the modelling of emulsions were discussed in chapter 1. For the comparison of the computer model results with experimental measurements, a phenomenological approach was required. A model of an emulsion on the scale used in creaming experiments can not trace the movement of individual particles, but must instead interpret the motion in terms of changes in concentration or other macroscopic quantities. Previous modelling in this area has been applied to the inverse problem of sedimentation, or to the related field of fluidisation (in which an upward flux of a carrier fluid is used to suspend heavier particles). The models of sedimentation due to Zimmels (1988, 1992) and Williams and Amarasinghe (1989, 1991) were considered to be the most appropriate starting points for the creaming model developed in this work. Each assigns a sedimentation velocity to particles, rather than solving the equations of motion for the whole system. Zimmels uses a set of horizontal "slabs" of particles of each size which move as a single unit. The local environment is defined using an additional fixed set of layers to calculate a total, local concentration.

Williams and Amarasinghe employ the technique of using horizontal layers to define a local concentration, but appear to track the movement of individual particles (or at least individual size fractions) in the system. The methods of horizontal layering, and of assigning particle velocities rather than solving the equations of motion, were employed in the model presented here. However, a somewhat different approach was employed to calculate the development of the concentration profiles.

2.1 Overview of model

The computer model is one-dimensional, the vertical direction determining the critical variation in concentration. The horizontal dimensions of emulsion samples in experiments are approximately 35 mm square, which is several orders of magnitude greater than the particle diameter (up to approximately 2 μm). Therefore, the size of the container might be assumed to be not a strong factor affecting the creaming rate of individual particles. Some effects of the cell wall may be felt especially by the particles near the walls, but these are likely to be small when compared with the concentration changes in the bulk of the sample. The horizontal dimensions of the sample are therefore assumed to be infinite in the model. The vertical dimension in the model is an adjustable parameter, but is usually taken to be 250 mm, as in the ultrasound scanner (see section 1.3). On the macroscopic level, the emulsion is completely defined locally by the concentration of oil (dispersed phase) and the particle size distribution. The presence of individual particles with their own identity can be overlooked. The definition of a sample in terms of the movement of identifiable particles is only practicable for a small scale model, otherwise the number of particles needed properly to model the system is unacceptably large.

As with any computer model, a certain amount of discretisation is necessary to enable numerical simulation. In the creaming model, the system is discretised spatially, temporally and into discrete particle size fractions. A schematic diagram of the model is shown in figure 2.1. The sample is split into horizontal layers, within which the concentration is uniform with height. The concentration profile in the sample is therefore described by a stepwise variation, which approaches a smooth profile as more, narrower, layers are used. For a polydisperse emulsion, there exists a continuous particle size distribution, which must also be split into discrete units. A certain concentration of

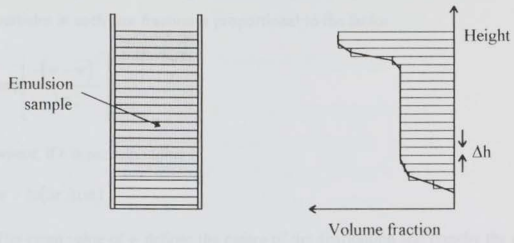

Figure 2.1 Schematic diagram of the representation of an oil in water emulsion in the phenomenological computer model.

dispersed phase is assigned to each one of a number of discrete size fractions (figure 2.2). As the number of size fractions is increased, each covering a smaller range of particle size, the discretised size distribution approaches the real, continuous distribution. The local concentration in each horizontal layer is the sum of the concentration over all particle size fractions.

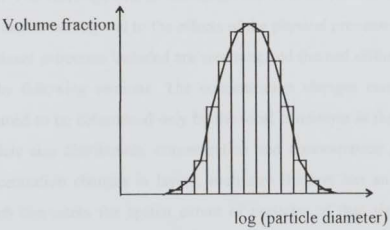

Figure 2.2 Discrete size fraction representation of a continuous particle size distribution in the computer model.

The particle size distribution used in the model was log-normal, which is typical of emulsions produced through a laboratory homogeniser. Thus, the concentration of particles in each size fraction is proportional to the factor

$$\exp\left[\frac{-\left(w-\overline{w}\right)^2}{2\sigma_w^2}\right] \qquad [2.1]$$

where, if r is particle radius

$$w = \ln(2r/\mu\mathrm{m}) \qquad [2.2]$$

The mean value of w defines the centre of the distribution and thereby the particle size at which the peak of the distribution occurs. The width of the distribution (the degree of polydispersity) is defined by the parameter σ_w. The distribution is divided into equal segments in w, in the range

$$-3\sigma_w \le \left(w-\overline{w}\right) \le 3\sigma_w \qquad [2.3]$$

with each segment representing a different size fraction.

The evolution of the sample is calculated using discrete time steps. As the length of the time step is reduced, the model of the sample approaches, in principle, the real situation of a continuous progression. In each time interval, the change in oil concentration in each layer is calculated, according to the equations of motion for the fluid. The rules applied to determine the volume flux of dispersed phase at the layer boundaries correspond to the effects of the physical processes included in the model. The dominant processes included are creaming and thermal diffusion, and these are discussed in the following sections. The concentration changes caused by these processes are assumed to be determined only by the local conditions in the adjacent layers, namely the particle size distribution, concentration and concentration gradient. In addition to the concentration changes in layers, each size fraction has an upper and lower boundary which represents the spatial extent of particles of that size. Initially these boundaries correspond to the top and bottom of the sample. However, during creaming, the particles which were initially at the bottom of the sample move upwards and their position at any time defines a lower boundary. In a monodisperse sample this is the serum interface, which is clearly defined if Brownian diffusion is negligible. During each time step, therefore, the position of the upper and lower boundaries for each size fraction must be

calculated. The following sections discuss the physical processes in the emulsions which determine the concentration changes in the layers and the movement of the boundaries.

2.2 Physical processes included in the model

The equations of motion for a single, continuous fluid are well known. They can be derived from the continuity equation (conservation of mass) and conservation of momentum (Newton's second law) and energy. When the fluid velocity is very low, as is the case in creaming, the inertial terms in the equations can be neglected (since they are second order in the flow speed). This is called the Stokes regime of flow, and corresponds to a very low Reynolds number. The equations of motion then take the famous Navier-Stokes form. In a multiphase system, the equations become more complicated, but the appropriate modifications can be found in works such as Shih et al. (1986), Roco (1992) and Gidaspow (1994). Additional constitutive equations are required, for example to obtain the drag force on each particle. The equations of motion are not reproduced here, since the phenomenological model does not directly solve these equations for the whole system. Some workers have applied finite difference or finite element methods to obtain a solution to the equations of motion in the sample. However, in the phenomenological model described here, the motion of the particles is defined in terms of the contributing physical processes (creaming and diffusion), for which the equations of motion have been solved separately. The effects of the multi-particle nature of the system are included implicitly in the numerical model through the combination of the creaming and diffusion properties of the individual particles, and through ensemble averaged hydrodynamic effects.

The dominant physical effects which occur in an emulsion, in the absence of direct particle interactions, are the gravitational force, thermal diffusion, viscous drag and hydrodynamic interactions. The net effect of the gravitational forces on a particle in an oil in water emulsion is to cause creaming, which is limited by the viscous drag exerted by the continuous phase fluid. The thermal energy of the particles causes them to execute random motion, again restricted by the viscous drag. This is the effect of diffusion, which acts to blur sharp concentration gradients. At finite concentrations, hydrodynamic interactions between particles, i.e. those that are mediated by the continuous phase fluid, may also be significant. The application of the equations of motion to these individual

processes results in expressions for particle movement which can then be applied in the phenomenological model. This approach avoids the need to solve the equations of motion directly for the entire multi-phase sample.

2.2.1 Gravity (creaming)

As Archimedes discovered, bodies immersed in a fluid experience an upward force (called the buoyancy force) due to the differential pressure acting over the surface of the body. This force slows the fall of particles which are more dense than the surrounding fluid, and causes particles which are less dense than the fluid to rise upwards or float. The magnitude of the buoyancy force is easily derived for an isolated cylindrical object (with its axis vertical) by considering the extra pressure acting upwards on the lower surface of the cylinder due to the additional weight of fluid at this lower depth. The result is equally valid for spheres and irregularly shaped objects. Archimedes principle states that the upward force due to the fluid is equal to the weight of fluid displaced by the object. The net force due to gravity on an object submerged in a fluid is therefore proportional to the density difference between the object and the surrounding fluid. For a sphere this takes the form

$$F_g = \frac{4}{3}\pi r^3 g \Delta\rho \qquad [2.4]$$

where r is the particle radius and $\Delta\rho$ is the density difference between the dispersed and continuous phases. In an oil in water emulsion, the dispersed phase (oil) is less dense than the continuous phase, and therefore the particles tend to rise to the top of the sample (to form a cream). The net gravitational force would tend to accelerate the particle, but in a viscous fluid its movement is restrained by the viscous drag exerted by the surrounding fluid. For a sphere, the Stokes drag is given by

$$F_d = 6\pi\eta r u \qquad [2.5]$$

where u is the particle's speed, and η is the viscosity of the surrounding fluid.

Since the particle movement in the creaming of emulsions is within the Stokes regime of flow, the inertial terms in the equations of motion can be neglected. For a single, isolated, spherical, solid particle in an infinite fluid medium, a particle will accelerate to a constant terminal velocity given by the balance of the gravitational force (equation 2.4), and the drag of the fluid on the particle (equation 2.5). Thus

$$F_g = F_d \qquad [2.6]$$

The resultant velocity is called the Stokes velocity and is given by the equation

$$u_0 = \frac{2r^2 g\Delta\rho}{9\eta} \qquad [2.7]$$

Equation 2.7 describes the speed at which a single oil droplet will rise to the top of the emulsion (in the absence of any other emulsion droplets). It can therefore be called the creaming velocity. The dependence of the creaming velocity on the parameters of particle size, density difference and viscosity is very important for the stabilisation of food emulsions, as discussed in chapter 1. The assumption of sphericity and rigidity (infinite viscosity) for the particle are reasonably valid for emulsion droplets coated with a protective layer of emulsifier or protein (Walstra and Oortwijn, 1975). Crystallised fat particles may not conform so well to this description, but a variety of modifications are available using shape factors to describe the non-sphericity.

In reality, equation 2.7 is only the infinite time asymptotic limit of the particle's speed, as the acceleration decreases to zero and the force balance is approached. However, in a typical oil in water emulsion, the drag on the particle is sufficiently large that the time taken for the particle to accelerate to within an accepted tolerance of its terminal velocity is negligible. Therefore, the particle can be considered to move with its terminal velocity at all times. In the model, the environment of the particle changes as it moves through the sample, and therefore its terminal velocity will also change. However, the time taken at each point for the particle to reach its terminal velocity is negligible compared with the time scale over which its environment changes significantly. Therefore, the model neglects particle acceleration and simply attributes a terminal creaming speed according to the local conditions.

Equation 2.7 is valid for an isolated particle in an infinite fluid medium. In a real emulsion with a finite concentration of dispersed phase particles, hydrodynamic interactions become significant and introduce concentration-dependent factors into the particles' speed. The modifications to the creaming speed include the effect of the backflow of the surrounding fluid, and the effective density and viscosity of the emulsion. Such hydrodynamic effects are discussed in section 2.2.3. Although the overall considerations of the effect of particle size, viscosity and density difference are still valid,

the hydrodynamic interactions can result in very different effective creaming speeds for the particles.

2.2.2 Thermal diffusion

Thermal diffusion is a term for the random process otherwise known as Brownian motion. The jittery motion of small specks of pollen on a pool of water was observed by Robert Brown in 1828 and was later attributed to the effect of random collisions of the water molecules by Goüy (see Dickinson, 1985). The random motion of the water molecules themselves is a result of their thermal energy. Similar random motion occurs on a colloidal scale in an emulsion due to the thermal energy of the oil droplets. If a particle is observed at various time intervals it can be seen to execute a convoluted and random motion, for example, the path shown in figure 2.3. Its true path is even more convoluted but this represents a sample of its position at regular intervals of time.

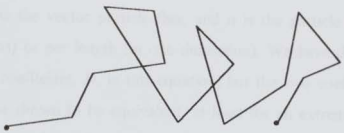

Figure 2.3 Thermal random walk.
A possible two-dimensional random walk path traced by recording a particle's position at a sequence of time steps

In one dimension, if the particle is equally likely to move in either direction, the average displacement from its original position must be zero. However, it has a non-zero root mean square displacement, which Einstein showed was given by

$$\left\langle (z - z_0)^2 \right\rangle^{1/2} = (2Dt)^{1/2} \qquad [2.8]$$

where z_0 is the initial position and D is a diffusion coefficient. In three dimensions the mean square displacement is simply three times as large, since there are three orthogonal co-ordinates. Thus, if the particle is initially at the origin,

$$\left\langle R^2 \right\rangle^{1/2} = (6Dt)^{1/2} \qquad [2.9]$$

For the purposes of the model, only one-dimensional diffusion need be considered. Although the particles do diffuse in all three directions, the system is assumed to be uniform in the two horizontal components, and the motion can be resolved into a single vertical direction. It is interesting to note the characteristic feature of random walk phenomena such as diffusion, that the distance travelled is proportional to the square root of the time taken. This is in contrast to the creaming behaviour in which the distance travelled is directly proportional to the time taken.

The description of thermal particle motion in terms of a random walk is not directly applicable in a phenomenological model. The effect of thermal diffusion in an emulsion must instead be defined in terms of the resultant changes in concentration. The usual phenomenological description is given by Fick's first law of diffusion

$$\boldsymbol{J} = -D\nabla n \qquad [2.10]$$

where $\boldsymbol{J}$ is the vector particle flux, and n is the particle density per volume (in three dimensions) or per length (in one dimension). We have defined another (macroscopic) diffusion coefficient, D, in this equation, but the two coefficients of equation 2.10 and 2.8 will be shown to be equivalent, at least for an extremely dilute system of identical particles. Equation 2.10 indicates that, in a phenomenological model, diffusion will only become significant in the presence of concentration gradients. In a uniform sample, the effects of diffusion are not visible on a macroscopic level. The process of creaming, however, creates concentration gradients, for example at the underside of the cream layer, or at the serum interface. Diffusion may, therefore, be significant in these regions. Equation 2.10 is the form of diffusion equation used in the model to calculate the volume flux moving between the horizontal layers.

Fick's second law of diffusion can be derived from equation 2.10 by considering the net flux in a small slice of sample (in one dimension), which is given by

$$\frac{\partial J_z}{\partial z} = -\frac{\partial n}{\partial t} \qquad [2.11]$$

from which Fick's second law is obtained

$$\frac{\partial n}{\partial t} = D\frac{\partial^2 n}{\partial z^2} \qquad [2.12]$$

The application of this equation to the case of a single particle provides the link to the random walk description. The initial probability distribution function of a single particle, whose position is known, can be described by a delta function. The "envelope" of the particle's likely location spreads with time, approaching asymptotically a uniform distribution in which the particle is equally likely to be at any position. Fick's second law (equation 2.12) can be solved for the particle probability distribution function with the boundary conditions appropriate for a single particle which are given by

$$n(z,t) = 0 \quad \begin{cases} z \neq z_0 \,, \; t = 0 \\ z \to \pm\infty \,, \; t \geq 0 \end{cases} \qquad [2.13]$$

and the normalisation condition

$$\int_{-\infty}^{\infty} n(z,t)\mathrm{d}z = 1 \qquad [2.14]$$

where z_0 is the particle's initial position. The result for the probability distribution of the particle's position at any time is a Gaussian function centred on the particle's initial position. Thus

$$n(z,t) = \frac{1}{\sqrt{4\pi D t}} \exp\left(\frac{-(z-z_0)^2}{4Dt}\right) \qquad [2.15]$$

where D is the diffusion coefficient. The root mean square displacement from the initial position can be calculated by integration, resulting in equation 2.8, which arose from the random walk description. This demonstrates the link between the phenomenological and random walk descriptions of diffusion, and also that the diffusion coefficients previously defined in each case are equivalent for a single isolated particle.

Although the phenomenological description of diffusion given by equation 2.10 is used in the model, it cannot be applied when the concentration gradient is not defined. This is the case at the upper and lower boundary of particles (which initially correspond to the top and bottom of the sample). These boundaries define the limit of particle concentration for each size fraction, and therefore represent a step-change in concentration. The concentration gradient at the step is not defined, and therefore equation 2.10 cannot be applied, although it is known physically that diffusion will blur the sharp change in concentration. The effect of diffusion on a step change in concentration can be found using the probability distribution of the position of a single

particle, equation 2.15. In mathematical terms, the overall particle number density distribution after a given time is the convolution of the individual particle probability distribution and the initial particle number density profile. On the microscopic level, the distribution is the superposition of the random walk trajectories of all the individual particles, whose starting positions are defined by the initial concentration profile. If the step change in concentration is at the origin, the initial particle number density profile is constant in the negative half-space and zero elsewhere.

$$n(z,0) = \begin{matrix} n_0 & \text{for } z \le 0 \\ 0 & \text{for } z > 0 \end{matrix} \qquad [2.16]$$

The convolution of the two functions, equations 2.15 and 2.16, gives the probability distribution of the number density of particles at time t. Thus

$$n(z,t) = \frac{n_0}{\sqrt{4\pi Dt}} \int_{-\infty}^{0} dz_0 \exp\left(\frac{-(z-z_0)^2}{4Dt}\right) \qquad [2.17]$$

By substituting the dummy variable

$$Z = \frac{(z-z_0)}{\sqrt{4Dt}} \qquad [2.18]$$

the distribution can be expressed in terms of the complementary error function, giving

$$n(z,t) = \frac{n_0}{\sqrt{\pi}} \int_{\frac{z}{\sqrt{4Dt}}}^{\infty} dZ \exp\left(-Z^2\right) = \frac{n_0}{2} \operatorname{erfc}\left(\frac{z}{\sqrt{4Dt}}\right) \qquad [2.19]$$

where

$$\operatorname{erfc}(z) = 1 - \operatorname{erf}(z) = \frac{2}{\sqrt{\pi}} \int_{z}^{\infty} dZ \exp\left(-Z^2\right) \qquad [2.20]$$

The evolution of a step change in concentration with time is illustrated in figure 2.4, using equation 2.19 to calculate the concentration profile. The initial sharp boundary becomes more diffuse with time, as the particle distribution spreads out. The boundary can be defined as the position at which the concentration is some specified proportion of the initial amplitude of the step, i.e.

$$n(z,t) = \alpha n_0 \qquad [2.21]$$

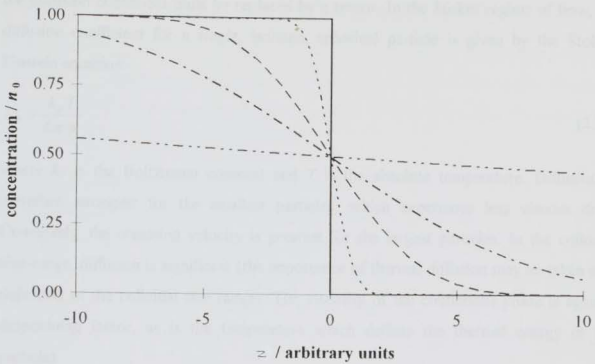

Figure 2.4 Effect of diffusion on a step-change in concentration.
The solid line is the initial concentration profile. The other lines represent the concentration profile after arbitrary time units of 1, 2, 3, and 10.

The distance moved by this boundary between the times t_1 and t_2 is given by

$$z_2 - z_1 = \sqrt{4D}\left(\sqrt{t_2} - \sqrt{t_1}\right)\mathrm{erfc}^{-1}(2\alpha) \qquad [2.22]$$

The upper and lower boundaries in the model can be related to this step change. The effect of diffusion is therefore embodied in an additional time-dependent displacement in each time step, given by equation 2.22, relative to the current boundary position. A boundary defined as being at half of the amplitude of the initial step does not move with time, but remains at the original position of the step change. For the model, the boundary was defined as the position at which the concentration is 25 % of the initial step amplitude. The displacement defined by equation 2.22 is superimposed on the displacement due to the creaming velocity for the lower and upper interfaces, to represent the spreading of the step interface

The magnitude of the effects of diffusion are embodied in the diffusion coefficient. The particle movement is a balance between the particle's thermal energy (which causes it to move about at random), and its mobility (which may be restricted by viscous drag, for example). The discussion is restricted to the isotropic case. In the more general case,

the diffusion coefficient must be replaced by a tensor. In the Stokes regime of flow, the diffusion coefficient for a single, isolated, spherical particle is given by the Stokes-Einstein equation:

$$D_0 = \frac{k_B T}{6\pi\eta r} \qquad [2.23]$$

where k_B is the Boltzmann constant and T is the absolute temperature. Diffusion is therefore strongest for the smallest particles, which experience less viscous drag. Conversely, the creaming velocity is greatest for the largest particles. In the colloidal size-range, diffusion is significant (the importance of thermal diffusion may be taken as a definition of the colloidal size range). The viscosity of the continuous phase is again a determining factor, as is the temperature which defines the thermal energy of the particles.

The Stokes-Einstein equation for the diffusion coefficient (equation 2.23) is valid only for a single, spherical particle in an infinite fluid medium. This corresponds to the conditions for the derivation of the Stokes creaming velocity (equation 2.7). At finite concentrations, the diffusion coefficient is modified due to the influence of the other particles. The thermal motion can then no longer be described by a single coefficient and is replaced by two different parameters. The *self*-diffusion coefficient quantifies the movement of a single labelled particle in a uniform environment. The *mutual*-diffusion coefficient defines the movement of particles in the presence of inhomogeneity such as concentration gradients (Dickinson, 1983). It is the second of these, the *mutual*-diffusion coefficient which is of relevance to the phenomenological model. In the following discussion the diffusion coefficient is assumed to be the mutual-diffusion coefficient throughout.

The modifications to the diffusion coefficient at finite concentration are due to both hydrodynamic and thermodynamic effects. Hydrodynamic interactions affect the particle mobility, M, which may be defined by the velocity, $\boldsymbol{U}$, attained by a particle due to the application of a steady force. Thus

$$\boldsymbol{U} = M\boldsymbol{F}^* \qquad [2.24]$$

where the velocity refers to axes in which the mean volume flux of continuous and dispersed phases is zero. For the creaming problem the velocity is therefore relative to

the container. The definition of the force, F^* (in Batchelor's notation) is such that the flux of dispersed phase is the same as if the particles are acted on by this force, and the continuous phase experiences no force (Batchelor, 1976). The hydrodynamic effects on particle mobility are discussed in the next section, since they are also relevant to the creaming speed.

The thermodynamic modification to the diffusion coefficient is introduced because of the greater volume available for the particle to occupy at lower concentrations. There is therefore a statistical influence which increases the probability of a particle moving down a concentration gradient. The statistical factor can be related to the concentration dependence of the osmotic pressure or chemical potential. Batchelor (1976, 1983) showed that the overall diffusion coefficient in a monodisperse system can be written as

$$D = M\frac{\phi}{1-\phi}\left(\frac{\partial \mu}{\partial \phi}\right)_{p,T} \qquad [2.25]$$

where μ is the chemical potential per particle and ϕ is the volume fraction. Alternatively, the coefficient can be expressed in terms of the osmotic pressure, Π thus

$$D = M\left(\frac{\partial \Pi}{\partial n}\right)_{p,T} \qquad [2.26]$$

At low concentrations, the thermodynamic factor in a monodisperse system is given by

$$\frac{\phi}{1-\phi}\left(\frac{\partial \mu}{\partial \phi}\right)_{p,T} = k_B T\left(1+8\phi+30\phi^2\right) \qquad [2.27]$$

(Batchelor, 1976). At higher concentrations, a more complete description is necessary, such as that provided by the Carnahan-Starling equation (Sami-Selim et al., 1993, and in approximate form in Glendinning and Russel, 1982), thus

$$\frac{\phi}{1-\phi}\left(\frac{\partial \mu}{\partial \phi}\right)_{p,T} = k_B T\frac{\left[(1+2\phi)^2+(\phi-4)\phi^3\right]}{(1-\phi)^4} \qquad [2.28]$$

The thermodynamic factor diverges as the concentration, ϕ, approaches unity. However, it can be seen from the next section that hydrodynamic effects dominate at high concentration and prevent particle movement. The diffusion coefficient therefore

decreases to zero in a concentrated emulsion. A useful review of the concentration dependence of the diffusion coefficient can be found in Sami-Selim et al. (1993).

2.2.3 Hydrodynamic interactions

The derivation of the Stokes creaming velocity, or the Stokes-Einstein diffusion coefficient assumed that there was a single isolated particle moving in an infinite fluid. The situation is modified when the volume fraction of particles is finite, due to hydrodynamic interactions. These are interactions between particles which are mediated by the continuous phase fluid. The movement of a particle causes a corresponding flow of the surrounding fluid, which, in turn, has an effect on any neighbouring particles. Thus the movement of any particle influences other particles through the reaction of the surrounding fluid. One of the contributions to the hydrodynamic interactions is the backflow of continuous phase fluid (which occurs to conserve volume). However, there are other contributions due to the velocity field created in the fluid by the particle motion. These are discussed in the dilute limit by Batchelor (1972).

A complete solution for the particle movement is theoretically possible for a given configuration of particles, provided the fluid flow field around a spherical particle is known. The complete equations of motion for the fluid could be solved numerically, but this is not practical for a large-scale model. Progress is required *via* analytical or empirical results. Experimentally, observations are made over time-scales which are very long compared with the time during which the system can explore the many different configurations of particle positions. Therefore, any measured properties are effectively an average over all particle configurations. The hydrodynamic interactions can thus be expressed as ensemble averages, assuming the particles to be randomly distributed. They can then be written as a function of the concentration, rather than the particle configuration.

The hydrodynamic effects are incorporated into the particle mobility, which was defined by Batchelor (1976) in terms of the velocity-force relationship, equation 2.24. This expression is valid for both diffusion and creaming, showing the connection between the hydrodynamic effects in each case. The force on each particle due to gravity (when the fluid is force-free) is given by equation 2.4. In Batchelor's definition, the density difference is (as written) between the particle and the continuous phase fluid, rather than

the suspension. Thus, in a monodisperse suspension, the creaming speed (relative to the container) is related to the mobility by

$$u = \frac{4}{3}\pi r^3 g \Delta\rho M \qquad [2.29]$$

The diffusion coefficient was related to the mobility through equation 2.25.

For a single, isolated, spherical particle, the mobility is given by

$$M = \frac{1}{6\pi\eta r} \qquad [2.30]$$

(from the Stokes drag law, equation 2.5). The mobility in a dispersion of finite concentration may be written as

$$M = \frac{h(\phi)(1-\phi)}{6\pi\eta r} \qquad [2.31]$$

where $h(\phi)$ is a hindrance factor. The reasons for the choice of this form will become apparent later. The creaming speed in a monodisperse suspension (equation 2.29) can therefore be expressed in terms of the Stokes velocity of the particles (equation 2.7) and the hydrodynamic factors (equation 2.31), thus

$$u = h(\phi)(1-\phi)u_0 \qquad [2.32]$$

Similarly, the diffusion coefficient in a monodisperse suspension can be written in terms of the Stokes-Einstein coefficient as

$$D = D_0 h(\phi)(1-\phi)\cdot\frac{1}{k_B T}\frac{\phi}{(1-\phi)}\left(\frac{\partial\mu}{\partial\phi}\right)_{p,T} \qquad [2.33]$$

(equations 2.31, 2.25 and 2.23).

Although Batchelor expresses all velocities relative to the zero-volume-flux axes (which is the laboratory frame of reference in the creaming problem), other workers have used a different reference frame. Much work in this area has been involved with fluidisation, in which a volume flux of fluid is used to maintain the buoyancy of heavy particles. The usual frame of reference in this case moves with the mean velocity of the continuous phase fluid. In other words, the frame of reference in which the mean flux of continuous phase is zero. The creaming speed of a particle in this frame of reference is

denoted by the subscript ϕ. When the suspension is at rest in a container (as is the case for creaming), the relationship between the frames of reference is given by

$$u = u_\phi + u_1 \qquad [2.34]$$

where all velocities are positive upwards. The continuous phase velocity, u_1, can be found by conserving the volume flux crossing any horizontal plane, thus for a monodisperse sample

$$u_1(1-\phi) + u\phi = 0 \qquad [2.35]$$

so that the relative velocity is given in this case by

$$u_\phi = \frac{u}{(1-\phi)} \qquad [2.36]$$

Thus

$$u_\phi = h(\phi)u_0 \qquad [2.37]$$

hence the reason for the choice of the form of the mobility in equation 2.31. Barnea and Mizrahi (1973) conclude that the results of previous workers, particularly Mertes and Rhodes (1955) have demonstrated that only the relative velocity can be used to compare results from the different experimental processes (sedimentation, fluidisation and others). Barnea and Mizrahi discuss the relationship between the relative and absolute velocities in each of the different methods. The determination of the hydrodynamic effects has therefore focused on the hindrance factor $h(\phi)$, mainly through the concentration dependence of the creaming or sedimentation velocity. A very useful review is presented by Williams and Amarasinghe (1989) of the results in the literature, and only the main results are drawn out here.

Analytical results for the hindrance factor are only accessible in the dilute limit, mostly also for monodisperse systems. The earliest attempts assumed either a regular arrangement of particles, or that the fluid flow around each particle was confined within a cell (usually spherical) where some boundary condition is applied. The first of these was by Smoluchowski (1913), who obtained the result

$$u = \frac{u_0}{\left(1 - 2.32\frac{r}{s}\right)} \qquad [2.38]$$

where s is the interparticle spacing. Each of these approaches predicts that the sedimentation velocity varies in the form

$$u = u_0\left(1 - a_\phi \phi^{1/3}\right) \qquad [2.39]$$

in the dilute limit. A review of these techniques and the results obtained can be found in Happel and Brenner (1965) and in Barnea and Mizrahi (1973).

Later, the ensemble average of a random arrangement of particles was attempted, first by Burgers (1941, 1942), and later by Batchelor (1972) and Reed and Anderson (1976, 1980). These methods based on a random particle arrangement predicted that the modification to the creaming velocity should be first order in concentration. The definitive work is considered to be that of Batchelor, who obtained the result

$$u = u_0\left(1 - 6.55\phi\right) \qquad [2.40]$$

or as a hindrance factor

$$h(\phi) = \left(1 - 5.55\phi\right) \qquad [2.41]$$

Batchelor (1972) also discusses the difference between the ensemble average approach and previous techniques with results of the form 2.39. He attributes the difference to the use in the earlier models of a characteristic length scale, usually the inter-particle spacing, which is inversely proportional to the one-third power of concentration. In a random system, no one particle separation has any special significance. It is interesting to note that Smoluchowski (who obtained the result 2.38) commented that if the particles were arranged at random, the leading order term in the third power of concentration would vanish. It is now generally accepted that the dilute limit should take the form of equation 2.40, although the coefficient of the concentration term varies somewhat.

The analytical method becomes extremely difficult beyond the dilute limit, and empirical and semi-empirical approaches have been used by later workers to obtain the hydrodynamic interactions at higher concentrations. Richardson and Zaki (1954) suggested the use of a hindrance factor of the form

$$h(\phi) = \left(1 - \frac{\phi}{\phi_{pack}}\right)^q \qquad [2.42]$$

which has the correct dependence in the dilute limit. The parameter ϕ_{pack} is a maximum packing fraction, but is usually taken to be unity. A variety of results for the coefficients exist, from theoretical, semi-empirical and empirical investigations. Many of these are included in the review by Williams and Amarasinghe (1989). The general consensus is that if $\phi_{pack}=1$, the coefficient q is around 4. The most widely used value is that given by Garside and Al-Dibouni (1977), $q=4.1$ (in the low Reynolds number limit), although they produced a more complicated formula valid for a wide range of Reynolds number. An alternative empirical correlation due to Dallavalle for a wide range of Reynolds number has also been used in some sedimentation models (Williams and Amarasinghe, 1989).

The other, very widely used correlation for the hindrance factor in a monodisperse suspension was determined by Barnea and Mizrahi (1973). They compiled a semi-empirical relationship for the creaming velocity, which was fitted to many sets of experimental data over a range of concentration and Reynolds number. The form of the relative velocity dependence was established by considering the component effects due to modifications to the suspension density, viscosity and drag force. These contributions can be seen in the force balance equation used to derive the Stokes velocity (equations 2.4, 2.5 and 2.6). A consideration of the Stokes drag force also indicates the possible source of the requirement to use the relative velocity in comparisons between experiments. The Stokes drag is derived by considering the pressure acting on the surface of a particle which is stationary in a uniform flow of fluid. The velocity in the drag force is therefore the relative velocity between the particle and the surrounding fluid at a large distance from the particle (where the flow is uniform if there is only one particle). Hence it appears sensible to use the relative velocity when defining the concentration dependence of the drag force.

The density difference in the gravitational force is modified by using the suspension density in the buoyancy component, rather than the density of the continuous phase. This introduces a factor of

$$(1-\phi) \qquad [2.43]$$

The viscosity of the suspension was written in an exponential form, consistent with earlier theoretical work (Barnea and Mizrahi include a review of previous work on viscosity of suspensions). The coefficients in the viscosity expression are determined empirically. Finally, they adopt a form for the additional hydrodynamic effects in the drag

force which varies with the one-third power of concentration. Unfortunately, their work was slightly too early to incorporate the result of Batchelor for the dilute limit, which is the preferred form of the hydrodynamic dependence. However, their expression for the relative velocity was fitted to a wide range of experimental results, and the empirical fit was given by a hindrance factor

$$h(\phi) = \frac{(1-\phi)}{\left(1+\phi^{1/3}\right)\exp\left\{\frac{5\phi}{3(1-\phi)}\right\}} \qquad [2.44]$$

Equation 2.44 is the form used for the hydrodynamic interactions in the creaming model. The creaming velocity and diffusion coefficient are related to it in a monodisperse system through equations 2.32 and 2.33.

Figure 2.5 shows the concentration dependence of the creaming velocity and diffusion coefficient in a monodisperse system as a proportion of their dilute limiting values (the Stokes velocity, equation 2.7, and the Stokes-Einstein coefficient, equation 2.23). The hydrodynamic concentration dependence was taken to be that given in equation 2.44, which is used in the model. The creaming speed decreases monotonically

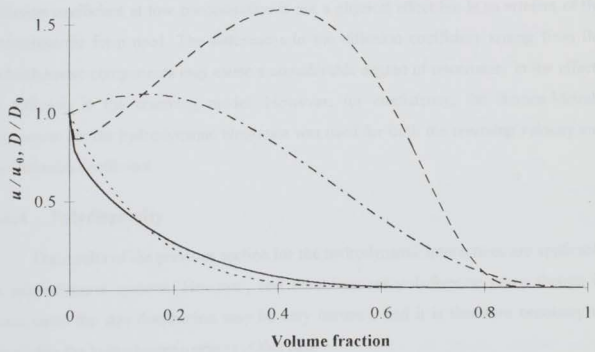

Figure 2.5 Concentration dependence of creaming speed and diffusion coefficient for a monodisperse sample.

The solid line is the creaming speed and the dashed line the diffusion coefficient used in the model. For comparison, the dotted line is the creaming speed and the dash/dot line the diffusion coefficient using a modified hindrance factor.

to zero as the concentration increases, which is due entirely to the hydrodynamic hindrance. The diffusion coefficient, however, initially falls, but then increases with increasing concentration, when the volume fraction is less than approximately 0.4, because of the statistical thermodynamic effects. It then decreases rather steeply to zero at high concentrations as the hydrodynamic hindrance becomes predominant.

For comparison, figure 2.5 also shows the creaming speed and diffusion coefficient which would be obtained using the Richardson-Zaki form for the hydrodynamic hindrance factor (equation 2.42) with $\phi_{pack}=1$ and the Batchelor coefficient of $q=5.55$. The form of the creaming speed remains unchanged, although the Barnea-Mizrahi version is somewhat steeper at low concentrations due to its limiting dependence in the one-third power of concentration. However, the diffusion coefficient is very different. The peak value and the volume fraction at which the peak occurs are considerably altered by this change in the hydrodynamic term. The fall in the diffusion coefficient at the lowest concentrations is only seen with the Barnea-Mizrahi form for the hydrodynamic hindrance. This feature is due to the one-third power concentration dependence of the hydrodynamic term at low concentrations. It has already been seen that this is steeper than the correct, linear form for the dilute limit. Hence, the drop in the diffusion coefficient at low concentration is not a physical effect but is an artefact of the hydrodynamic form used. The differences in the diffusion coefficient arising from the hydrodynamic components may cause a considerable degree of uncertainty in the effects of diffusion in the creaming model. However, for consistency, the Barnea-Mizrahi expression for the hydrodynamic hindrance was used for both the creaming velocity and the diffusion coefficient.

2.2.4 Polydispersity

The results of the previous section for the hydrodynamic interactions are applicable to monodisperse systems. However, real emulsions are polydisperse (even though in some cases the size distribution may be very narrow), and it is therefore necessary to determine the hydrodynamic effects in this case.

Batchelor (1983) showed how the mobility formulation (equations 2.24, 2.25 and 2.29) can be extended to a polydisperse system. The hydrodynamic interactions now include pair-wise interactions between each combination of particle sizes. The hydrodynamic interactions in the dilute limit for a polydisperse system were examined by

Batchelor (1982) in terms of the sedimentation velocity, and numerical results were given (Batchelor and Wen, 1982) for some limiting cases of the nature of the polydispersity and flow. However, the case of a pauci-disperse system (in which there exists a range of particle sizes around a mean value), which is the usual case in emulsions, does not appear to be addressed directly, and the range of the Péclet number for the creaming emulsions does not appear to fall into the special cases. When the density of all particles is the same, the coefficients for a small range of particle size are very similar, and therefore the hydrodynamic factor approaches the monodisperse case, using the total volume fraction.

It is difficult to see how the dilute limit results might be extended to more concentrated systems. Davis and Grecol (1994) suggested a modification of the form of the Richardson-Zaki expression for the monodisperse case (equation 2.42), using the coefficients calculated by Batchelor and Wen (1982) for the dilute limit. However, the numerical values for the coefficients are not certain, as discussed in the preceding paragraph. Several workers have postulated modifications to the monodisperse hindrance factors appropriate for polydisperse systems. Mirza and Richardson (1979) included an extra correction factor

$$(1-\phi)^{0.4} \qquad [2.45]$$

in the Richardson-Zaki equation for their bidisperse settling experiments. Others suggested the inclusion in the suspension density only of those particles smaller than the particle whose velocity is being calculated (Selim et al., 1983). However, the modifications adopted have mainly been empirical, with little assessment of the applicability to a general polydisperse suspension.

The formulation for polydispersity used in the present model has been adopted previously by several workers in sedimentation modelling (Stamatakis and Chi Tien, 1992, Zimmels, 1983,1988, Williams and Amarasinghe, 1989, 1991). The hydrodynamic effects are considered to be due to the overall flow of particles and are thus related to the total concentration, rather than to the detailed particle size distribution. The hydrodynamic factors derived for monodisperse systems can then be applied to the relative velocity in the polydisperse case, using the total dispersed phase concentration. Equation 2.37 is valid for each individual component, giving

$$u_{\phi i} = h(\phi) u_{0i} \qquad [2.46]$$

for the relative velocity of a particle of size fraction i. The conservation of volume flux in the laboratory frame can be used to calculate the continuous phase velocity, and thereby the particle velocity relative to the container. Thus

$$\sum_i u_i \phi_i = -u_1 \left(1 - \sum_i \phi_i\right) \qquad [2.47]$$

Substitution of the solution for the fluid velocity into a polydisperse version of equation 2.34 leads to

$$u_i = u_{\phi i} - \frac{\sum_j u_j \phi_j}{\left(1 - \sum_j \phi_j\right)} \qquad [2.48]$$

Multiplication by the concentration of species i followed by summation over all particle species leads to

$$\frac{\sum_j u_j \phi_j}{\left(1 - \sum_j \phi_j\right)} = \sum_j u_{\phi i} \phi_j \qquad [2.49]$$

whence the absolute particle velocity of species i can be obtained:

$$u_i = u_{\phi i} - \sum_j u_{\phi j} \phi_j \qquad [2.50]$$

This is the form used in the model for the polydisperse emulsions. The hindrance factor used in the relative velocity (equation 2.46) was the Barnea-Mizrahi formulation, 2.44.

A form for the diffusion coefficient in a concentrated polydisperse suspension has not become available. Batchelor (1983) gave general results for the diffusion and cross-diffusion coefficients but these include complicated expressions in the chemical potential, dependent on the interactions between particles. The monodisperse form of the diffusion coefficient and the diffusive flux was therefore used in the model, using the total volume fraction. The diffusive flux for each size of particle is given by equation 2.10, using the concentration gradient of particles of that size. Thus

$$\boldsymbol{J}_i = -D_i \nabla n_i \qquad [2.51]$$

The diffusion coefficient is given by equation 2.33, with the Stokes-Einstein coefficient for the correct particle size, and using equation 2.44 for the hydrodynamic hindrance factor (using the total volume fraction). The thermodynamic factor is calculated from equation 2.28, also using the total volume fraction. Although this is not an exact result

for diffusion, it is the creaming velocity which should be dominant in the model, and therefore the precise concentration dependence of the diffusion coefficient is of secondary importance.

2.3 Time evolution

The sample is initially uniform in terms of concentration and particle size distribution. The evolution of the concentration profile is modelled by calculating the concentration changes in the horizontal layers and the movement of the upper and lower limits of each size fraction in a series of small time steps. The processes affecting these contributions have been discussed in the previous sections, and now the application of these results in the model is detailed.

2.3.1 Calculation of change in concentration at layer boundaries

The volumetric flux of dispersed phase particles crossing the boundary between adjacent layers is calculated in each time interval. There are two contributions, due to creaming and diffusion. The flux in both cases is determined entirely from the local environment (that is the concentration and particle size distribution in the two layers). The total volume fraction at the interface is taken to be the average of the volume fraction in the two layers. The hydrodynamic hindrance factor is calculated from this average total concentration using the Barnea-Mizrahi relation, equation 2.44. The creaming velocity of particles of each size fraction is determined by equations 2.46, and 2.50. The diffusion coefficient is calculated using equations 2.33, and 2.28, again using the total average concentration.

The volumetric flux of particles of size fraction i due to creaming, is proportional to their velocity and the local concentration of particles of that size, thus

$$\Delta\phi_{i,\mathrm{crm}} = \phi_i u_i \frac{\Delta t}{\Delta h} \qquad [2.52]$$

For diffusion, the flux is proportional to the concentration gradient, equation 2.51,

$$\Delta\phi_{i,\mathrm{diff}} = -D_i \frac{\left(\phi_{i,h+} - \phi_{i,h-}\right)}{\Delta h} \frac{\Delta t}{\Delta h} \qquad [2.53]$$

where the difference in concentration is for particles of the same size fraction between the two layers. Both of these fluxes have been defined as positive in the upward direction.

2.3.2 Boundary velocities for each size fraction

The lower and upper limits of particles of each size fraction are defined as boundaries, which move with a velocity determined by the local conditions. In the absence of diffusion, the boundaries move with the local creaming velocity of particles of the same size. Diffusion causes the change in concentration at these limits to become less well defined as time progresses. This effect is modelled using an additional boundary velocity, which was derived from the evolution, due to diffusion, of a step-change in concentration. The extra displacement of the boundary was defined in equation 2.22. In the model, the boundary was defined as the position where the concentration is 25 % of the initial concentration, which gives an extra time-dependent velocity of

$$u_{i,\mathrm{diff}} = \frac{0.95}{\Delta t}\sqrt{D_i}\left(\sqrt{t} - \sqrt{t-\Delta t}\right) \qquad [2.54]$$

2.4 Choice of discrete units

2.4.1 Layer thickness

The layer thickness, Δh, must be small enough to represent accurately any regions of rapidly varying concentration, and to avoid a significantly stepped effect in the concentration profile. Creaming experiments using the ultrasound scanner (figure 1.1) have a resolution of 1 mm and the creaming model ought to have at least as fine divisions. The layer thickness is reduced in size (for the same overall sample height) until there is no significant difference in the concentration profiles and ultrasound velocity profiles obtained. For polydisperse samples, a layer thickness of 0.5 mm was found to be sufficient, but for monodisperse samples, in which the concentration gradients can be much larger, better accuracy was obtained using a layer thickness of 0.25 mm. This may also be true for a polydisperse sample when there is no diffusion, and the concentration gradients again become steeper.

2.4.2 Time interval

The time interval, Δt, used in the model is not fixed in an absolute manner. In order for the model to produce accurate results, the volumetric flux crossing a layer boundary during any time step must not be a large proportion of the volume of particles in the layer. Otherwise the conditions in the layer at the beginning of the time step, which were used to calculate the flux, are not truly representative of the conditions during the whole time interval. One way of ensuring sufficiently small changes in each time step is to define the time interval in terms of the largest distance which could be travelled by a particle in a single time step, as a proportion of the layer thickness. The fastest particle speed is the Stokes velocity for the largest particles in the sample. The actual particle speed will be significantly lower than the Stokes velocity due to hydrodynamic hindrance, but the Stokes velocity can be used to set an upper limit. The time step is therefore defined by

$$\Delta t = \alpha \frac{\Delta h}{u_{max}} \qquad [2.55]$$

Thus in one time step, no particle can travel further than a proportion α of the layer thickness. It was found that a value of $\alpha = 0.5$ was sufficient to obtain consistent concentration profiles. A maximum time interval of 10 minutes was specified.

2.4.3 Size range in each size fraction

The continuous particle size distribution is split into discrete size fractions as shown in figure 2.2. It was chosen to restrict the distribution to three standard deviations either side of the mean, as given in equation 2.3. The number of size fractions therefore defines the range of particle size assigned to a single size fraction. This is especially significant at the larger particle size limits, where the same interval (on the logarithmic scale) represents a wider range of particle sizes. Also, since the creaming velocity is proportional to the square of particle size, the difference in speed between the smallest and largest particles in the size fraction is greatest for the largest particle sizes. The concentration profiles are step-like, with each step corresponding to the lower boundary of the particles of a given size fraction. As the number of size fractions is increased, the volume fraction of particles assigned to the size fraction is reduced, and the steps in the total concentration profile decrease in size, until the profile is smooth. Also, the

difference in position of the lower boundary between consecutive size fractions decreases as the number of size fractions is increased. The number of size fractions used in the model was 101, which was found to be sufficient to obtain acceptably smooth concentration profiles.

2.5 Computer requirements

The computer code was written in FORTRAN 77. The development was carried out on the Sun SPARCenter 2000 system, and jobs were run on the Silicon Graphics Challenge XL server at the University of Leeds. A flow diagram of the calculation is shown in figure 2.6, and the program is given in Appendix A1. The polydisperse sunflower oil in water samples take approximately 2 days of CPU time to complete. The monodisperse samples are much faster.

2.6 Ultrasound velocity and attenuation calculations

One of the objectives of developing the computer model was to provide data which would be representative of real creaming emulsions, in order to compare different theories for interpreting ultrasound velocity measurements. The data from the model are completely characterised in terms of the concentration and particle size distribution, whereas any experimental system includes unknown variables, particularly height-dependent changes in particle size distribution. To this end, the calculation of ultrasound velocity, using multiple scattering theory and the Urick equation, was incorporated into the creaming model. The different theories of ultrasound propagation are discussed in chapter 4, along with a description of the computer program used to calculate the ultrasound velocity and attenuation. The programs have been organised so that the ultrasound velocity profiles in the creaming model can be obtained using the separate ultrasound calculation subroutines. The ultrasound program need only be invoked when the model results are output, to obtain the ultrasound velocity and attenuation for the particle size distribution in each layer.

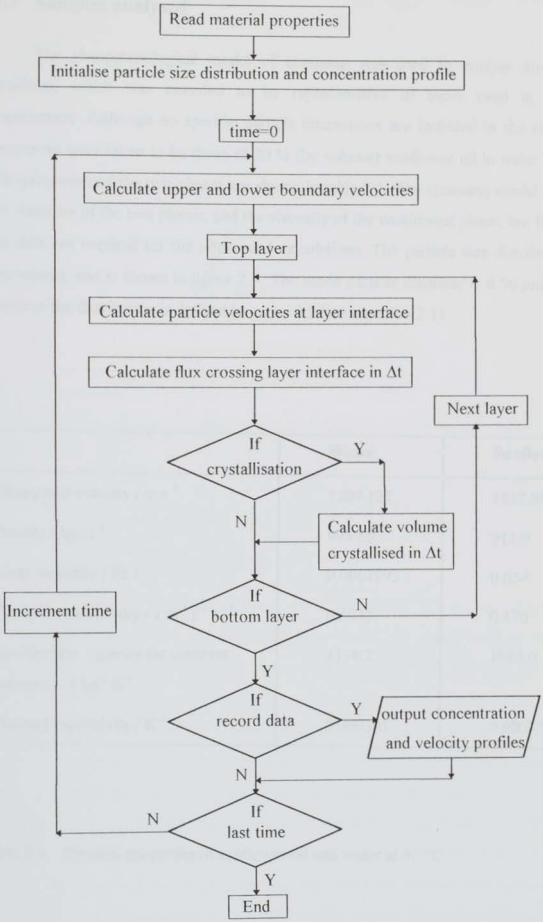

Figure 2.6 Flow diagram of the calculation for the phenomenological creaming model.

2.7 Samples analysed

The phenomenological model of creaming was used to analyse an idealised emulsion, which was intended to be representative of those used in creaming experiments. Although no specific particle interactions are included in the model, the properties were taken to be those of 20 % (by volume) sunflower oil in water at 30 °C. The properties of the two phases are shown in table 2.1. The creaming model uses only the densities of the two phases, and the viscosity of the continuous phase, but the rest of the data are required for the ultrasound calculations. The particle size distribution was log-normal, and is shown in figure 2.7. The mode particle diameter is 0.56 μm, and the width of the distribution is defined by $\sigma_w = 0.5$ (see equation 2.1).

	Water	**Sunflower oil**
Ultrasound velocity / m s^{-1}	1509.127	1437.86
Density / kg m^{-3}	995.65	912.9
Shear viscosity / Pa s	0.0007973	0.054
Thermal conductivity / J m^{-1} s^{-1} K^{-1}	0.6032	0.170
Specific heat capacity (at constant pressure) / J kg^{-1} K^{-1}	4178.2	1980.0
Thermal expansivity / K^{-1}	0.000301	0.0007266

Table 2.1 Physical properties of sunflower oil and water at 30 °C.

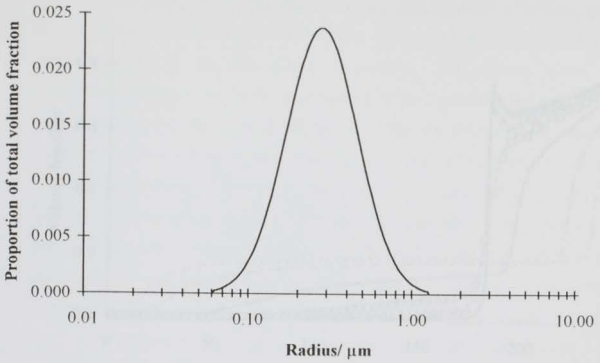

Figure 2.7 Initial particle size distribution for the sunflower oil in water emulsion used in creaming model.

2.8 Results

2.8.1 Total oil concentration profiles

Figure 2.8 shows the predicted total concentration of oil as a function of height in the polydisperse sunflower oil in water emulsion at various time intervals during creaming. The corresponding profiles for a monodisperse sample (with particle diameter 0.56 μm) are shown in figure 2.9. The bottom of the sample corresponds to zero height. The concentration profiles of the monodisperse sample can be divided into three sections: the cream (a high concentration region at the top of the sample), uniform emulsion, and serum (an oil-deficient region at the bottom of the sample). The serum layer interface is sharply defined, and moves up the system at a rate which is uniform until it meets the cream. The underside of the cream is also well defined, and moves downwards until it meets the serum interface. The emulsion between the serum and cream interfaces remains uniform at the initial concentration. Thus creaming can be thought of as an "end effect" in which parts of the emulsion which are far enough from either end are unchanged in a monodisperse sample.

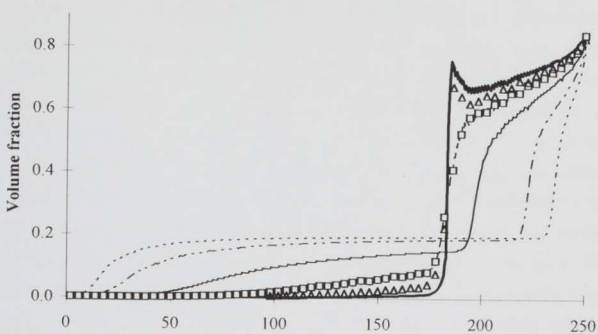

Figure 2.8 Predicted total volume fraction of oil as a function of height and time for a polydisperse sunflower oil in water emulsion.

The profiles correspond to · · · 50 days, - · - · 100 days, — 250 days, □ 500 days, △ 700 days, — 1000 days.

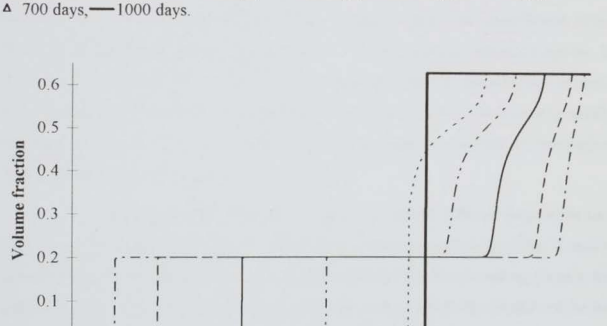

Figure 2.9 Predicted volume fraction of oil as a function of height and time for a monodisperse sunflower oil in water emulsion.

The profiles correspond to — · — 50 days, – – 100 days , — 200 days, - · - · 300 days, · · · 400 days, — 700 days.

In the polydisperse sample (figure 2.8) the concentration varies more gradually with height in the lower regions. It would be difficult in this case to define a serum interface, except in the early stages of creaming. The step-like nature of the concentration profile is due to the contributions of the component size fractions. Since larger particles cream more quickly, the lower interface for these particles (equivalent to the serum interface in a monodisperse sample) has reached a higher level at a given time than for smaller particles. The total concentration therefore increases with height because more of the particle size fractions are present at higher levels. The difference in the height of the lower interfaces of particles of different sizes increases with time, so that the increase in concentration with height becomes more gradual at later times. The concentration in the bulk of the sample falls with time at a given position, as the lower interface of more and more size fractions passes that point. This contrasts with the monodisperse case in which the emulsion remains unchanged between the serum and cream interfaces.

The cream interface is sharp in both the monodisperse and polydisperse samples. The interface moves downwards at a very similar rate in the two systems, although the polydisperse sample is marginally faster. This is probably due to the contribution of the more rapid creaming of larger particles which are present in the polydisperse system. In both cases, the concentration increases rapidly with height up to a concentration of about 50 %, but above this level, the concentration in the cream increases much more gradually with height. This is due to the strong hydrodynamic hindrance at high concentration, which slows the particle creaming rate considerably.

The concentration profile within the cream takes a rather different form in the two cases. In the monodisperse system, the model restricts the concentration so that it cannot be higher than 63 %, which is the approximate maximum (random) packing fraction for identical spheres. In a polydisperse system, however, the concentration is allowed (in the model) to take any value up to 100 %, and is only determined by the hydrodynamic factor in the creaming velocity. The hydrodynamic hindrance factor tends to zero as the volume fraction approaches unity, and this factor is applied in the model to both the monodisperse and polydisperse systems. The concentration profile for the polydisperse sample (figure 2.8) shows that the concentration only reaches a value of approximately

85 %, and does not rapidly approach an unrealistic volume fraction of unity. The creaming rate at concentrations higher than this must be negligible.

It is clear that, physically, the maximum packing fraction is determined by the degree of polydispersity, since smaller particles can occupy the interstices of larger particles. The hydrodynamic effects (which determine particle mobility and should incorporate obstruction) are therefore dependent, at high concentrations, both on the total concentration and the particle size distribution. However, the hydrodynamic description used in the model assumes that the hydrodynamic interactions can be entirely accounted for by the total volume fraction, neglecting the particle size distribution. The particle mobility in this case tends to zero only as the volume fraction approaches 1.0. If the sample is monodisperse, the particle mobility should decrease to zero around the maximum packing fraction of 0.63. The creaming velocity in a monodisperse system is therefore non-zero, in the model, at the maximum packing fraction (which is imposed on the system in the monodisperse case), and this may affect the concentration profile in the cream to some degree. Conversely, the maximum concentration attained in a polydisperse sample may be higher than the real value if the degree of polydispersity is low. These discrepancies are due to the assumption of the form of the hydrodynamic interactions, and the lack of a generally applicable description of particle mobility in a polydisperse system.

The effect of diffusion on the concentration profiles is shown in figure 2.10 for the polydisperse sample and figure 2.11 for the monodisperse sample. In both cases, the neglect of diffusion causes the concentration gradients to become sharper, as might be expected. The influence of diffusion in the polydisperse sample is not as significant as in the monodisperse system because the creaming profile (in the polydisperse case) is more predominantly determined by the larger particles, for which diffusion is weaker. It will be seen in the following sections that diffusion has a greater effect on the concentration profiles of the individual size fractions, and thereby the particle size distribution in the polydisperse system.

It is perhaps surprising that the effect of diffusion is more noticeable at the cream interface, rather than at the serum interface. The spreading of the serum interface due to diffusion is counteracted by the concentration dependence of the creaming velocity. As the interface spreads, the lower particles are in a less concentrated region and therefore

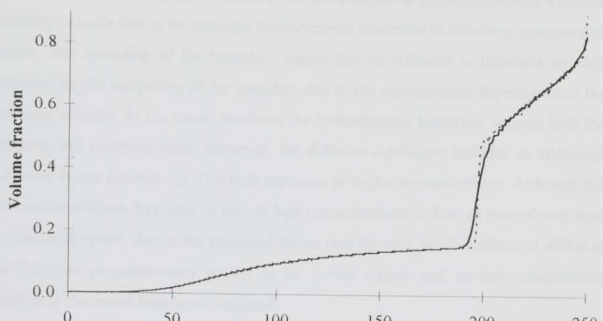

Figure 2.10 Effect of diffusion on the total concentration profiles after 250 days in a polydisperse sunflower oil in water emulsion.

The solid line includes diffusion. The dotted line is when diffusion is neglected.

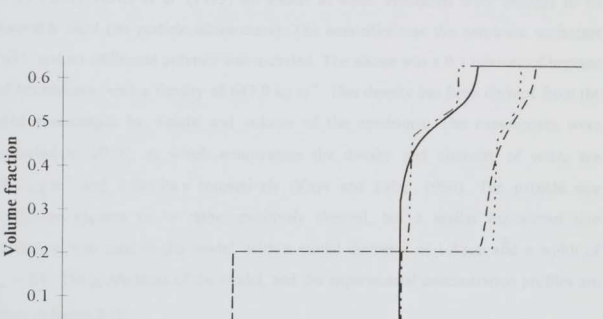

Figure 2.11 Effect of diffusion on concentration profiles in a monodisperse sunflower oil in water emulsion.

The dashed and solid lines are the concentration profiles with diffusion included after 200 and 400 days respectively. In the absence of diffusion the profiles are the dotted and dashed/dotted lines respectively.

cream (upwards) more quickly. Particles which are higher up the interface have a smaller creaming velocity due to the stronger hydrodynamic hindrance in this more concentrated region. The spreading of the boundary region due to diffusion is therefore strongly restricted by the sharpening of the boundary due to the concentration dependence of the creaming velocity. At the cream interface, the hydrodynamic hindrance reduces both the diffusion and creaming rates. However, the diffusion coefficient includes an additional statistical factor (section 2.2.2) which increases at higher concentrations. Although the diffusion coefficient decreases to zero at high concentrations, it does so more slowly than the creaming speed, due to the statistical factor (see figure 2.5). The effects of diffusion are therefore proportionately greater in the cream region, and so the concentration gradient at the cream interface is reduced.

The total concentration profiles predicted by the model can be compared with experimental results. Many of the experimental systems studied do not fit into the idealised assumptions of the model, since they include particle interactions (electrostatic interactions, for example) or there is some degree of flocculation. Experiments carried out by Fillery-Travis et al. (1993) on alkane in water emulsions were thought to be reasonably ideal (no particle interactions). The emulsifier was the non-ionic surfactant Brij35 and no additional polymer was included. The alkane was a 9:1 mixture of heptane and hexadecane, with a density of 643.0 kg m^{-3}. This density has been derived from the stated percentages by weight and volume of the emulsions. The experiments were conducted at 20 °C, at which temperature the density and viscosity of water are 998.2 kg m^{-3} and 0.001 Pa s respectively (Kaye and Laby, 1986). The particle size distribution appears to be rather positively skewed, but a similar log-normal size distribution was used in the model, with a modal diameter of 1.4 μm and a width of $\sigma_w = 0.5$. The predictions of the model, and the experimental concentration profiles are shown in figure 2.12.

The form of the concentration profiles predicted by the model below the cream region compares well with the experimental results. However, the creaming rate is more rapid experimentally than in the model, especially at early times. This may be due to the form of the hydrodynamic hindrance used in the model, which perhaps overestimates the reduction in creaming speed due to the other particles. In the cream region, the shape of the concentration profiles differs markedly between model and experimental results. The sharp change in concentration gradient in the cream occurs at a much higher

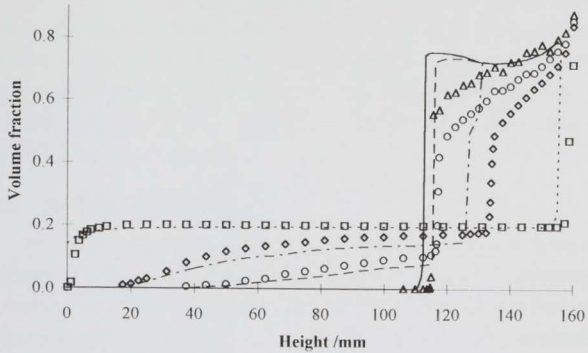

Figure 2.12 Comparison of experimental (Fillery-Travis et al., 1993) and modelled creaming profiles for a polydisperse alkane in water emulsion.

The squares, diamonds, circles and triangles are the model predictions after 0.25, 5, 12.5 and 50 days respectively. The experimental results represented by the dotted, dot/dashed, dashed and solid lines are after 0.22, 5.14, 12.12 and 57.2 days respectively.

concentration in the experiments (around 70 %), compared with 50 % in the model. This causes the concentration profile to look very different in the two cases. The peak in concentration at the bottom of the cream which is seen experimentally in the profiles after 12 days and 57 days, is not present in the modelled results. However, the predictions of the model for the sunflower oil in water emulsion (figure 2.8) after a long period did show such a peak in concentration. This feature takes longer to form in the model than in the experiment.

The differences between experiment and model may be attributable to the simplified description of the hydrodynamic interactions in the model, especially in the most concentrated region. In an earlier section, the hydrodynamic effects in concentrated regions were discussed, noting that polydispersity must have an influence at high concentrations. These effects are not included in the model, and therefore the model can not be expected to provide a complete description of the concentration profile in the cream region. The agreement between the concentration profiles at lower concentrations

is evidence that the hydrodynamic interactions used in the model (the hindrance factor determined solely by the local oil concentration) is a good description in this less-concentrated region. A second contribution to the discrepancy between the experimental and modelled results is the possible existence of non-hydrodynamic interactions in the experimental system, which are not included in the model. The magnitude and effect of any such interactions are not known for this system.

2.8.2 Particle size distribution

The quadratic variation of the Stokes creaming velocity with particle size inevitably has an effect on the variation with height of the particle size distribution in a polydisperse sample, since larger particles cream considerably faster than smaller particles. The effect of this difference in creaming rate has already been seen in the total concentration profiles. Although not included in the model, colloidal interactions may also cause particle size dependent effects. The creaming velocities of particles of different sizes are influenced by the hydrodynamic interactions, mainly through the backflow of the continuous phase fluid. The velocity of each size fraction relative to the container is determined from equation 2.50, which includes the opposing flow of continuous phase fluid. Under some circumstances, it is possible that the backflow of the surrounding fluid is sufficient to carry the smallest particles downwards. Only when the local size distribution changes, due to the loss of the larger particles, can the smaller particles reverse their direction and cream upwards. This phenomenon was noted in the particle trajectories derived by Zimmels (1988). The creaming behaviour of the different particle size fractions is therefore influenced not only by the Stokes velocity dependence on particle size, but also by the flow of the surrounding fluid which causes smaller particles to move downwards.

The effect of the different size fractions in a polydisperse sample on its creaming behaviour can be demonstrated by observing the concentration profiles of the individual size fractions, and the variation in particle size distribution with position and time. Figure 2.13 shows the calculated concentration profiles of particles of various sizes after 250 days for the sunflower oil in water emulsion. The total concentration profile at this time is also shown as a reference. A clear lower boundary can be seen for each size fraction, corresponding to the position of particles which were initially at the bottom of the sample. Below the boundary for each fraction there are no particles of that size. The position of the lower

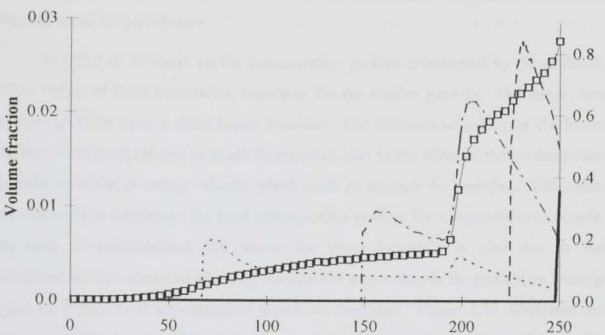

Figure 2.13 Concentration as a function of height for different particle size fractions after 250 days in a sunflower oil in water emulsion.

The size fractions are for radii of - - - 0.154 μm, — · — 0.28 μm, — — 0.51 μm — 1.25 μm. The total concentration is shown by □ and refers to the right hand axis.

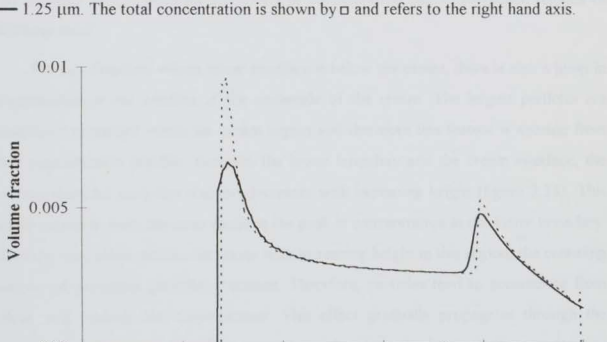

Figure 2.14 Effect of diffusion on the concentration profile of a single size fraction in a sunflower oil in water emulsion.

The profiles are for a radius of 0.154 μm after 250 days. The solid line includes diffusion, and the dotted line is in the absence of diffusion.

boundary is higher up the sample for the larger particles, due to the dependence of the creaming speed on particle size.

The effect of diffusion on the concentration profiles is indicated by the rounded, diffuse nature of these boundaries, especially for the smaller particles. The larger, less diffusive particles have a sharp lower boundary. The diffusive spreading of the lower interface is not as significant as might be expected, due to the effect of the concentration dependence of the creaming velocity which tends to sharpen the boundary. This effect was discussed in relation to the total concentration profiles for a monodisperse sample. The peak in concentration just above the lower boundary is also due to the concentration-dependence of creaming, as particles accumulate in the more slow moving region of higher total concentration above the boundary. Figure 2.14 illustrates the influence of diffusion on the concentration profile of one of the smaller particles in the sample, with a radius of 0.154 μm. In the absence of diffusion the lower boundary is very sharp, and the peak is narrower and larger. It would appear that diffusion rounds off and reduces the peak in the concentration profile. This is consistent with the understanding that diffusion acts to promote uniformity of concentration and so to reduce regions of inhomogeneity.

For size fractions whose lower interface is below the cream, there is also a jump in concentration at the position of the underside of the cream. The largest particles are completely contained within the cream region and therefore this feature is missing from their concentration profiles. Between the lower boundary and the cream interface, the concentration for each size fraction decreases with increasing height (figure 2.13). This would appear to have the same cause as the peak in concentration at the lower boundary. Since the total concentration increases with increasing height in this region, the creaming velocity of individual particles decreases. Therefore, particles tend to accumulate from below, and increase the concentration. This effect gradually propagates through the system, from the lower boundary upwards, and causes the increase in concentration towards the lower boundary seen in the plots.

Within the cream, the concentration of most sizes of particle decreases towards the top of the sample (figure 2.13). The largest particles (those with a radius of 1.25 μm are shown here) occupy only a very small region at the top of the sample, and their concentration increases with height. These are the most rapidly creaming particles, and

dominate the creaming process at early times. For most particle sizes, as more cream develops, a greater number of the larger size fractions are absent at the lower interface of the cream, and the smaller particles can occupy a larger proportion of the space. The concentration profile therefore decreases towards the top of the sample. In addition to the more rapid upward motion of the large particles, the fluid backflow also contributes to the particle size balance. The smaller particles are carried downwards in the continuous phase flow in the early stages of creaming, and so there is a reduced volume of these particles at the top of the emulsion. The diffusive spreading of the upper interface for these small particles causes them still to be present at the top of the sample, but the concentration is reduced as particles lower down move downwards. In the absence of diffusion, the upper boundary for the smallest particles (that is, the particles initially at the very top of the sample) does move downwards a little way. The position of the upper boundary can be seen in figure 2.14. The top layer in this case contains none of the smallest particles.

The effects of polydispersity described in the preceding paragraphs can also be identified in the variation of the particle size distribution with height. It is the local particle size distribution (and concentration) which will determine the ultrasound velocity in the emulsion at any position. It is therefore informative to compare the particle size distribution at various points in the sample with the initial distribution, which was shown in figure 2.7. Figure 2.15 shows the particle size distribution at three different heights in the bulk of the emulsion after 250 days. In each distribution there is a sharp cut-off at the large particle size limit, due to the absence of particles larger than a specific size. The lower interfaces of all particles larger than this limit have moved higher up the sample than the position at which the distribution is taken. Near the bottom of the sample, only the smallest particles remain, due to their slower creaming speed, and to the effect of diffusion. The concentration of particles of a given size can be seen to decrease with increasing height, as was observed in the concentration profiles. It is clear that in this region the particle size distribution may be very different from that in the initial uniform sample.

The particle size distribution in the cream varies even more strongly with height, as shown in figure 2.16. These distributions correspond to 500 days, when the cream is more extensive. At the top of the sample, the average particle size is considerable larger

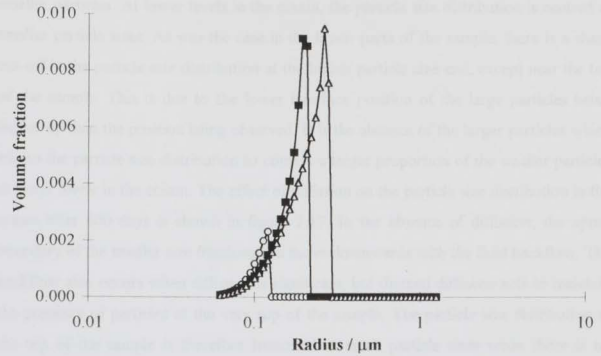

Calculated

Figure 2.15 Particle size distribution in the bulk of the polydisperse sunflower oil in water emulsion after 250 days.

The distributions correspond to heights of ○ 50 mm, ▪ 100 mm and ▵ 150 mm from the bottom of the sample.

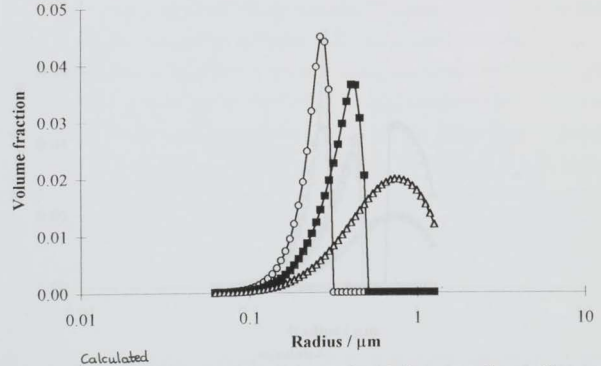

Calculated

Figure 2.16 Particle size distribution in the cream of a polydisperse sunflower oil in water emulsion after 500 days.

The distributions correspond to heights of ○ 200 mm, ▪ 225 mm and ▵ 250 mm from the bottom of the sample.

than the initial mean size, due to the differential creaming rates, and the backflow of the smaller particles. At lower levels in the cream, the particle size distribution is centred at smaller particle sizes. As was the case in the lower parts of the sample, there is a sharp cut-off in the particle size distribution at the higher particle size end, except near the top of the sample. This is due to the lower interface position of the large particles being higher up than the position being observed. It is the absence of the larger particles which allows the particle size distribution to contain a larger proportion of the smaller particles at lower levels in the cream. The effect of diffusion on the particle size distribution in the cream after 500 days is shown in figure 2.17. In the absence of diffusion, the upper boundary of the smaller size fractions can move downwards with the fluid backflow. The backflow also occurs when diffusion is significant, but thermal diffusion acts to maintain the presence of particles at the very top of the sample. The particle size distribution at the top of the sample is therefore truncated at small particle sizes when there is no diffusion (figure 2.17).

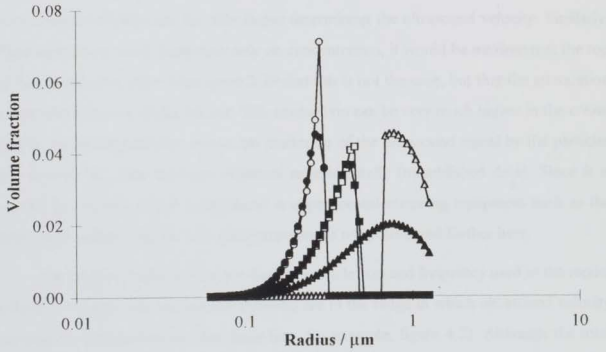

Figure 2.17 Effect of diffusion on the calculated particle size distribution in the cream after 500 days in a sunflower oil in water emulsion.

Open symbols represent no diffusion, filled symbols represent diffusion. The heights are the same as in the previous figure.

2.8.3 Ultrasound velocity and attenuation profiles

Figures 2.18 and 2.19 show ultrasound velocity and attenuation profiles generated by the model for the polydisperse sunflower oil in water emulsion. The ultrasound parameters have been calculated using multiple scattering theory, and the frequency was 1 MHz. The theories of ultrasound propagation commonly used to interpret ultrasound measurements are discussed in more detail in chapters 4 and 5, and only the main points are presented here.

The ultrasound velocity in the pure oil phase is lower than in the aqueous phase. A simple interpretation would therefore expect that an increase in oil concentration at one position in the emulsion would correspond to a decrease in ultrasound velocity at that position. This is indeed true in the lower regions of the sample (compare figure 2.18 with the total concentration profiles, figure 2.8). In the cream, the concentration always increases towards the top of the sample (apart from a small peak at the bottom of the cream). The ultrasound velocity does decrease with height in the cream at early times. However, at later times the ultrasound velocity increases with increasing height in the cream layer (after 1000 days, for example). At intermediate times (500 days) the ultrasound velocity in the cream is almost constant. It is clear, then, that the total concentration of oil is not the only factor determining the ultrasound velocity. Similarly, if the attenuation were dependent only on concentration, it would be maximum at the top of the sample. It is clear from figure 2.19 that this is not the case, but that the attenuation peaks below the top of the sample. The attenuation can be very much higher in the cream than in the initial emulsion, due to the scattering of the ultrasound signal by the particles (see chapter 4). This has been observed experimentally (unpublished data). Since it is usually the velocity which is measured in experimental creaming equipment such as the ultrasound scanner (figure 1.1), the attenuation is not considered further here.

The results of chapter 4 show that the particle size and frequency used in the model (which are typical of experimental systems) are in the range in which ultrasound velocity increases as the particle size increases (see, for example, figure 4.2). Although the total concentration of oil increases towards the top of the sample (causing a decrease in sound speed), the particle size distribution also becomes skewed towards the larger particles (causing an increase in sound speed). These two factors have an opposing influence on

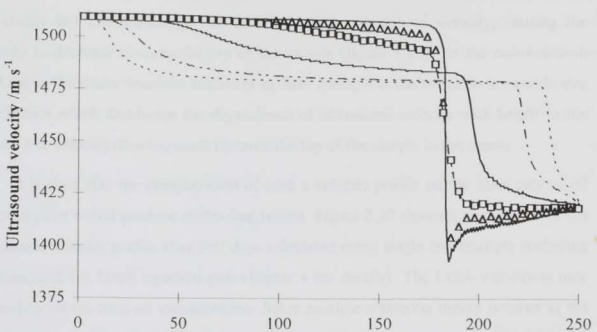

Figure 2.18 Ultrasound velocity profiles calculated from multiple scattering theory from the creaming model for a sunflower oil in water emulsion.

The profiles correspond to··· 50 days, - - - 100 days,— 250 days, □ 500 days, △ 700 days,— 1000 days.

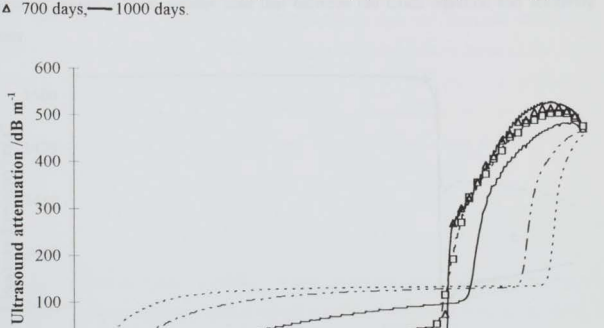

Figure 2.19 Ultrasound attenuation profiles from the creaming model for a sunflower oil in water emulsion.

The profiles correspond to··· 50 days, - - - 100 days,— 250 days, □ 500 days, △ 700 days,— 1000 days.

the ultrasound velocity. At early times, the concentration varies strongly with height in the cream and this dominates the variation of the ultrasound velocity, causing the velocity to decrease towards the top of the sample (figure 2.18). As the concentration gradient in the cream becomes shallower at later times, it is the variation in particle size distribution which dominates the dependence of ultrasound velocity with height in the cream. The velocity then increases towards the top of the sample in the cream.

It is clear that the interpretation of such a velocity profile on the basis only of oil concentration would produce misleading results. Figure 2.20 shows a comparison of the ultrasound velocity profile after 500 days calculated using single and multiple scattering theories, and the Urick equation (see chapter 4 for details). The Urick velocity is only dependent on the total oil concentration. Since multiple scattering theory is taken as the benchmark, it is clear that the Urick equation would produce totally unreliable data for this system. The difference between the single and multiple scattering theories is included to illustrate that at the oil concentrations present in the cream, multiple scattering effects can be very significant. However, the difference between the single and multiple scattering results is much smaller than that between the Urick equation and scattering theory.

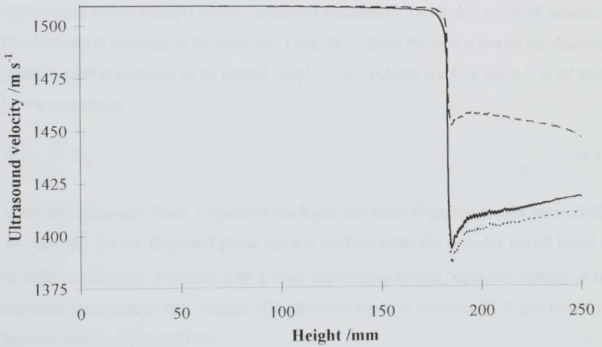

Figure 2.20 Comparison of ultrasound velocity theories after 1000 days from the creaming model for a sunflower oil in water emulsion.

The solid line is calculated from multiple scattering theory, the dotted line from single scattering theory, and the dashed line using the Urick equation.

The ultrasound technique for creaming studies is based on the determination of local oil concentrations from the measured velocity profiles. The difficulties discussed here of the effects of particle size distribution need to be avoided if simple interpretations of ultrasound measurements are to be possible. Chapter 5 discusses the ways in which simplified interpretations can be used, and under what circumstances they may be applied. The results of the creaming model have shown up the potential problems of ultrasound measurements used in this way, but have also indicated some ways to overcome them.

2.9 Creaming and crystallisation

Combined crystallisation and creaming behaviour in emulsions containing a mixture of solid and liquid droplets was investigated by including a solid fat dispersed phase in the model, in addition to the usual liquid oil phase. Each size fraction has its own solid and liquid volume fraction, and upper and lower boundaries for the solid and liquid particles. Crystallisation is modelled by converting, in each time step, some volume of liquid phase droplets into solid droplets of a corresponding size. Since the solid phase is more dense, the volume of a particle decreases when it crystallises. Although the volume change (and radius change) of the particles is included in the model, the total volume of the emulsion is assumed to be constant. Thus, the volume fraction when all the dispersed phase is solid is assumed to be related simply to the volume fraction when it is all liquid by the expression

$$\Phi_L = \frac{\rho_3}{\rho_2}\Phi_S \qquad [2.56]$$

where the subscripts 2 and 3 represent the liquid and solid dispersed phases respectively. Φ_L and Φ_S are the dispersed phase volume fraction when the particles are all liquid or all solid respectively. Equation 2.56 is only approximately true, since the volume of the emulsion also changes (the volume of continuous phase is conserved). It can be shown that the relationship should be

$$\Phi_L = \frac{\rho_3}{\rho_2}\Phi_S\left[1+\left(\frac{\rho_3}{\rho_2}-1\right)\Phi_S\right]^{-1} \qquad [2.57]$$

Equation 2.56 is therefore a good approximation at low concentrations of dispersed phase, but may not be as good in the cream, especially where the density difference between solid and liquid phases is quite large, as for hexadecane. However, inclusion of the volume change of the emulsion is an added complication in the creaming model, since it represents a variation in thickness of the horizontal layers used to define the volume fraction profile. Therefore, a change in solid volume fraction due to the solidification of a given volume fraction of liquid droplets was calculated using the ratio of the densities only (equation 2.56).

2.9.1 Crystallisation kinetics

Recent studies of creaming and crystallisation have been carried out on *n*-hexadecane in water emulsions (Ma, 1995), for which earlier crystallisation studies had also been made (McClements et al., 1993, Dickinson et al., 1993b). The analysis of the crystallisation kinetics is, however, applicable to any emulsion containing solid and liquid particles, provided the dominant crystallisation mechanism is the same. The only difference is in the rate constant. The crystallisation kinetics in such emulsions were investigated using an ultrasound technique (McClements et al., 1993, Dickinson et al., 1993b), which is discussed in more detail in chapter 5. The principle of the method is that the proportion of the dispersed phase which is solid can be calculated from the measured ultrasound velocity in the emulsion. Every particle is assumed to be either wholly solid or wholly liquid. Initially 50 % by weight of the dispersed phase is solid, and the rest is liquid. This is achieved by dividing the emulsion into two equal parts, and freezing one part so that all the oil crystallises. The parts are then remixed to make a partially crystalline emulsion. The ultrasound velocity in the mixed emulsion is measured as a function of time to determine the time dependence of the solid fat content and thereby the crystallisation kinetics (McClements et al., 1993).

One possible mechanism for crystallisation in this mixed emulsion is a heterogeneous process, involving collisions between solid and liquid dispersed particles. Other possibilities exist, such as homogeneous nucleation (Turnbull and Cormia, 1961), or a mechanism which is dependent on mass-transport of oil or fat due to solubilisation by the emulsifier (Dickinson et al., 1996). For the purposes of the model, the heterogeneous mechanism was assumed to be valid, since it had been shown to be consistent with the previous crystallisation study (McClements et al., 1993). According

to this mechanism, crystallisation of a liquid droplet occurs due to a collision with an already crystalline droplet, which nucleates crystal growth in the liquid. Following nucleation, the droplet rapidly solidifies completely. Not every such collision results in the solidification of the liquid particle, however, due to an energy barrier (partly caused by the protective layer of emulsifier around the droplet).

The heterogeneous crystallisation kinetics can be described in terms of a binary collision process between solid and liquid particles. The rate equation includes both the particle collision rate, and the proportion of collisions which result in crystallisation. In a monodisperse sample, the rate of crystallisation can therefore be expressed in terms of the proportions of solid and liquid droplets. If α_s is the proportion of dispersed phase droplets which are solid, the rate equation can be written as

$$\frac{\mathrm{d}(1-\alpha_s)}{\mathrm{d}t} = -K\alpha_s(1-\alpha_s) \qquad [2.58]$$

where K is a rate constant (McClements et al., 1993. They use the symbol ϕ for α_s). The rate constant determined in the experiments (McClements et al., 1993) was specific to the samples used (which were nearly monodisperse), and is particle size and concentration dependent. In a polydisperse sample, the binary collision rate includes contributions from collisions between particles of all different sizes. The rate of change of the number density, n_i, of liquid droplets of species (size fraction) i due to collisions with solid particles of species (size fraction) j can be written as

$$\frac{\mathrm{d}n_{i,j}}{\mathrm{d}t} = -\varepsilon\beta_{i,j}n_i n_j \qquad [2.59]$$

where ε is a collision efficiency factor (the proportion of collisions which result in solidification of the liquid droplet) and $\beta_{i,j}n_i n_j$ is the binary collision rate between these species.

Interparticle collisions in an emulsion are the result of some form of relative motion between the particles (Colbeck, 1994). The relative motion may be caused by a number of different processes, but the predominant effects in the present work are due to Brownian diffusion and creaming. Brownian diffusion causes random particle collisions in both monodisperse and polydisperse emulsions. In contrast, the effect of creaming on the collision rate is only significant in a polydisperse emulsion. Although some collisions

may occur in a monodisperse sample as a result of creaming, the particles all move, on average, with the same velocity, and the collision rate is consequently low. However, in a polydisperse emulsion, particles of different sizes move with different creaming velocities and collisions are much more likely. The binary collision rate in the emulsion is, therefore, the sum of the two contributing processes, so that the factor $\beta_{i,j}$ can be written

$$\beta_{i,j} = \beta_{i,j,\text{diff}} + \beta_{i,j,\text{cm}} \qquad [2.60]$$

where $\beta_{i,j,\text{diff}}$ and $\beta_{i,j,\text{cm}}$ are the factors in the collision rates due to Brownian diffusion and the relative particle creaming rates respectively. Short range hydrodynamic effects are neglected.

The binary collision process has been extensively investigated in the context of flocculation and coalescence. Expressions for the collision rates have been obtained from works on flocculation by Melik and Fogler (1984), Lawler (1993) and Abel et al. (1994). The collision rates for Brownian diffusion are based on the early work of Smoluchowski, later extended to polydisperse systems. In this case, the collision factor is given by

$$\beta_{i,j,\text{diff}} = 8\pi \frac{\left(D_i + D_j\right)}{2} \frac{\left(r_i + r_j\right)}{2} \qquad [2.61]$$

In a monodisperse sample, the collision rate is independent of particle size (for a given particle number density). Smaller particles have a larger diffusion coefficient, being more mobile, but their collision cross-section is small. Large particles are less mobile but have a large collision area. Hence, the overall collision rate is independent of particle size. In a polydisperse sample, the Brownian collision rate may be significantly increased due to collisions between particles of different sizes (Colbeck, 1994). For example, a small, very mobile particle is much more likely to collide with a larger particle (with a large collision cross-section) than with a particle identical to itself. The combination of the size-dependent diffusion coefficients and collision areas leads to an increased collision rate in a polydisperse system.

The gravitationally-induced collision rate is proportional to the volume swept out by the relative velocity of the two species of particle, and to the effective cross-sectional area of the collision. Thus

$$\beta_{i,j,\text{cm}} = \pi\left(r_i + r_j\right)^2 \left|u_i - u_j\right| \qquad [2.62]$$

Lawler (1993) has an extra factor of 0.5 in his expression. Melik and Fogler (1984) discuss some modifications to the effective collision cross-section due to the hydrodynamics of the fluid flow. However, for the purposes of the model, the binary collision rate was taken in its simplest form, given above. It is clear that the degree of polydispersity in an emulsion is a determining factor in the significance of the gravitational contribution to the binary collision rate. In addition, the gravitational collision rate is strongly particle size dependent.

Although the binary collision rates are most easily derived using the number density of particles (as in the preceding equations), the phenomenological creaming model (and the crystallisation study) uses the volume fraction of each species. Remembering that a subscript of "2" represents the liquid dispersed phase, and a subscript of "3" the solid dispersed phase, equation 2.59 can be written as

$$\frac{d\phi_{2,j}}{dt} = -\frac{\varepsilon\left(\beta_{i,j,\text{diff}} + \beta_{i,j,\text{crm}}\right)}{\left(\frac{4}{3}\pi r_j^3\right)} \cdot \phi_{2,j}\phi_{3,j} \qquad [2.63]$$

By writing the volume fractions in terms of the proportion of the dispersed phase, and comparing with the crystallisation rate (equation 2.58) given by McClements et al. (1993), it can be seen that the rate constant in the monodisperse case is given by

$$K = \frac{\varepsilon\left(\beta_{i,j,\text{diff}} + \beta_{i,j,\text{crm}}\right)}{\left(\frac{4}{3}\pi r_j^3\right)} \cdot \Phi_S = \varepsilon\left(\beta_{i,j,\text{diff}} + \beta_{i,j,\text{crm}}\right)n_0 \qquad [2.64]$$

where n_0 is the number density of particles. Thus, the rate constant is itself dependent on the total concentration of dispersed phase and on particle size. However, the collision efficiency can be assumed to be independent of these parameters and was derived in the crystallisation study (McClements et al., 1993). The collision rate was calculated by McClements et al. using the monodisperse form of the diffusion collision frequency, equation 2.61, neglecting the effect of the density change on solidification. The densities of water, liquid hexadecane and solid hexadecane at 6 °C are 999.9, 783.3 and 909.4 kg m^{-3} respectively (Kaye and Laby, 1986, Allegra and Hawley, 1972). The particle diameter with a Tween20 emulsifier had a value of d_{32}=0.36 μm (the volume-surface average) when the particles are liquid. The contribution of relative creaming

speeds in these emulsions was small and can be ignored. Thus, the collision efficiency factor can be calculated from equation 2.61, and is approximately

$$\varepsilon = 8.0 \times 10^{-8} \qquad [2.65]$$

This corresponds to an energy barrier of around $16k_BT$, as given by McClements et al. (1993).

Since the collision efficiency can be assumed to be relatively insensitive to particle size and temperature, the crystallisation rate can be calculated in the model using equation 2.63, with the value of equation 2.65. The crystallisation rate can therefore be calculated for a polydisperse hexadecane in water emulsion, at any concentration. The equations are not precisely valid at high concentrations because tertiary and higher collisions would then become significant. The binary collision rates are given by equations 2.61 and 2.62. The creaming speeds include the hydrodynamic hindrance. The Brownian collision rate is determined by the diffusive motion of individual particles within the medium. However, the diffusion coefficients used in the model are the phenomenological mutual diffusion coefficients which describe the flux of particles in a concentration gradient. These coefficients were used throughout, for simplicity, with the concentration dependence previously detailed.

2.9.2 Modelling of combined creaming and crystallisation

The computer program for modelling creaming and crystallisation is included in Appendix A1. The creaming and crystallisation behaviour of a 20 vol. % hexadecane in water emulsion with a mixture of solid and liquid particles was determined at 8 °C using the creaming model. This system was recently studied experimentally by Ma (1995) using the ultrasound scanner (figure 1.1). The crystallisation rate in the absence of creaming was initially measured, and it was found to be consistent with the results of McClements et al. (1993). The physical properties of the constituent phases are shown in table 2.2 (Kaye and Laby, 1986, Allegra and Hawley, 1972). The particle size distribution (obtained in the experimental samples) peaks at a diameter of 0.42 μm, with a width of $\sigma_w = 0.5$, when all particles are liquid. This is consistent with the volume-surface diameter of d_{32}=0.36 μm. The frequency used in the calculations of ultrasound velocity was 1.6 MHz (as in the creaming experiments).

	Water	Hexadecane (liquid)	Hexadecane (solid)
Ultrasound velocity / m s^{-1}	1439.1	1400.0	2200.0
Density / kg m^{-3}	999.9	781.9	908.2
Shear viscosity / Pa s	0.0014	0.00385	
Shear rigidity / Pa			7.0×10^8
Thermal conductivity / J $m^{-1}s^{-1}K^{-1}$	0.572	0.140	0.185
Specific heat capacity at constant pressure / J kg^{-1} K^{-1}	4195	2092	2092
Thermal expansivity / K^{-1}	0.000075	0.000895	0.00066

Table 2.2 Physical properties of hexadecane and water at 8 °C.

Results from the model for the concentration profiles after 2.5 days, of solid and liquid phases and the total dispersed phase concentration are shown in figure 2.21. Very little creaming has occurred after this time, but crystallisation is well advanced. The liquid volume fraction is very much reduced, whereas most of the dispersed phase is now solid. After 5 days, the concentration of liquid oil is only approximately 1 % (1/10 of its initial value). The crystallisation process is considerably faster than the creaming rate in the ideal emulsion (in which the particles cream independently). This is clear from the time scale of ideal creaming behaviour in the model (of the order of 200 days) compared with the time scale of the crystallisation experiment by McClements et al. (1993), (500 hours). Therefore, crystallisation is almost complete before a significant amount of creaming occurs, and all the dispersed phase is then solid.

The creaming behaviour is therefore dominated by the solid dispersed phase. The density difference between hexadecane particles and the continuous phase fluid is considerably smaller for solid particles than for liquid particles. Hence, the solid particles cream more slowly, and the creaming rate in the mixed emulsion is dramatically reduced compared to the all-liquid ideal emulsion. Figure 2.22 shows the total concentration of the dispersed phase after 30 days in the mixed emulsion (whose particles are practically

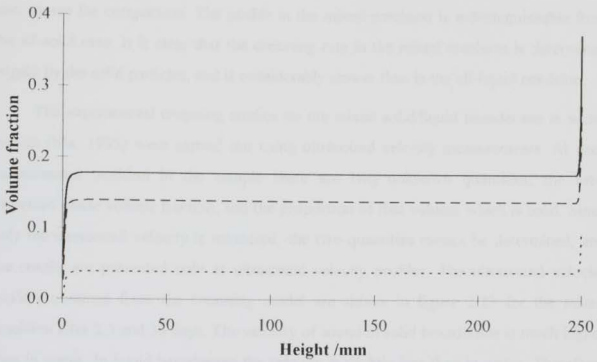

Figure 2.21 Profiles of liquid, solid and total dispersed phase concentration after 2.5 days of creaming in a mixed hexadecane in water emulsion at 8°C.

The dotted, dashed and solid lines correspond to the liquid, solid and total dispersed phase respectively.

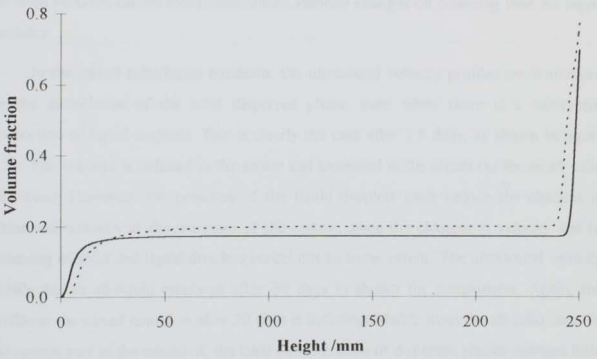

Figure 2.22 Profiles of total dispersed phase concentration after 30 days in mixed solid/liquid and all-liquid hexadecane in water emulsions at 8°C.

The dotted and solid lines correspond to the all-liquid and mixed emulsions respectively.

all solid at this time). The corresponding results for creaming in the all-liquid emulsion is also shown for comparison. The profile in the mixed emulsion is indistinguishable from the all-solid case. It is clear that the creaming rate in the mixed emulsion is determined largely by the solid particles, and is considerably slower than in the all-liquid emulsion.

The experimental creaming studies on the mixed solid/liquid hexadecane in water system (Ma, 1995) were carried out using ultrasound velocity measurements. At each measurement position in the sample there are two unknown quantities, the total dispersed phase volume fraction, and the proportion of that volume which is solid. Since only the ultrasound velocity is measured, the two quantities cannot be determined, and the results are presented only as ultrasound velocity profiles. The ultrasound velocity profiles obtained from the creaming model are shown in figure 2.23 for the mixed emulsion after 2.5 and 30 days. The velocity of sound in solid hexadecane is much higher than in water. In liquid hexadecane the velocity is slightly less than in water. Therefore, in the all-liquid emulsion, the ultrasound velocity would be expected to decrease at high oil concentration (in the cream) and increase in the serum. The opposite is true for the all-solid dispersed phase emulsion – the velocity increases in the cream and decreases in the serum. The larger velocity difference between the dispersed and continuous phases for solid particles causes more pronounced velocity changes on creaming than for liquid particles.

In the mixed solid/liquid emulsion, the ultrasound velocity profiles are dominated by the distribution of the solid dispersed phase, even when there is a substantial proportion of liquid droplets. This is clearly the case after 2.5 days, as shown in figure 2.23. The velocity is reduced in the serum and increased in the cream (as for an all-solid emulsion). However, the presence of the liquid droplets must reduce the changes in ultrasound velocity at the extremes of the system, since the changes in velocity due to creaming of solid and liquid droplets cancel out to some extent. The ultrasound velocity profile for an all-liquid emulsion after 30 days is shown for comparison. Again, the profile in the mixed emulsion after 30 days is indistinguishable from the all-solid case. In the central part of the emulsion, the total concentration of dispersed phases changes little in the early stages of creaming. The variation with time of the ultrasound velocity in this region corresponds entirely to the crystallisation of liquid particles. The crystallisation rate in the system can therefore be calculated in such an ideal system using the same

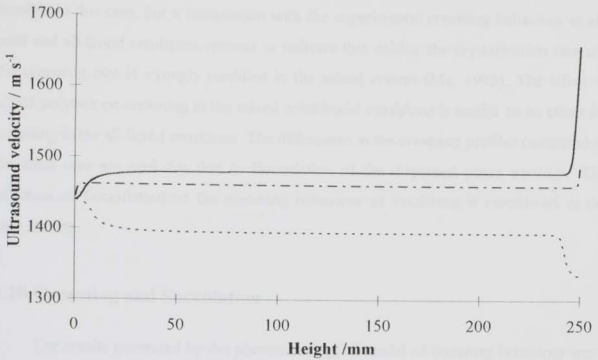

Figure 2.23 Ultrasound velocity profiles for the creaming and crystallisation model of a hexadecane in water emulsion at 8°C.

The dashed/dotted and solid lines are the profiles in the mixed solid/ liquid emulsion after 2.5 and 30 days respectively. The dotted line is for an all-liquid emulsion after 30 days.

principles as in the crystallisation studies (McClements et al., 1993).

The experimental study examined the effects on the creaming behaviour due to the presence of additional non-adsorbing polymer in the continuous phase. In the absence of polymer, the creaming rate is so slow that the only observable effect over the time scale of the experiment is the increase in velocity throughout the emulsion due to crystallisation. This case corresponds qualitatively to the model results. It was observed that the crystallisation rate was little different from that measured in the "static" crystallisation experiments. In the creaming model it can also be seen that the crystallisation kinetics (section 2.9.1), assuming a binary collision mechanism, are dominated by the Brownian term (equation 2.61) rather than the sedimentation term (equation 2.62) in this system. The addition of polymer causes the creaming rate to increase dramatically in some cases, and to become negligible in others, depending on the polymer concentration. Where the creaming rate is increased, crystallisation is no longer complete before significant creaming occurs, as in the idealised emulsion. The ultrasound velocity profile is then determined both by the modification due to creaming at the serum and cream, and an increase in velocity corresponding to the crystallisation of the liquid

droplets. Quantitative analysis of the creaming and crystallisation behaviour is not yet possible in this case, but a comparison with the experimental creaming behaviour in all-solid and all-liquid emulsions appears to indicate that neither the crystallisation rate nor the creaming rate is strongly modified in the mixed system (Ma, 1995). The effect of added polymer on creaming in the mixed solid/liquid emulsions is similar to its effect on creaming in the all-liquid emulsions. The differences in the creaming profiles compared to the ideal case are probably due to flocculation of the dispersed phase particles. The influence of flocculation on the creaming behaviour of emulsions is considered in the next section.

2.10 Creaming and flocculation

The results generated by the phenomenological model of creaming behaviour were compared in section 2.8.1 with experimental results on a near-ideal system (Fillery-Travis et al., 1993). Qualitatively, the modelled concentration profiles compare well with experimental results except in the cream region. Quantitatively, the hydrodynamic hindrance used in the model seems to be overestimated, since the model predicts a slower creaming rate than that observed. Deficiencies in the description of the hydrodynamic interactions were also thought to explain the different concentration profiles in the highly concentrated region.

However, the creaming behaviour of many experimental systems is quite dissimilar to the predictions of the model. A recent study of the effect of the polysaccharide xanthan on the creaming behaviour of emulsions (Dickinson et al., 1994; Ma, 1995) produced concentration profiles with markedly different serum and cream profiles from the "ideal" case. An example of the results is shown in figure 2.24. It is clear that, although the sample is polydisperse, the concentration profile has a sharp serum interface which develops rapidly. This interface does not move up the sample with time, but remains in the same position. The influence of xanthan was also examined in the studies of creaming and crystallisation (Ma, 1995) in hexadecane in water emulsions, and was found to cause similar changes to the creaming profiles as occurred in the absence of crystallisation. Recent creaming experiments with excess caseinate in the aqueous phase have been carried out by Golding (as yet unpublished). In some cases, creaming was seen completely to cease, following the development of a serum layer, and the whole sample

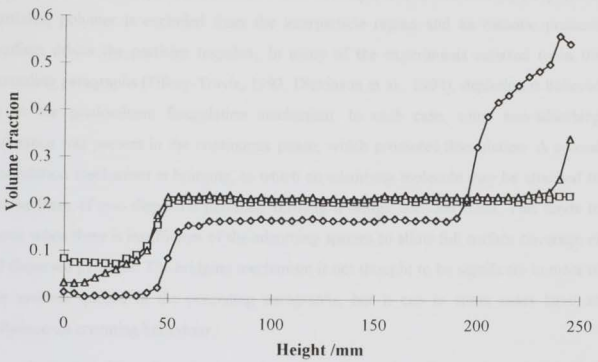

Figure 2.24 Creaming behaviour of a 20 % sunflower oil in water emulsion with 0.03 wt. % xanthan in the aqueous phase at 30 °C (Ma, 1995).

The profiles corresponding to the squares, triangles and diamonds were taken after 0.5 hours, 1.5 hours and 10 days respectively.

became solid-like. The work by Fillery-Travis et al. (1993), which was used to obtain an example of an ideal emulsion, also includes other examples of creaming in the presence of added polymer, producing a variety of forms of concentration profiles.

The common factor in these studies is thought to be the occurrence of flocculation of the oil particles. The term flocculation refers to the sticking together (reversibly or irreversibly) of two or more dispersed phase particles, which then behave as a single unit. Each droplet in the floc retains its individual identity, rather than coalescing with others to form a single larger particle. As discussed in chapter 1, flocculation occurs due to the existence of a favourable energy state when particles are close together. This may be caused by a long-range attractive potential between particles, or by an attractive force which is significant only when particles become close together, due to random collisions.

One short-range attraction which may cause flocculation is the depletion interaction, proposed by Asakura and Oosawa (1954, 1958). Depletion flocculation occurs in the presence of large polymer molecules or micelles in the continuous phase.

When two particles approach within a distance comparable to the size of the polymer particles, polymer is excluded from the interparticle region and an osmotic pressure gradient drives the particles together. In many of the experiments referred to in the preceding paragraphs (Fillery-Travis, 1993, Dickinson et al., 1994), depletion is believed to be the predominant flocculation mechanism. In each case, some non-adsorbing substance was present in the continuous phase, which promotes flocculation. A second flocculation mechanism is bridging, in which an adsorbing molecule may be attached to the surfaces of two dispersed particles, forming a bridge between them. This tends to occur when there is insufficient of the adsorbing species to allow full surface coverage of all dispersed particles. The bridging mechanism is not thought to be significant in most of the systems quoted in the preceding paragraphs, but it can in some cases have an influence on creaming behaviour.

It is clear from the experimental studies of creaming discussed previously that flocculation can have a very significant effect on creaming behaviour. In some cases, flocculation caused a large increase in creaming rate. It may be suggested that this is due to the faster creaming speed of flocs (due to their size), provided that they remain free to move relatively unhindered. In other cases, the extent of flocculation is so great as to produce a particle gel, in which creaming is greatly reduced, and the emulsion becomes much more stable. Previously the creaming model has assumed that all particles are free to move independently, and do not stick together. In fact, any particle interactions were omitted. Since the effect of flocculation on creaming behaviour is so significant, and the types of additives causing it are commonly present in food systems, an attempt was made to include these effects in the phenomenological model.

In the present phenomenological model, flocculation is irreversible: particles remain stuck together once they have flocculated. Reversible flocculation is difficult to implement in the phenomenological description, since no trace is kept of each individual floc, only of the volume fraction of flocs of a given size (as was the case for single particles). In order to allow particles to break off from a floc, its composition must be known in terms of the size of each of the particles in the floc. When creaming occurs, flocs of the same geometric size may have a different composition, depending on their growth and creaming rate history. Hence there is no simple, unique means of recording the particle size distribution in a floc. If floc break-up were then allowed, an assumption

as to the sizes of the particles breaking off may lead to non-conservation of the single particle size distribution in the emulsion as a whole. Therefore, only irreversible flocculation was included in the phenomenological model. Floc break-up in a monodisperse system can, however, be modelled, as demonstrated by Hsu and Tsao (1992), in the absence of creaming.

The driving force for depletion flocculation is the presence of a non-adsorbing species (such as a polymer) in the continuous phase. Its concentration is one determining factor in the flocculation rate. As flocs form, the polymer is excluded, to some extent, from the volume occupied by the floc. This floc volume includes a quantity of continuous phase fluid since the flocs are sparse. Hence as flocs grow, the concentration of polymer external to the flocs increases, because of the reduced "free" volume of continuous phase fluid. This increase in concentration in turn affects the flocculation rate between other particles or flocs. Polymer is likely to be completely excluded from a small, compact floc. However, as the flocs grow larger, and become more sparse, or even begin to form a network, some polymer must be trapped within the flocs or network.

A quantitative description of the polymer concentration and exclusion from flocs is not simple. A model which assumed complete exclusion of polymer from flocs would be unrealistic, since some polymer is likely still to be present when the flocs form a network which fills the whole space. In the other extreme, if the polymer concentration is assumed to be uniform throughout the continuous phase, including that incorporated into flocs, no changes in polymer concentration (with height and time) will be observed. An explicit description of the polymer was, therefore, omitted from the model. The flocculation process was assumed rather to occur at the same rate throughout the sample, with no account taken of variations in polymer concentration. So, the *effect* of the polymer in inducing flocculation is modelled, without explicitly including the polymer itself, except as a parameter in the flocculation rate.

There are three principal components to a phenomenological model of flocculation and creaming. Firstly, the kinetics of flocculation must be defined in terms of local characteristics such as the particle concentration. Secondly, the average structure of flocs must be quantifiable by a small number of parameters. Finally, the average dynamic properties of the flocs thus formed must be related to the floc characteristics, such as its effective size. Since the model is a phenomenological one, the description of floc

structure and the dynamic properties of flocs can only be a representational average over many different possible configurations. These three components are considered in the following sections.

2.10.1 Flocculation kinetics

The kinetics of flocculation are based on identical principles to the heterogeneous crystallisation mechanism described in section 2.9.1. Flocculation occurs due to collisions between two particles or flocs which then stick together. In the case of depletion flocculation the components need not collide but only approach within a distance comparable to the polymer size, which causes exclusion of the polymer from the space between them. Since the radius of gyration of a typical polymer is considerably smaller than most of the oil particles in the emulsions being studied, the contribution of the polymer size to the collision cross-section has been neglected in the model.

As in the crystallisation case, there are two factors determining the overall flocculation rate, namely the frequency of collisions between particles or flocs, and the probability of the components sticking together once they have collided. The rate of binary collisions due to thermal diffusion, and to the relative creaming speeds of particles of different sizes were given in section 2.9.1 (equations 2.61 and 2.62). These rate equations are generalised in the model by attributing to flocs a diffusion coefficient, creaming speed and geometric radius. The dynamic properties of flocs are discussed in section 2.10.3, and the geometric size in section 2.10.2. Collision rates between any combination of particles or flocs of different sizes can therefore be calculated using the binary rate equations (2.61 and 2.62). The rate equation 2.59 now represents the loss of particles (or flocs) of size fraction i due to flocculation with particles (or flocs) of size fraction j.

The collision efficiency introduced for crystallisation is also applicable to flocculation. In the case of crystallisation it represented the proportion of solid-liquid encounters which resulted in the solidification of the liquid droplet. When applied to flocculation it is equivalent to the proportion of particle encounters which result in the component species sticking together. In the case of depletion flocculation, the sticking probability is determined, in part, by the concentration of the non-adsorbing species (polymer). Since this concentration was assumed, in the model, to be constant

throughout the emulsion, the collision efficiency was simply retained as a variable parameter. It is also assumed to be independent of particle size and concentration (as for crystallisation). Where more information is available about the flocculating potential, a more complex form for the sticking probability could be used, incorporating, for example, the effects of particle size.

2.10.2 Floc structure

Flocs are not compact structures (unlike the droplets formed by coalescence), but become less space-filling the larger they grow. The detailed structure of such a floc may be very complex, but, on average, it may be parametrised by using the concept of fractal geometry. A more detailed description of the fractal nature of flocculation and its effect on creaming and diffusion rates can be found in the next chapter in the context of the lattice model. At this stage, it is sufficient to state that the floc structure is characterised by a fractal dimensionality, which describes the degree of sparsity as the floc increases in size. Thus, the volume of oil in a floc with an effective geometric radius r_f, is given by the expression

$$V_{oil} = \gamma_f r_f^{d_f} \qquad [2.66]$$

where the parameter d_f is the fractal dimension (or dimensionality). The fractal dimension is less than or equal to three. A value of three (equal to the Euclidean dimension) is equivalent to a random or homogeneous distribution of particles, and in this case the density of particles in the floc is uniform. A fractal dimension substantially less than three represents the increasingly sparse nature of the floc structure as the number of particles in the floc increases.

If the sample is monodisperse, and equation 2.66 is applied in the limit of a single particle in the floc, the proportionality constant can be written

$$\gamma_f = \frac{4}{3}\pi r^{3-d_f} \qquad [2.67]$$

where r is the radius of an individual particle. The fractal dimension has been determined by experiment or by simulation for a number of different aggregates (Meakin, 1988, Jullien, 1990). A value of 2.0 was found to be appropriate for many aggregates or flocs, and this is the value used in the model.

2.10.3 Floc mobility

The creaming speed and diffusion coefficient of flocs are crucial in determining the overall creaming characteristics of a flocculating emulsion. For the purposes of the phenomenological model, these dynamic properties must be related to the geometric size of the floc. Both the creaming speed and the diffusion coefficient are determined by the mobility of the floc, or alternatively, the viscous drag force caused by the continuous phase fluid. For single, isolated, spherical particles, this mobility was given by equation 2.30. As a first approximation, the mobility of an isolated floc may similarly be related to its geometric radius. In practice, isolated floc mobility may better be determined by a different, "hydrodynamic" radius, rather than by its geometric dimensions. However, this modification was neglected in the model, and any hydrodynamic effects on mobility were combined with the concentration-dependent hydrodynamic interactions described in the following paragraphs. The hydrodynamic radius may be smaller than r_f.

In the preceding section, the volume of oil in a floc of a given geometric radius was related to the fractal dimension, which characterises the floc structure. Hence, the average net buoyancy force on the floc (which is due only to the oil in the floc) can be obtained directly. The modified "Stokes" creaming velocity and "Stokes-Einstein" diffusion coefficient for a floc of geometric radius r_f were, therefore, defined as follows:

$$u_{f,0} = \frac{\gamma_f r_f^{(d_f - 1)} g \Delta\rho}{6\pi\eta} \qquad [2.68]$$

$$D_{f,0} = \frac{k_B T}{6\pi\eta r_f} \qquad [2.69]$$

The mobility of flocs and single particles in the flocculated emulsion is affected by the hydrodynamic interactions, which are modified by the existence of flocs. In sections 2.2.3 and 2.2.4, the effect on particle mobility of hydrodynamic interactions in a non-flocculated emulsion were expressed in terms of the local particle concentration. Since all the particles in a floc move together, their combined effect on the flow field in the surrounding fluid is different from their individual contributions if they existed separately as single particles. Similarly, the floc cannot be considered as a solid sphere of radius equal to the geometric radius of the floc, since some of the continuous phase fluid incorporated in the floc remains free to move with the surrounding fluid.

The effect of flocs on the hydrodynamic interactions is, therefore, dependent on the structure of the floc, particularly on the freedom of fluid to flow through or within the floc. Modifications to the hydrodynamic interactions due to these effects have been considered by Chhabra and Prasad (1991). They derived an expression for the viscous drag, including hydrodynamic effects, on a sphere with a solid core and a permeable shell. The cell model introduced by Happel was used to determine the hydrodynamic effects, in spite of the demonstration by Batchelor (1972) of its doubtful validity. The result is applicable for a monodisperse system of flocs, in which all particles are flocculated, and all flocs are the same size. The extension of the expression to a diverse suspension of flocs and single particles may be difficult. Bedenko et al. (1983) also considered the sedimentation of flocculated suspensions, in which most of the dispersed phase was flocculated. The flocs were large and nearly monodisperse. The hydrodynamic component in the sedimentation speed was, in this case, calculated by considering the flocs as "solid" spheres, in which no fluid flows in or out.

In the absence of a satisfactory phenomenological description of the hydrodynamic effects in a flocculated emulsion, two limiting conditions were investigated in the creaming model. In the first limit, the hydrodynamic hindrance factor (section 2.2.3) is calculated using only the concentration of oil, as in the unflocculated emulsion. This corresponds to the assumption that the flow field of the continuous phase fluid is unchanged by the presence of flocs, and that the effect of trapped fluid inside flocs may be neglected. In the other extreme, if the fluid incorporated into the floc is considered to be completely bound to the floc, the hydrodynamic hindrance factor is determined by the total concentration of flocs and particles (including the continuous phase fluid inside the flocs). This was the formulation used in an early study by Michaels and Bolger (1962) for dilute, flocculated suspensions, and also by Bedenko et al. (1983). In applying this hydrodynamic condition to the flocculating emulsion, the effective total concentration increases as the flocculation becomes more extensive, until no further movement is possible. Both cases are simplifications of the true situation, which is dependent on the details of floc structure and the flow field around flocs.

2.10.4 Samples analysed

The computer program for the modelling of creaming and flocculation is given in Appendix A2. The calculations on creaming and flocculation were carried out on smaller

scale systems than those presented in the preceding sections. The binary collisions used in the flocculation kinetics are computationally intensive and therefore the system size was reduced to improve computation speed. The sample properties correspond to a 20 % (by volume) sunflower oil in water emulsion at 30 °C, whose properties were given in table 2.1. The sample height was 40 mm, and the particle size distribution was characterised by a modal diameter of 0.56 μm and width of $\sigma_w = 0.42$ (giving a maximum diameter of 2 μm). Only 11 size fractions were used in the initial distribution. The flocculation characteristics are described by the parameters of the proportionality constant

$$\gamma_f = 4.2 \times 10^{-7} \text{m} \qquad [2.70]$$

and the flocculation probability, which is variable. Flocs were allowed to grow to a maximum diameter of 20 μm, and 20 size fractions were used in the floc size distribution. The value of the time interval is defined so as to ensure that the model does not attempt to flocculate more particle or floc volume than is present in any layer, thus conserving oil volume. At high flocculation efficiencies, a very small time interval must be used and so the calculations become rather slow.

2.10.5 Creaming and flocculation results

Creaming profiles predicted by the model for the sunflower oil in water emulsion after 4 days are shown in figure 2.25. The hydrodynamic interactions in these results were calculated using the total concentration of flocs and particles. The results of two different flocculation probabilities are shown, along with the creaming profile in the absence of flocculation. The emulsion with the larger flocculation probability hardly develops a serum or cream before the whole emulsion is constrained in a particle network structure which prevents further creaming. This condition is represented by a large value of the total volume fraction, due to the presence of many space-filling flocs. Although the oil concentration is still low, particles are extensively connected and movement of flocs is restricted. A reduction in the flocculation probability allows free creaming to proceed, at least over the time period shown. However, the creaming profile does not indicate an increase in creaming speed compared to the emulsion with no flocculation. It would appear that when the hydrodynamic interactions are determined by

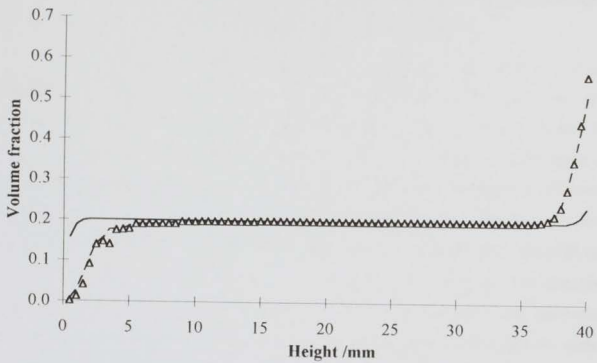

Figure 2.25 Concentration profiles of flocculation and creaming after 4 days using hydrodynamic interactions based on total floc concentration.

The solid and dashed lines represent flocculation efficiencies of 10^{-7} and 10^{-9} respectively. The open triangles are the results in the absence of flocculation.

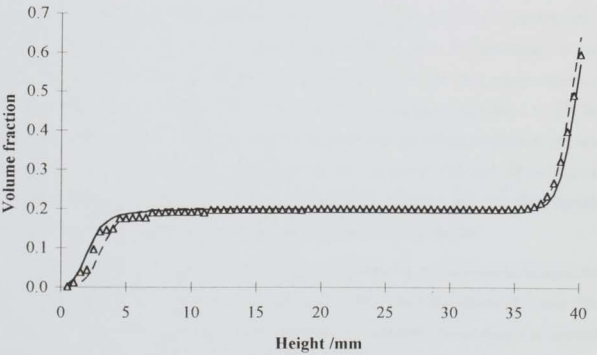

Figure 2.26 Concentration profiles of flocculation and creaming after 5 days using hydrodynamic interactions based on oil concentration only.

The solid and dashed lines represent flocculation efficiencies of 10^{-7} and 10^{-6} respectively. The open triangles are the results in the absence of flocculation.

the total volume fraction of flocs, the additional hindrance caused by the growth of many flocs outweighs their increase in creaming speed due to their larger size.

The alternative limiting condition for the hydrodynamic interactions is for the hindrance to be a function only of the oil concentration, rather than the total concentration of flocs. Creaming profiles under these conditions are shown in figure 2.26 for two different flocculation probabilities, after 5 days. The results in the absence of flocculation are again included for comparison. At the lower flocculation efficiency, creaming appears to be slightly slower than for single particles, whereas a marginal increase in creaming rate is observed at a higher flocculation probability. Although the flocs are still fairly free to move with the hydrodynamic factor applied in this case, the total volume fraction nominally included in flocs at this stage is much greater than unity. A more appropriate description of the system is, therefore, as a particle network, rather than as many individual flocs. The present hydrodynamic description allows greater freedom of movement of flocs, compared with the use of the total concentration in the hindrance factor. However, no dramatic increase in creaming rate has been observed, even in this case (figure 2.26).

A comparison of the creaming profiles obtained using the two extreme hydrodynamic descriptions is illustrated in figure 2.27. The flocculation probability (10^{-7}) was the same in both cases. The result obtained in the absence of flocculation is also shown. When the hydrodynamic interactions are determined by the total concentration of flocs and particles, creaming rapidly ceases, because of the growth of flocs to fill the whole space. This condition is an approximate representation of the interlinking of flocs into a particle gel, in which little particle movement will occur. The use only of the oil concentration in the hindrance factor has no equivalent limiting state, and flocs remain free to move, even when a networked structure is likely to have formed.

An increase in creaming rate was not observed when the hydrodynamic interactions were determined by the total floc concentration. This may be expected, since this condition is likely to overestimate the hydrodynamic reduction in creaming rate caused by the growth of flocs. However, the alternative hydrodynamic description also failed to produce a significantly increased creaming rate. In this case, the use of the oil concentration in the hydrodynamic hindrance factor leads to an underestimate of the effect of flocs on the hydrodynamic interactions. Hence, an increase in creaming rate

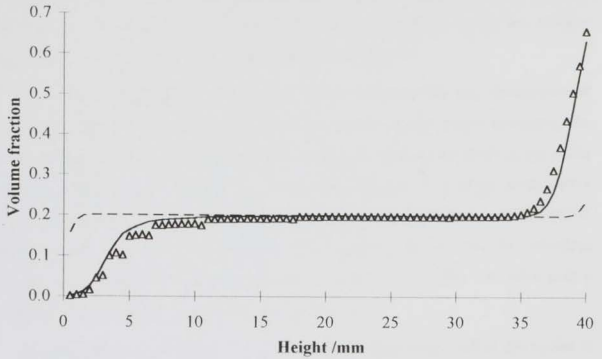

Figure 2.27 Concentration profiles of flocculation and creaming after 8 days comparing hydrodynamic interactions.

The solid and dashed lines represent hydrodynamic interactions calculated using the oil concentration, and the total concentration respectively. The open triangles are the results in the absence of flocculation.

might be expected in this case, due to the larger effective size of flocs compared with individual particles.

There are a number of possible reasons why a dramatic increase in creaming rate has not been observed in the model. Firstly, the "Stokes" creaming speed of a floc does not increase as steeply with radius as it does for a single particle (equation 2.68). This is because the proportion of oil in the floc decreases as the floc grows larger, so reducing the additional buoyancy force caused by the increased floc volume. Hence, the creaming speed of a moderately sized floc may not be as large as expected intuitively. For example, a floc of diameter 5 μm has a ("Stokes") creaming speed only three times larger than the speed of a single particle of diameter 0.56 μm. The Stokes creaming speed of the largest flocs allowed in the model (r_f=10 μm) is identical to the speed of the largest particles in the unflocculated emulsion. In the early stages of creaming, therefore, the difference in creaming rate may not be immediately apparent in a polydisperse emulsion. In such emulsions, the larger particles affect the creaming rate, especially in the early stages. The time taken for the sample to flocculate delays the onset of the increase in

creaming speed, since the model assumes that the emulsion is completely unflocculated at the start of creaming. The creaming behaviour of a sample which has already flocculated may show a more apparent increase in creaming rate.

The results illustrated in the previous figures indicate that the description of flocculation included in the phenomenological creaming model cannot reproduce the creaming behaviour observed in practice. The significant features observed under some conditions in flocculating emulsions are a rapid development of a serum layer, and a cessation of creaming due to the formation of a particle network structure. Although the creaming model was able to reproduce the constraint of particles by extensive flocculation, in neither limiting case of the hydrodynamic interactions was there seen a significant increase in the creaming rate in the early stages.

The description of the flocculation and creaming behaviour used in the model is inadequate for a partially flocculating emulsion. The early stages of flocculation in a dilute emulsion may be reasonably well represented by the model, since flocs can form but still remain free to move independently. The formation of a particle gel either by extensive flocculation in a relatively dilute system, or by flocculation in a very concentrated system may also be characterised. The model was able to represent this condition through a limiting form of the hydrodynamic interactions. An alternative description has been investigated by Buscall and White (1987) and Buscall (1990). They modelled the evolution of the network of a strongly flocculated suspension in terms of compressive stress, and of the continuous phase fluid draining from the network. A similar, strongly-flocculated model has also been presented by Auzerais et al. (1988). However, the intermediate region between the "dilute" and "concentrated" (or networked) limits is difficult to model satisfactorily. Flocs begin to fill the space, and cease to behave as individual entities. Their dynamic properties lie somewhere between those of isolated particles and those of a particle network. An appropriate phenomenological description of the characteristic structure and behaviour of flocs in this type of system has yet to be achieved.

The phenomenological model has therefore been unable to reproduce even the qualitative characteristics observed experimentally in some flocculating emulsions. This is largely due to the lack of adequate phenomenological descriptions of creaming and flocculation behaviour in partially flocculated emulsions. It seems likely that any

successful model of creaming in flocculated systems will have to include a more detailed structural description of the emulsion at the level of individual particles.

2.11 Conclusions of model

The basic phenomenological creaming model includes no direct particle interactions and therefore corresponds to an idealised emulsion. Within the limitations of these assumptions, a number of significant conclusions could be drawn from the results.

- The differential creaming rates of particles of different sizes causes strong variation in the particle size distribution in the sample.
- The backflow of the continuous phase fluid can carry some of the smaller particles with it so that they move downwards in the first stages of creaming.
- The concentration profile in the cream is determined by the hydrodynamic interactions at high concentrations. A description of the hydrodynamic effects in terms of the total concentration is insufficient to model the size-distribution dependent packing of particles in the cream.
- Under some conditions the ultrasound velocity in the emulsion is dependent on particle size distribution. The variation in particle size distribution, especially in the cream, can mask the concentration dependence of the velocity.
- Interpretation of ultrasound velocity measurements in these circumstances in terms only of the total concentration of oil may produce misleading results.
- Thermal diffusion does not have a strong effect on profiles of total oil concentration for the particle sizes modelled, but may influence the particle size distribution, and thereby the ultrasound velocity.
- Crystallisation in an ideal hexadecane emulsion containing solid and liquid droplets has little effect on creaming. Crystallisation is relatively rapid, and therefore the creaming behaviour is characterised by the creaming of solid particles.
- The concentration profiles in an ideal, modelled emulsion are very different from some experimental systems in which flocculation is occurring.

- Modelling of combined flocculation and creaming behaviour was characterised by the space-filling nature of extensive flocculation, which prevents further creaming.
- No appropriate description of the hydrodynamics in flocculated systems was found to accurately represent the creaming behaviour.

The failure of the phenomenological model to predict the creaming behaviour of flocculated emulsions has led to a different, smaller scale modelling approach to combined flocculation and creaming. The next chapter describes a statistical model which is designed to investigate the effect of flocculation characteristics on creaming profiles, by simulating the system at the level of the individual particles rather than through a phenomenological description.

Chapter 3 : Lattice Modelling of Creaming and Flocculation

The creaming model presented in the previous chapter illustrated the qualitative form of the concentration profiles which would be expected in an ideal emulsion. Initially, no direct particle interactions were included. It was noted that many experimental studies have observed markedly different profiles to those predicted by the model. These differences are thought to be due to direct particle interactions, specifically flocculation, which were omitted from the phenomenological model. While an attempt was made to include the effects of flocculation in the model in a phenomenological manner, the numerical results were not able to reproduce the concentration profiles which have been observed in practice. The analysis indicated the difficulty of incorporating into a phenomenological model a process which occurs at the level of individual particles.

For this reason, a model was developed to assess the effect of flocculation on creaming behaviour by simulating these processes at the particulate scale. Inevitably, such a model can only represent a very small sample, because of the large number of particles contained in an emulsion. It can no longer represent the emulsion at the scale of creaming experiments in the ultrasound scanner, but is intended to indicate the form of concentration profiles expected in the presence of flocculation. The aim of the model is to determine whether the creaming behaviour observed in experimental systems is explicable solely in terms of particles sticking together to form flocs (and thereby creaming more rapidly) or whether other processes are at work.

3.1 The fractal nature of flocculation

Fractal geometry has been shown to provide a useful, simple description of flocs generated by a variety of means (Meakin, 1988, Jullien, 1990). The fractal dimension (or dimensionality) can be applied to obtain the scaling relationships of properties such as the creaming speed, or floc size, in terms of the number of particles in the floc. The fractal dimension of an aggregate or floc also holds information on the degree of compactness of any particle network which might be generated through flocculation. Before these

techniques are described in relation to the lattice model, it is first necessary to provide a brief introduction to the concept of fractal geometry.

The term "fractal" was first introduced by Mandelbrot (1975) to describe ramified structures which do not lend themselves to definition by Euclidean geometry. The need for such a concept was indicated by the existence in nature of convoluted physical forms such as coastlines, clouds, and aggregates. The Euclidean geometry of squares, triangles, etc. comes nowhere near a proper description of such structures. Fractal structures are those that can be characterised by a non-integer dimensionality (Mandelbrot, 1982, Vicsek, 1989). This fractional (fractal) dimension can be defined in terms of the number of small measuring units (of dimension equal to the Euclidean dimension of the embedding space) which are required to cover the structure completely. This is a measure of how space-filling the structure is. In a fractal object, the required number of measuring units, n_L, scales with the size of the object, L, in the form

$$n_L \propto L^{d_f} \qquad [3.1]$$

It is clear from this relationship that, if the fractal dimension d_f is equal to the Euclidean dimension of the embedding space, the object fills the space uniformly. In three dimensions this may correspond to a homogeneous dispersion. A non-integer dimension represents the sparse, convoluted nature of fractal objects. For example, a coastline is embedded in (approximately) two-dimensional space, but may have a fractal dimension between one and two. This represents its greater space-filling capability than a straight line, but its inability to fully cover a two-dimensional surface. An aggregate grown in three dimensions typically has a fractal dimension less than 3, indicating that it becomes more sparse the larger it grows. In many real cases, the fractal scaling behaviour is not universal, but applies over a limited range of length scales.

Many fractals have a property called self-similarity, which arises from the scale-invariant nature of equation 3.1. Self-similarity means that the structure of the fractal object is invariant under an isotropic change of length scale. This quality applies precisely in mathematically generated fractal structures, for example in the illustrations presented by Mandelbrot (1982). In real, physical systems, however, self-similarity is only true statistically, or on average. In other words, taking aggregation as an example, an expanded view of one section of an aggregate will not exactly match the original aggregate in structure. It does, however, correspond to the structure of an aggregate

which could statistically have been produced by the same aggregation process. An alternative type of fractal is one in which different fractal dimensions are required to define the scaling behaviour in different co-ordinate directions. Such fractals are called self-affine.

In relation to flocculation, the results of fractal geometry have been shown to be applicable to many aggregation phenomena in two and three dimensions. The suitability of a fractal description of aggregates (or flocs) is evidenced both by the structure of experimentally produced samples, and by computer simulations of their growth which have demonstrated fractal scaling behaviour. Meakin (1988) presents an example of an experimentally produced colloidal gold aggregate which exhibits self-similarity and for which a fractal dimension can be calculated. A substantial amount of work over the last 15 years has been devoted to computer simulation of aggregation growth phenomena. In all cases, a fractal description of the aggregates was found to apply. Useful reviews of the computational techniques and results for the fractal dimensions under various conditions can be found in the works of Jullien (1990) and Meakin (1988). Many different techniques have been used, relating to deposition of particles onto a surface, the growth of an aggregate by the addition of single particles in turn, the aggregation of particles into clusters and clusters into larger clusters, etc. The fractal dimension is affected by the physical conditions represented by the computer simulation, and in some cases by the spatial constraints of the model (for example, the shape of the lattice in lattice models). However, the results of the computational studies indicate that fractal geometry is a valid description of aggregating (or flocculating) systems, and is therefore applicable to the present work.

The fractal nature of flocculation is relevant to the lattice model of creaming and flocculation in two respects. Firstly, the fractal dimension of the flocs can be used to define the scaling behaviour of the creaming speed and diffusion coefficient with floc mass. Fractal geometry is of great benefit in similar generalised descriptions of the dependence of physical parameters of an aggregate with its size or mass. It does not define the detailed structure of the individual floc, but acts as a description of the statistical average of the properties of such aggregates. In the lattice model, a fractal dimension of the flocs is assumed, based on previous results, in order to determine the creaming and diffusion rates of flocs of varying sizes. Thus, the properties of the flocs

are defined in a statistically averaged manner, rather than considering the structure of an individual floc to assess the effect on its mobility. The second use of the fractal dimension in the model is to quantify the degree of compactness of any space-filling particle network which may be formed. The fractal dimension was calculated over a region of the sample, to compare the structures formed under different conditions.

The flocs considered in this study are assumed to be self-similar, so that a single fractal dimension is valid. It could be argued that in a creaming (or sedimenting) field, preferential growth may occur in the vertical direction, resulting in a self-affine fractal. However, self-similarity and a single fractal dimension are assumed for the lattice model. The fractal relationship between the number of particles, $N(R)$, within a sphere of radius R is given by

$$N(R) \propto R^{d_f}, \; N(R) = \left(\frac{R}{r}\right)^{d_f} \qquad [3.2]$$

For a single floc, the radius R is equivalent to the radius of the floc, r_f, and N then represents the number of particles in the floc. This applies to a floc which is composed of many identical spheres. The second equality has been provided for consistency down to the scale of a single particle (of radius r). This need not always be true, but is convenient for the lattice model. Equation 3.2 can be used as a simpler definition of the fractal dimension in its application to flocculation. This relationship (equation 3.2) provides the basis for the scaling behaviour of creaming and diffusion coefficients, which are described in later sections. It is also the expression used to obtain the fractal dimension of the particle networks generated by the flocculation and creaming processes.

3.2 Overview of model

A very simple approach to the problem of creaming and flocculation has been adopted for the small-scale model developed in this study. In order to enable a reasonable size of system to be modelled, and for computational simplicity, a lattice model was used, rather than a more complex continuum Brownian dynamics simulation. It was based on two previously published models of sedimentation (van der Knaap et al., 1994, Huang and Somasundaran, 1988), both of which were in two dimensions, and only one of which included flocculation (van der Knaap et al., 1994). The essence of a lattice

model is that the positions of the particles are constrained to coincide with the nodes of an imposed lattice structure. Particle movement is achieved by pseudo-random steps between lattice sites, weighted according to the required physical rate of motion (for example, the creaming speed or diffusion coefficient).

The model developed for the study of creaming and flocculation is three-dimensional and is based on a cubic lattice. Figure 3.1 shows a schematic diagram of the lattice model. The excluded volume of rigid particles is accounted for by choosing a lattice spacing equal to the particle diameter. The model is therefore restricted to monodisperse systems. Each lattice site can only be occupied by a single particle at any time. Initially, particles are assigned at random to positions on the lattice, up to the required proportion of occupation. Particle movement is executed by selecting a particle at random and moving it to a new site according to its predefined creaming and diffusion rate. During each time interval, every particle is given the opportunity to move. No hydrodynamic interactions are included other than the obstruction caused when a particle attempts to move to an already occupied lattice site. Such movement is forbidden by the single-occupancy criterion.

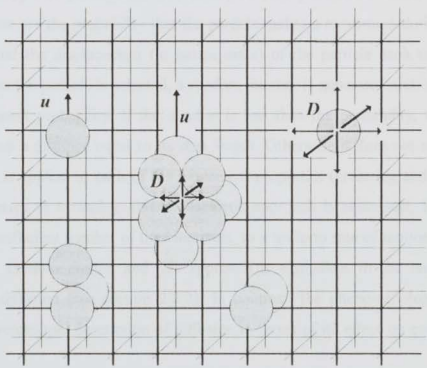

Figure 3.1 Schematic diagram of lattice model of creaming and flocculation.

Creaming is always upwards and the speed is denoted by u. Diffusion occurs in any direction, and the diffusion coefficient is denoted by D. The lengths of the arrows represent the relative magnitudes of each motion for single particles and flocs.

The effects of flocculation are included in the model by allowing neighbouring particles to stick together. The presence of polymer (which is the driving force for depletion flocculation) is not included explicitly, but its effects are accounted for through the formation of flocs, with an adjustable "bonding" probability, P_{bond}. Once particles have stuck together to form a floc, the floc moves as a single unit and is assigned its own motion characteristics according to its size. It was expected intuitively that the greater creaming velocity attributed to individual flocs would increase the overall creaming rate in the system when flocculation was included. The break up of flocs is also included, representing reversible flocculation in which the thermal energy is sufficient to separate previously "bonded" particles. The degree of reversibility is determined by a bond breakage probability, P_{break}. The modelling procedure is very similar to that adopted by Haw et al. (1995), in the study of gel formation, although creaming was not included in their systems.

3.3 Physical processes included in the model

For each type of particle motion, there are two parameters which define the movement. These are the probability that the particle makes a movement during a single time interval, and the displacement (in lattice units) of the particle each time it does move. Each time the particle is selected, a random number is generated and is compared with the movement probability. If the number is less than the probability, the particle attempts to move a distance equal to its step length. Otherwise it does not move at all. This procedure is applied to each of the movement properties (creaming and diffusion). For a process such as creaming, this probabilistic approach is equivalent, for a single particle over a sufficient number of time intervals, to a uniform rate of motion. Diffusion is essentially a random motion and this approach is equivalent to the random walk description of diffusion (see section 2.2.2). In contrast, the phenomenological model adopted the macroscopic description of diffusion in terms of its effect on concentration gradients.

3.3.1 Gravity (creaming)

The creaming process was described in section 2.2.1. It was shown that a particle reaches a terminal, uniform velocity equal to the Stokes velocity (equation 2.7) in an infinite medium in the absence of other particles. Hydrodynamic interactions reduced the

average creaming speed by an amount dependent on the particle concentration. Hydrodynamic interactions are not included in the lattice model, except for the obstruction of particle movement due to other particles occupying the destination lattice site. In a monodisperse sample in which no flocculation occurs, the creaming speed is the same for all particles. However, the presence of flocs causes the creaming speed to vary, according to the size of the floc. It was shown in section 3.1 that the number of particles in a fractal floc is related to its effective radius by equation 3.2. The effective density of the floc can be calculated from this result, and thereby the net gravitational force on the floc. If the "Stokes" drag on the floc is proportional to the floc radius (just as it is proportional to the radius of a rigid sphere), the force balance equation can be used to show that the "Stokes" creaming speed of the floc is given by

$$u_{0,N} = \frac{2r^2 g\Delta\rho}{9\eta} \cdot N^{\left(1-\frac{1}{d_f}\right)} = u_0 N^{\left(1-\frac{1}{d_f}\right)} \qquad [3.3]$$

where d_f is the fractal dimension and u_0 is the Stokes velocity of a single particle of radius r. This relationship is valid for a fractal floc made up of N identical particles. Equation 3.3 is equivalent to the creaming velocity used for flocs in the phenomenological creaming model (equation 2.68). The larger the floc, the faster its creaming rate, in the absence of additional obstruction. A fractal dimension of 2 was used in the calculation of creaming speeds for all flocs. This value is approximately that obtained by computer simulations of aggregation under a variety of conditions. Many of these values can be found in the review of Jullien (1990). Although the fractal dimension is slightly different for different modes of aggregation, the effect of this variation on the creaming speed is negligible compared to the dominant influence of floc size.

Although the creaming process is not in essence a random one, it can be described in terms of randomly generated motion in order to be compatible with the lattice model. The motion is described by a probability of movement during each time interval, and a step length (in lattice units), which is the distance moved by the particle or floc when it does make a movement. If the creaming speed is written in lattice units per time interval, the relationship is given by

$$p_{\mathrm{crm},N} l_{\mathrm{crm},N} = u_{0,N} \frac{\Delta t}{2r} \qquad [3.4]$$

The lattice unit is equal to the particle diameter. The step length is chosen for each floc size in order to keep the probability within predefined limits (it certainly cannot be greater than unity). A maximum step length of six lattice units was specified. When a particle or floc is to be moved, a random number is generated. If the number is less than the creaming probability of the particle, p_{crm}, a displacement is attempted. The particle tries to move a vertical distance equal to its step length l_{crm} (in lattice units). If this displacement is obstructed by other particles, it moves as far as it can vertically, up to its allowed step length.

3.3.2 Thermal diffusion

Thermal diffusion was discussed in section 2.2.2. The diffusion coefficient for a single isolated particle in an infinite medium is given by the Stokes-Einstein equation (equation 2.23). For flocs, the Stokes drag force is related to the radius of the floc, r_f, which was expressed in terms of the number of particles in the floc by equation 3.2. Thus the modified Stokes-Einstein diffusion coefficient for flocs can be written as

$$D_{0,N} = \frac{k_B T}{6\pi\eta r} \cdot N^{-\frac{1}{d_f}} = D_0 N^{-\frac{1}{d_f}} \qquad [3.5]$$

where d_f is the fractal dimension and D_0 is the diffusion coefficient of a single particle. The equation is again valid for a floc made up of N identical particles. The diffusion coefficient is reduced as more particles are added to the floc. The fractal dimension was defined to be 2 for these calculations, for the reasons discussed in the previous section. Rotational diffusion was neglected in this model.

The description of diffusion in the lattice model is that of a random walk. This is in contrast to the phenomenological model of creaming in which the only effect of diffusion was to smooth out concentration gradients. The two parameters defining the diffusive motion are again a probability of movement in each time step, and a step length (in lattice units). The step length is the displacement of the particle or floc in any direction when it makes a movement. The random walk result for the mean square displacement of an object was derived by Einstein, and was presented in chapter 2 (equation 2.9). In terms of the diffusion coefficient, it can be written as

$$\langle R^2 \rangle = 6Dt \qquad [3.6]$$

The lattice model requires the motion to be expressed in relation to the movement probability and step length. Another random walk result is useful here. If an object executes a random walk, with each step being the same length l_{walk}, its mean square displacement after m steps is given by

$$\langle R^2 \rangle = l_{walk}^2 m \qquad [3.7]$$

In the lattice model, the object (particle or floc) has a constant step length, and the number of steps executed in any time period is related to the movement probability. Therefore, the diffusion parameters can be expressed as

$$l_{walk} = l_{diff,N}(2r), \quad m = p_{diff,N}\frac{t}{\Delta t} \qquad [3.8]$$

The units of length have been converted to the lattice spacing, which is equal to the particle diameter. A comparison of equations 3.7 and 3.6 with these results shows that the movement probability should be related to the diffusion coefficient by

$$p_{diff,N} = 6 \cdot \frac{D_{0,N}\Delta t}{(2r)^2} \cdot \frac{1}{\left(l_{diff,N}\right)^2} \qquad [3.9]$$

The factor which includes the diffusion coefficient is equivalent to the diffusion coefficient expressed in units of the lattice spacing and the time interval.

In the case of diffusion, the step length was restrained always to be equal to a single lattice unit. This avoided difficulties relating to non-uniformity of concentration profiles caused by particles making large steps near the edges of the system. A random number is generated to determine whether the particle takes a step in the current time interval. If the number is less than the diffusion probability, the particle or floc will move. Its displacement is equally likely to be in any of the six co-ordinate directions, and is of a size equal to one lattice unit (provided no obstruction is encountered).

It is important at this stage to highlight the differences in particle movement between the present lattice model and previous models on which the work is based (van der Knaap et al., 1994, Huang and Somasundaran, 1988). In each of the previous models, the creaming and diffusion rates are characterised by a parameter representing the ratio of creaming and diffusion probabilities. In the model of Huang and Somasundaran, the probability of particle movement in each direction is determined

according to the net effect of sedimentation and diffusion. Particles move by a single lattice unit in the selected direction. Flocculation was not included, and therefore the movement probability and step length are the same for all particles.

Van der Knaap et al. (1994) simulated the effects of diffusion by selecting each particle in turn and calculating its displacement according to the predetermined probability, as in the present model. However, the creaming motion was executed for all particles at the same time. On each time step, a single random number determines whether a creaming step will be made in this interval (according to the creaming probability), and all particles are moved by the appropriate distance. This procedure avoids the unphysical obstruction of particles which would otherwise cream at the same speed, which can occur in the present model. The relative creaming and diffusion rates of flocs of different sizes are controlled only through the step length in the model of van der Knaap et al. (1994). The probability of movement by creaming or diffusion is the same for flocs of all sizes, and creaming occurs for all flocs at the same time. However, the distance moved by the floc depends on its size. A maximum step length of five lattice units for creaming and three lattice units for diffusion were defined (van der Knaap et al., 1994). Therefore, there are only five discrete creaming rates, and three discrete diffusion rates, since particles can only move between lattice sites.

In the present model, both the movement probability and the step length can be varied according to floc size. Hence, a near-continuous range of creaming and diffusion rates are permitted. Since the creaming probability is now different for each size of floc, the model follows the method of Huang and Somasundaran for creaming movement. Each particle is moved in turn, as is the case for diffusion. Some obstruction of particles with the same creaming speed will result, but the effect is expected to be small.

3.3.3 Flocculation

Flocculation is the tendency of particles to stick together, when they touch or approach within a certain distance of each other (see sections 1.1.2 and 2.10). In the case of depletion flocculation, this mutual attraction is driven by the presence of polymer or other entities (e.g. surfactant micelles) in the continuous phase. Although the lattice model does not explicitly include such an additional species, its effects are simulated through the sticking probability of particles. In many physical systems flocculation is

reversible, in the sense that the thermal energy of some flocculated particles is sufficient to pull them apart again. This feature can be characterised by the probability that a flocculated "bond" will break apart. The two key parameters which determine flocculation in the lattice model are therefore the bonding and break up probabilities, P_{bond} and P_{break} respectively. The bonding probability, P_{bond}, is the likelihood that a bond will form between neighbouring particles in each time interval. The break up probability, P_{break}, is the probability that an existing bond will break during each time interval.

Flocculation in the lattice model is only permitted between the nearest neighbours on the lattice. Since a cubic lattice is used, there are six such neighbouring sites, each separated from the central particle by one lattice unit. The next nearest neighbours are at a distance of $\sqrt{2}$ times the lattice unit from the central particle, there are 12 such neighbours. The limitation of bond formation to the nearest neighbours therefore corresponds to a very short-range potential (which is the case for depletion flocculation). The reversibility of flocculation relates to the breaking of each "bond" rather to an individual particle breaking off from a floc. A particle which is bonded to more than one nearest neighbour in a floc is less likely to break off than a particle with a single connection. Thus, a more compact structure is favoured in the model, not through an attractive non-bonded potential between particles, but through the greater stability of more closely structured flocs.

The bonding and break up probabilities can be interpreted in terms of an interparticle potential. Figure 3.2 shows a schematic diagram of the interparticle potential energy as a function of their separation, as represented in the lattice model. The plot is not to scale. The spatial extent of the regions of negative and positive energy is negligible in the lattice model, since particles can occupy neighbouring sites with or without being flocculated, and a bond can break without particles moving away to another lattice site. At a separation of $2r$, the potential tends to infinity, which corresponds to the volume exclusion of the rigid particles. The other two notable features are the negative potential well, and the positive energy barrier. The potential well represents the favourable energy state of particles which are flocculated. However, particles at a larger separation must overcome the energy barrier in order to reach the flocculated state. The probability of a particle having sufficient energy to "cross" the energy barrier can be written as a

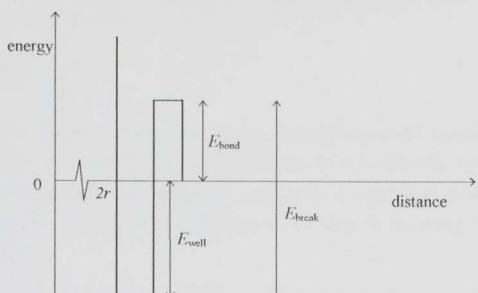

Figure 3.2 Schematic representation of interparticle potential as a function of distance for the lattice model.

E_{bond} is the energy barrier to flocculation, E_{well} the depth of the potential minimum and E_{break} the energy required to escape from the potential well.

Boltzmann factor. This probability is equal to the bonding probability used in the lattice model. Thus

$$P_{bond} \propto \exp\left(-\frac{E_{bond}}{k_B T}\right) \qquad [3.10]$$

The limit of zero bonding probability corresponds to an infinite energy barrier, whereas a probability of one is equivalent to no barrier to flocculation at all. The Boltzmann factor relationship for the bonding probability is valid for this process if the energy barrier is reasonably high (several $k_B T$), and narrow.

The extent of reversibility of the flocculation is determined by the depth of the potential well, as well as the height of the energy barrier. The energy required by a particle to escape from the potential well is represented by E_{break} as shown in figure 3.2, and is the sum of the well depth and the barrier height, thus

$$E_{break} = E_{bond} + E_{well} \qquad [3.11]$$

The break up probability can again be related to the energy required to break the bond through a Boltzmann factor

$$P_{break} \propto \exp\left(-\frac{E_{break}}{k_B T}\right) \qquad [3.12]$$

An infinitely deep potential well represents completely irreversible flocculation, since particles can not escape from the well, once flocculated. It is clear from equations 3.11 and 3.12 that this situation corresponds to $P_{break}=0$. The rate of flocculation is still determined by the height of the energy barrier, and thus, in the model, through the parameter P_{bond}.

A shallower potential well represents a more loosely linked floc, in which particles can break off relatively easily. As the well becomes shallower, the energy required to separate flocculated particles decreases, and the probability of break up increases. The condition at which the potential well vanishes, is equivalent to

$$P_{break} = P_{bond} \qquad [3.13]$$

Although the flocculated energy state in this case is no longer favourable, the energy barrier still prevents particles escaping once a bond is formed. The break up probabilities studied in the lattice model were in the range from zero up to the bonding probability. If the break up probability is larger than the bonding probability, the "flocculated" state is a less favourable energy state for particles than a random distribution. Hence the energy barrier to particles escaping from the "bonded" state is lower than the barrier to formation of that state. This is not physically representative of most real flocculating systems.

3.4 Time evolution

The evolution of the sample is modelled by executing particle motion in a series of small time intervals. In each interval, every particle is selected once at random to execute a displacement. The order in which particles are chosen to be moved is random from within the set of particles which have not yet moved during this time step. Since flocs include many particles, they are more likely to be moved first, because the probability is equal for each particle, rather than for each unit (particle or floc, a floc counts as a single

unit). However, each floc is only allowed one attempt to move during any one time interval.

Having selected the unit (particle or floc) to be moved, the displacement of the particle or floc is determined by its probability and step length for each of the physical processes included in the model (see sections 3.3.1 and 3.3.2). Having calculated the required displacement (which is zero if the particle is not allowed to move in this interval), the destination sites for all the particles in the floc are examined. If any of these sites are already occupied by particles from a different unit (another floc or particle), the displacement is refused. If the displacement was more than one lattice unit, an attempt is made to achieve a smaller displacement without obstruction. It is clear that although flocs have a faster creaming speed, they are also more likely to be obstructed than single particles, because of their larger collision cross-section. After the unit's displacement has been determined, all neighbouring particles are examined. These may be new neighbours due to the new position of the unit, or existing adjacent particles within the floc. Each neighbouring pair which is not already bonded is allowed to bond, according to the bonding probability. Each existing bond is given the opportunity to be severed, according the break up probability.

This process of displacement followed by flocculation is repeated with each randomly selected particle or floc until all have had opportunity to move during this time interval. A sequence of many such time steps simulates the evolution of the creaming and flocculation behaviour.

3.5 Boundary conditions

3.5.1 x and y periodic boundaries

Periodic boundary conditions are used in many simulations in order to model the effect of a much larger system, whilst only in fact simulating the motion of a relatively small number of particles. The two opposite boundary walls are made to "wrap-around" so that any particle moving out of one side of the system appears at the other side. Instead of only looking at a single computational "box", the system behaves like an infinite array of identical "boxes" neighbouring each other. No new information is contained in the other boxes, since they are identical, but the technique removes the need

to impose containing walls on each side of the computational area, which would confine the particles and influence their motion. Periodic boundaries were adopted in the lattice model in the two horizontal directions (x and y).

3.5.2 z boundaries

The effects of creaming cannot be seen without an impenetrable boundary in the vertical direction, corresponding to the top or bottom of the sample. Adoption of a periodic boundary in the vertical direction would allow creaming, diffusion and flocculation to continue, but the sample would remain essentially uniform. A serum or cream can only be observed in the presence of an impenetrable boundary. The lower limit of the vertical co-ordinate (z) is simply treated like the bottom surface of an emulsion. No particles are supplied from below, so that when particles move up from the bottom, the concentration of particles is reduced, just as in the development of a serum layer. Similarly, the top boundary of the system was treated like the top of an emulsion, that is, no particles are allowed to move beyond the top boundary. Therefore, a more concentrated region is expected to develop at the top of the sample. Periodic boundaries were used in this model only to study diffusion limited and reaction limited aggregation, since the effects of creaming were then removed (see section 3.9.1).

3.6 Calculation of fractal dimension

The fractal dimension is a useful parameter for describing aggregate structure, in particular the degree of compactness of flocs. In many previous studies of aggregation processes, the fractal dimension was calculated for a single floc, which was grown by simulation or experiment. However, in a relatively concentrated system, such as that simulated by the lattice model, the definition of individual flocs as fractal entities becomes inappropriate, as the flocs link together and form a particle network. However, a fractal (or scaling) dimension can still be specified for the structure as a whole, since it is a characteristic of the particle density (equation 3.2). The particle distribution is equally well defined for a particle network as for an individual floc. For any selected particle, the dependence on distance of the number of particles within a given distance can readily be calculated. These particles need not necessarily be connected. If a linear

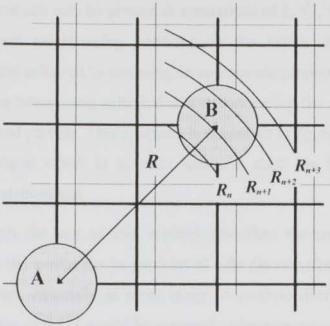

Figure 3.3 Calculation of the particle distribution function in the lattice model. A proportion of the volume of particle B, which is at a distance R from particle A, is assigned to each of the spherical shells denoted by R_n etc.

region can be found in the relationship between $\log(N(R))$ and $\log(R)$, the gradient of this region is equal to the fractal (scaling) dimension of the structure (equation 3.2).

In the lattice model, the particle distribution is calculated using, as central points, each of the particles which are present in a specified horizontal layer. For each of these particles (for example particle A in figure 3.3) the distance from it of all other particles is calculated. For example, particle B in figure 3.3 is at a distance R from particle A. The particle distribution is then obtained by counting the numbers of particles within each distance range, R_n. The distance ranges are equivalent to spherical shells, each of a specified thickness, as shown in the diagram. The particle distribution is specified by the number of particles within each shell. A sum of the distributions over all of the central particles yields an average particle distribution function in the locality of the horizontal layer.

Initially, the distribution was calculated by recording each particle at the position of its lattice site (its centre of mass). However, it was found that this caused a significantly lumpy distribution due to the existence of only discrete particle separations because of the geometry of the cubic lattice. For example, in the close proximity of a particle,

another particle can only be present at separations of 1, $\sqrt{2}$, $\sqrt{3}$ etc. (lattice units), which are the closest neighbouring positions on the lattice. Refinement of the particle distribution was achieved by assigning an appropriate proportion of the particle's volume to each of the intersecting spherical shells representing the consecutive distance ranges from the central particle. This approach is illustrated in figure 3.3. The proportion of the particle's volume which is in each spherical shell can be calculated from simple geometrical relationships.

Although the use of this method smoothes the particle distribution function considerably, the availability to particles of only discrete sites on the lattice still distorts the distribution, especially at close range. A random distribution of particles with a volume fraction of 0.524 would be expected to have on average an equivalent volume of 3.655 particles within a distance of 1 particle diameter of any other particle. However, a fully occupied cubic lattice (which has the same volume fraction of 0.524) has only the equivalent of 2.609 particles within this range. The uneven nature of the particle distribution in the lattice model is to some extent smoothed out in the overall distribution function $N(R)$ especially at distances larger than a few diameters. However, to remove some of the artificial effects of the lattice structure on the distribution function, all results were scaled according to the distribution which would be obtained if the lattice were fully occupied.

In the fully occupied lattice, the numbers of particles in each distance range is a measure of the maximum volume available to particles on the lattice within that range. $G_0(R_n)$ represents the number of particles (as an equivalent volume) on a fully occupied cubic lattice in the distance range denoted by the argument R_n. The argument R_n represents the spherical shell between a distance of R_n and R_{n+1}, as shown in figure 3.3. The calculated number of particles in this distance range in another lattice simulation is represented by $G(R_n)$. Therefore, the *proportion* of the available volume occupied by particles in this shell is $G(R_n)/G_0(R_n)$. Hence the *effective* number of particles in this range should be equal to this proportion, scaled by the actual spatial volume in the spherical shell (which is the available volume if the particles were not restricted to lattice sites). Thus

$$G_{\text{eff}}(R_n) = \frac{G(R_n)}{G_0(R_n)} \cdot \frac{4\pi}{3}\left[R_{n+1}^3 - R_n^3\right] \qquad [3.14]$$

The total number of particles $N(R)$ is obtained by summation over all the distance ranges (shells) up to the required distance. The fractal dimension itself is determined from the gradient of a linear fit to the logarithmic relationship of $N(R)$.

In the lattice simulations, the fractal dimension is calculated over the range four to ten particle diameters, which was found to obey fractal scaling in all cases. At smaller length scales, the floc structure causes fluctuations in the particle distribution, and a fractal scaling description is invalid. At long distances, the particle distribution becomes homogeneous, and the fractal dimension approaches 3. The fractal dimension over the chosen length scale is characteristic of the scaling properties of the structure in the locality of the horizontal slice used for the central particles. It is only meaningful in a region in which the particle concentration is approximately constant, since in the presence of a concentration gradient, the particle distribution is affected by the changes in average concentration as well as by the structure of the dispersion. Therefore, the fractal dimension was only calculated in the region of the sample between the serum and cream regions, where the concentration is reasonably uniform.

3.7 Computer requirements

The lattice model program was written in FORTRAN 77, and was executed using the Sun SPARCenter 2000 and Silicon Graphics Challenge XL servers at the University of Leeds. Random number generation was achieved using the Numerical Algorithms Group FORTRAN Library subroutines (mark 15). A single pseudo-random number sequence was used for each program run. A flow diagram of the program is shown in figure 3.4, and the code is given in Appendix A3. An expanded flow diagram of the flocculation section which forms and breaks bonds is shown in figure 3.5. The model is CPU-intensive, and the size of the system and number of particles were tailored to the available resources. A typical simulation of 100,000 particles, with 2400 time steps takes up to 5 days of CPU time to run when floc break up is included. The program requires approximately 24 Mbytes of memory.

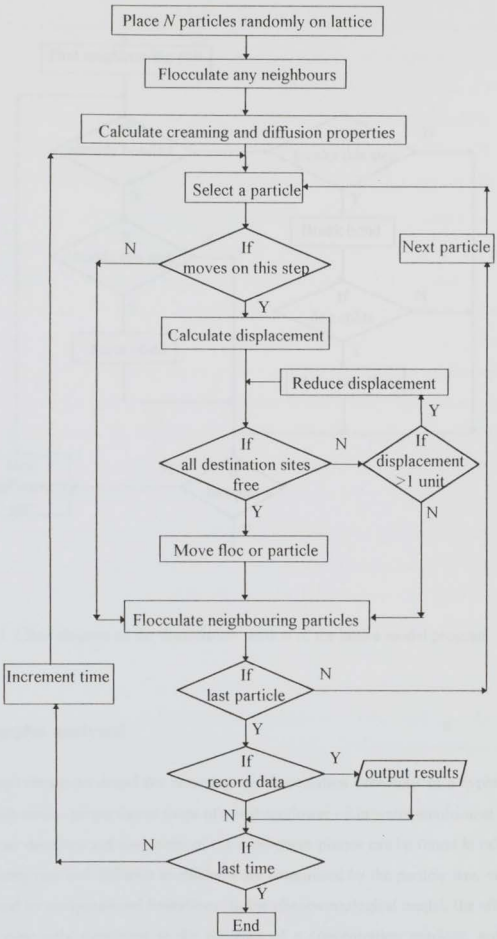

Figure 3.4 Flow diagram of lattice model program of creaming and flocculation

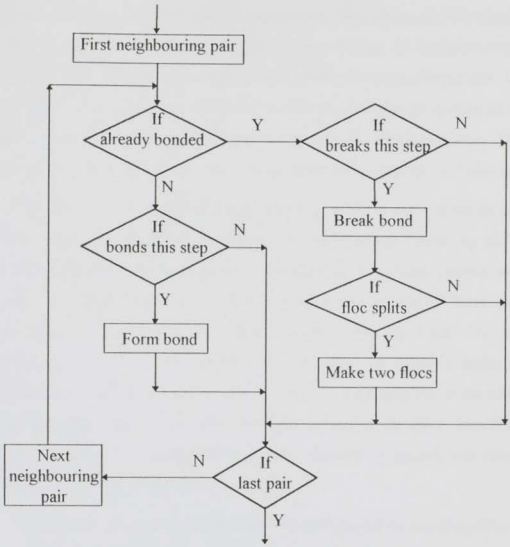

Figure 3.5 Flow diagram of the flocculation section of the lattice model program.

3.8 Samples analysed

It was chosen to model the creaming and flocculation behaviour of a hypothetical sample with similar properties to those of a real sunflower oil in water emulsion at 30 °C. The relevant densities and viscosities of the component phases can be found in table 2.1. The creaming rate and diffusion coefficients are determined by the particle size, which is largely fixed by computational limitations. In the phenomenological model, the effects of diffusion were only significant in the presence of a concentration gradient, and were found to be relatively small. However, individual particles of colloidal size are very

diffusive, executing extensive random walk motion. The lattice model incorporates this random walk motion and therefore requires a large amount of computational resources to model the diffusion, for only a small development of creaming behaviour. A relatively large particle size was chosen, therefore, so that the creaming properties of the system could be observed without excessive computation of diffusive motion. The particle diameter used in the calculations was 1.2 μm, and this also defines the lattice spacing.

Equations 3.4 and 3.9 define the movement probability and step length for particles and flocs. Since the movement probability for each process (creaming and diffusion) must be less than unity, the time step is constrained by the limiting displacement allowed for each movement. The fastest creaming speed is for the largest flocs, whereas the largest diffusion coefficient is for single particles. The step length for creaming is permitted to be as much as six lattice units. However, the diffusive displacement was defined to be a single lattice unit in all cases, due to inconsistencies in the concentration profiles when this was not the case. The time interval is therefore determined by the diffusion probability for single particles. A time step of 0.25 seconds was chosen for the modelling of the sunflower oil in water system.

The number of particles in the sample is determined by the proportion of lattice sites which are occupied. In the systems analysed, an initial occupancy of 10 % was used. This corresponds to a volume fraction of 0.052 (due to the volume of a sphere compared with its circumscribing cube). An occupancy of 100 % is therefore equivalent to a volume fraction of only 52 %, so the high concentrations observed in some creams are not possible in the model. The dimensions of the lattice were usually taken to be 70×70×200. The calculation of fractal dimension takes an average over all particles in a single layer, so that each determination is an average of approximately 490 particle distribution functions. In order to obtain good statistical averages of all the system properties, five simulations were carried out for each set of parameters. For the diffusion limited and reaction limited aggregation, different lattice dimensions and volume fractions were used, and these are defined in section 3.9.1.

3.9 Results

3.9.1 Diffusion limited and reaction limited aggregation

Two cases of the growth of aggregates under different limiting conditions are well-established: diffusion limited aggregation and reaction limited aggregation. Both of these conditions have previously been simulated in the absence of a gravitational field, with particle motion determined by diffusive random walks. The two conditions correspond to different limiting values of the bonding probability. In the diffusion limited case, the bonding probability is unity, so that as soon as one particle touches another particle, they stick together. The aggregation process is therefore characterised by the dynamics of particle motion. In the other extreme, if the bonding probability is very low, as in the reaction limited case, particles must collide many times before a bond is formed. This is equivalent to a significant energy barrier which must be overcome to stick particles together. The characteristics of particle motion are secondary to the size of the energy barrier in determining flocculation in this case.

In the lattice model, these two conditions were simulated to calculate the fractal dimension for comparison with previous work. Periodic boundary conditions were imposed on the top and bottom boundaries in the vertical direction for these simulations, and the lattice dimensions were $100 \times 100 \times 100$. All creaming speeds were set to zero, to represent the absence of a gravitational field. The samples were extremely dilute, as was the case in previous simulations, with a lattice occupation of 0.005, or 5000 particles. No break up of flocs was permitted, and the system was allowed to evolve until all particles had aggregated into a single cluster. For the diffusion limited case, the bonding probability was unity, and for reaction limited kinetics a bonding probability of 0.001 was used. Ten simulations were carried out for each set of parameters. The calculations of the particle distribution $N(R)$ were carried out using every particle in turn as the centre for the distribution, so in each case the distribution is an average over 5000 particles.

The fractal dimension was determined over the range 4 to 10 particle diameters from the gradient of the logarithmic plot of the particle distribution function (figure 3.6). The fractal dimension obtained in the diffusion limited case was 1.8 and for the reaction limited conditions 1.9, although the difference in gradient can not be identified visually. Quoted results in the literature are 1.8 and 2.1. for the diffusion and reaction limited

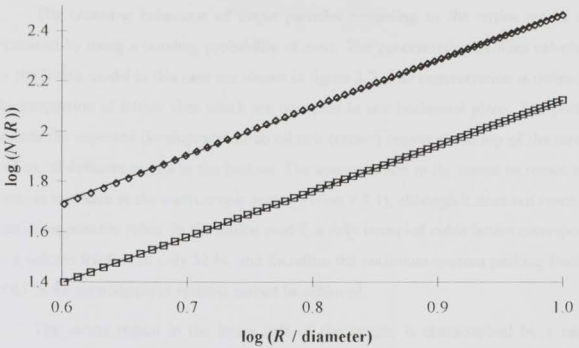

Figure 3.6 Number of particles *N(R)* within a distance *R* for diffusion limited and reaction limited aggregation.

□ is for diffusion limited aggregation and ◇ for reaction limited aggregation. The lines are the best straight-line fits.

conditions respectively. The lattice model result for diffusion limited aggregation is therefore in agreement with previous work. The reaction limited value is rather low for the lattice model, but it is at least larger than the diffusion limited case. It may be that the bonding probability used (0.001) is not sufficiently small to obtain the limiting fractal dimension at low bonding probability. A lower probability takes too long to simulate (the lattice model is not optimised for this type of simulation) and was not attempted. In addition, the concentration of particles may be too great to allow the isolated growth of small flocs before these link together to form a single aggregate. The spatial restriction on floc growth would influence the fractal dimension obtained. As flocs become larger, the fractal dimension in the reaction limited case approaches the diffusion limited value anyway. The results indicate sufficient confidence in the lattice model to draw conclusions from the calculations of fractal dimension in creaming and flocculation studies. It is likely that the differences in fractal dimension obtained under various flocculation conditions are of most interest, rather than their absolute values.

3.9.2 Single particles

The creaming behaviour of single particles according to the lattice model was examined by using a bonding probability of zero. The concentration profiles calculated by the lattice model in this case are shown in figure 3.7. The concentration is defined as the proportion of lattice sites which are occupied in any horizontal plane. The profiles include the expected development of an oil rich (cream) region at the top of the sample and an oil deficient region at the bottom. The concentration in the cream increases with time, as was seen at the macroscopic scale (section 2.8.1), although it does not reach the maximum possible value. In the lattice model, a fully occupied cubic lattice corresponds to a volume fraction of only 52 %, and therefore the maximum random packing fraction of 63 % for monodisperse systems cannot be achieved.

The serum region in the lower half of the sample is characterised by a rather gradual increase in concentration with height. A monodisperse, non-diffusive emulsion would be expected, at the macroscopic level, to show a sharp serum interface, between an oil deficient region (serum) and the uniform emulsion (see for example, the results of section 2.8.1). The concentration profiles from the lattice model in the absence of diffusion are shown in figure 3.8. A comparison of figures 3.7 and 3.8 demonstrates that the spreading of the serum interface is caused by the effects of thermal diffusion. This may be somewhat surprising considering the size of particles used (diameter 1.2 μm). The macroscopic results (section 2.8.1) showed that the effect of diffusion was very small for more diffusive particles of diameter 0.56 μm. The apparently strong influence of diffusion is due to two effects. Firstly, the spreading of a step change in concentration due to diffusion was shown in section 2.2.2 to be most rapid in the early stages. Hence, although the interface has spread significantly over the time scale observed in the lattice model, the rate of spreading will slow down considerably at later times. Secondly, the samples analysed are only 200 particle diameters in vertical extent. The width of the serum interface is therefore only of the order of a few tens of micrometers. On the scale of the model, this appears to be significant, but its width is negligible on the macroscopic scale. If the spreading rate of the interface reduces with time, the interface width can be expected to be reasonable at the macroscopic level.

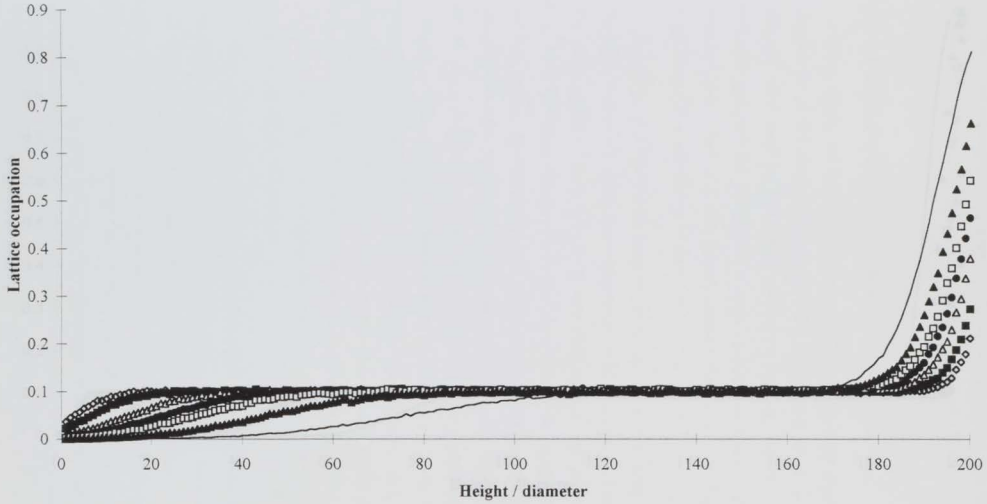

Figure 3.7 Proportion of lattice sites occupied as a function of height, for single particles.
The profiles are for ◇ 1, ■ 2, △ 4, ● 6, □ 8, ▲ 12 and —20 minutes.

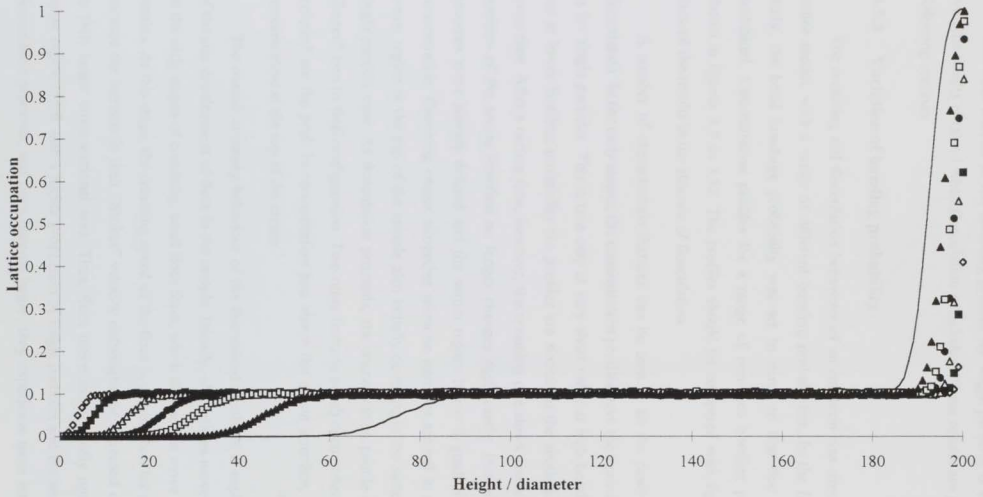

Figure 3.8 Proportion of lattice sites occupied as a function of height, for single particles, in the absence of diffusion. The profiles are for ◇ 1, ▪ 2, △ 4, ● 6, □ 8, ▲ 12 and — 20 minutes.

The main interest in the creaming profiles for single particles is as a comparison with the results obtained when flocculation is included. These results are presented in the following sections.

3.9.3 Variation of bonding probability

The creaming and flocculation behaviour of an emulsion was simulated using the lattice model, with a range of different bonding probabilities. In the first part of the study, the bond breakage probability was set to zero, so that floc break up was prohibited. Concentration profiles for a range of non-zero bonding probabilities are shown in figures 3.9 to 3.12. The profiles should be compared with figure 3.7, which showed the results in the absence of flocculation.

A number of characteristic features can be seen in all the cases which include flocculation. In the early stages, the concentration profiles have the same qualitative form as for single particles. This is true only at very short times at high bonding probability, but at lower bonding probability the profiles are similar to the single particle case for some time. After a certain time, however, the creaming rate slows considerably, and the position of the serum interface no longer changes significantly. Instead, the interface becomes more sharply defined and the serum region below it gradually decreases in concentration. Creaming ceases altogether when no particles are left in the serum. The cream region at the top of the sample also initially develops in the same way as in the single particle case. As flocculation proceeds, the concentration profile in the cream is "frozen" into its final configuration. Two other features which occur when flocculation is included are the peak in concentration just above the serum interface, and the dip in concentration at the top of the cream.

The overall creaming behaviour of the flocculated emulsion is explicable in terms of the size development of flocs in the sample. Initially, all particles move independently. In the early stages of creaming, small flocs form, which themselves move as independent entities. At this stage, the creaming speed of the flocs is greater than for single particles, because the increase in their "Stokes" velocity outweighs the increased obstruction due to their larger cross-sectional area. Thus, flocs move more rapidly upwards, and the lower region is left with a higher proportion of single particles and the smallest flocs. As flocculation proceeds, and flocs become larger, they experience more interference from

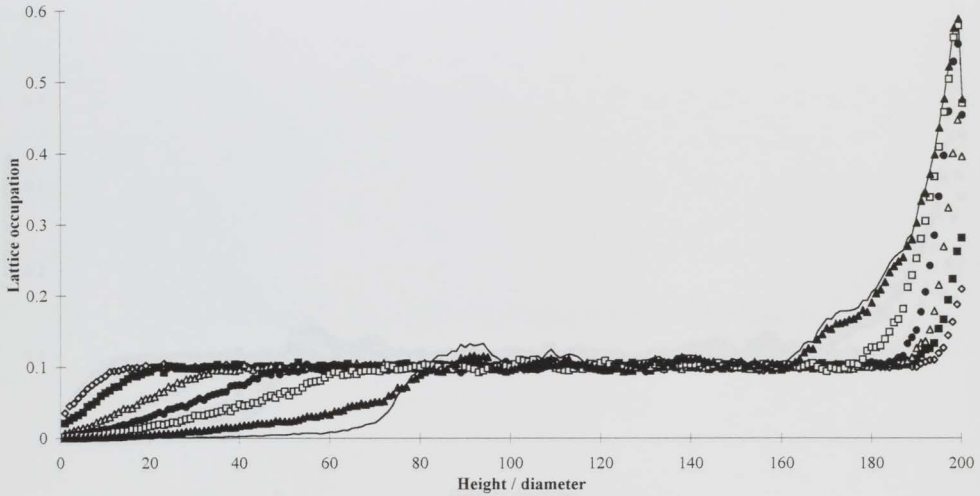

Figure 3.9 Proportion of lattice sites occupied as a function of height, with a bonding probability of 0.001, and no floc break up. The profiles are for ◇ 1, ▪ 2, △ 4, ● 6, □ 8, ▲ 12 and — 20 minutes.

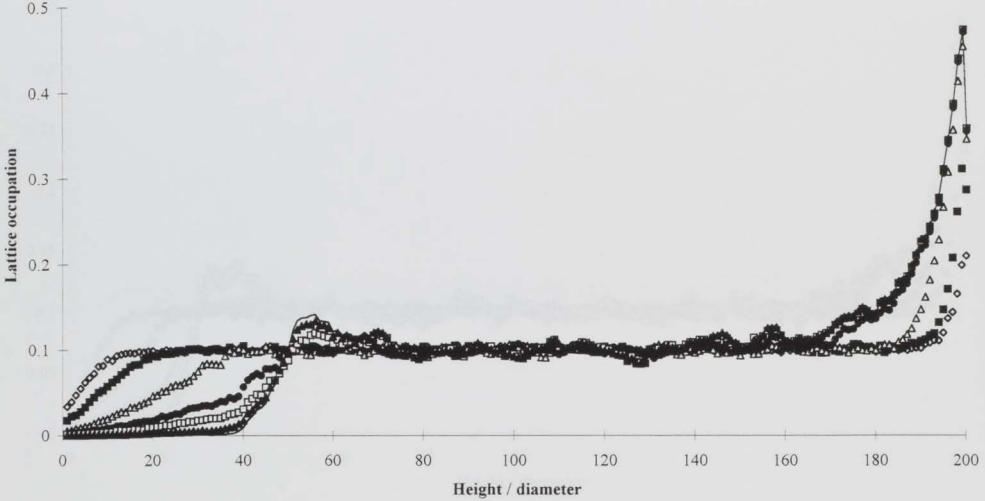

Figure 3.10 Proportion of lattice sites occupied as a function of height, with a bonding probability of 0.002, and no floc break up. The profiles are for ◇ 1, ■ 2, △ 4, ● 6, □ 8, ▲ 12 and — 20 minutes.

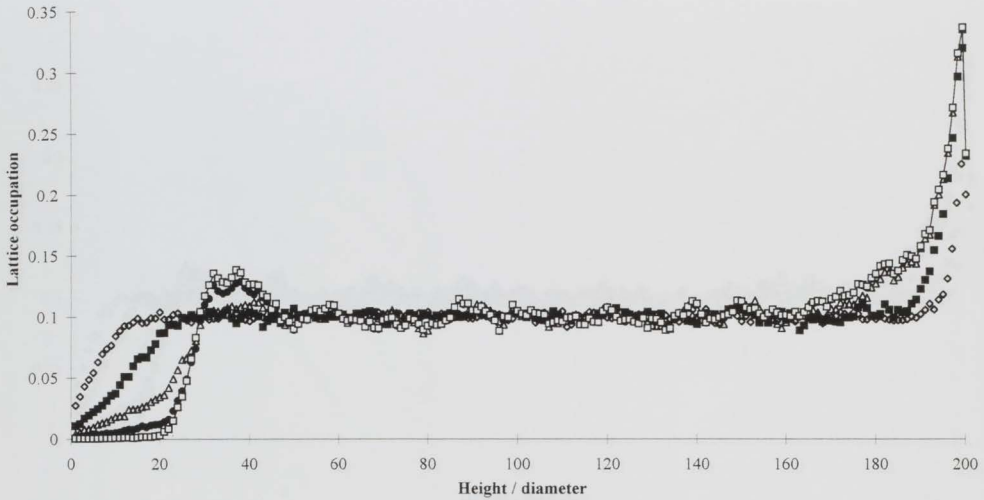

Figure 3.11 Proportion of lattice sites occupied as a function of height, with a bonding probability of 0.005, and no floc break up. The profiles are for ◇ 1, ■ 2, △ 3, ● 5 and ⊟ 10 minutes.

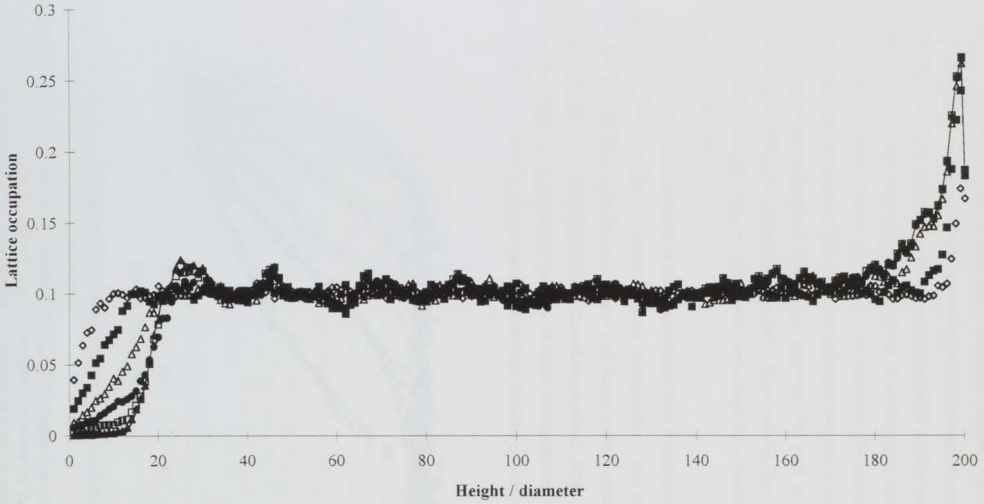

Figure 3.12 Proportion of lattice sites occupied as a function of height, with a bonding probability of 0.01, and no floc break up.
The profiles are for ◇ 0.5, ■ 1, △ 1.5, ● 2, □ 3, ▲ 5 and — 10 minutes.

one another. Flocs link together to form more extensively bonded regions, which have significantly reduced mobility, and which eventually become a single space-filling particle network. The serum has a lower concentration and includes smaller flocs and single particles, due to the relative creaming rates. Hence, it is the region above the serum interface which becomes extensively linked to form a network. The single particles and small flocs in the lower region are still relatively mobile and continue to cream until they meet and bond to the underside of the network structure. The peak in concentration above the serum interface is caused by the smaller, faster moving flocs and particles catching up with and penetrating into the slower networked flocs, thereby forming an accumulation of particles.

In the early stages of flocculation, the production of flocs causes an increase in the creaming rate due to the faster "Stokes" velocity of larger flocs. This can be seen by comparison with the single particle case. Figure 3.13 shows a series of comparisons of concentration profiles in flocculating and non-flocculating systems. After 2 minutes, the concentration profile for a bonding probability of 0.005 shows that creaming is more advanced than for single particles after the same time. Similarly, faster creaming has

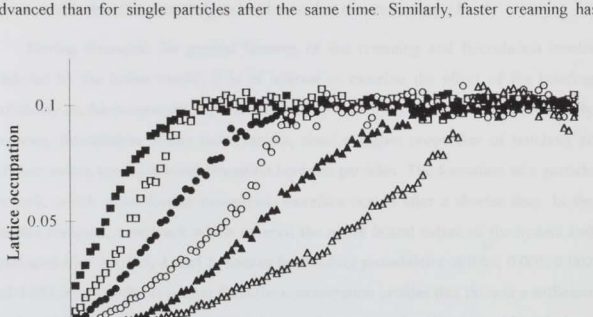

Figure 3.13 Comparison of concentration profiles in flocculated and non-flocculated systems illustrating the change in creaming rate.

Squares represent the profiles after 2 minutes for P_{bond}=0.005 (open squares) and for single particles (closed squares). After 5 minutes, the open circles are for P_{bond}=0.002 and closed circles for single particles. Triangles are for the profiles after 10 minutes of a sample with P_{bond}=0.001 (open triangles) and for single particles (closed triangles).

occurred for a bonding probability of 0.002 after 5 minutes than for single particles. A marked increase in creaming rate can be seen for the sample with a bonding probability of 0.001 after 10 minutes, compared with single particles, also after 10 minutes. At high bonding probability, it is only at very short times that the increased rates can be seen. The difference between the flocculated and non-flocculated systems is more pronounced at later times, provided the system is still free to move.

Flocculation causes the concentration in the cream to be reduced compared to the single particle case (figures 3.9 to 3.12). Particles which are linked together in flocs cannot adopt the most compact packing structure, and therefore the concentration is lower. The dip in concentration at the top of the system is caused by the prevention of flocs or particles penetrating above the top boundary. An approximately spherical floc, which has an extent larger than a single lattice unit, can only move vertically until its uppermost point reaches the top boundary. Hence, the top layer contains a smaller proportion of particles than exists lower down, nearer the centre of mass of the floc. This reduced concentration will only extend one or two particle diameters from the top of the sample, and is therefore not likely to be observed at the macroscopic level.

Having discussed the general features of the creaming and flocculation results predicted by the lattice model, it is of interest to examine the effect of the bonding probability on the concentration profiles (figures 3.9 to 3.12). As the bonding probability increases, flocculation occurs more rapidly, since a higher proportion of touching or collision events results in bond formation between particles. The formation of a particle network, which slows further movement, therefore occurs after a shorter time. In the samples analysed, a network which covered the entire lateral extent of the system had developed after 1.5, 2.5, 4, and 5 minutes for bonding probabilities of 0.01, 0.005, 0.002 and 0.001 respectively. It is clear from the concentration profiles that there is a sufficient number of free particles to allow some degree of creaming after this time, although these eventually join the network and become immobile.

The extent to which a serum or cream is formed in the sample is reduced as the bonding probability increases, because of the shorter time available before the particles are immobilised in the network. The limited time which is available for particles to cream relatively unhindered affects the concentration reached in the cream region. As the bonding probability increases, the concentration of the cream decreases, since it is

formed over a shorter period, before its configuration is "frozen-in" by flocculation. The concentration in the cream may also be affected by the size of the flocs which initially formed it. At low bonding probabilities, the initial creaming behaviour is characterised by smaller flocs and single particles, which are more compact. At higher bonding probabilities, flocs grow to a larger, and therefore more sparse, size before significant creaming can occur, and therefore pack less efficiently in the cream. Hence, the space-filling character of the flocs which formed the cream determinesits concentration. The same effect was observed in two-dimensional simulations of van der Knaap et al. (1994). A relationship between sediment porosity and the form of the interparticle potential was also demonstrated by Ansell and Dickinson (1986).

The time period over which creaming occurs relatively freely also affects the final position of the serum interface, which represents the lower limit of the particle network. At a higher bonding probability, flocculation occurs more rapidly, and therefore the final position of the serum interface is closer to the bottom of the sample. This is clear from a comparison of the concentration profiles, figures 3.9 to 3.12. Although particle movement has not completely ceased at the lowest bonding probabilities simulated, the serum position is still clearly defined in this case. Only a further reduction in the concentration of the serum is yet to occur in these samples.

The variation of the height of the serum interface with bonding probability is shown in figure 3.14. A comparable dependence was demonstrated in two-dimensions by van der Knaap et al. (1994). A functional relationship can be derived between the two parameters of serum interface height and bonding probability. The correct limiting conditions must be obtained at the two extreme values of bonding probability (zero and unity). For single particles (a bonding probability of zero), the height of the interface tends to infinity, since, if the sample is infinitely high, the interface continues to move with a uniform creaming speed. In the other extreme, a bonding probability of unity causes very rapid flocculation. However, the extent of serum formation before networking occurs depends on the initial concentration of particles. At high concentrations, all particles are initially likely to be touching at least one other particle, and therefore linkage occurs immediately and no creaming is possible. At low concentrations, creaming may develop significantly before sufficient contact is achieved to prevent further movement. Hence the limiting condition on the serum height at a

bonding probability of unity is concentration dependent, although at the concentrations used in the simulations it is likely to be very small.

In order to relate the serum position to the flocculation rate, it is more convenient to use the height of the energy barrier as the flocculation parameter, rather than the bonding probability. Zero bonding probability represents an infinitely high barrier, whereas a bonding probability of unity corresponds to the absence of an energy barrier. This semi-infinite range for the energy makes derivation of a relationship with serum height simpler. An appropriate function with the correct limiting dependence was found to be a linear relationship between the energy barrier and the logarithm of serum height. The best fit for this set of data was found to be

$$\ln\left(h_{serum}/2r\right) = 0.3475 + 0.5806\left(E_{bond}/k_B T\right) \qquad [3.15]$$

where h_{serum} is the height of the serum interface relative to the bottom of the sample. The curve generated from this equation is included in figure 3.14. For the systems studied in the lattice model, the bonding probabilities used correspond to a range of the energy barrier from 4.5 to 7 $k_B T$.

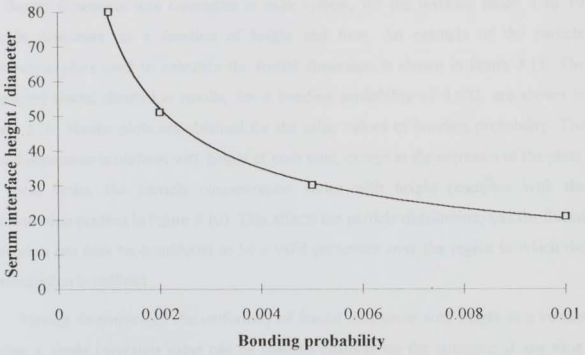

Figure 3.14 The serum interface position as a function of bonding probability in the absence of floc break up.

Open squares are the simulation results, and the solid line is the best fit (equation 3.15)

The final position of the serum interface in a system with irreversible flocculation is specific to the dynamic properties of the particles in the system. These are dependent on both the material properties and on particle size. However, the parameters used in the model are not dissimilar to real experimental systems. Extrapolation of the relationship calculated from the lattice modelling results to a macroscopic scale may be of dubious value. However, assuming that a sample is completely unflocculated at the start of creaming, a serum height of 10 mm, corresponds to an energy barrier to flocculation of the order of 15 $k_B T$, according to equation 3.15. This is certainly not an unreasonable value for a real system. The relationship is of course logarithmic, and therefore a large change in serum position relates to a rather small increase in the energy barrier. The determination of the serum interface position in irreversibly flocculated samples may perhaps be used as an indication of the energy barrier to flocculation under various conditions.

The values of the fractal dimension in the creaming and flocculating samples provides information on the nature of the flocculated structure formed. In these systems, the fractal dimension is a scaling parameter characterising the particle distribution, and is a property of the local network structure, rather than of an individual floc. The value of the fractal dimension was calculated in each system, for the distance range 4 to 10 particle diameters, as a function of height and time. An example of the particle distribution plots used to calculate the fractal dimension is shown in figure 3.15. The calculated fractal dimension results, for a bonding probability of 0.002, are shown in figure 3.16. Similar plots are obtained for the other values of bonding probability. The fractal dimension is uniform with height at each time, except at the extremes of the plots. At these limits, the particle concentration varies with height (compare with the concentration profiles in figure 3.10). This affects the particle distribution, and the fractal dimension can only be considered to be a valid parameter over the region in which the concentration is uniform.

Having demonstrated the uniformity of fractal dimension with height in a certain region, a single (average) value can be used to characterise the structure at any time. Figure 3.17 shows the variation in fractal dimension with time, for each of the irreversibly flocculating systems simulated in the lattice model. In each case, the fractal dimension decreases with time from its initial value of 3 (equal to the dimension of the space). At first, the fractal dimension decreases gradually, but later rather more steeply,

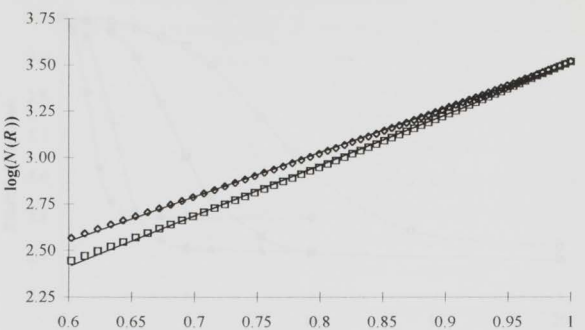

Figure 3.15 Plot of number of particles *N(R)* within a distance *R* used to calculate the fractal dimension.

□ is the distribution after 2 minutes and ◇ after 10 minutes. The bonding probability was 0.005, and the distribution was calculated at a height of 100 diameters.

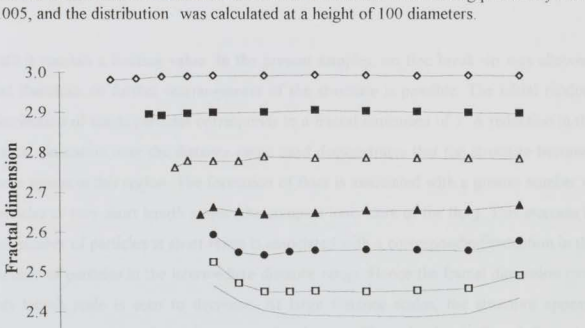

Figure 3.16 Fractal dimension as a function of height and time for a bonding probability of 0.002.

The profiles are for ◇ 1, ■ 3, △ 4, ▲ 5, ● 6, □ 8 and — 20 minutes.

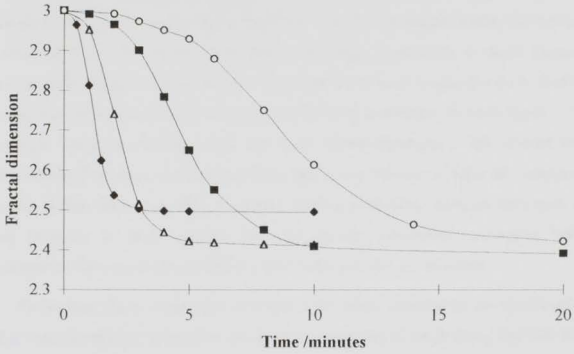

Figure 3.17 Fractal dimension in the uniform region as a function of time for different values of the bonding probability.

The bonding probabilities are◆ 0.01, △ 0.005, ■ 0.002 and○ 0.001.

until it reaches a limiting value. In the present samples, no floc break up was allowed, and therefore no further rearrangement of the structure is possible. The initial random distribution of single particles corresponds to a fractal dimension of 3. A reduction in the fractal dimension over the distance range used demonstrates that the structure becomes more sparse in this region. The formation of flocs is associated with a greater number of particles at very short length scales (the compact inner core of the floc). This increase in the number of particles at short range is associated with a corresponding reduction in the number of particles in the intermediate distance range. Hence the fractal dimension over this length scale is seen to decrease. At large distance scales, the structure appears homogeneous and the dimension approaches 3 again. The reduction in fractal dimension over the distance scale analysed, demonstrates, therefore, the development of compact flocs which later link together into a network. The decrease in fractal dimension becomes more rapid after the initial gradual decline, due to the greater capture efficiency of sparse flocs. The limiting value of the fractal dimension characterises the final structure in the systems in which no break up is permitted.

The effect of bonding probability on the time-dependence and limiting value of the fractal dimension can be clearly seen in figure 3.17. As the bonding probability decreases, the time taken for the fractal dimension to decrease significantly is much longer. However, the limiting fractal dimension of the particle network is also lower. It should be noted that the fractal dimension at the lowest bonding probability shown in figure 3.17 has not yet reached its limiting value. The lower fractal dimension of the network for lower bonding probability indicates that flocs have more freedom to form into compact structures before linking together. At higher bonding probability, particles have such a strong tendency to stick together that the particle distribution undergoes little rearrangement from a random distribution before the particles are all linked.

The limiting fractal dimensions obtained in the lattice simulations are significantly greater than the value (2.0) used for the dynamic properties of single flocs, and than the standard values for diffusion limited and reaction limited aggregation at infinite dilution. It has previously been noted that at finite particle concentrations the fractal dimension can vary significantly from these values. Van Garderen et al. (1995) studied the effect of concentration on fractal dimension and concluded that at very short range, the dilute limit is obtained. However, in the intermediate and long ranges, the fractal dimension gradually increased towards the spatial dimension. Hence values of fractal dimension significantly higher than the dilute limit could be obtained. Similarly high dimensions were found in the simulations of Bijsterbosch et al. (1995), which included an attractive potential between particles. The work includes a useful discussion of the factors which influence the fractal dimension. The relatively large fractal dimension obtained in the intermediate distance range was attributed to interpenetration of the smaller flocs before the structure is "frozen" by the extensive cross-linking. This does not occur in very dilute systems. Although the fractal dimension of the network structure is larger than 2.0, this value may still be applied to the local formation of individual flocs and therefore to the creaming and diffusion properties of the flocs.

3.9.4 Variation of break up probability

The effect of floc break up on the creaming behaviour of flocculated dispersions was investigated by varying the floc break up probability. Simulations were carried out for a bonding probability of 0.005, with no floc break up, and with break up probabilities of 0.001 and 0.002. The concentration profiles are shown in figures 3.18 and 3.19. These

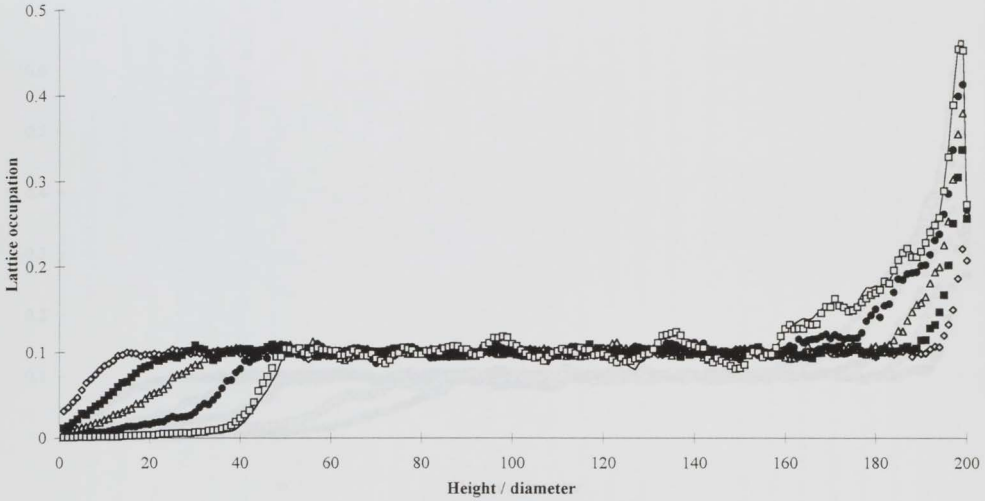

Figure 3.18 Proportion of lattice sites occupied as a function of height, with a bonding probability of 0.005, and a break up probability of 0.001. The profiles are for ◇ 1, ■ 2, △ 3, ● 5, □ 10 and — 12 minutes.

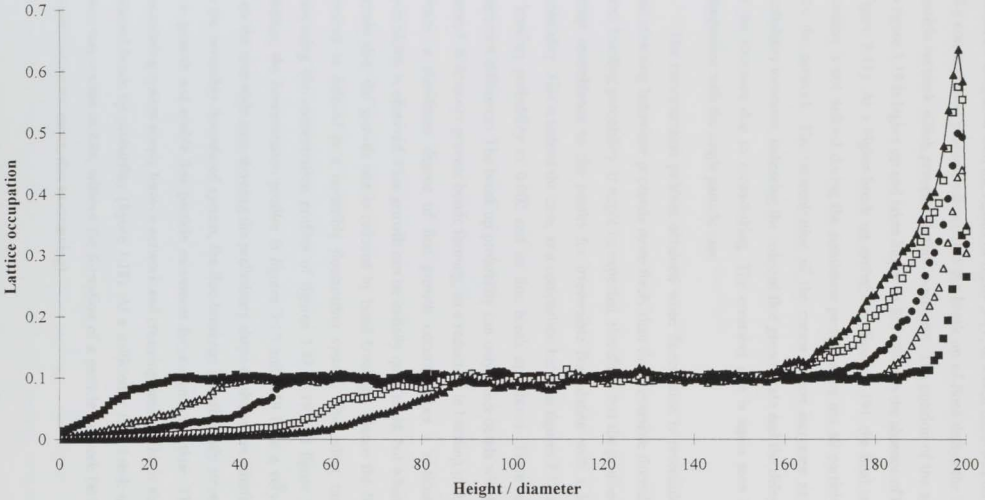

Figure 3.19 Proportion of lattice sites occupied as a function of height, with a bonding probability of 0.005, and a break up probability of 0.002. The profiles are for ■ 2, △ 4, ● 6, □ 10 and -▲-14 minutes.

should be compared with the results of figure 3.11, in which there was no floc break up. The concentration profiles indicate that the break up of flocs delays the formation of a particle network which prevents further movement. The position of the serum interface in figure 3.18 is higher up and takes longer to form than in the absence of bond breakage (figure 3.11). At a higher break up probability (figure 3.19), the final serum interface position is not defined during the simulation period, since not all particles have linked into the network. The concentration of the cream region increases as the break up probability increases, indicating the reduced floc growth rate and the delay in "freezing" of the structure due to cross-linking. The creaming rate is again seen to increase in comparison with the single particle case.

The concentration profiles obtained when flocculation is reversible demonstrate that creaming behaviour proceeds more freely than for irreversible flocculation with the same bonding probability. It might be expected, therefore, that the profiles would bear a closer resemblance to the results for irreversible flocculation with a lower bonding probability. This is indeed the case, as a comparison between figures 3.18 and 3.10 (with a bonding probability of 0.002 and no floc break up) shows. There is however, an important difference. The break up probability can only affect bonds which have already formed. It does not prevent bonds forming, as a reduction in bonding probability would. Hence, a significant degree of floc growth occurs before a noticeable effect of reversibility is observed. Floc growth can be initially quite rapid, but when flocs reach a certain size, the growth rate is reduced by bond breakage. Hence the formation of a network is delayed in a reversibly flocculating system. This effect can be seen by comparing the concentration profiles of figures 3.18, 3.19 and figure 3.10. After 6 minutes, the concentration profiles in figures 3.10 and 3.19 have a very similar form, with the reversible case showing the preliminary shape of the serum interface. However, in the reversibly flocculated system, the floc breakage is sufficiently strong to limit the floc growth and enable free particle movement for a significant time. The irreversibly flocculating system simply forms a network and creaming ceases. This is also true for the reduced break up probability (figure 3.18). At a sufficiently high break up probability, flocs may remain mobile, without the formation of a particle network (at least until the concentration increases, due to creaming).

The lattice simulation does not explicitly favour formation of more compact structures, as would be the case with an attractive interparticle potential. However, the inclusion of the breakage of bonds implicitly attributes greater stability to more compact configurations. A particle which is connected to a floc by a single bond is more likely to break off from that floc than one which has, for example, three connections to other particles in the floc. Since each bond has equal probability of breaking, the probability of any *particle* breaking off from the floc is equal to the bond breakage probability raised to the power of the number of bonds connected to the particle. Thus

$$P_{particle} = \left(P_{break}\right)^{Nbonds} = \exp\left(-Nbonds \times E_{break}/k_B T\right) \qquad [3.16]$$

where *Nbonds* is the number of bonds between the particle and its neighbours. This is a very steep function of the number of connections, and therefore more compact structures (in which particles are connected to a number of other particles, rather than only one) should be more favourable. The effect of the breakage probability has been investigated by Haw et al. (1995) with lattice simulations carried out using a bonding probability of unity (the diffusion limited case). A larger break up probability was shown to produce more compactly structured flocs on a short length scale. The competition between short range compactification of the flocs (by bond breakage) and linkage of neighbouring flocs into a network can result in rather different structural forms. If the rearrangement of flocs into a more compact form is more rapid than the space-filling growth of the floc, the flocs may not grow sufficiently to cause cross-linking into a networked structure (Haw et al., 1995). This was observed in the present lattice model, in the relatively free creaming behaviour at higher break up probability, demonstrating that the flocs are still mobile.

The fractal dimension is plotted as a function of time in figure 3.20, for each of the break up probabilities simulated. As discussed in the previous section, a reduction in the fractal dimension over the length scale used here is indicative of a more compact structure at short length scales, and correspondingly sparse structure in the distance range used. When flocculation is irreversible (P_{break}=0), the fractal dimension decreases until it reaches a limiting value. No rearrangement of the structure into a more compact form is possible after all the particles are linked together. As the break up probability is increased it is clear from figure 3.20 that the fractal dimension decreases at a much slower rate. It does not reach a limiting value when an extensive network is formed, but

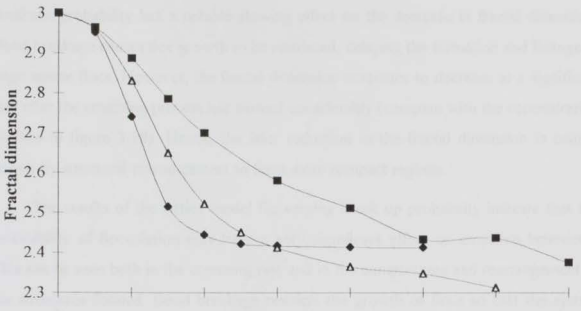

Figure 3.20 Fractal dimension as a function of time, for variable break up probability, with a bonding probability of 0.005.
The profiles are for break up probabilities of ◆ 0.0, △ 0.001 and ■ 0.002.

continues to decrease. This is because the breakage of bonds allows rearrangement of particles into a more stable, compact configuration, resulting in a smaller fractal dimension in the intermediate length range. It is clear, however, that reversible flocculation leads to a structure with a lower fractal dimension than irreversible flocculation with the same bonding probability. The fractal dimension reached in the simulation period for reversible flocculation is also lower than for the irreversibly flocculated structures formed at the lower bonding probabilities analysed (figure 3.17).

A comparison of figures 3.20 (for reversible flocculation) and 3.17 (irreversible flocculation) indicates the difference between the effect of bond breakage, and the effect of the rate of bond formation. As the bonding probability is decreased, in the absence of floc break up (figure 3.17), the fractal dimension takes longer to decrease from the initial plateau. However, an increase in break up probability, at the same bonding probability (figure 3.20) does not significantly change the very early variation in fractal dimension. This is because the initial formation of flocs is solely determined by the bonding probability. The rate of bond breakage only becomes significant in the presence of a

substantial number of bonds. After the initial development of flocs, an increase in breakage probability has a notable slowing effect on the decrease in fractal dimension. Bond breakage causes floc growth to be restricted, delaying the formation and linkage of large sparse flocs. However, the fractal dimension continues to decrease at a significant rate after the creaming process has slowed considerably (compare with the concentration profiles in figure 3.18). Hence, the later reduction in the fractal dimension is caused largely by structural rearrangement to form more compact regions.

The results of the lattice model for varying break up probability indicate that the reversibility of flocculation may have a very significant effect on emulsion behaviour. This can be seen both in the creaming rate and in the compactness and rearrangement of the structures formed. Bond breakage restricts the growth of flocs so that the system remains mobile for a longer period. However, the flocs formed have a larger creaming speed than single particles, and therefore an increase in the creaming rate should be observed. A speed up of creaming was also observed for irreversible flocculation, but the networking of flocs as they continue to grow causes the earlier onset of immobility. A lower bonding probability delays this process, but creaming is then determined by smaller flocs which cream more slowly. Rearrangement of the structure due to reversibility of flocculation allows more compact packing, and may permit further movement of particles, and the collapse of the network.

The difference in particle network structure produced under different flocculation conditions can be seen in figures 3.21-3.23. Each picture is a section of the lattice in the height range 80-100 diameters. In each case, the structure is shown at the end of the simulation period. The structures look somewhat unnatural because of the geometry of the lattice, which constrains the possible particle positions. For irreversible flocculation with a high bonding probability (figure 3.21) the structure is characterised by many small clumps of particles which are cross-linked. At lower bonding probability (irreversible), figure 3.22 shows that larger, more compact regions have formed. Reversible flocculation at the same bonding probability (figure 3.22) is characterised by only a few regions of densely packed particles. However, many single particles are still present in this case because the network was not fully developed by the end of the simulation run. These visual images are consistent with the interpretation of the fractal dimension results.

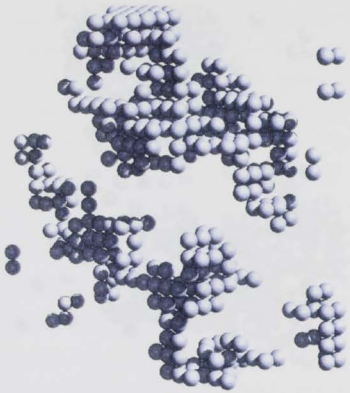

Figure 3.21 Pictorial representation of the particle network structure formed with a bonding probability of 0.01 and no floc break up.

The section corresponds to a height range of 80-100 particle diameters after 10 minutes.

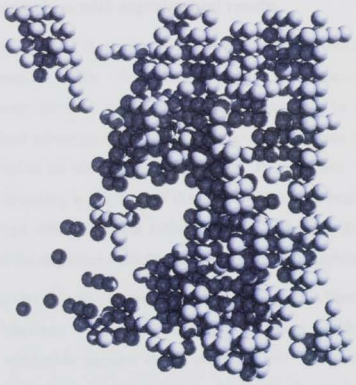

Figure 3.22 Pictorial representation of the particle network structure formed with a bonding probability of 0.005 and no floc break up.

The section corresponds to a height range of 80-100 particle diameters after 17 minutes.

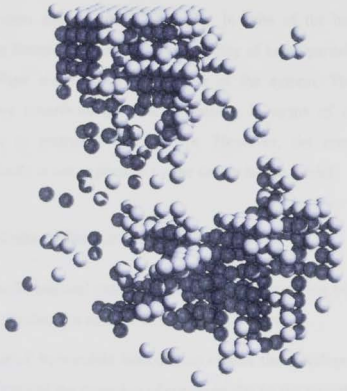

Figure 3.23 Pictorial representation of the particle network structure formed with a bonding probability of 0.005 and a break up probability of 0.002.
The section corresponds to a height range of 80-100 particle diameters after 14 minutes.

3.9.5 Comparison with experimental results

A comparison of the lattice model concentration profiles for flocculated systems with experimental results (for example, figure 2.24) shows that some qualitative agreement exists between the simulated and real results. The lattice model reproduces the well-defined serum interface, whose formation is followed by a gradual reduction in the concentration of the serum region below the interface. The model predicts the cessation of creaming in the bulk of the system due to the extensive linkage of particles in a networked structure. This initial creaming behaviour followed by almost entire immobility of the dispersed particles has been observed experimentally.

A particular feature of some experimental studies has been the very rapid formation of a serum interface, whose position does not change significantly after it is formed. Although a noticeable increase in the creaming rate was observed in the flocculation simulations of the lattice model (see figure 3.13), this does not appear to be sufficient to explain the rapid serum development observed on a macroscopic scale. In addition, the experimental results shown in figure 2.24 show that the cream region continues to develop extensively after the serum interface has been formed. The concentration in the

bulk of the system also decreases gradually, in spite of the immobility of the serum interface. These features indicate that the mobility of some particles in the system is still sufficient to allow creaming in some parts of the system. The reversible nature of flocculation may contribute to these processes, in terms of allowing some particle movement due to restricted floc growth. However, the complex nature of these experimental results is not explicable by the simple lattice model.

3.10 Conclusions of lattice model

The three-dimensional lattice simulations of the creaming behaviour of flocculating emulsions have produced a number of interesting features.

- The presence of irreversible flocculation causes the development of a well-defined serum interface and the cessation of creaming due to the formation of a network.
- The height of the serum interface is related to the bonding probability, or to the height of the energy barrier to flocculation.
- Reversibility of flocculation delays the formation of a particle network, allowing flocs to remain mobile for longer. Creaming may continue at a reduced rate after a network is formed.
- An increase in creaming rate is observed in both reversible and irreversible flocculating systems before the system is fully networked. This is due to the more rapid movement of flocs of moderate size.
- The fractal dimension of the developing particle network is influenced by both bonding and break up probabilities. More compact structures are formed with reversible flocculation, since rearrangement is permitted.

The results of the lattice model are qualitatively consistent with experimental observations of the development of a sharp serum interface, followed by almost complete cessation of creaming. Although an increase in creaming rate in the early stages was seen in the simulations, it is difficult to conclude that this is sufficient to explain the very rapid formation of the serum which has been observed in practice. Hence, the simple model of creaming and flocculation adopted by the lattice simulation does explain some features of real emulsions. Nevertheless, the rapid movement of oil in the early stages of creaming probably requires an alternative mechanism to fully account for the experimental results.

Obstruction of larger flocs by smaller flocs in the model may unrealistically reduce creaming rate.

Chapter 4 : Theory of Ultrasound Propagation

4.1 Aims of theoretical ultrasound work

Low power ultrasound can be used as a non-destructive probe of dispersed systems, such as emulsions (see section 1.3). The two measurable quantities characterising the ultrasound propagation in the sample are its velocity and attenuation, and these can be related to useful physical properties of the sample being measured. This relationship between velocity and attenuation and a quantity such as the dispersed phase volume fraction or solid fat content is the key to the value of the ultrasound technique. The ultrasound scanner (figure 1.1), used to study creaming in emulsions, relies on the ultrasound velocity being directly related to the volume fraction of oil at any point in the sample. Concentration profiles of the emulsion can therefore be determined as creaming progresses. Similarly, investigations of crystallisation rates in emulsions utilise the difference in ultrasound velocity between the solid and liquid oil droplets. The measured ultrasound velocity in the sample can be related to the proportion of the dispersed phase which is solid. Measurements of sound speed in the crystallising emulsion are therefore a means of studying the crystallisation kinetics.

The main ultrasound applications used at Leeds are based on velocity (or speed) measurements. Attenuation measurements have been made for a number of different applications, but the error in attenuation measurements was found to be considerably higher than for the velocity measurements. Attenuation measurements suffer more strongly from effects such as dispersion (which affects the shape of the waveform), diffraction and probe variation, and therefore velocity measurements are both more accurate and more reproducible. Other workers have used attenuation measurements to some degree of success. The majority of the discussion in the following sections and in the next chapter is therefore directed towards the relationship between ultrasound velocity and the system parameters, rather than the attenuation.

The aim of the ultrasound work was to evaluate various ways of interpreting ultrasound measurements, particularly of creaming, flocculation and crystallisation in emulsions. Hence, the focus of the study was initially the theory of ultrasound

propagation in such systems. This chapter considers the basic ultrasound theories which are commonly used to interpret measurements in dispersed systems. The important special cases of the theory are discussed, along with the circumstances under which each of these cases can be applied. A number of practical techniques for obtaining the relationship between ultrasound velocity and the dispersed phase concentration are developed in chapter 5.

4.2 Homogeneous descriptions of dispersed systems

The speed at which a sound wave propagates through an isotropic, homogeneous fluid is given by the equation

$$v = \frac{1}{\sqrt{\kappa_0 \rho_0}} \qquad [4.1]$$

(Wood, 1964, p. 261, and earlier editions), where v is the ultrasound velocity, κ_0 is the compressibility of the fluid and ρ_0 its density. In most cases, sound wave propagation is adiabatic and therefore the adiabatic compressibility is usually used. Under conditions of isothermal propagation, the isothermal compressibility should be used instead. In some circumstances the propagation is neither adiabatic nor isothermal, in which case the velocity falls somewhere between the two limiting speeds. A discussion of this problem can be found in Pierce (1981, p. 34-36).

Urick (1947) suggested that, in a dispersion in which the dispersed particles are much smaller than the wavelength of the sound wave, the density and compressibility in equation 4.1 should be replaced by the terms

$$\rho_0 = \phi\rho_2 + (1-\phi)\rho_1$$

$$\kappa_0 = \phi\kappa_2 + (1-\phi)\kappa_1 \qquad [4.2]$$

where subscripts 1 and 2 denote the continuous and dispersed phases respectively, and ϕ is the dispersed phase volume fraction. These quantities are the volume-averaged values of the density and compressibility of the suspension. Equation 4.2 had already been used for fluid mixtures (Wood, 1941, p. 361), since ρ_0 and κ_0 are the overall density and compressibility of the system. Urick proposed that a suspension in which the particles were much smaller than the wavelength of sound should be treated in the same way. The

equation was found by Urick to agree with experimental measurements on xylene in water emulsions. It was then used to determine the compressibility of the oil droplets in an emulsion.

This approach is a homogeneous description of the system, considering the suspension itself as a homogeneous fluid, with a modified density and compressibility corresponding to the volume-averaged values for the suspension. It does not consider the interaction of the sound wave with the individual particles.

4.3 Ultrasound scattering theory

The theory of ultrasound propagation on which much of this work has been based is scattering theory. The term scattering may be used to describe any effect which removes energy from the sound wave and makes it unavailable to the propagating acoustic field. In an emulsion, scattering is caused by the presence of the individual dispersed phase particles, which disturb the propagating wave. Energy is lost from the forward direction of the wave by being scattered in all directions and also by thermal and viscous dissipation around the particle. The wave also undergoes a phase shift which is apparent in the change in velocity of the propagating wave. The basis of scattering theory as applied to acoustic propagation in an emulsion is that the particles can be considered as independent scattering centres, each affecting the sound wave separately from the other particles. Other approaches to the acoustic problem were introduced in chapter 1. There have been several reviews of different solutions to acoustic propagation in dispersed systems, to which the reader is referred (Harker and Temple, 1988), and these alternative theories will not be considered further.

The scattering theory method provides some intuitive understanding of the physical processes which occur at the particles. It appears to be particularly appropriate in the long wavelength limit, in which the wavelength of the propagational acoustic wave is much larger than the particle radius (this is also known as the Rayleigh limit, after Lord Rayleigh who investigated the scattering of sound by small particles in this limit). Under these conditions, the effect of the emulsion on the sound wave can be described by a series of different scattering modes. In the long wavelength regime this series may usually be terminated above the first order mode (dipole scattering). At higher frequencies, the effect involves many higher order scattering modes and other

approaches to the acoustic problem then become more suitable. In addition, in the long wavelength region, only "single" and "double" (scattering by two particles) scattering effects need normally be taken into account. Therefore, the multiple scattering theory description of sound propagation is most appropriate in the long wavelength limit. The use of ultrasound signals of the order of MHz to characterise emulsions with particle sizes of the order of μm, means that the long wavelength condition is valid. Therefore the scattering theory description of ultrasound propagation is suitable for the study of emulsions and was used as the basis for this work.

The groundwork of the theories of ultrasound propagation are well-established. Lord Rayleigh considered the effect of a sound wave on a spherical obstacle in the long wavelength limit, arriving at the famous theory that attenuation is proportional to the fourth power of frequency (Strutt, 1872, 1896). Since then, numerous attempts have been made to improve and extend the knowledge of the modification to the sound wave caused by a particle, for example by including thermal effects (Epstein and Carhart, 1953), or a shell-like coating on the particle (Anson and Chivers, 1993). Considerable effort has also been expended in determining the effect of the whole set of particles which exist in an emulsion, each having their own scattering properties. These two aspects still remain the crucial elements of the scattering theory technique. Firstly, to determine the effect of a planar sound wave on a single, isolated particle, and secondly to determine the effect of the ensemble of particles in the dispersion on the sound wave (in terms of the scattering properties of the individual particles). The following sections describe the methods for each of these stages. The details may be found in the references, but sufficient information is given for an understanding of the subsequent discussions and developments.

4.3.1 General theory of sound propagation

The propagation of a sound wave in a medium can be defined by a single complex value called the wavenumber which is related to the two measurable parameters – the velocity and attenuation. The acoustic field properties, such as pressure or displacement, are oscillatory and include a factor of

$$\exp\{i(\mathbf{k}.\mathbf{r}-\omega t)\} \qquad [4.3]$$

where $\mathbf{k}$ is the wavevector and its modulus, k, the wavenumber. The time variation,

$\exp(-i\omega t)$, is omitted from all the following equations, since it appears in every field quantity. It can be seen that the wavenumber is in general given by

$$k = \frac{\omega}{v} + i\alpha \qquad [4.4]$$

where ω is the angular frequency, v is the speed at which the wave propagates and α is the attenuation. The detectable acoustic mode is called the propagational mode, because the wave's energy can travel over considerable distances in this mode. In a homogeneous fluid the velocity of the propagational mode is the normal sound speed in the medium, and α the measured attenuation.

In addition to the propagational mode, a medium can support two other modes of acoustic wave motion: thermal and shear waves. Thermal waves are compressional waves which arise due to thermal conduction. Shear waves are transverse waves which occur because of viscous effects. The equations of motion and the thermodynamic relations in the medium determine the wavenumbers of the various modes to be

$$\frac{1/k^2}{1/k_t^2} = \frac{v^2}{2\omega^2}\left\{1 - i\left(e_k + \gamma f_k\right) \pm \left[1 - 2ie_k - 2if_k(\gamma - 2) - \left(e_k - \gamma f_k\right)^2\right]^{\frac{1}{2}}\right\} \qquad [4.5]$$

where v is the sound speed of the propagational mode and e_k and f_k are given by

$$e_k = \frac{4}{3}\frac{(\eta + \mu/2)\omega}{\rho v^2}, \quad f_k = \frac{\sigma\omega}{v^2} \qquad [4.6]$$

$$k_s = (1+i)\sqrt{\frac{\omega\rho}{2\eta}} \qquad [4.7]$$

where η/ρ is the kinematic viscosity (Epstein and Carhart, 1953). A full list of symbols is given at the end of this thesis. A very good approximation for the thermal mode is

$$k_t = (1+i)\sqrt{\frac{\omega}{2\sigma}} \qquad [4.8]$$

where σ is the thermometric conductivity. It can be seen from equations [4.7] and [4.8] that both the thermal and shear modes are dissipative (i.e. the real part of the wavenumber is equal to the imaginary part). The consequence of this is that both of these modes are strongly attenuated over a distance of only a few wavelengths. The thermal mode represents energy lost through thermal conduction processes, and the shear mode

the work done against viscous forces in the fluid or solid. Because of their dissipative nature, they are only present in the region around the interface where they are produced and do not contribute to the acoustic field over a long range. They are produced at interfaces where the properties of the medium changes and are therefore present when scattering occurs at the emulsion particles.

4.3.2 Plane wave incident on a single particle

The first stage in the scattering theory approach is to consider the effect of a plane wave incident on a single isolated particle. The key work on this problem was carried out by Epstein and Carhart (1953) and Allegra and Hawley (1972). The two papers give approximations at different stages, for example in the wavenumbers, or in the relationship between the potential and the temperature. For the purpose of completeness the fullest solution was used in each case in this work. These equations may therefore look slightly different from either of the two cited works, but are in fact an amalgamation of the most detailed results from each.

The incident wave is a propagational mode, but at the particle surface waves of the other modes are also produced, both inside and outside the particle. The acoustic field observed far from the particle is the sum of the incident wave and the outgoing propagational wave produced at the particle surface. A change of sound velocity is observed because the addition of these two waves produces an apparent phase change in the (originally) plane wave. Attenuation occurs because of the energy dissipated in the thermal and shear modes inside and outside the particle, and also because the energy in the scattered propagational mode is radiated in all directions, rather than being focused in the propagation direction of the incident wave.

The equations of motion in a fluid are satisfied by a fluid velocity, given by

$$\mathbf{v} = -\nabla\varphi + \nabla \times \mathbf{A} \qquad [4.9]$$

where φ is a scalar potential, and $\mathbf{A}$ is a vector potential. The acoustic motion can be described in terms of such potentials: scalar potentials for the compressional modes, and a vector potential for the shear mode. It should be noted that the vector $\mathbf{v}$ and its components refer to the local velocity of the fluid. The scalar quantity v refers to the speed (loosely also termed velocity) at which the sound wave propagates through the medium. The determination of the effects of scattering consists of finding appropriate

potentials which satisfy the boundary conditions at the particle surface. This process is assisted by the use of partial wave analysis, in which each wave potential is described by a sum of wave motions having different angular dependencies (spherical, dumb-bell etc.). Spherical co-ordinates are used with the origin at the centre of the particle, which is assumed to be spherical at this stage to simplify the symmetry of the problem. The appropriate radial and angular functions required to construct the wave potentials are the spherical Bessel functions and the Legendre polynomials. A single frequency is considered. If the time variation is omitted, the incident plane wave can be written as

$$\varphi_0 = e^{ikz} = \sum_{n=0}^{\infty} i^n (2n+1) j_n(kR) P_n(\cos\theta) \qquad [4.10]$$

the z-axis being the propagation direction.

A constant factor representing the actual amplitude of the sound wave, which is related to the acoustic intensity, is omitted for convenience. The acoustic intensity in a plane wave is equal to the sound speed multiplied by the acoustic energy density (Pierce, 1981, p. 39). This energy density is twice the kinetic energy per volume due to the sound field. With the use of equations 4.9 and 4.10, the omitted amplitude factor can therefore be expressed as

$$\sqrt{\frac{I}{\rho k^2 v}} \qquad [4.11]$$

where I is the acoustic intensity. The intensity is equivalent to a power per unit area normal to the propagation direction. All parameters which are proportional to the incident scalar potential should be multiplied by this factor.

The waves produced at the particle by the incident plane wave, can similarly be written as sums of the radial and angular functions, with unknown coefficients. The planar symmetry of the problem reduces the vector potential of the shear wave to a single component in the azimuthal direction, written $A_\psi = A$. The amplitude factor is again omitted in each case. Thus

$$\varphi_R = \sum_{n=0}^{\infty} i^n (2n+1) A_n h_n(kR) P_n(\cos\theta) \qquad [4.12]$$

$$\varphi_t = \sum_{n=0}^{\infty} i^n (2n+1) B_n h_n(k_t R) P_n(\cos\theta) \qquad [4.13]$$

$$A = \sum_{n=1}^{\infty} i^n (2n+1) C_n' h_n(k_s R) P_n^1(\cos\theta) \qquad [4.14]$$

$$\varphi' = \sum_{n=0}^{\infty} i^n (2n+1) A_n' j_n(k' R) P_n(\cos\theta) \qquad [4.15]$$

$$\varphi_r' = \sum_{n=0}^{\infty} i^n (2n+1) B_n' j_n(k_t' R) P_n(\cos\theta) \qquad [4.16]$$

$$A' = \sum_{n=1}^{\infty} i^n (2n+1) C_n' j_n(k_s' R) P_n^1(\cos\theta) \qquad [4.17]$$

where j_n and h_n are the spherical Bessel and Hankel functions, and P_n and P_n^1 are the Legendre and associated Legendre polynomials respectively. Primed symbols refer to the interior of the particle.

The terms in the series represent different modes of scattering, defined by their angular dependence. The zero order mode is spherically symmetric, caused by pulsation of the particle, whereas the first order mode represents dipole radiation, caused by particle movement forwards and backwards along the incident wave direction. Strutt (1896) showed that a disturbance of compressibility acted as a zero-order source of waves (that is, spherically symmetric), whereas a disturbance of density acted as a dipole source. In the long wavelength limit, the lower order scattering modes are most significant and the series can usually be truncated above the first order mode. Hence, the partial wave analysis scattering approach lends itself to a description of ultrasound propagation in the long wavelength regime. At higher frequencies the higher order scattering modes become more significant and all the terms in the series are important.

The effect of the spherical particle on the sound wave is encapsulated in the coefficients of the scattered waves, particularly in the scattered propagational mode, which will be present at large distances from the particle. The coefficients A_n are called the single particle scattering coefficients for this reason. These coefficients describe how the sound wave is modified by the presence of the particle. The coefficients are determined by applying boundary conditions at the particle surface, $R = r$. It has been shown, however, that the equations are identical if the displacement of the particle surface is also taken into account (Chow, 1964). The six boundary conditions which must be satisfied at the particle surface are the continuity of velocity, stress, temperature

and heat flux. The velocity and stress conditions each include three components, but the azimuthal symmetry due to the planar incident wave reduces this to two in each case.

The boundary equations for fluid particles were given by Epstein and Carhart (1953) and later converted for solid particles by Allegra and Hawley (1972). The conversion is simple – the fluid's viscosity is replaced by a modified bulk modulus for the solid, thus

$$\eta = \frac{\mu}{(-i\omega)} \qquad [4.18]$$

All terms for the solid material are also multiplied by a factor of $-i\omega$. This factor arises from the use of a displacement potential in the solid case, whereas a velocity potential is used in a fluid (equation 4.9). All time derivatives are equivalent to multiplication by this factor. The details are given by Allegra and Hawley (1972).

In applying the boundary conditions at the particle surface, the physical quantities of temperature, stress etc. must be related to the wave potentials. The velocity is simply derived from equation 4.9, with equations 4.10 to 4.17. The relationship between temperature and the wave potential can be derived from the energy equation and thermodynamic relations, and is found only to be related to the scalar potentials. The shear mode does not contribute to any temperature change in the medium, so only the thermal and propagational modes involve heat terms. If the symbol T denotes the deviation in temperature from the ambient value, then this change is related to the scalar potential by

$$T = G\varphi \qquad [4.19]$$

where

$$G = \frac{-ik^2(\gamma - 1)}{\omega\beta\left(1 + \frac{i\gamma\sigma k^2}{\omega}\right)} \qquad [4.20]$$

The stress component P_{rr} is made up of two terms: the pressure and the viscous stress. For the scalar modes, which contribute to the hydrostatic pressure, these terms combine to give

$$P_{rr} = \left(i\omega\rho - 2\eta k^2\right)\varphi - 2\eta\frac{\partial^2\varphi}{\partial R^2} \qquad [4.21]$$

The shear mode only includes viscous stress terms.

$$P_{rr} = \frac{2\eta}{\sin\theta}\frac{\partial}{\partial\theta}\left[\sin\theta\left(-\frac{A}{R^2} + \frac{1}{R}\frac{\partial A}{\partial R}\right)\right] \qquad [4.22]$$

The other stress component, $P_{r\theta}$, is given by

$$P_{r\theta} = 2\eta\frac{\partial}{\partial\theta}\left(\frac{\varphi}{R^2} - \frac{1}{R}\frac{\partial\varphi}{\partial R}\right) \qquad [4.23]$$

for the compressional modes and

$$P_{r\theta} = \eta\left[\left(\frac{2A}{R^2} - \frac{\partial^2 A}{\partial R^2}\right) + \frac{1}{R^2}\frac{\partial}{\partial\theta}\left(\frac{1}{\sin\theta}\frac{\partial}{\partial\theta}\left(A\sin\theta\right)\right)\right] \qquad [4.24]$$

for the transverse (shear) mode.

Boundary conditions must be applied at the surface of the particle, which is a sphere of radius r. It is clear that the omitted amplitude in each wave function is a common factor in each equation, and therefore has no effect on the solution for the coefficients. The boundary conditions for fluid particles in a fluid medium are therefore (in the order: radial velocity, temperature, heat flux, the P_{rr} stress component, tangential velocity and the $P_{r\theta}$ stress component):

$$aj_n'(a) + A_n a h_n'(a) + B_n b h_n'(b) - C_n n(n+1)h_n(c)$$

$$= A_n' a' j_n'(a') + B_n' b' j_n'(b') - C_n' n(n+1) j_n(c') \qquad [4.25]$$

$$G_p j_n(a) + G_p A_n h_n(a) + G_t B_n h_n(b) = G_p' A_n' j_n(a') + G_t' B_n' j_n(b') \qquad [4.26]$$

$$\tau\left\{G_p a j_n'(a) + G_p A_n a h_n'(a) + G_t B_n b h_n'(b)\right\} = \tau'\left\{G_p' A_n' a' j_n'(a') + G_t' B_n' b' j_n'(b')\right\} \qquad [4.27]$$

$$\left[\left(i\omega\rho - 2\eta k^2\right)j_n(a) - 2\eta k^2 j_n''(a)\right] + A_n\left[\left(i\omega\rho - 2\eta k^2\right)h_n(a) - 2\eta k^2 h_n''(a)\right]$$

$$+B_n\left[\left(i\omega\rho - 2\eta k_t^2\right)h_n(b) - 2\eta k_t^2 h_n''(b)\right] + 2n(n+1)\eta C_n'\frac{\left[ch_n'(c) - h_n(c)\right]}{r^2}$$

$$= A_n'\left[\left(i\omega\rho' - 2\eta' k'^2\right)j_n(a') - 2\eta' k'^2 j_n''(a')\right]$$

$$+B_n'\left[\left(i\omega\rho' - 2\eta' k_t'^2\right)j_n(b') - 2\eta' k_t'^2 j_n''(b')\right]$$

$$+2n(n+1)\eta' C_n'\frac{\left[c'j_n(c') - j_n(c')\right]}{r^2} \qquad [4.28]$$

$$j_n(a) + A_n h_n(a) + B_n h_n(b) - C_n'\left[h_n(c) + ch_n'(c)\right]$$

$$= A_n' j_n(a') + B_n' j_n(b') - C_n'\left[j_n(c') + c' j_n'(c')\right] \qquad [4.29]$$

$$\eta\left[aj_n'(a) - j_n(a)\right] + \eta A_n\left[ah_n'(a) - h_n(a)\right] + \eta B_n\left[bh_n'(b) - h_n(b)\right]$$

$$-\frac{1}{2}\eta C_n'\left[c^2 h_n''(c) + \left(n^2 + n - 2\right)h_n(c)\right]$$

$$= \eta' A_n'\left[a' j_n'(a') - j_n(a')\right] + \eta' B_n'\left[b' j_n'(b') - j_n(b')\right]$$

$$-\frac{1}{2}\eta' C_n'\left[c'^2 j_n''(c') + \left(n^2 + n - 2\right)j_n(c')\right] \qquad [4.30]$$

where G_p and G_t are the thermal factors calculated from equation 4.20 for the propagational and thermal modes respectively. A primed function represents a spatial derivative. Otherwise, prime denotes the dispersed phase inside the particle.

The solution of this set of equations for each mode (denoted by n) produces a value for the single particle scattering coefficient, A_n, of that mode. The fifth and sixth of these equations (for the tangential velocity and the stress $P_{r\theta}$) are invalid for the zero order mode, because the angular function factor which was cancelled throughout is zero in this case. No shear waves are produced in the zero order mode. Although analytical results can be obtained in special cases, the general solution for the scattering coefficients is calculated numerically. A discussion of the special limiting cases of the single particle scattering properties is reserved for a later section.

4.3.3 Effect of many scattering centres : single and multiple scattering

Having determined the coefficients of the scattered waves generated when a plane acoustic wave impinges on a particle, it is necessary to consider the effect of an assembly of such particles (for example in an emulsion) on the velocity and attenuation of the wave. It is these quantities which can be measured, and can provide information on the properties of the system.

Strutt (1872, Baron Rayleigh), estimated the energy lost from a sound wave by comparing the amplitude of the scattered and incident fields at large distances from the particle. For small particles he found that the scattered intensity was proportional to the inverse of the fourth power of the wavelength. He used this result to explain why the sky is blue. However, this was only for a single particle, and he neglected thermal and shear waves. In their work on scattering in dispersed systems, Epstein and Carhart (1953) and Allegra and Hawley (1972) similarly defined the attenuation of the wave by calculating the energy in the scattered propagational mode at a large distance. At this distance, both the thermal and shear modes have fully dissipated and contribute a negligible amount. These studies each assumed that the effect of the particles was additive, so that the total energy lost was proportional to the number of particles. Thus, their attenuation result might be called a single scattering theory, since scattering by one particle is considered to have no effect on other particles. The result for the attenuation coefficient is

$$\alpha = -\frac{3\phi}{2k_1^2 r^3}\sum_{n=0}^{\infty}(2n+1)\,\mathrm{Re}\,A_n \qquad [4.31]$$

These authors were only concerned with attenuation and did not derive expressions for the velocity in the suspension.

A sound wave propagating through an emulsion will of course interact with more than one particle. The acoustic field surrounding a particle is the sum of the incident plane wave and the scattered fields from all other particles. The single scattering approaches used by Epstein and Carhart (1953) and Allegra and Hawley (1972) are limited to dilute dispersions or to very weak scattering. In these circumstances, the proportion of the acoustic field incident on a particle which is due to scattering at other particles is negligible. As the concentration of particles in the sample increases, the scattered field due to all other scatterers becomes a significant proportion of the acoustic

field incident on a given particle. Analysis of the propagation characteristics in this case is called multiple scattering theory.

There have been various approaches to the multiple scattering problem in a dispersed system. An early multiple scattering model was applied by Urick and Ament (1949). They used a "thin slab approximation" to obtain the effective wavenumber of an emulsion in terms of the single particle scattering amplitudes. They calculated the forward and backward scattered wave amplitudes from a thin slice of dispersion (much smaller than the wavelength) in terms of the scattering coefficients. These were then compared with the reflected and transmitted waves which would be obtained from a homogeneous slice of fluid with a given wavenumber. Thus the apparent wavenumber of the dispersion was determined. Their result, to zero and first order scattering modes is

$$\left(\frac{K^2}{k_1^2}\right)=\left(1-\frac{3i\phi}{k_1^3r^3}A_0\right)\left(1-\frac{9i\phi}{k_1^3r^3}A_1\right) \qquad [4.32]$$

The scattering calculation assumed that each particle in the slice experienced the same acoustic field, so neglecting the influence of the scattered waves transverse to the propagation direction. In other words, only longitudinal multiple scattering is allowed, not transverse multiple scattering. The result given by Urick and Ament (1949) therefore omits some terms included by later workers.

Later work on multiple scattering has approached the problem in very different ways. The two theories which are widely used for the analysis of ultrasound measurements and have formed the basis for this work are by Lloyd, Berry and Ziman (Ziman, 1966, Lloyd, 1967a, 1967b, Lloyd and Berry, 1967) and by Waterman, Truell and Fikioris (Waterman and Truell, 1961, Fikioris and Waterman, 1964). Waterman and Truell (1961) determined the wavenumber in a dispersion by using the hierarchy method and ensemble averaging to obtain the acoustic field. These methods were introduced by earlier workers (Foldy, 1945 and Lax, 1951, 1952). The ensemble averaging processes involves an average over all possible configurations of particle positions. The hierarchy is formed from the relationship between the ensemble average with n particles in fixed positions to the ensemble average with $n+1$ particles fixed. The total field which would be observed is the ensemble average with no particle positions fixed.

Waterman and Truell calculated the acoustic field present in the region of a scatterer, due to the incident wave and to the scattered fields from all other particles. The termination of the resulting hierarchy of equations in order to obtain a solution can only practically be done at the first level – the exciting field at a scatterer is considered to be equal to the total field there (although the total field would include the contribution from the scattered field from the same particle). The exciting field at a particle at position $\mathbf{r}_1$ is therefore the sum of the incident wave and the scattered fields from all particles. Thus

$$\left\langle \varphi^E\left(\mathbf{r}|\mathbf{r}_1\right)\right\rangle = \varphi_0\left(\mathbf{r}\right) + \int \mathrm{d}\mathbf{r}' n\left(\mathbf{r}'\right) T\left(\mathbf{r}'\right) \left\langle \varphi^E\left(\mathbf{r}|\mathbf{r}'\right)\right\rangle \qquad [4.33]$$

using the notation of Waterman and Truell (1961). The superscript E denotes the exciting field at a particle. The scattering operator, T, defines the scattered wave produced at the particle in terms of the exciting wave. In the partial wave formulation, it can be described by the transformation

$$T\left(\mathbf{r}_1\right) j_n\left(k|\mathbf{r}-\mathbf{r}_1|\right) P_n\left[\cos\theta\left(\mathbf{r}-\mathbf{r}_1\right)\right] = A_n h_n\left(k|\mathbf{r}-\mathbf{r}_1|\right) P_n\left[\cos\theta\left(\mathbf{r}-\mathbf{r}_1\right)\right] \qquad [4.34]$$

The case of a plane wave incident on a dispersed medium of randomly distributed spherical point-like scatterers is obtained by writing the total field (or exciting field) in the region of a particle in a form similar to those used to calculate the scattering coefficients.

$$\left\langle \varphi^E\left(\mathbf{r}|\mathbf{r}_1\right)\right\rangle = \sum_{n=0}^{\infty} E_n\left(z_1\right) j_n\left(k|\mathbf{r}-\mathbf{r}_1|\right) P_n\left(\cos\theta\left(\mathbf{r}-\mathbf{r}_1\right)\right) \qquad [4.35]$$

The solution proceeds by assuming a planar form for the acoustic field in the propagation direction, so that

$$E_n\left(z_1\right) = E_n^0 \exp\left(iKz_1\right) \qquad [4.36]$$

where K is the effective wavenumber of the dispersion. Equations 4.10, and 4.35-4.36 are substituted into equation 4.33. Following the spatial integration over the dispersion, the wavenumber is calculated by matching the coefficients of the plane wave solutions in the unperturbed wavenumber k and the effective wavenumber of the medium K.

The first attempt by Waterman and Truell (1961) produced a wavenumber which agreed with the single scattering attenuation derived by Epstein and Carhart (1953) and Allegra and Hawley (1972). It also agreed with the thin-slab approximation of Urick and

Ament (1949). However, a later determination of the integration stages of the calculation by Fikioris and Waterman (1964) corrected an earlier error in the exclusion of particle interpenetration. They obtained an infinite series of equations to be solved for the wavenumber and for the amplitudes of the modes of the exciting field. An explicit solution for the wavenumber can be obtained by terminating the series above the required scattering mode, for example to include only zero and first order scattering modes. In this case the wavenumber is given by

$$\left(\frac{K^2}{k_1^2}\right) = 1 - \frac{3i\phi}{k_1^3 r^3}\left(A_0 + 3A_1\right) - \frac{27\phi^2}{k_1^6 r^6}\left(A_0 A_1 + 2A_1^2\right) \qquad [4.37]$$

The work of Lloyd and Berry (1967) provides a different approach to the problem of calculating the wavenumber of a dispersion in terms of the single particle scattering amplitudes. It forms part of a series of papers (Ziman, 1966, Lloyd, 1967a, 1967b and Lloyd and Berry, 1967) concerned with the density of energy states in a medium and in deriving the refractive index (which is proportional to the wavenumber). The acoustic problem was found to be closely related and the calculation of the effective wavenumber is produced almost as a side issue. It has been found to produce reliable results in many systems, and has been widely adopted as the correct form of the multiple scattering theory result. The series is terminated here after the second-order scattering terms, since these are in most cases sufficient to describe the propagation. The wavenumber in the dispersion is given by

$$\left(\frac{K^2}{k_1^2}\right) = 1 - \frac{3i\phi}{k_1^3 r^3}\left(\sum_{n=0}^{\infty}(2n+1)A_n\right)$$

$$- \frac{27\phi^2}{k_1^6 r^6}\left(A_0 A_1 + \frac{10}{3}A_0 A_2 + 2A_1^2 + 11A_1 A_2 + \frac{230}{21}A_2^2\right) \qquad [4.38]$$

The result agrees with the Fikioris and Waterman (1964) result, equation 4.37, to the first order scattering mode. Higher orders have not been compared. Lloyd and Berry (1967) includes many references to earlier work on scattering, including the many different approaches to the multiple scattering problem.

Equations 4.37 and 4.38 form the basis for the theories of interpretation of ultrasound measurements in this work. Although the Lloyd and Berry and Fikioris and Waterman results agree, the approach used by the latter workers is much more

straightforward and easy to understand. The Lloyd and Berry methodology is rather opaque to those not familiar with their particular field of work, and therefore any modification of their theory to include additional effects would be difficult. The Waterman and Truell approach offers the possibility to generalise the theory to compensate for some of the effects discussed in the next section, such as a non-random particle distribution. Such modifications have not, however, been attempted in the present work.

4.4 Assumptions of scattering theory

As with any theory, the single particle scattering theory and the multiple scattering theories make a number of assumptions about the system in order to obtain a result for the wavenumber in a dispersion. It is in these assumptions that the restrictions of applicability of the theory may be found, but also the possibility of modification in order to obtain a more general result. Some of the basic assumptions were discussed by the original authors of the work presented in the previous sections. The assumptions listed by Epstein and Carhart (1953) are that the momentum equation is used in the Navier-Stokes form, thermal stresses are neglected, the gradual changes in temperature and pressure caused by the wave are neglected, no phase changes are allowed (vaporisation or crystallisation), the equations are linearised with respect to the oscillatory variations in the field quantities (velocity, pressure etc.), and that the temperature variation of the viscosity and heat conduction is neglected. These preliminary assumptions pose no real problem to the application of the work to emulsions. However, other restrictions are applied which do have implications for the applicability of the theory. In this section, those assumptions which have a bearing on the application of ultrasound measurements in food systems are examined, especially those relating to the multiple scattering theory formulation.

4.4.1 Scattering is weak

Most scattering theories rely on the premise that the scattered wave amplitude is small compared with the incident wave. For food systems, this is usually satisfied unless resonant scattering occurs, such as in the presence of bubbles.

4.4.2 System is static

Each particle is assumed not to move during the sound wave oscillation other than in the acoustic field, otherwise its movement will affect the way it interacts with the sound wave. The characteristic times for creaming and diffusion (the dominant kinetic processes in a colloidal dispersion) are typically much longer than the duration of the ultrasound pulse used to probe the emulsion (a few microseconds). Therefore the particles may be considered to be stationary.

4.4.3 Particles are spherical

The boundary conditions for the single particle scattering coefficients are applied at the surface of a sphere. Many emulsion droplets which have a coating of emulsifier or stabiliser on their surface are approximately spherical. However, the effect of the coating itself is usually ignored, simply treating the particle as purely of the dispersed phase substance. Some analyses have attempted to include the "shell" around the particle (Anson and Chivers, 1993), but it is rather difficult to define the material properties of such an adsorbed layer. The problem of non-sphericity also occurs in crystallised emulsion droplets, in which the fat crystals may be needle-shaped rather than spherical. However, experimental measurements on such systems seem to indicate that even in this case the assumption of sphericity can produce good results. The determination of the scattering coefficients experimentally, as described in the next chapter, overcomes this problem, since the actual scattering properties of the system are measured, rather than predicted theoretically.

4.4.4 Infinite time irradiation

The multiple scattering theories appear to assume that the sample has been irradiated with a continuous ultrasound signal for ever. This is implicit in the inclusion of the influence of scattered waves from all other particles at any distance from a scatterer, regardless of the time taken for those waves to reach it. The "exciting field" at a scatterer used by Waterman and Truell (1961) is integrated over the complete half-space, so including scattering from particles an infinite distance away. In reality, a short ultrasound pulse is used to stimulate the emulsion, and therefore multiple scattering will only be possible on a very local basis. Delayed multiple scattering from more and more widely separated scatterers will be received at later and later times. The real samples are also

finite in extent, rather than infinite as assumed in the model. The Lloyd and Berry (1967) approach is more difficult to describe in these terms, but they also seem to consider a "soup" of acoustic field in the medium, almost in a long-time steady-state model. In principle, it must be possible to include a time-delay factor in the scattered fields, in a similar way to the modifications of electromagnetic theory for relativistic effects. The influence of these assumptions on the scattering theory results is difficult to assess. However, it is likely that the strongest influence on multiple scattering occurs due to the particles which are closest together. Therefore the correction for finite samples and short pulses is likely to be small and to affect only the multiple scattering term (single scattering is unaffected).

4.4.5 Point-like particles

The analytical multiple scattering results for the wavenumber (equations 4.37 and 4.38) were obtained by assuming a random particle distribution and point-like particles. This considerably simplifies the integration steps of the problem and reduces the number of parameters required to describe the system. The scattering properties of the individual particles, incorporated in the single particle scattering coefficients, *do* include the effects of particle size. It is the determination of the combined effect of a dispersion of such scatterers which assumes them to be point-like, for the purposes of the spatial integration.

Real particles obviously have a finite size, and therefore other particles are excluded from the region inside and immediately around the particle. However, if the particle distribution is random, apart from the excluded volume of the particle itself, then the approximation will not be overly restrictive. This is because the single particle scattering will still depend approximately on the number density of particles. The effect of the excluded volume will again influence the multiple scattering effects, which are significantly weaker than the dominant single-scattering effects.

4.4.6 Random particle distribution

As described in the previous section the particle distribution is assumed to be completely random, although the multiple scattering analyses do retain the generality of an arbitrary distribution for as long as possible. In a flocculated emulsion, the particle distribution is not random, and particles are more likely to be closer together than in a

non-flocculated emulsion. Modification to the single scattering terms can only arise due to a difference in the summation of the scattered waves from non-randomly distributed particles. Multiple scattering is influenced by the greater proximity of particles to each other, probably leading to stronger multiple scattering. The quantitative effect of the non-randomness of the particle distribution is not known, nor whether it is likely to be a significant effect in flocculated systems. Its determination is probably only possible through numerical solution of the general analytical equations provided by workers such as Waterman and Truell (1961) before resorting to the random, point-like assumption. A calculation of the magnitude of the correction, especially for the single scattering result, is required in order to indicate the significance of this effect in flocculated systems.

4.4.7 No overlap of thermal and shear waves

The multiple scattering theories assume that the thermal and shear waves produced at the particle surface have no influence on nearby particles. Multiple scattering only occurs due to the scattered propagational modes. This is certainly valid at high frequencies or very low concentrations where the dissipation length (skin depth) of both thermal and shear waves is much shorter than the average distance between particles. However, for many emulsions this is not the case, and it is possible for a substantial amplitude of the thermal or shear waves produced by one particle to be present at the surface of another particle. The effect on the velocity and attenuation occurs through the conversion of the thermal or shear component back into a propagational mode on scattering by another particle. This is clearly a multiple (not single) scattering effect but its magnitude is not known. It will be most significant when flocculation occurs, since the particles are more likely to be closer together and therefore the waves overlap to a greater extent. Waterman and Truell (1961) invoked symmetry arguments (the incident wave is planar) to suggest that the shear waves will have no effect on multiple scattering. It is necessary to extend the analysis to include thermal waves in the "exciting field" incident on a particle (which consists of the incident wave and the scattered waves from all other particles). It may only be possible to quantify the effect of thermal wave overlap through numerical simulation.

4.4.8 No interactions between particles

Each particle is assumed to be free to move independently of the other particles. In multiple scattering theory, the scattering properties of a single particle are used to characterise the sample. If there are connections between particles, their movement in response to the sound wave may become more co-operative, so that the scattering properties are determined by the whole dispersion or local arrangement of particles, rather than by each particle individually. This may occur in a flocculated system, in which the sound wave is scattered by a floc, rather than by the component particles. However, the "bonds" between weakly flocculated particles tend to be rather loose and may be insignificant in terms of the particles' response to the sound wave. There may also be some interaction between the oscillatory energy supplied in the acoustic field and the breaking and reforming of such connections in a floc. This is another unquantified effect on the ultrasound propagation, but it is only likely to be relevant in flocculated systems.

4.4.9 No phase changes

The particles are assumed to be solid, or fluid, but are not allowed to undergo a phase transition during the passage of a sound wave. This was mentioned by Epstein and Carhart (1953) for the vaporisation of liquid droplets in a fog. It is also relevant to crystallising or melting droplets in an oil in water emulsion. The theory assumes that each droplet is either completely solid or completely liquid and that its phase is unaffected by the sound wave. Whilst this is true in most cases, it is conceivable that, if the energy barrier to the phase change is of the order of the fluctuation in thermal energy caused by the sound wave, the oscillation of heat in and out of the particle may involve a phase change of the particle. In this case, the scattering coefficient must include an additional term due to the heat involved with the phase change. This effect may be a way of observing the dynamic crystallisation of the droplets themselves.

From the assumptions which are discussed above, it can be seen that, in a non-flocculated emulsion, multiple scattering theory provides a reasonable basis for a description of ultrasound propagation. The effects of flocculation on the propagation characteristics are largely unquantified as yet, although there is some experimental evidence that it can have a marked effect on velocity and attenuation (McClements,

1994). Theoretically, this may be due to the overlap of thermal waves, to the non-random particle distribution, to the co-operative movement of particles in a floc, or to dissipation in the forces between flocculated particles. As yet, no adequate theoretical description exists of ultrasound propagation in a flocculated dispersion. Future analysis may require numerical simulation of flocs in a sound field in order to make progress in this area. The issue of melting or crystallisation caused by the ultrasound wave has also not yet been quantified.

4.5 Numerical calculations using scattering theory

The results of sections 4.3.2 and 4.3.3 illustrate that the determination of ultrasound velocity and attenuation in an emulsion is a non-trivial problem. Although analytical solutions exist in the long wavelength region for the single particle scattering coefficients of section 4.3.2, a general solution for polydisperse emulsions, with solid or liquid droplets is only practicable by numerical calculation. A computer program has therefore been written to obtain the velocity and attenuation in an emulsion using the boundary equations of section 4.3.2 to obtain the single particle scattering coefficients, and equation 4.38 for the complex wavenumber according to multiple scattering theory. The velocity and attenuation in the emulsion are directly obtained from equation 4.4.

A flow chart of the computer program is shown in figure 4.1, and the program code is given in Appendix A4. This program calculates the ultrasound velocity and attenuation for a set of input parameters, which includes the oil concentration and particle size distribution as well as the properties of the component phases. An interface exists by which this calculation links with the model of creaming (chapter 2), or with a another, "front-end" computer program, to obtain the required data. An example of such a program which determines the variation of the ultrasound parameters with particle size and frequency is given in Appendix A5. The program was written in FORTRAN 77, and uses the Numerical Algorithms Group FORTRAN Library subroutines (mark 15) to calculate the Bessel functions and to obtain the matrix solution of the complex boundary equations. The calculations were carried out on the University of Leeds Sun SPARCenter 2000 and Silicon Graphics Challenge XL servers.

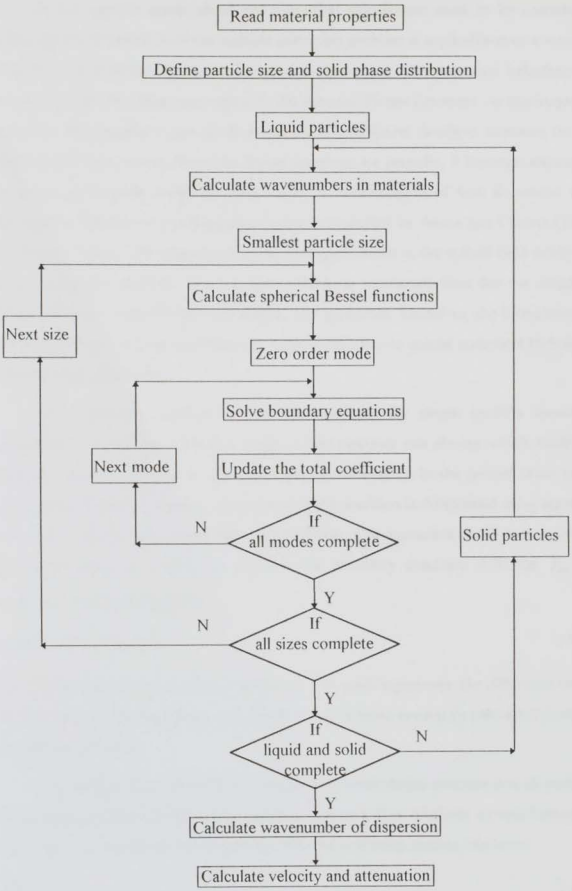

Figure 4.1 Flow chart of the computer program to calculate ultrasound velocity and attenuation in emulsions, according to scattering theory.

A few specific points about the numerical calculations need to be considered. Although the formulation of the multiple scattering problem is applicable over a range of frequency (if sufficient terms are included in the series), the numerical calculation is restricted to the low frequency region by the spherical Bessel functions. As the frequency increases, the imaginary part of the argument of the Bessel functions increases for the thermal and shear waves. Since the Bessel functions are periodic, it becomes impossible to obtain an accurate result for their value. A consideration of how to extend such calculations beyond the low frequency region is presented by Anson and Chivers (1993) and other workers. The majority of ultrasound applications in the colloid field satisfy the long wavelength condition, and it is also in the long wavelength limit that the simplified relationships developed in the next chapter are applicable. Therefore, the formulation of the previous sections was used directly, without recourse to special numerical techniques to avoid these difficulties.

The computer program is able to calculate the single particle scattering coefficients, A_n, for any scattering mode, n (the operator can choose which modes to include). For the purposes of this study only coefficients up to the second order mode were calculated. The complex wavenumber of the emulsion is determined using equation 4.38, up to second order in particle concentration. One numerical detail is that for the first order scattering mode, the terms in the boundary condition 4.30 for P_{n0} are modified, using the relationship

$$aj_1'(a) - j_1(a) = -aj_2(a) \qquad [4.39]$$

for both the Bessel and the Hankel functions. For small arguments, the difference on the left hand side of this equation is very small, and so is more accurately calculated from the second order function.

The wavenumber derived from multiple scattering theory assumes that all particles (scatterers) are identical (the same size and material). It is relatively straightforward to show that, in a dispersion which includes different scattering species, the terms

$$\frac{\phi A_n}{r^3} \qquad [4.40]$$

in equation 4.38, should be replaced by

$$\sum_i \frac{\phi_i A_{ni}}{r_i^3} \qquad [4.41]$$

where the sum is over the different scattering species. Equation 4.41 is an average according to the number density of scatterers. This is relevant to dispersions in which there are particles of different sizes (polydisperse) or some solid and some liquid particles. The single particle scattering coefficient must be determined for each species of scatterer separately: for each size of particle and for solid and liquid particles. The scattering coefficients for solid scatterers are obtained by converting the equations 4.25 to 4.30 in the way specified by Allegra and Hawley (1972). The shear viscosity of the fluid is replaced by the bulk modulus of the solid in the form given in equation 4.18. In addition, all the terms in the boundary equations relating to the solid droplets must be multiplied by a factor of $-i\omega$. In the computer program, the solid droplets are assumed to be of the same material (solidified) as the liquid droplets, so that the particle size distribution is simply converted for solid droplets using the ratio of the solid to liquid densities. The proportion of particles which are solid at each radius must also be specified. The computer program calculates the combined scattering coefficient, given the particle size distribution, and the proportion of particles which are solid.

A numerical solution for the ultrasound propagation parameters of velocity and attenuation can therefore be calculated for any polydisperse, mixed solid/liquid emulsion. This allows the comparison and development of ultrasound theories applicable for the interpretation of experimental measurements on emulsions. The interpretation of ultrasound velocity measurements of creaming in emulsions was of particular interest, such as those obtained from the equipment shown in figure 1.1. These emulsions are generally polydisperse and the particle size distribution at any height varies with time. Therefore it was vital to be able to calculate the predicted ultrasound velocity for any given oil concentration and particle size distribution. This work was aided by the computer modelling of creaming which is described in chapter 2. The model enabled the construction of fully characterised data on particle size distribution and concentration profiles which could then be used to compare ultrasound theories and help to develop new simplified ways of interpreting ultrasound measurements. To this end, the numerical scattering theory calculations were integrated into the creaming model described in chapter 2, allowing the calculation of the ultrasound velocity and attenuation predicted by multiple scattering theory for the constructed creaming emulsions. The benefit of the

computer model is that all of the system parameters are known, whereas in an experimental system, the particle size distribution is not known as a function of height and time, and the concentration is only extracted from the measured ultrasound velocity. Therefore, with the computer model and the ultrasound theory calculations, accurate assessment can be made of the applicability of various ultrasound models in interpreting the ultrasound data.

The ability to calculate ultrasound parameters for solid and liquid particles in an emulsion assists in the study of the applicability of simplified scattering theories for crystallisation experiments in emulsions. Measurements of ultrasound velocity have been used to calculate the proportion of the dispersed phase droplets which are solid (the solid fat content) and thereby examine crystallisation kinetics (Dickinson et al, 1993b). The interpretation of ultrasound measurements in both creaming and crystallising systems is discussed specifically in chapter 5.

4.6 Important limiting solutions of scattering theory

The formulation described in the preceding sections allows numerical calculation of the ultrasound velocity and attenuation in an emulsion, whose properties are known. These calculations are not convenient for routine use in interpreting ultrasound measurements. In some cases, however, simplified forms of the velocity and attenuation exist, which may be more appropriate and more easily implemented. The numerical calculations were used to investigate the limiting forms of the scattering theory results, to establish simpler expressions, and to determine the conditions under which these might be applied.

The applications of ultrasound measurements in colloid science are usually in the long wavelength limit (the wavelength of the sound wave is much larger than the particle size). The wavelength of sound in pure water at 30 °C is approximately 1.5 mm at 1 MHz, compared with the colloidal particle sizes of approximately 1 μm. It is in this region that the useful simplified theories of ultrasound propagation can be applied. At higher frequencies the variation of velocity and attenuation with frequency can be very strong and is more difficult to predict. Therefore, all the further work on ultrasound propagation is restricted to the long wavelength region. This limit is sometimes called the Rayleigh limit, after Lord Rayleigh who first investigated the scattering of sound by

obstacles, and determined the scattered intensity under the long wavelength condition (Strutt, 1872, 1896). The definition of the long wavelength limit is given by

$$kr \ll 1 \qquad [4.42]$$

or in terms of the wavelength, and defining the inequality

$$\frac{2\pi r}{\lambda} < \frac{1}{10} \qquad [4.43]$$

In the long wavelength limit, the ultrasound velocity and the attenuation per wavelength ($\alpha\lambda$) vary with the parameter $r\sqrt{f}$ which is proportional to the thermal and shear wavelengths. The limit of the long wavelength region can be written in terms of this parameter as

$$r\sqrt{f} < \sqrt{\frac{v}{20\pi}} \cdot \sqrt{r} \qquad [4.44]$$

showing that at smaller particle sizes the limit occurs at smaller values of the scaling parameter. Conversely, at higher frequencies but with the same particle size, the long wavelength limit applies for a smaller range of the scaling parameter $r\sqrt{f}$. Thus the velocity and attenuation variation discussed in the following sections, which apply in the long wavelength region, must be truncated at the limit defined by equation 4.44. For smaller particle sizes, some of the features at large values of the scaling parameter may be absent, because they would occur outside the long wavelength region.

The ultrasound velocity and attenuation over a range of frequency and particle size were calculated numerically for a nominal 20 vol. % sunflower oil in water emulsion at 30 °C, and are shown in figures 4.2 and 4.3. The particle radius used for the calculations was 50 μm in order to obtain a large range of the scaling parameter $r\sqrt{f}$ within the long wavelength region. The physical data of the component phases which is required for the ultrasound scattering calculations is shown in table 4.1. These are identical to the emulsion properties used in the modelling of creaming behaviour (chapter 2).

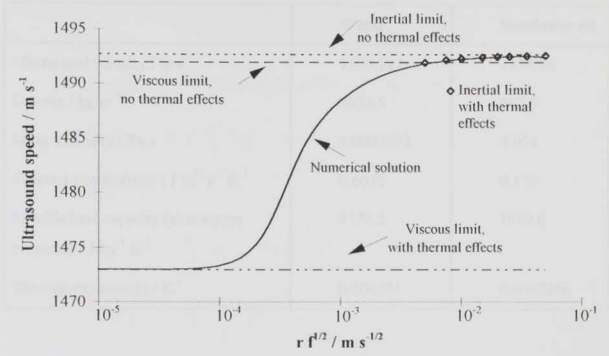

Figure 4.2 Ultrasound velocity as a function of the scaling parameter $r\sqrt{f}$ for a 20 vol.% sunflower oil in water emulsion at 30 °C.

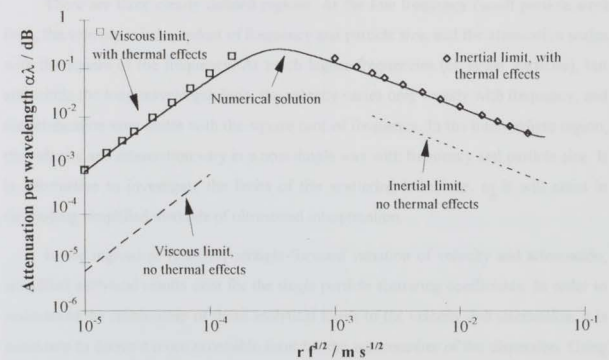

Figure 4.3 Ultrasound attenuation per wavelength as a function of the scaling parameter $r\sqrt{f}$ for a 20 vol.% sunflower oil in water emulsion at 30 °C.

	Water	Sunflower oil
Ultrasound velocity / m s^{-1}	1509.127	1437.86
Density / kg m^{-3}	995.65	912.9
Shear viscosity / Pa s	0.0007973	0.054
Thermal conductivity / J m^{-1} s^{-1} K^{-1}	0.6032	0.170
Specific heat capacity (at constant pressure) / J kg^{-1} K^{-1}	4178.2	1980.0
Thermal expansivity / K^{-1}	0.000301	0.0007266

Table 4.1 Physical properties for sunflower oil and pure water at 30 °C.
The data for water were taken from Kaye and Laby (1986). The properties of sunflower oil were given by McClements (1988).

There are three clearly defined regions. At the low frequency (small particle size) limit, the velocity is independent of frequency and particle size, and the attenuation scales with the square of the frequency. At much higher frequencies (or larger particles), but still within the long wavelength limit, the velocity varies only weakly with frequency, and the attenuation now scales with the square root of frequency. In the intermediate region, the velocity and attenuation vary in a non-simple way with frequency and particle size. It is informative to investigate the limits of this scattering behaviour, as it will assist in developing simplified methods of ultrasound interpretation.

In the regions of relatively straight-forward variation of velocity and attenuation, simplified analytical results exist for the single particle scattering coefficients. In order to understand the relationship of these analytical forms to the velocity and attenuation, it is necessary to derive a more accessible form for the wavenumber of the dispersion. Using a modified scattering parameter, the multiple scattering theory result, equation 4.37 can be used to show that

$$K = k_1\left[1+\frac{\phi}{2}\left(a_0+3a_1\right)-\frac{\phi^2}{8}\left(a_0^2-6a_0a_1-15a_1^2\right)\right] \qquad [4.45]$$

where

$$a_n = -\frac{3iA_n}{k^3 r^3} \qquad [4.46]$$

whence the dominant terms in the velocity give

$$\frac{1}{v} = \frac{1}{v_1}\left[1 + \frac{\phi}{2}\mathrm{Re}(a_0 + 3a_1) - \frac{\phi^2}{8}\mathrm{Re}\left(a_0^2 - 6a_0a_1 - 15a_1^2\right)\right] \qquad [4.47]$$

and for the attenuation

$$\alpha = \frac{\omega}{v_1}\left[\frac{\phi}{2}\mathrm{Im}(a_0 + 3a_1) - \frac{\phi^2}{8}\mathrm{Im}\left(a_0^2 - 6a_0a_1 - 15a_1^2\right)\right]$$

$$+\alpha_1\left[1 + \frac{\phi}{2}\mathrm{Re}(a_0 + 3a_1) - \frac{\phi^2}{8}\mathrm{Re}\left(a_0^2 - 6a_0a_1 - 15a_1^2\right)\right] \qquad [4.48]$$

Alternatively, the velocity can be written in the form

$$\frac{1}{v^2} = \frac{1}{v_1^2}\left[1 + \phi\,\mathrm{Re}(a_0 + 3a_1) + \phi^2\left(3\,\mathrm{Re}\,a_0\,\mathrm{Re}\,a_1 + 6\left(\mathrm{Re}\,a_1\right)^2\right)\right] \qquad [4.49]$$

or, equivalently

$$\frac{1}{v^2} = \frac{1}{v_1^2}\left[\left(1 + \phi\,\mathrm{Re}\,a_0\right)\left(1 + 3\phi\,\mathrm{Re}\,a_1\right) + 6\phi^2\left(\mathrm{Re}\,a_1\right)^2\right] \qquad [4.50]$$

An additional term in the velocity equations was neglected, since the attenuation in the continuous phase is small, and the imaginary part of the modified scattering coefficients (4.46) are also much smaller than their real part. The second term in the attenuation of equation 4.48 is often neglected, especially if only the first order in concentration is of interest. However, the first order contribution to the second term may not be negligible compared with the second order contribution to the first term. Therefore both terms have been given here.

It is clear from equations 4.47 and 4.48 that the first order effects (in concentration) on the velocity are related to the real part of the modified scattering coefficients (4.46), and on the attenuation to the imaginary part of these coefficients. In order to understand the variation of the velocity and attenuation with particle size and frequency, the special cases of the modified scattering coefficients must be found. Simplified results for the single particle scattering coefficients can be obtained by making

a number of assumptions about the properties of the materials. Table 4.2 defines the conditions used to obtain the limiting analytical cases of the coefficients for fluid particles in a fluid medium. In the long wavelength limit, all of these conditions are valid for most fluids.

Condition	Description
$kr \ll 1,\ k'r \ll 1$	Propagational wavelength much larger than particle radius (Rayleigh limit)
$\left\|\frac{k^2}{k_t^2}\right\| \ll 1,\ \left\|\frac{k'^2}{k_t'^2}\right\| \ll 1$	Thermal wavelengths much smaller than the propagational wavelengths
$\left\|\frac{k^2}{k_s^2}\right\| \ll 1,\ \left\|\frac{k'^2}{k_s'^2}\right\| \ll 1$	Shear wavelengths much smaller than the propagational wavelengths
$\alpha'^2 \ll \frac{\omega^2}{v'^2},\ \alpha'^2 \ll \frac{\omega^2}{v'^2}$	Attenuation in bulk phases negligible

Table 4.2 Criteria applied to obtain limiting values of single particle scattering coefficients for fluid particles.

The zero order scattering mode represents spherically symmetric scattering. In the long wavelength limit, the zero order scattering coefficient for fluid particles in a fluid medium is given by

$$A_0 = \frac{ik^3r^3}{3}\left(\frac{\rho' k'^2}{\rho k^2} - 1\right) + ikr\frac{G_p}{G_t}\left(1 - \frac{\tau' G_t'}{\tau G_t}\right)^2 \cdot \frac{1}{F} \qquad [4.51]$$

where

$$F = \frac{h_0(b)}{bh_1(b)} - \frac{\tau}{\tau'}\frac{j_0(b')}{b' j_1(b')} \qquad [4.52]$$

(Epstein and Carhart, 1953 and Allegra and Hawley, 1972). The coefficient consists of two terms, and can be written as

$$A_0 = A_{01} + A_{02} \qquad [4.53]$$

The limiting analytical values of these terms under various conditions are given in table 4.3.

The first term of equation 4.51 can be simplified by substituting the propagational wavenumber (4.4), and using the Wood equation 4.1 for sound speed. The real part of the modified scattering coefficient (equation 4.46) is therefore proportional to the difference in compressibility between the two phases, as shown in the table. This result was obtained by Rayleigh (Strutt, 1872, 1896) (although Rayleigh incorrectly converted the sound speed, density and compressibility relationship). He considered the problem in the absence of thermal and viscous effects (no thermal or shear waves were included, no shear stress was present and the thermal boundary conditions were neglected). Thus the only waves to be considered were the incident, internal and scattered propagational modes. The continuity condition at the boundary was imposed on the radial velocity and the pressure. This illustrates that the first part of the zero order scattering coefficient is not influenced by thermal effects.

An examination of the radial velocity and pressure in the long wavelength limit for the incident wave and the propagational wave inside the particle, shows that the ratio of these properties for the two modes is in proportion to the compressibility. By definition, the compressibility of a material defines the fractional change in volume caused by a given pressure. For a spherical surface, this volume change is directly proportional to the radial velocity at the surface. The propagational wave inside the particle produces a different radial velocity for the same pressure from that caused by the incident wave because of the compressibility difference between the two materials. Therefore, a scattered propagational wave must be produced to maintain the continuity of radial velocity as well as pressure. Thus the amplitude of the scattered wave is proportional to the difference in compressibility of the internal and external materials.

The radial velocity of the propagational modes in the absence of thermal waves is in phase with the incident wave (this is the case considered by Rayleigh, but he also neglected shear stress). However, the phase of the radial stress for the scattered propagational mode varies with frequency, as shown in figure 4.4. At low frequencies the viscous stress dominates in the scattered propagational wave, but the pressure term is predominant in the incident and internal propagational waves. At the high frequency

Scattering coefficient	Condition	Description
$A_{01} = \frac{ik^3 r^3}{3} \cdot \left\{ \frac{\Delta\kappa}{\kappa} + 2i\frac{\kappa'}{\kappa}\Delta\left(\frac{v\alpha}{\omega}\right) \right\}$		
$A_{02} = \frac{ik^3 r^3(\gamma-1)}{3} \cdot \frac{\rho' C_p'}{\rho C_p} \left[\frac{\Delta\left(\frac{\beta}{\rho C_p}\right)}{\left(\frac{\beta}{\rho C_p}\right)} \right]^2 \cdot \left\{ 1 + \frac{i\omega r^2 \rho' C_p'}{3\tau}\left(1 + \frac{\tau}{5\tau'}\right) \right\}$	$\lvert k_i r\rvert \ll 1, \quad \lvert k_i' r\rvert \ll 1$	Thermal wavelength much larger than particle radius
$A_{02} = \frac{ik^3 r^3}{3} \cdot \frac{3(\gamma-1)}{r\sqrt{2\omega}} \left[\frac{\Delta\left(\frac{\beta}{\rho C_p}\right)}{\left(\frac{\beta}{\rho C_p}\right)} \right]^2 \cdot \sqrt{\frac{\tau\tau' \rho' C_p'}{\rho C_p}} \cdot \frac{(1+i)}{\left(\sqrt{\tau' \rho' C_p'} + \sqrt{\tau \rho C_p}\right)}$	$\lvert k_i r\rvert \gg 1, \quad \lvert k_i' r\rvert \gg 1$	Thermal wavelength much shorter than particle radius

Table 4.3 Limiting analytical expressions for the zero order single particle scattering coefficient for fluid particles. The criteria in table 4.2 must also be satisfied.

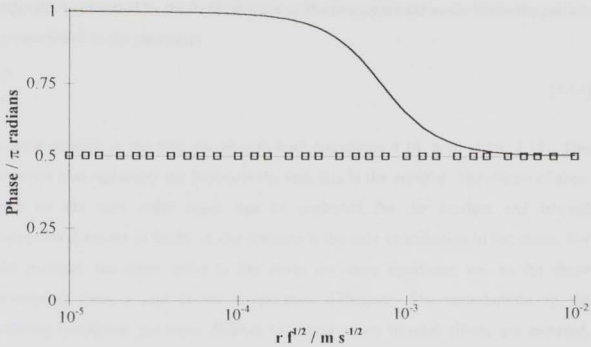

Figure 4.4 Phase angle of the stress at the particle surface for the zero order mode of 20 vol.% sunflower oil in water at 30 °C in the absence of thermal effects.
□ is the incident wave, and ——— the scattered propagational mode.

limit, the pressure is most important in the radial stress for the scattered wave, and therefore the stress is in phase with the incident and internal waves. This variation due to the viscous stress does not have a significant effect on the modified scattering coefficient, since the stress is dominated by the incident and internal wave modes.

Comparison of the first term of the zero order coefficient in table 4.3 with equations 4.47 and 4.48 shows that its effect on the velocity and attenuation (to first order in concentration) is independent of frequency. The attenuation must be determined carefully, since in this case both terms in equation 4.48 must be included. This is in contradiction to Allegra and Hawley (1972) who used the form of equation 4.31 to calculate attenuation, which omits some significant terms in this case. For the other scattering coefficients Allegra and Hawley's and Epstein and Carhart's expression for attenuation (4.31) is an acceptable approximation, because the losses due to the scattering mechanisms are much larger than the attenuation of the bulk phase.

The second term in the zero order scattering coefficient (equations 4.51 and 4.53) incorporates the thermal effects. For fluid particles this is due to the difference in the

temperature-pressure coupling in the different materials. For a given pressure, the temperature generated by the incident wave or the propagational mode inside the particle is proportional to the parameter

$$\frac{\beta}{\rho C_p} \qquad [4.54]$$

for each material in the long wavelength limit (equations 4.19, 4.20, 4.10, 4.15). This parameter also represents the factors in the heat flux in the material. The effects of shear stress on the zero order mode can be neglected for the incident and internal propagational modes in fluids, so the pressure is the only contribution to the stress. For solid particles, the shear terms in the stress are more significant and so the shape deformation plays a part in the temperature difference. The contributions to the scattering coefficient are more difficult to isolate when thermal effects are included, because there are four waves generated at the particle surface, and four boundary conditions to be satisfied. However, it is clear that the thermal waves must be generated to maintain the continuity of temperature at the particle surface, given that the incident wave and the propagational wave inside the particle produce a different temperature change for the same pressure field. The differing heat flow properties inside and outside the particle also contribute to the magnitude and phase of the generated waves.

The value of the thermal term varies with frequency and particle size, and is determined by the magnitude of the thermal wavelength in the two materials. The form of the scattering coefficient contribution due to thermal effects is given in table 4.3. When the thermal wavelength is much larger than the particle size (low frequency) the term takes the first form in the table. The contribution to the velocity (compare equation 4.47) is independent of frequency in this region, and the attenuation (equation 4.48) varies as the square of frequency. If the thermal wavelength is much shorter than the particle size ("high" frequency), the thermal effect in the scattering coefficient takes the second form of table 4.3. The effect on the velocity is much smaller in this region and decreases as the frequency (or particle size) increases. The thermal effects become negligible at sufficiently high frequency. This may, however, no longer be in the long wavelength region for which the analytical results are valid. The thermal attenuation in the short thermal wavelength region varies as the square root of frequency.

The contributions of the two components (compressibility and thermal differences) of the zero order mode to the scattering amplitude can be illustrated by examining the phase of the different wave modes at the surface of the particle. Figures 4.5 to 4.8 show the phase of the radial velocity, stress, temperature and heat flux at the particle surface for each of the wave modes inside and outside the particle. The presence of the thermal waves modifies the scattered wave so that its radial velocity is no longer always in phase with the incident wave. It is clear that the magnitude of the thermal wavelength relative to the particle size has an effect on the form of the heat flow, radial velocity, stress and temperature relationship to the incident wave. Most noteworthy is that the thermal effects on ultrasound velocity at low frequency correspond to the temperature in the thermal waves oscillating 90° out of phase with the other waveforms. At higher frequencies the temperature oscillations in all waves gradually come into phase with each other, manifested in the "high frequency" form of the thermal contribution to velocity. The attenuation still increases with frequency because of the greater energy in the thermal waves at higher frequency.

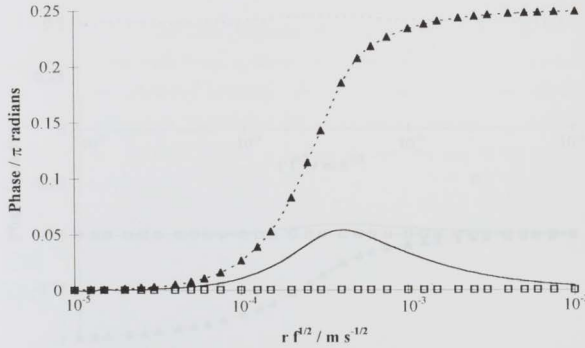

Figure 4.5 Phase angle of the radial velocity at the particle surface for the zero order mode of a 20 vol.% sunflower oil in water emulsion at 30 °C.

□ is the incident wave, —— the scattered propagational mode, ▲ the thermal mode, and - - - - the internal thermal mode.

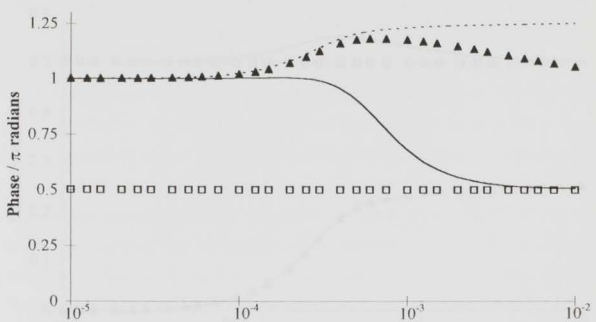

Figure 4.6 Phase angle of the stress component P_{rr} at the particle surface for the zero order mode for a 20 vol.% sunflower oil in water emulsion at 30 °C.

□ is the incident wave, —— the scattered propagational mode, ▲ the thermal mode, and ···· the internal thermal mode.

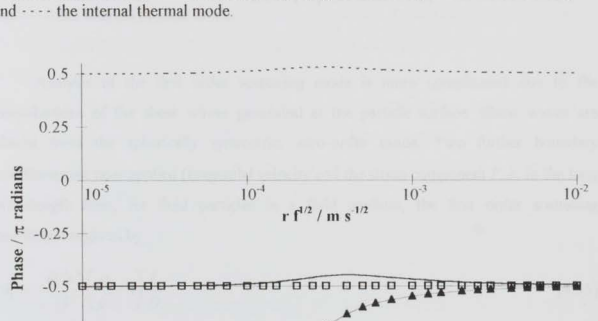

Figure 4.7 Phase angle of the temperature at the particle surface for the zero order mode for a 20 vol.% sunflower oil in water emulsion at 30 °C.

□ is the incident wave, —— the scattered propagational mode, ▲ the thermal mode, and ···· the internal thermal mode.

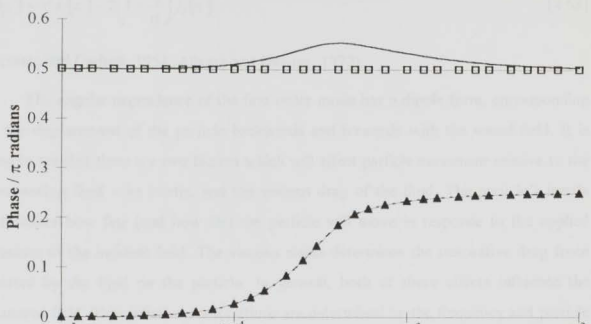

Figure 4.8 Phase angle of the heat flux at the particle surface for the zero order mode for a 20 vol.% sunflower oil in water emulsion at 30 °C.

□ is the incident wave, —— the scattered propagational mode, ▲ the thermal mode, and - - - - the internal thermal mode.

Analysis of the first order scattering mode is more complicated due to the contributions of the shear waves generated at the particle surface. Shear waves are absent from the spherically symmetric, zero-order mode. Two further boundary conditions are now applied (tangential velocity and the stress component $P_{r\theta}$). In the long wavelength limit, for fluid particles in a fluid medium, the first order scattering coefficient is given by

$$A_1 = -\frac{ik^3r^3}{3}\left(\frac{\rho}{\rho'}-1\right)\frac{L}{D} \qquad [4.55]$$

where

$$L = h_2(c)Q(c') - \frac{\eta}{\eta'}ch_1(c)j_2(c') \qquad [4.56]$$

$$D = Q(c')\left[3\frac{\rho}{\rho'}h_2(c) + 2\left(\frac{\rho}{\rho'}-1\right)h_0(c)\right] - \frac{\eta}{\eta'}\left(\frac{\rho}{\rho'}+2\right)ch_1(c)j_2(c') \qquad [4.57]$$

$$Q(c') = c' j_1(c') - 2\left(1 - \frac{\eta}{\eta'}\right) j_2(c') \qquad [4.58]$$

(Epstein and Carhart, 1953, Allegra and Hawley, 1972).

The angular dependence of the first order mode has a dipole form, corresponding to the displacement of the particle backwards and forwards with the sound field. It is easy to see that there are two factors which will affect particle movement relative to the surrounding fluid – its inertia, and the viscous drag of the fluid. The particle's inertia determines how fast (and how far) the particle will move in response to the applied pressure of the incident field. The viscous stress determines the restorative drag force exerted by the fluid on the particle. In general, both of these effects influence the scattered field. Their relative contributions are determined by the frequency and particle size, and the scattering coefficient is therefore frequency dependent. However, two important limits exist in which either the inertial or viscous effects dominate.

When the wavelength of shear waves is much shorter than the particle size ("high" frequency), the effect of the inertia of the particle is much stronger than the viscous drag. The motion of the particle caused by the incident pressure is different from the motion of the fluid (because of their different density). The viscous drag is insufficient to force the particle to move with the surrounding fluid, so the particle moves out of phase with it. The fluid then appears to the sound wave to have an additional inertia due to the presence of the particle. The scattering coefficient takes the second form given in table 4.4, if the particle is very viscous. A more general result is complicated. The additional inertia due to the particle is contained in the factor

$$\frac{\rho' - \rho}{2\rho' + \rho} \qquad [4.59]$$

This may be called the inertial limit. Rayleigh considered this problem in the absence of viscous drag from the surrounding fluid, by neglecting the shear waves. Thus the term represents the limit of negligible continuous phase viscosity compared with inertial forces. Thermal waves were also neglected by Rayleigh, but in the long wavelength limit the coupling between thermal and viscous effects in fluids is negligible anyway. The contribution of the inertial effect to velocity is independent of frequency (equation 4.47), but the attenuation in this region varies with the square root of frequency (equation 4.48).

Scattering coefficient	Condition	Description
$A_1 = \frac{ik^3r^3}{9}\cdot\frac{\Delta\rho}{\rho}\left[1+\frac{2i}{9}\cdot\frac{\omega\rho r^2}{\eta}\cdot\frac{\Delta\rho}{\rho}\right]$	$\lvert k_s r\rvert \ll 1,\ \lvert k_s' r\rvert \ll 1$ $\eta' \gg \eta$	Shear wavelength much larger than particle radius Particle very viscous Viscous effects dominate over inertial effects
$A_1 = \frac{ik^3r^3}{3}\cdot\frac{(\rho'-\rho)}{(2\rho'+\rho)}\left[1+\frac{3i}{r}\sqrt{\frac{2\eta}{\omega\rho}}\cdot\frac{(\rho'-\rho)}{(2\rho'+\rho)}\right]$	$\lvert k_s r\rvert \gg 1,\ \lvert k_s' r\rvert \gg 1$ $\eta' \gg \eta$	Shear wavelength much shorter than particle radius Particle very viscous Inertial effects dominate over viscous effects

Table 4.4 Limiting analytical expressions for the first order single particle scattering coefficient for fluid particles. The criteria in table 4.2 must also be satisfied.

When the shear wavelength is much larger than the particle size (low frequency), the effect of the viscous drag of the surrounding fluid is much stronger than the inertial forces on the particle. The particle is forced by the viscous drag to move in phase with the surrounding fluid. In some cases, if the density difference between dispersed and continuous phases is very large, the inertial effects still dominate in this region. However, for most food systems and for the emulsions studied in this work the density difference is relatively small, and the viscous stress is most significant. The scattering coefficient is therefore dependent only on the density difference between particle and fluid, and takes the form given in table 4.4 for very viscous particles. Lamb (1932, p. 514) obtained the same limiting results for the first order mode for rigid solid particles (no waves inside the particle) in the absence of thermal effects. Therefore, these limiting conditions are determined simply by the particle's motion in the surrounding fluid, and not by the response of the material inside the particle to the sound wave.

The phase angles of the critical quantities at the particle surface are shown in figures 4.9 to 4.14. Although the variation of the relative contributions for each of the seven wave modes is very complicated, a significant variation in the phase of the scattered propagational mode appears only to occur in the stress component P_{rr} (figure 4.11). At low frequencies the stress due to the scattered wave is 90° out of phase with the incident wave, but at "high" frequencies it is in anti-phase. In the other stress component (figure 4.12) it may be noticed that the internal and external shear waves are 90° out of phase at low frequencies, but at higher frequencies their shear stress becomes in phase with each other. It is difficult to draw conclusions from the individual wave motions as to the movement of the particle itself (partly due to the fact that the wave solutions are in spherical co-ordinates, whereas the particle motion is one-dimensional and along the incident wave propagation direction). The simpler approaches of Lamb and Rayleigh are more informative in this regard, as described above, since they illustrate the two limiting solutions for the visco-inertial scattering in terms of the particle motion relative to the surrounding fluid.

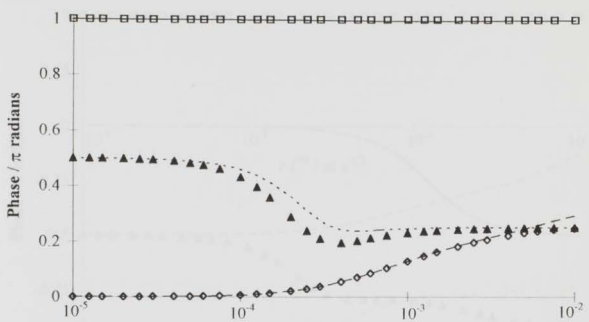

Figure 4.9 Phase angle of the radial velocity at the particle surface for the first order mode for a 20 vol.% sunflower oil in water emulsion at 30 °C.

□ is the incident wave, —— the scattered propagational mode, ▲ the thermal mode, ···· the internal thermal mode, ◇ the shear mode, and – – – the internal shear mode.

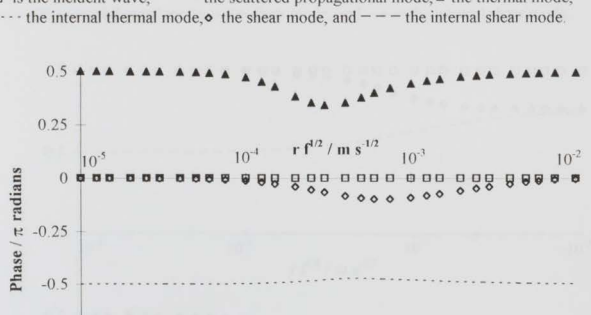

Figure 4.10 Phase angle of the tangential velocity at the particle surface for the first order mode for a 20 vol.% sunflower oil in water emulsion at 30 °C.

□ is the incident wave, —— the scattered propagational mode, ▲ the thermal mode, ···· the internal thermal mode, ◇ the shear mode, and – – – the internal shear mode.

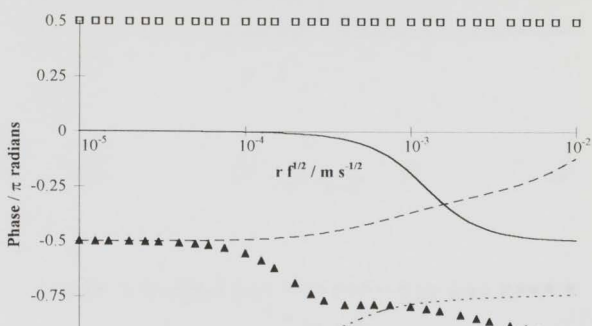

Figure 4.11 Phase angle of the stress component P_{rr} at the particle surface for the first order mode for a 20 vol.% sunflower oil in water emulsion at 30 °C.

□ is the incident wave, —— the scattered propagational mode, ▲ the thermal mode, - - - - the internal thermal mode, ◇ the shear mode, and – – – the internal shear mode.

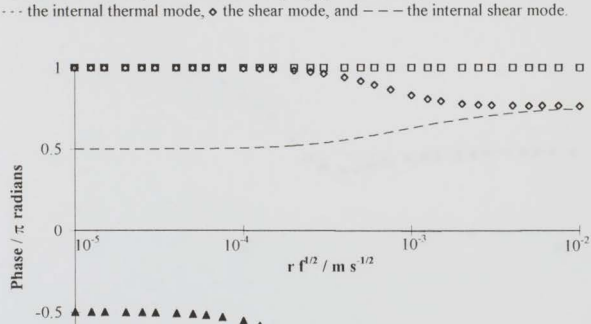

Figure 4.12 Phase angle of the stress component $P_{r\theta}$ at the particle surface for the first order mode for a 20 vol.% sunflower oil in water emulsion at 30 °C.

□ is the incident wave, —— the scattered propagational mode, ▲ the thermal mode, - - - - the internal thermal mode, ◇ the shear mode, and – – – the internal shear mode.

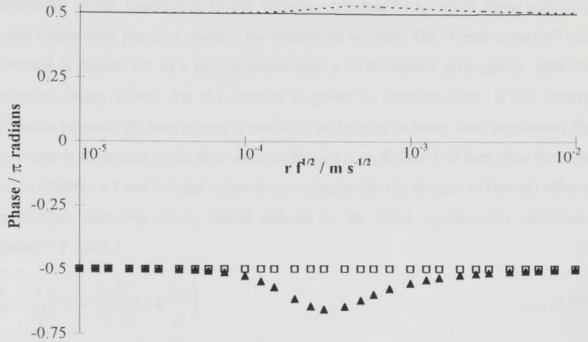

Figure 4.13 Phase angle of the temperature at the particle surface for the first order mode for a 20 vol.% sunflower oil in water emulsion at 30 °C.

□ is the incident wave, —— the scattered propagational mode, ▲ the thermal mode, - - - - the internal thermal mode.

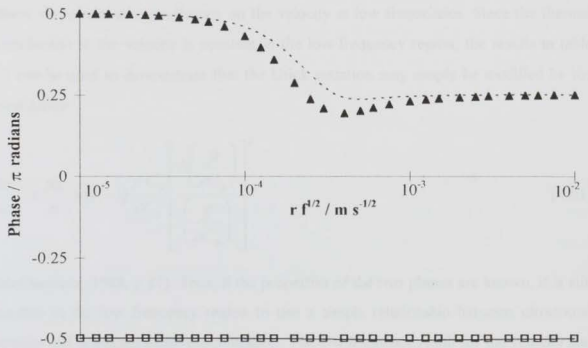

Figure 4.14 Phase angle of the heat flux at the particle surface for the first order mode for a 20 vol.% sunflower oil in water emulsion at 30 °C.

□ is the incident wave, —— the scattered propagational mode, ▲ the thermal mode, - - - - the internal thermal mode.

Having established the special cases of the scattering coefficients and the relationship of the coefficients to the velocity, it is helpful to relate these scattering theory results with previous theories for ultrasound velocity. The "Urick equation" was presented in section 4.2 as a homogeneous theory of ultrasound propagation. Multiple scattering theory shows that the velocity is given by equation 4.50. If the density difference between the two phases is small (as is the case in many food emulsions) the extra term in the square of the first order coefficient is negligible. It is then clear from the results of tables 4.3 and 4.4 that at low frequencies, and in the absence of thermal effects, the multiple scattering theory model reduces to the Urick equation for ultrasound velocity 4.1 and 4.2.

$$\frac{1}{v^2} = \frac{1}{v_1^2}\left(1+\phi\frac{\Delta\kappa}{\kappa}\right)\left(1+\phi\frac{\Delta\rho}{\rho}\right) \qquad [4.60]$$

Urick and Ament (1949) recognised that this equation was a special case of scattering theory, but omitted thermal effects in their analysis. They used the "thin slab approximation" described in the previous section, along with the results of Lamb (1932) for the first order scattering coefficients. The Urick velocity from this equation is shown for the sunflower oil in water emulsion in figure 4.2. It is clear that in this case thermal effects do have a strong influence on the velocity at low frequencies. Since the thermal contribution to the velocity is constant in the low frequency region, the results in table 4.3 can be used to demonstrate that the Urick equation may simply be modified by the substitution

$$\frac{\Delta\kappa}{\kappa} \rightarrow \frac{\Delta\kappa}{\kappa} + (\gamma-1)\frac{\rho' C_p'}{\rho C_p}\left[\frac{\Delta\left(\frac{\beta}{\rho C_p}\right)}{\left(\frac{\beta}{\rho C_p}\right)}\right]^2 \qquad [4.61]$$

(McClements, 1988, p.27). Thus, if the properties of the two phases are known, it is still possible in the low frequency region to use a simple relationship between ultrasound velocity and dispersed phase concentration. The low frequency result for the velocity and attenuation using the limiting values of table 4.3 are shown in figures 4.2 and 4.3.

In the high frequency region within the long wavelength limit, the second set of results in tables 4.3 and 4.4 are valid. If the thermal term were neglected, and if the

densities of the two phases were again similar, the "Urick" equation would take another modified form:

$$\frac{1}{v^2} = \frac{1}{v_1^2}\left(1 + \phi\frac{\Delta\kappa}{\kappa}\right)\left(1 + \phi\frac{3\Delta\rho}{\left(2\rho' + \rho\right)}\right) \qquad [4.62]$$

This result was also presented by Urick and Ament (using their thin slab approximation for multiple scattering), in the absence of thermal effects. This "inertial limit" is shown in figures 4.2 and 4.3 for the sunflower oil in water emulsion. It is worth noting that when the densities of the two phases are very similar, the density term in the inertial limit approaches the viscous limit expression. In other words, the difference between the results of equations 4.60 and 4.62 may be within experimental error in velocity. It is clear even for sunflower oil in water (figure 4.2), that the inertial and viscous limits in the absence of thermal effects are very similar.

The thermal effect on velocity at the high frequency end of the long wavelength limit is more troublesome, because it is frequency dependent (table 4.3). It can obviously be included explicitly using the previous quoted results but removes a degree of simplicity from the velocity relationship. However, the magnitude of this term may not be very great. Figure 4.2 shows that for a wide range of frequency, its contribution is no greater than the difference between the viscous and inertial limits for the first order scattering mode. It is reasonable, therefore, to omit the thermal term for the purposes of obtaining a simple relationship between velocity and concentration. Were the thermal term to be very significant in this region, it would render the frequency range less suitable for use in polydisperse systems in which the size distribution is unknown or varying. For this purpose, it is necessary to have very little variation of velocity with particle size, and thus the low frequency limit is more appropriate. This point is discussed in greater detail in the next chapter, in which alternative methods for obtaining a velocity-concentration dependence are presented.

4.7 Summary of scattering theory results

The investigation of scattering theory was intended to determine the usefulness and applicability of various theoretical formulations to the interpretation of ultrasound measurements in emulsions. The main points of the chapter are as follows:

- Multiple scattering theory allows a physical understanding of the interaction of a sound wave with the particles in an emulsion.
- The multiple scattering formulation is particularly suitable in the long wavelength regime, in which many emulsion measurements are made.
- The scattering properties of particles, and the velocity and attenuation in an emulsion, can be calculated numerically, provided that the physical properties of the constituent phases are known.
- Some ranges of frequency and particle size exist for which simplified, analytical solutions are possible for ultrasound velocity. The limiting solutions are presented in tables 4.3 and 4.4.
- The limiting conditions of scattering theory can be related to previously used velocity–concentration formulae.

In summary, the multiple scattering theory formulation is an appropriate theoretical basis for interpreting ultrasound measurements. Although a general solution requires numerical techniques, some simpler expressions exist which can be applied in an experimental situation. However, the physical properties of the materials in an emulsion are often not known, and the calculation of scattering characteristics is then difficult. In chapter 5, a number of practical solutions are presented for the determination of the scattering properties of emulsions, without recourse to a full scattering theory calculation.

Chapter 5 : Methods for Interpreting Ultrasound Measurements

In the previous chapter, the theory of ultrasound propagation in dispersed systems was discussed. In principle, the results presented there can be used to calculate ultrasound velocity and attenuation in any well-characterised emulsion, subject to the criteria of section 4.4. By 'well-characterised' is meant a knowledge of the particle size (and size distribution), the concentration of dispersed phase, the frequency, and all the relevant physical properties of the constituent phases.[1] Conversely, if all of these parameters are known except for the dispersed phase concentration, a measurement of ultrasound velocity can be used to determine this quantity. The results of multiple scattering theory have been used to calculate the ultrasound velocity in a variety of well-characterised emulsions, and these have been found to agree well with experimental measurements (McClements, 1992, McClements and Povey, 1989). However, some workers have found significant discrepancies between the predictions of this theory and their experimental results on other dispersions (Holmes and Challis, 1993, Holmes et al., 1993, 1994). This may be due to the violation of some of the fundamental assumptions of the theory, such as the absence of particle interactions or flocculation, as discussed in chapter 4. Alternatively it may be that the values of the physical properties used for the phases (e.g. viscosity, thermal conductivity) do not correspond exactly to the real values of the system being measured. The differences may be due to experimental uncertainties in the values or to variation in the materials. Holmes et al. (1993) studied the effect of uncertainties in a number of parameters on the calculation of ultrasound velocity and attenuation. In some cases, the effects were very significant. The errors involved in making attenuation measurements were found at Leeds to be much greater than for measurement of sound speed, although other workers have made accurate attenuation measurements. Thus, most of this work has concentrated on ultrasound velocity rather than attenuation.

Assuming that all the system parameters are known and that scattering theory does provide an accurate prediction of ultrasound velocity, a full scattering theory calculation

[1] An example of the data required is shown in table 5.1, later in this chapter.

could be used for concentration determination. However, it does not lend itself to this technique, because the determination of the scattering coefficients is a complex numerical problem which would need to be carried out for each sample used. Some, simpler analytical solutions exist under various limiting conditions (see section 4.6), for example the Urick equation. However, even these simplified expressions may require a substantial amount of physical data for the system being measured. The paucity of such data for many food components, particularly their thermal properties, causes a problem for the use of scattering theory. In addition, the application of the theory to some systems has been found to be inaccurate and therefore it cannot be relied upon to produce acceptable results.

The aim of the present work is to develop simple methods of finding the relationship between measured ultrasound velocity and dispersed phase concentration (or solid fat content). To be valuable for routine use, these methods must avoid the need for an inconvenient scattering theory calculation and the difficulties and restrictions associated with it. The results presented in this chapter are concerned with ultrasound velocity and attenuation measurements in emulsions, particularly creaming and crystallisation. Several techniques are discussed for determination of the ultrasound velocity–concentration relationship from experimental measurements in these systems.

5.1 Experimental determination of scattering coefficients

The central result of multiple scattering theory is an equation for the square of the wavenumber of the dispersion in the form of a series in ascending powers of particle concentration (or volume fraction of dispersed phase). The velocity may be calculated from the wavenumber, and hence from the scattering coefficients, as given by equations 4.47 and 4.49. The latter will be the preferred form for this chapter because of its similarity with the Urick equation. Thus the velocity, v, may be written as

$$\frac{1}{v^2} = \frac{1}{v_1^2} + \delta\phi + \varepsilon\,\phi^2 + \mathrm{O}\left(\phi^3\right) \qquad [5.1]$$

Subscript 1 represents the continuous phase in this context, and ϕ is the volume fraction. The coefficients are related to the Urick equation by

$$\delta = \frac{1}{v_1^2}\left[\frac{\Delta\kappa}{\kappa_1} + \frac{\Delta\rho}{\rho_1}\right], \varepsilon = \frac{1}{v_1^2}\left[\frac{\Delta\kappa}{\kappa_1} \cdot \frac{\Delta\rho}{\rho_1}\right] \qquad [5.2]$$

and to the modified scattering coefficients (see equation 4.46) by

$$\delta = \frac{1}{v_1^2}\mathrm{Re}(a_0 + 3a_1), \quad \varepsilon = \frac{1}{v_1^2}\left[3\,\mathrm{Re}\,a_0\,\mathrm{Re}\,a_1 + 6(\mathrm{Re}\,a_1)^2\right] \qquad [5.3]$$

where $\Delta\kappa$ and $\Delta\rho$ are the differences in compressibility and density between the dispersed and continuous phases respectively, and a_n are the modified scattering coefficients. Since it is the velocity which is measured, and the concentration to be determined, we can write

$$\phi = \delta_v\left(\Delta 1/v^2\right) + \varepsilon_v\left(\Delta 1/v^2\right)^2 \qquad [5.4]$$

where

$$\Delta 1/v^2 = \frac{1}{v^2} - \frac{1}{v_1^2} \qquad [5.5]$$

and

$$\delta_v = \frac{1}{\delta} \quad \varepsilon_v = -\frac{\varepsilon}{\delta^3} \qquad [5.6]$$

The coefficients of the equations (5.1 and 5.4) are related to the scattering coefficients of the particles, and may be calculated using the results of the previous chapter if all the system properties are known. However, the form of equations 5.1 or 5.4 is exactly the approach which would be taken if an empirical relationship were to be found between velocity and concentration. A linear relationship would be attempted to fit experimental data, then a quadratic relationship, and so on. Following such an empirical procedure in this case is effectively a determination of the scattering characteristics of the particles in the sample, or the scattering properties of the collective dispersion (if flocculation is present, for example). The violations of the scattering theory assumptions may be incorporated into a modification of the scattering properties. If these scattering characteristics are determined directly for the system of interest these modifications are taken into account. Such modifications might include non-sphericity, particle interactions, or flocculation.

Therefore, measurements to find the relationship between ultrasound velocity or attenuation and dispersed phase concentration can be thought of as a determination of the scattering characteristics, not necessarily of the individual particles, but of the collective properties of the system. Experimental methods for obtaining the scattering properties for a sample also avoid the difficulties associated with finding the physical data for the materials. The scattering coefficients are related to the experimental velocity coefficients when there is a single dispersed component by

$$\mathrm{Re}\,a_0 = -\frac{\delta v_1^2}{2}(1 \pm 3S) \qquad [5.7]$$

$$\mathrm{Re}\,a_1 = \frac{\delta v_1^2}{2}(1 \pm S) \qquad [5.8]$$

where

$$S = \sqrt{1 - \frac{4\varepsilon}{3\delta^2 v_1^2}} \qquad [5.9]$$

True correspondence with scattering theory, and with the dipole and monopole characteristics of the scattering modes, requires the choice of the "minus" solution of these equations.

The results of this chapter are designed to enable the determination of the scattering properties of a sample from experimental data, in a variety of applications. These build on the principles of scattering theory, and aim to produce simple and convenient methods along the lines of the popular Urick equation.

5.2 Particle size and frequency dependence

The principal applications of this work are concerned with a velocity–concentration relationship. It was seen in chapter 4 that the ultrasound velocity in a scattering system varies with particle size and frequency (figures 4.2 and 4.3). In some regions this variation may be quite strong, whereas in other frequency ranges the velocity is independent of frequency and particle size. These limiting conditions of scattering theory were discussed in chapter 4. The implication of this dependence is that any velocity–concentration relationship is valid only for the frequency and particle size (and size distribution) for which it was determined. A change in the size distribution or the

frequency may cause the velocity relationship to become invalid. In the scattering theory formulation, this is equivalent to the scattering properties being functions of frequency and particle size, and their values being only applicable to a specific particle size and frequency.

Computer modelling of creaming in emulsions (chapter 2) has demonstrated that in a polydisperse sample there can be strong size fractionation especially in the cream layer. The particle size distribution may vary strongly with height in the sample, and at any point may be quite different from the size distribution in the initial uniform sample. This can clearly cause a problem for the interpretation of ultrasound velocity measurements. The ultrasound velocity profiles predicted from multiple scattering theory for the results of the computer model show that velocity variation in the cream takes quite a different form from the concentration dependence (section 2.8.3). If velocity measurements on this system were interpreted using a constant velocity–concentration relationship the volume fraction profiles would look quite different from the true profile. Figure 5.1 shows the result of applying the renormalisation method (described in section 5.4) to these velocity profiles. The velocity–concentration relationship has been assumed constant for the entire system, and has been calculated by ensuring that the total volume of oil in the sample remains constant. The renormalisation coefficients were calculated using the initial emulsion and the velocity profile after 500 days. It is clear that the concentration profile calculated by renormalisation is far from the true profile (figure 5.1), because the particle size variation in the cream has the opposite influence on the velocity to the concentration variation. This clearly illustrates the difficulties of particle size dependence of velocity measurements, especially when the particle size distribution is so strongly varying. The computer modelling results for ultrasound velocity in a creaming emulsion are discussed in more detail section 2.8.3.

The computer model enables us to make such comparisons which are not possible with experimental data because the concentration and particle size variation with height are unknown, and only the ultrasound velocity is measured. The model results can be used in both ways — to examine the velocity profiles predicted from different theories, and to compare the model's predicted concentration profiles with those which would be obtained from the ultrasound data if standard velocity–concentration relationships were applied. Multiple scattering theory is taken as the benchmark in these cases.

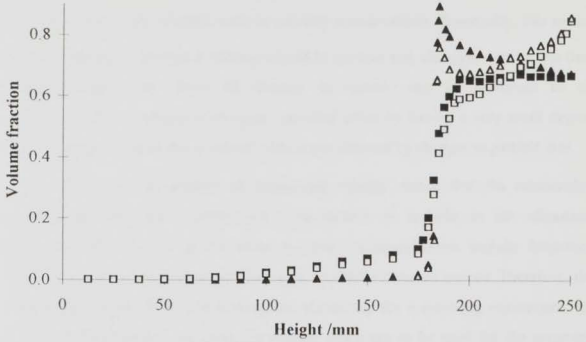

Figure 5.1 Comparison of renormalised concentration profiles with the actual profiles, generated by the computer model (section 2.8.3).

The sample is 20 vol.% sunflower oil in water at 30 °C, and the profiles are after 500 days (squares) and 1000 days (triangles). Open symbols represent the actual concentration and closed symbols the concentration calculated by renormalisation.

The particle size dependence clearly does not cause a problem in a monodisperse sample, since there can be no changes in particle size distribution. In a polydisperse sample, however, it is necessary to ensure that the velocity does not vary significantly over the range of particle size distributions in the system. If this is true, the fractionation in the cream will not affect the velocity–concentration relationship. This can be achieved either by reducing the degree of polydispersity in the sample, to avoid variations of particle size, or by choosing the particle size and frequency range so that the velocity is relatively insensitive to differences in particle size. In chapter 4, the velocity was shown to have two limiting conditions in the long wavelength region in which it varies little with particle size (section 4.6). The "high frequency" limit may not be present in the long wavelength region when the particle size is small. The low frequency region is therefore recommended for creaming experiments. A quantitative restriction on the application of a constant velocity–concentration relationship in a creaming experiment might be written as

$$v(\phi_{max}, r_{max}) - v(\phi_{max}, r_{min}) < \Delta v_{exp} \qquad [5.10]$$

where Δv_{exp} is the experimental error in velocity measurements. Essentially, this means that any variation in ultrasound velocity caused by particle size changes must be less than the experimental error. Thus, all changes in velocity can be attributed to oil concentration. The condition is obviously satisfied either by having a very small degree of size variation, or by having a velocity that is not affected by changes in particle size.

The frequency dependence of ultrasound velocity means that the relationship determined between the velocity and concentration is specific to the ultrasonic transducers used. Probes of the same nominal frequency often include frequency components over a range of frequencies which may differ between probes. Therefore, the determination of the velocity–concentration relationship for a creaming experiment, for example, must be carried out using the probes which are to be used for the creaming experiment itself.

5.3 Calibration

Previous creaming experiments for which the Urick equation was found to be invalid, were interpreted by a calibration technique (for example, Dickinson et al., 1994). A series of emulsions of known composition was made with a range of dispersed phase concentration. The ultrasound velocity was measured in each case, and a regression fit of velocity as a function of concentration was calculated. In this way, the concentration of oil could be determined from measured velocity profiles in subsequent creaming experiments. In the light of multiple scattering theory analysis, it is clear that this method is an experimental determination of the scattering properties of the sample. Although the velocity–concentration relationship has been written in terms of the inverse square of the velocity (equations 5.1 or 5.4), the principles apply equally well to a direct correspondence between the velocity and a power series in concentration. The calibration curve must of course be measured using the same ultrasound probes as used for the experiment. The method is not restricted to creaming experiments, but could be used to determine concentration in any samples, provided that a set of well-characterised emulsions can be made, in order to "calibrate" the velocity relationship.

The restrictions on the particle size distribution variation and on the dependence of velocity with particle size, as described in the previous section, must be applied for the calibration method to be valid. A test of the validity of the technique in creaming experiments is to calculate the total volume fraction of oil in the whole sample, as determined from the calibrated velocity measurements. The calculated volume fraction averaged over the height of the sample should remain equal to the initial volume fraction of oil in the uniform emulsion, which is usually known. A deviation of this quantity from the initial value is an indication that the velocity–concentration relationship is changing with time, or is not constant with height in the sample. In other words, the fractionation effect is influencing the ultrasound velocity, and the calibration curve does not apply over the whole sample.

The calibration technique was applied to recent measurements on a 20 vol.% sunflower oil in water sample at 30 °C, with a variety of concentrations of xanthan gum added to the aqueous phase. These measurements were made by Jian Guo Ma using the ultrasound scanner illustrated in figure 1.1 (Ma, 1995). The effect of xanthan on the ultrasound velocity in the aqueous phase was found to be negligible at the concentrations used (Dickinson et al., 1994). However, the effect of unadsorbed Tween20 in the water does have a significant effect on velocity, and all emulsions were made so that the concentration in the aqueous phase was 1 wt. % Tween20. A calibration curve was constructed using measurements made with the ultrasound scanner (operating at 1.19 MHz) and also with the *Ultrasound Velocity Meter* (UVM1) (operating at 2.25 MHz). The volume–surface average particle size, d_{32}, was 0.56 μm. The measured velocity as a function of oil concentration in each case is shown in figure 5.2. The difference between the two curves indicates that for these emulsions the particle size and frequency fall in the range in which ultrasound velocity does vary with these parameters. Therefore, the determination of concentration profiles using the calibration curve depends on the size distribution not varying so strongly in the cream that the curve becomes invalid.

The calibration curve measured in the ultrasound scanner was used to calculate the volume fraction profiles in creaming experiments on these emulsions. The resulting profiles for a 20 vol.% sunflower oil in water emulsion with 2 wt.% Tween20 and 0.03 wt.% xanthan are shown in figure 5.3. After 10 days the total volume fraction in the

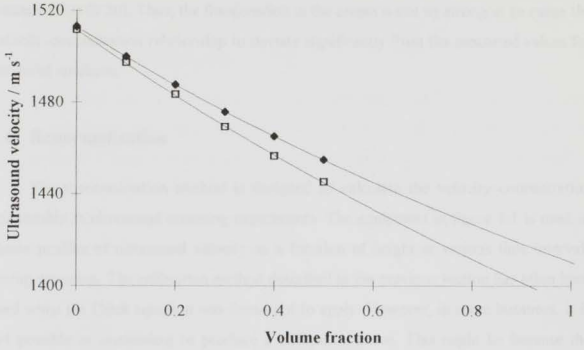

Figure 5.2 Calibration curves of ultrasound velocity as a function of oil concentration for emulsions of sunflower oil in water at 30 °C (Ma, 1995).

□ measured in the ultrasound scanner (1.19 MHz), ◆ measured in the ultrasound velocity meter (2.25 MHz), with their respective fitted curves

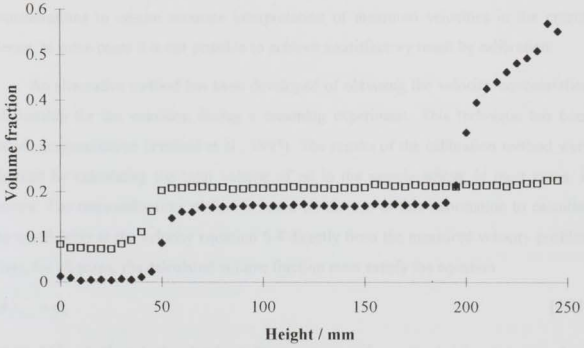

Figure 5.3 Calibrated oil volume fraction against height for a 20 vol.% sunflower oil in water emulsion with 2 wt.% Tween20 and 0.03 wt.% xanthan at 30 °C (Ma, 1995).

□ is the first scan, and◆ after 10 days.

sample, according to the calibrated results is within 0.01 of the initial known concentration (0.20). Thus, the fractionation in the cream is not so strong as to cause the velocity–concentration relationship to deviate significantly from the measured values for the initial emulsion.

5.4 Renormalisation

The renormalisation method is designed to calculate the velocity–concentration relationship in ultrasound creaming experiments. The equipment in figure 1.1 is used to obtain profiles of ultrasound velocity as a function of height at various time intervals during creaming. The calibration method described in the previous section has often been used when the Urick equation was found not to apply. However, in some instances, it is not possible or convenient to produce a calibration curve. This might be because the precise components of the sample are not known, and so it would not be possible to make corresponding emulsions with different oil concentrations. Emulsions with a lower oil concentration could be made by dilution from the emulsion of interest, provided there were no components in the continuous phase which affected ultrasound velocity. However, it is necessary to have points on the calibration curve at reasonably high concentrations to ensure accurate interpretation of measured velocities in the cream. Hence, in some cases it is not possible to achieve a satisfactory result by calibration.

An alternative method has been developed of obtaining the velocity–concentration relationship for the emulsion during a creaming experiment. This technique has been called renormalisation (Pinfield et al., 1995). The results of the calibration method were checked by calculating the total volume of oil in the sample which, in most cases, is known. The renormalisation method is based on the use of this information to calculate the coefficients in the velocity equation 5.4 directly from the measured velocity profiles. Thus, for all scans, the calculated volume fraction must satisfy the equation

$$\langle \phi \rangle_{h,t} = \phi_0 \qquad [5.11]$$

where $\langle \phi \rangle_{h,t}$ is the calculated volume fraction averaged over the height of the sample at time t and ϕ_0 is the initial volume fraction of oil in the emulsion. This criterion, applied to equation 5.4 (the velocity–concentration relationship) enables the determination of the

coefficients of the velocity equation from the measured velocity profiles. The procedure is described in the following sections.

5.4.1 Linear renormalisation

On the first scan of a creaming experiment, the sample tends to be still reasonably uniform, and there is very little cream (high concentration of oil). If the sample is not too concentrated it is likely that the quadratic term in equation 5.4 will be negligibly small on this scan. This is equivalent to the neglect of multiple scattering at the concentration of the initial sample. The application of equation 5.11 to equation 5.4 on the first scan leads to an estimate for the linear renormalisation coefficient.

$$\delta_v = \frac{\phi_0}{\left\langle \Delta 1/v^2 \right\rangle_{h,0}} \qquad [5.12]$$

The application of equation 5.4 in this case leads to a result

$$\phi = \delta_v \Delta\left(1/v^2\right) \qquad [5.13]$$

for the volume fraction at any position. This result can be used as the linearly renormalised estimate for oil concentration on the first and subsequent scans.

The linear renormalisation method was applied to the results of creaming experiments referred to in the previous section (Ma, 1995). For the first scan, the linearly renormalised volume fraction profile is shown in figure 5.4. There is no formation of a cream on this scan, so the neglect of the quadratic term is probably reasonable at the relatively low concentration in the sample. Figure 5.4 also shows the volume fraction profile calculated from the Urick equation (equations 4.1 and 4.2) and from the calibration curve which was discussed in the previous section, and was shown in figure 5.2. The linearly renormalised and calibrated results agree to within 0.015 in volume fraction, although the average volume fraction calculated from the calibrated results was only 0.187. It is clear that in this case, the Urick equation is invalid.

On later scans, as a cream layer develops, the linear approximation becomes less accurate because the quadratic terms in equation 5.4 become more significant, especially in the cream. A further application of the renormalisation principle is required in order to obtain the quadratic renormalisation coefficient.

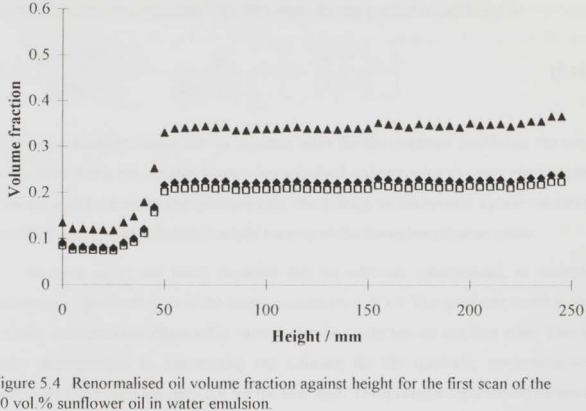

Figure 5.4 Renormalised oil volume fraction against height for the first scan of the 20 vol.% sunflower oil in water emulsion.

◆ is the linearly renormalised volume fraction, □ the calibration curve results, and ▲ the Urick equation result.

5.4.2 Quadratic renormalisation

When more concentrated regions develop in the emulsion (cream forms), or if multiple scattering is particularly significant even at the initial concentration, the quadratic terms of equation 5.4 must be included. There are then two coefficients to be determined. The renormalisation condition 5.11 can be applied to each scan, and therefore two significantly different scans are required to calculate the two coefficients.

The first order coefficient can be estimated from the first scan, in which the second order effects can usually be neglected, as seen in section 5.4.1. The estimate for the linear renormalisation coefficient is given in equation 5.12, and the linearly renormalised volume fraction profiles are calculated using equation 5.13. On later scans, the quadratic terms can be calculated when the linearly renormalised concentrations produce an average volume fraction (over the height of the sample) which deviates from the true concentration by more than, say, 0.01. The linearly renormalised results no longer satisfy equation 5.11. When this occurs, the quadratic renormalisation coefficient can be

calculated by the application of equations 5.11 and 5.4 to this scan, substituting for the linear coefficient from equation 5.12. The result for the quadratic coefficient is

$$\varepsilon_v = \frac{\phi_0 - \delta_v \left\langle \Delta 1/v^2 \right\rangle_{h,t}}{\left\langle \left(\Delta 1/v^2\right)^2 \right\rangle_{h,t}} = \frac{\phi_0}{\left\langle \left(\Delta 1/v^2\right)^2 \right\rangle_{h,t}} \cdot \left(1 - \frac{\left\langle \Delta 1/v^2 \right\rangle_{h,t}}{\left\langle \Delta 1/v^2 \right\rangle_{h,0}} \right) \qquad [5.14]$$

The term in brackets shows that an accurate value for the quadratic coefficient can only be obtained when the average linearly renormalised concentration deviates significantly from the initial concentration. Alternatively, the average of the inverse square velocities must have changed significantly, usually because of the formation of some cream.

In some cases, the initial emulsion may be relatively concentrated, or multiple scattering is significant even at the initial concentration of oil. The quadratic terms in the velocity–concentration relationship cannot then be neglected on the first scan. This is easily demonstrated by substituting the estimate for the quadratic renormalisation coefficient (5.14) into equation 5.4 for the first scan. The quadratic term should be much smaller than the initial concentration, if the above estimates for the linear and quadratic coefficients are accurate. If this is not the case, then the quadratic term must be included for the first scan, and the two coefficients must both be calculated from the data from two significantly different scans. In this case, the linear and quadratic coefficients are given by the equations

$$\delta_v = \left[\frac{\phi_0}{\left\langle \Delta 1/v^2 \right\rangle_{h,0}} \right] \cdot \left(1 - \frac{\left\langle \left(\Delta 1/v^2\right)^2 \right\rangle_{h,0}}{\left\langle \left(\Delta 1/v^2\right)^2 \right\rangle_{h,t}} \right) \cdot \frac{1}{\Xi} \qquad [5.15]$$

$$\varepsilon_v = \left[\frac{\phi_0}{\left\langle \left(\Delta 1/v^2\right)^2 \right\rangle_{h,t}} \right] \cdot \left(1 - \frac{\left\langle \left(\Delta 1/v^2\right) \right\rangle_{h,t}}{\left\langle \left(\Delta 1/v^2\right) \right\rangle_{h,0}} \right) \cdot \frac{1}{\Xi} \qquad [5.16]$$

where

$$\Xi = \left(1 - \frac{\left\langle \left(\Delta 1/v^2\right)^2 \right\rangle_{h,0}}{\left\langle \left(\Delta 1/v^2\right)^2 \right\rangle_{h,t}} \cdot \frac{\left\langle \Delta 1/v^2 \right\rangle_{h,t}}{\left\langle \Delta 1/v^2 \right\rangle_{h,0}} \right) \qquad [5.17]$$

These might be called the "exact" solutions. Again, accurate results can only be obtained when a significant change has taken place relative to the first scan, otherwise the bracketed terms are too similar and poor solutions are obtained. The values for the coefficients calculated by equations 5.12 and 5.14 or by equations 5.15 and 5.16 are valid for all scans of the same sample. The best solutions for the coefficients are obtained when the difference between the scans is greatest (for example, using the first and last scans to calculate the coefficients).

The quadratically renormalised concentration profiles for the sunflower oil in water emulsions investigated by Ma (1995) are shown in figure 5.5. This calculation was made using the "estimated" solutions (equations 5.12 and 5.14) to determine the renormalisation coefficients, using the first scan, and the scan after 10 days. These were substituted into equation 5.4 to obtain the volume fraction. The linearly renormalised profile is also shown, illustrating the significance of the quadratic terms in the cream layer. The linearly renormalised volume fraction on this scan still gave an average volume fraction of oil in the whole sample of 0.206. The results of the calibration curve and the Urick equation are also shown for comparison. The quadratic renormalisation and the calibration results agree on oil volume fraction to within 0.01.

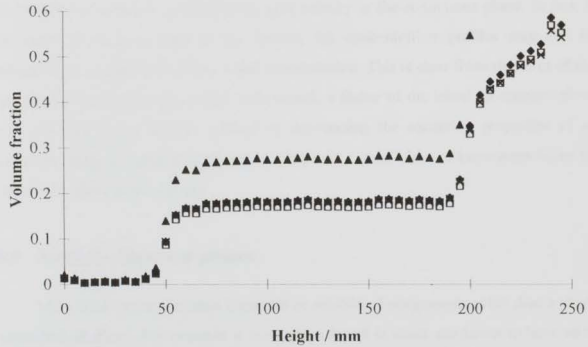

Figure 5.5 Quadratically renormalised oil volume fraction against height for the 20 vol.% sunflower oil in water emulsion after 10 days.

× is the quadratically renormalised volume fraction, ◆ the linearly renormalised volume fraction, □ the calibration curve results and ▲ the Urick equation result.

Section 5.2 discussed the restrictions on the applications of techniques such as renormalisation due to particle size dependence of the ultrasound velocity. This is especially relevant in creaming experiments in which there may a strong variation of particle size, especially in the cream. Should any particle size variation in the sample cause a significant change in the coefficients of the velocity–concentration relationship (equation 5.4), the renormalisation method would become inappropriate. It should be possible to detect any such discrepancies, by testing the average volume fraction of oil in the sample on each scan. The renormalisation coefficients are calculated from the first scan and one later scan. When these values are applied to calculate the volume fraction on all other scans, the results should yield the correct value for the average concentration (equal to the initial value) in all cases. If this does not occur, it is an indication that the parameters in equation 5.4 are different for the different scans. In other words, there is a significant change in the velocity–concentration relationship with time, usually caused by variation in particle size distribution from the initial emulsion.

The results of this section can be used to obtain the relationship between ultrasound velocity and oil concentration directly from the measured velocity profiles. The only information which is necessary to achieve this is the initial concentration of oil in the uniform emulsion, and the ultrasound velocity in the continuous phase. In fact, if the initial oil concentration is not known, the concentration profiles may still be calculated as a proportion of the initial concentration. This is clear from the form of the renormalisation coefficients, which each include a factor of the initial oil concentration. The technique is an indirect method of determining the scattering properties of an emulsion during a creaming experiment, using only a small piece of knowledge based on the conservation of oil volume.

5.5 Multiple dispersed phases

Many food systems contain dispersed or solubilised components other than a single emulsified oil phase. For example, it is common for oil in water emulsions to have some polymer present in the aqueous phase. Studies of crystallisation in emulsions can also be considered as having two different dispersed phases — solid and liquid particles. In order to develop practical approaches for the interpretation of ultrasound measurements in these systems, it is first expedient to consider the general theoretical results for samples

with multiple dispersed phases. The basis of the development of a theory for mixed systems is multiple scattering theory, as described in chapter 4. Each dispersed component must satisfy the conditions discussed in section 4.4. This precludes interactions between different components or between similar components (such as flocculation). Each component entity must act independently and be randomly distributed. The imaginary parts of the modified scattering coefficients (equation 4.46) are neglected throughout the following analysis.

For each component phase, the velocity is given by equation 5.1. In the combined system, the scattering coefficients are calculated by summing the coefficients for each phase in proportion to their number density. The combined coefficient is given by equation 4.41, just as for a polydisperse sample (each size fraction can be treated as a separate dispersed phase component). Explicitly, the velocity in the combined system can be written as follows

$$\frac{1}{v^2} = \frac{1}{v_1^2}\left[1 + \sum_i \left(\phi_i \operatorname{Re} a_{0i} + 3\phi_i \operatorname{Re} a_{1i}\right)\right.$$

$$\left. +3\left\{\left(\sum_i \phi_i \operatorname{Re} a_{0i}\right)\left(\sum_i \phi_i \operatorname{Re} a_{1i}\right) + 2\left(\sum_i \phi_i \operatorname{Re} a_{1i}\right)^2\right\}\right] \qquad [5.18]$$

where i represents a dispersed phase species. Using the relationship between the individual scattering coefficients and the velocity equation for each phase separately (equations 5.1 and 5.3), this can be simplified to

$$\frac{1}{v^2} = \frac{1}{v_1^2} + \sum_i \left(\delta_i \phi_i + \varepsilon_i \phi_i^2\right) + \sum_i \sum_{j>i} \Gamma_{i,j} \phi_i \phi_j \qquad [5.19]$$

where

$$\Gamma_{i,j} = \frac{3}{v_1^2}\left(\operatorname{Re} a_{0i} \operatorname{Re} a_{1j} + \operatorname{Re} a_{0j} \operatorname{Re} a_{1i} + 4 \operatorname{Re} a_{1i} \operatorname{Re} a_{1j}\right) \qquad [5.20]$$

Single scattering effects in the inverse square velocity equation are simply additive. Multiple scattering is not so straightforward. In this case only double scattering events are included. A double scattering event might be scattering from two particles of the same component, or scattering from two different species. The former effects are again additive in this equation. The final term in equation 5.19 accounts for the effects of

scattering from two different components. This is the only term in the equation which cannot be directly determined from the experimental coefficients without further rearrangement or assumptions. However, if the scattering coefficients can be written in the form of equations 5.7 and 5.8, the extra term can be simplified, giving

$$\Gamma_{i,j} = \frac{3}{2} v_1^2 \delta_i \delta_j \left(1 - S_i S_j\right) \qquad [5.21]$$

where the scattering factor S is given in equation 5.9.

The attenuation calculated by multiple scattering theory was given in equation 4.48. It is clear that the solution in a multiphase system will follow the same dependence as for the velocity. The quadratic terms in attenuation are often negligible, but their relationship to the scattering coefficients is difficult to determine in the multiphase case because of the many terms involved. Also it is not known which terms of equation 4.48 must be included. However, the form of the attenuation relationship can be written directly

$$\alpha = \sum_i \left(\chi_i \phi_i + \varsigma_i \phi_i^2\right) + \sum_i \sum_{j>i} \zeta_{i,j} \phi_i \phi_j \qquad [5.22]$$

All the terms in the attenuation which are quadratic in concentration may be negligible.

The Urick equation in a multiple phase system produces similar results for the ultrasound velocity, but it differs in the "cross-term" due to the omission of one of the multiple scattering terms (see section 4.6). Thus we have

$$\Gamma_{i,j} = \frac{1}{2} v_1^2 \delta_i \delta_j \left(1 - S_{Ur,i} S_{Ur,j}\right) \qquad [5.23]$$

where the Urick scattering parameter is now given by

$$S_{Ur,i} = \sqrt{1 - \frac{4\varepsilon_i}{\delta_i^2 v_1^2}} \qquad [5.24]$$

The results of this section can be applied to specific examples of multi-phase systems which are relevant in the study of food emulsions. Two such applications are discussed in the following sections.

5.6 Polymer/oil systems

Many food emulsions contain polymer dissolved or dispersed in the continuous phase. This may be for the purposes of modifying the rheological properties of the food for texture or stability reasons (for example a gum), or it may be present naturally (casein in milk). The presence of the additional dissolved or dispersed component may or may not influence significantly the ultrasonic properties of the system. If it does have an effect, this must be taken into account when applying techniques to determine the concentration of oil, such as those discussed in the preceding sections. The first consideration is how the properties of the multi-phase system are related to the properties of samples containing each dispersed phase independently. This will be of use in determining the volume fraction of oil in a sample with an added polymer or other component, when the effect of the additional component in water alone is already known.

For the polymer dispersion in the continuous phase, in the absence of oil

$$\frac{1}{v^2} = \frac{1}{v_1^2} + \delta_{pol}\phi_{pol} + \varepsilon_{pol}\phi_{pol}^2 \qquad [5.25]$$

$$\alpha = \chi_{pol}\phi_{pol} + \varsigma_{pol}\,\phi_{pol}^2 \qquad [5.26]$$

and for the emulsion in the absence of polymer

$$\frac{1}{v^2} = \frac{1}{v_1^2} + \delta_{oil}\phi_{oil} + \varepsilon_{oil}\phi_{oil}^2 \qquad [5.27]$$

$$\alpha = \chi_{oil}\phi_{oil} + \varsigma_{oil}\,\phi_{oil}^2 \qquad [5.28]$$

It is usually possible to determine all of these coefficients experimentally using a range of well-characterised emulsions and dispersions. The concentration used in these equations is expressed as a volume fraction. For polymers or other molecules, their volume may be difficult to define, and it is more usual to measure concentration as a percentage weight, or as a weight in a specified volume. For the purposes of scattering theory, the relevant quantity is the number of scattering centres per unit volume of the sample. In the case of emulsion particles, this is proportional to the volume fraction (at a specified particle size). For the polymer, any measure of concentration must be specified as a proportion of a volume of the sample. The quantity used may be a weight or mass, but it must be in

relation to a volume of sample, not to the continuous phase only. For example the concentration may take the units of kg m^{-3}. Alternatively, the number of molecules in a given volume could be used. Whatever the measure, it must be proportional to the number of scattering centres per volume of the sample.

For the combined system, the results of section 5.5 are directly applicable. Equations 5.19 and 5.20 or 5.21 can be used for velocity and equation 5.22 for attenuation. Hence the multi-phase system can be characterised simply, so that the velocity and attenuation for any concentration of oil or polymer can be calculated. Conversely, if the polymer concentration is known, the oil concentration can be determined. The combined scattering term in the velocity and attenuation (equations 5.19-5.21 and 5.22) may be difficult to calculate accurately, either from the theoretical scattering coefficients or from the experimentally determined parameters. The quadratic experimental coefficient of the velocity is often a relatively small contribution to the overall variation with concentration, and its error from a regression fit may be significant. This leads to uncertainty in the value of the combined scattering term in the velocity. Also, the form of this combined scattering effect depends on the relationship of the experimental parameters to the scattering coefficients (equation 5.3). If some of the assumptions of scattering theory are not applicable, this correspondence may not be exact, although the form of the velocity and attenuation dependence is still valid. Therefore the combined scattering term should be approached with some care. A sensible, practical solution to the problem would simply be to calibrate this combined term using an ultrasound measurement for a single multi-phase system in which all the other parameters are known (the concentrations of polymer and oil in this case).

Previously, the effect of the added component in creaming experiments was accounted for by calibrating the ultrasound velocity as a function of oil concentration with the known quantity of polymer already present in the aqueous phase. This was the approach taken for the sunflower oil in water emulsions studied by Ma (1995), in which there was an excess of the emulsifier Tween20. The emulsions were produced so that the concentration of Tween20 dispersed in the aqueous phase was the same in all cases, and the oil calibration was carried out at this concentration of emulsifier. This approach is entirely appropriate when the concentration of the additional dispersed phase can be kept constant. A more general approach is needed when the concentration of the added

component may also vary (although its value may be known). It is impractical to calibrate the ultrasound parameters (velocity and attenuation) for every combination of oil and polymer concentration. The equations presented above allow calibration as a function of oil concentration in the absence of polymer, and calibration as a function of polymer concentration in the absence of oil. A calibration point for a single sample of known polymer and oil concentration may also be necessary to obtain an accurate value for the combined scattering term. From these data, the ultrasound parameters in any combined system of these two components can be determined.

The discussion thus far has been directed towards the determination of oil concentration when the concentration of polymer is known, usually using ultrasound velocity measurements. However, since there are two ultrasound parameters which can be measured (velocity and attenuation), it should be possible to apply the results to the determination of both polymer and oil concentration. This is particularly relevant to the study of creaming in emulsions containing polymer in the continuous phase. The oil in water emulsion and polymer solution may undergo some degree of phase-separation, with the polymer being driven in the opposite direction to the natural creaming of the oil droplets. Thus the concentration of polymer (or other additive) in the aqueous phase may not be constant throughout the sample. A higher concentration may occur in the serum region, and a lower concentration in the cream. This variation is over and above that created by the change in volume fraction of the aqueous phase itself. The polymer concentration within the continuous phase can change, as well as its concentration as a proportion of the emulsion locally. Useful information would be obtained on the phase separation process if it were possible to determine the concentration profiles of both the oil and the polymer during creaming. Although such a phase separation may be accompanied by flocculation, whose effect on the ultrasound signal has not been quantified, a first step would be to determine the concentration profiles without accounting for flocculation.

The equipment shown in figure 1.1 is currently used to obtain ultrasound velocity profiles as creaming progresses. The results of the present and the previous chapters show how these may be converted into oil concentration profiles. If the equipment were modified to measure ultrasound attenuation accurately, as well as velocity, the results of this section could be used to calculate the polymer and oil concentration. The inversion of the equations for velocity and attenuation to solve for the concentration of each

component can only be carried out numerically as they stand. However, at the concentrations used in many creaming experiments, the polymer has a negligible effect on attenuation. Thus, the only significant terms in the attenuation are likely to be (from equation 5.22)

$$\alpha = \chi_{oil}\phi_{oil} + \varsigma_{oil}\phi_{oil}^{2} \qquad [5.29]$$

The oil concentration should therefore be calculated directly from the attenuation. This value is likely to be significantly less accurate than the results obtained from ultrasound velocity measurements, when the polymer concentration is constant. The polymer concentration can then be calculated from the velocity. The quadratic terms in polymer concentration are often (but not always) negligible in experiments. They are retained here for completeness.

$$\frac{1}{v^2} = \frac{1}{v_1^2} + \delta_{oil}\phi_{oil} + \varepsilon_{oil}\phi_{oil}^2 + \delta_{pol}\phi_{pol} + \varepsilon_{pol}\phi_{pol}^2 + \Gamma_{oil,pol}\delta_{oil}\delta_{pol}\phi_{oil}\phi_{pol} \qquad [5.30]$$

The coefficient of the combined scattering term, $\Gamma_{oil,pol}$, is determined experimentally or from the theoretical expressions given earlier (equations 5.20 or 5.21). These results open the way to study the changes in polymer concentration alongside the changes in oil concentration during creaming. The renormalisation method could in principle also be applied to these equations to obtain the concentration profiles when it is not possible to characterise the two component systems separately.

5.7 Crystallisation

The second example of the application of ultrasound measurements in systems with multiple dispersed phases is the study of crystallisation in oil in water emulsions containing both solid and liquid particles. The two dispersed phases are now the solid and liquid particles. The measurement of ultrasound velocity has been used as a non-destructive technique to probe the crystallisation kinetics of the oil droplets (McClements et al., 1990a, Dickinson et al., 1991, McClements et al., 1993, Dickinson, et al., 1993b). The results can be compared with theories of crystallisation to improve understanding of how crystallisation or melting is occurring, and what effects surfactants and other components have on the process. The use of ultrasound velocity measurements in this area relies on the existence of a relationship between the velocity and the proportion of

the dispersed phase particles which are solid (the volume fraction of the solid particles in the whole system is usually called the solid fat content). It is this relationship which is discussed in this section.

The Urick equation (which is a limiting solution of multiple scattering theory) takes a very simple form when the densities of the constituent phases are similar. In the crystallisation problem there are three phases in the system: the continuous phase (liquid), fully liquid dispersed phase particles (oil) and fully solid dispersed phase particles (fat). Partially crystallised droplets may sometimes also be present, but these are not accounted for in this analysis. If the densities of the three phases are equal, the Urick equation reduces to the form

$$\frac{1}{v^2} = \sum_{i=1}^{3} \frac{\phi_i}{v_i^2} \qquad [5.31]$$

where v is the ultrasound velocity in the emulsion, but the other velocities are those in the pure phases. The sum includes the continuous phase (i=1). Application of this equation to the case in which all the particles are liquid and all the particles are solid, followed by some rearrangement leads to the following expression for the solid volume fraction

$$\phi_S = \frac{\left(\frac{1}{v^2} - \frac{1}{v_L^2}\right)}{\left(\frac{1}{v_S^2} - \frac{1}{v_L^2}\right)} \cdot \Phi_S \qquad [5.32]$$

The ultrasound velocities v_L and v_S are now the velocities in the emulsion when all the dispersed phase is liquid and all solid respectively. These are not the velocities in the bulk oil or fat. Φ_S is the total dispersed phase volume fraction when all of the dispersed phase is solid. The densities of all three phases are assumed to be identical in deriving this equation.

Equation 5.32 for the solid volume fraction has been found to work well experimentally, even in samples in which scattering of ultrasound was known to occur. Although Dickinson et al. (1991) gave a brief explanation of why this should be so, it warrants a closer investigation. A sound theoretical basis for the equation, or an extension to it to include scattering effects, would allow the use of a simple equation to

analyse the kinetics of crystallisation in a variety of emulsions. Intuitively, it is clear that the scattering properties of the liquid particles are included in the velocity measured when all the dispersed phase is liquid. Similarly the scattering properties of the solid particles are included in the velocity measured when all the dispersed phase is solid. The results of section 5.5 showed that the single scattering effects were additive in the inverse square of velocity. Hence, it may be that the form of equation 5.32 allows the cancellation of some of the effects of scattering, which would otherwise invalidate the Urick equation.

Since the semi-crystalline emulsion contains two dispersed phases, equation 5.18 can be applied directly to obtain the ultrasound velocity. In this case, however, two further pieces of information greatly simplify the problem. The total mass of dispersed phase remains constant (this is not a creaming problem in which the concentration can change locally). The mass is related to the total volume fraction when all the dispersed phase is solid, Φ_S, and this can therefore be used as a reference. The volume of a liquid droplet is related to its volume when solid through the ratio of the densities of the two phases. Therefore, the volume fraction of droplets which are liquid can be written as

$$\phi_L = \frac{\rho_3}{\rho_2}\left(\Phi_S - \phi_S\right)\left[1 + \left(\frac{\rho_3}{\rho_2} - 1\right)\Phi_S\right]^{-1} \qquad [5.33]$$

The velocity of the combined sample is given by equation 5.18, thus

$$\frac{1}{v^2} = \frac{1}{v_1^2}\left[1 + \mathrm{Re}\left\{\left(\phi_L a_{0L} + \phi_S a_{0S}\right) + 3\left(\phi_L a_{1L} + \phi_S a_{1S}\right)\right\}\right.$$

$$\left. +3\,\mathrm{Re}\left\{\left(\phi_L a_{0L} + \phi_S a_{0S}\right)\left(\phi_L a_{1L} + \phi_S a_{1S}\right) + 2\left(\phi_L a_{1L} + \phi_S a_{1S}\right)^2\right\}\right] \qquad [5.34]$$

The velocities in the all-liquid and all-solid case are given by

$$\frac{1}{v_L^2} = \frac{1}{v_1^2}\left[1 + \delta_L\Phi_L + \varepsilon_L\Phi_L^2\right] \qquad [5.35]$$

$$\frac{1}{v_S^2} = \frac{1}{v_1^2}\left[1 + \delta_S\Phi_S + \varepsilon_S\Phi_S^2\right] \qquad [5.36]$$

where Φ_L is the volume fraction when all the dispersed phase is liquid. These equations (5.33 to 5.36) together with equation 5.3 produce the result for solid volume fraction

$$\phi_S = \frac{\left(\frac{1}{v^2} - \frac{1}{v_L^2}\right)}{\left(\frac{1}{v_S^2} - \frac{1}{v_L^2}\right)} \cdot \Phi_S + \frac{3\Phi_S(\Phi_S - \phi_S)\phi_S}{\left(\frac{1}{v_S^2} - \frac{1}{v_L^2}\right)v_1^2} \cdot \xi \qquad [5.37]$$

where the scattering factor is given by

$$\xi = \mathrm{Re}\left[\left(a_{1S} - \frac{\Phi_L}{\Phi_S}a_{1L}\right)\left\{\left(a_{0S} - \frac{\Phi_L}{\Phi_S}a_{0L}\right) + 2\left(a_{1S} - \frac{\Phi_L}{\Phi_S}a_{1L}\right)\right\}\right] \qquad [5.38]$$

The first term of equation 5.37 is the same as the Urick equation result 5.32. Single scattering effects are all accounted for in the first term. The additional term represents the effects of multiple scattering, including the residual effects not accounted for in the separate all-liquid and all-solid systems. The second term may be called a "scattering correction" for this reason. In fact, the correction depends on the difference in the scattering properties between the liquid and solid phases. The major difference occurs through their difference in compressibility, which affects the zero order scattering mode. When the densities of the solid and liquid dispersed phases are similar, the effect of the scattering correction is much reduced because of its dependence on the visco-inertial scattering properties, which are small in this case. For many food emulsions therefore, the additional term is negligible and the first term of equation 5.37 can be used on its own without significant error.

At constant total oil concentration, the scattering correction varies quadratically in the solid volume fraction, and is maximum when the solid volume fraction is half of the total volume fraction if the dispersed phase were all solid, i.e.

$$\phi_S = \frac{\Phi_S}{2} \qquad [5.39]$$

The leading term in the denominator of the scattering correction is proportional to the total solid volume fraction Φ_S. Thus, the peak value of the scattering correction varies approximately with the square of this total solid volume fraction. This is a favourable result since many crystallisation studies are carried out at volume fractions ≤ 0.5. The scattering term is considerably reduced in this case.

The magnitude and form of the "scattering correction" has been investigated for a hexadecane in water emulsion at 8 °C. The physical properties of the constituent phases

are shown in table 5.1. These properties correspond to the system which was studied in previous crystallisation and creaming experiments (Ma, 1995), and also in the modelling of combined crystallisation and creaming (section 2.9). The particle diameter was 1.0 μm and the frequency 1 MHz. The correction term was calculated for a range of values of total concentration, and for each of these a range of solid volume fraction was used. The results are shown in figure 5.6. The theoretical value of the scattering correction was calculated using the known value of the solid volume fraction. However, in an experiment the solid volume fraction is the quantity which is to be determined. Its value can be estimated from the first term of equation 5.37, and substituted into the scattering correction to obtain an estimate of the correction. An example of this estimated scattering correction is also shown in figure 5.6, for a total concentration of 0.7.

The results in figure 5.6 clearly show the quadratic dependence of the scattering correction on solid volume fraction (at constant total volume fraction). The increase in its peak value with increasing total volume fraction is also apparent. Thus the neglect of the scattering correction becomes considerably more appropriate at lower concentrations. For this system, an accuracy of 0.005 in volume fraction could be achieved using only the first term of equation 5.37 for a total concentration in the range

$$\Phi_s \leq 0.34 \qquad [5.40]$$

An accuracy of 0.01 (or 1%) in volume fraction without using the scattering correction is possible in the range

$$\Phi_s \leq 0.48 \qquad [5.41]$$

The peak value of the scattering correction is not negligible for all concentrations. In such cases, a determination of the solid volume fraction would require the inclusion of the scattering correction term in equation 5.37. The "estimated" and "theoretical" values of the scattering correction for a total concentration of 0.7 can be compared in figure 5.6. The difference between the estimated correction and the exact value for this system is everywhere less than 0.0009, and it is therefore satisfactory to use the estimated correction. An iterative procedure could be used to obtain a better value for the solid volume fraction, but this would not be necessary in this case. A single repeat of the substitution of the corrected solid volume fraction back into the scattering correction would show whether the result was within the required error. Equation 5.37 is a quadratic equation in solid volume fraction which could be solved directly. However, the

	Water	Hexadecane (liquid)	Hexadecane (solid)
Ultrasound velocity / m s^{-1}	1439.1	1400.0	2200.0
Density / kg m^{-3}	999.9	781.9	908.2
Shear viscosity / Pa s	0.0014	0.00385	
Shear rigidity / Pa			7.0×10^8
Thermal conductivity / J $m^{-1}s^{-1}K^{-1}$	0.572	0.140	0.185
Specific heat capacity at constant pressure / J kg^{-1} K^{-1}	4195	2092	2092
Thermal expansivity / K^{-1}	0.000075	0.000895	0.00066

Table 5.1 Physical properties of water, and liquid and solid hexadecane at 8 °C.

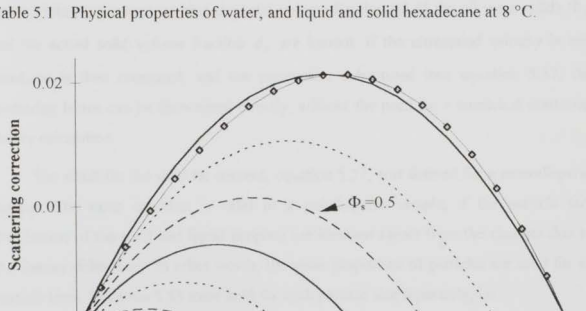

Figure 5.6 Plot of scattering correction in solid volume fraction determination for hexadecane in water at 8 °C.

The lines are for different values of total volume fraction Φ_s ranging from 0.1 to 0.7. The curve ◇ represents the estimated correction calculated using an estimate of solid volume fraction from the first term of equation 5.37.

simplified method of using the scattering correction to adjust the first estimate where required is recommended. The error in the "exact" calculation of the correction term due to the neglect of the attenuation in the derivation of the equation, was everywhere less than 3×10^{-5}.

As shown from the above calculations, it is possible to use multiple scattering theory to determine the scattering factor. However, the same problems are encountered as exist for the use of multiple scattering theory in other applications. The physical data for the constituent phases can be difficult to find or determine, and the theoretical scattering coefficient may not be exactly equal to its real apparent value. The particle sizes or size distribution may also be unknown. The scattering factor (equation 5.38) requires only a single determination as it is itself independent of the solid volume fraction. This allows the use of an experimental technique to determine the scattering factor, using a well-characterised semi-crystalline emulsion. An emulsion can be made, split into two quantities, half of which is frozen (so that all the oil crystallises), and half is not. The semi-crystalline emulsion is produced by mixing the two emulsions in appropriate proportions, so that the total volume fraction (if all the oil were solid) Φ_S and the actual solid volume fraction ϕ_S are known. If the ultrasound velocity in this emulsion is then measured, and the parameters substituted into equation 5.37, the scattering factor can be determined directly, without the need for a numerical scattering theory calculation.

The result for the solid fat content, equation 5.37, was derived for a monodisperse system. The same equation is valid in a polydisperse sample, if the particle size distribution of the solid and liquid droplets are identical (apart from the changes due to the density difference). In other words, the same proportion of particles are solid for all particle sizes. Equation 5.33 must hold for each particle size separately, i.e.

$$\phi_{il} = \frac{\rho_3}{\rho_2}\left(\Phi_{iS} - \phi_{iS}\right)\left[1 + \left(\frac{\rho_3}{\rho_2} - 1\right)\Phi_S\right]^{-1} \qquad [5.42]$$

where the index i now represents a single particle size and Φ_S is the total volume fraction of all particle sizes when all are solid. However, in reality the crystallisation rate is a function of particle size. In particular, in the case of homogeneous nucleation, the crystallisation rate is proportional to the volume of the oil droplet. Thus it is likely that a

higher proportion of the larger particles will be solid at any time. It is important to remember that the theory requires that each particle must be completely solid or completely liquid. The scattering properties used are for solid or liquid particles, not for a partially crystalline droplet. The result of equation 5.37 is not precisely valid for polydisperse systems. However, the discrepancy will depend on the degree of polydispersity in the sample, and on the sensitivity of the scattering correction to particle size. This is comparable with the validity criterion for the use of calibration and renormalisation techniques in creaming experiments. In that situation, both the variation in particle size distribution in the cream and the sensitivity of the ultrasound velocity to changes in particle size were relevant, and a combined criterion could be written in the form of equation 5.10.

The variation of the scattering correction with particle size is shown in figure 5.7 in the long wavelength region, at a frequency of 1 MHz. Although the curve appears rather steep, the overall variation is less than 0.003 in volume fraction over the range of particle size 0.01-10.0 μm. This is an encouraging result for the application of the equation 5.37 to polydisperse systems. When the crystallisation rate is a function of particle size, there will be an added contribution to the correction term due to the imbalance of the size distribution for solid and liquid particles. This effect may outweigh the dependence of the monodisperse scattering correction on particle size.

The effect of the imbalance of the solid and liquid size distribution was calculated for the hexadecane in water system, using the most skewed case possible. All particles larger than a given size are solid, and all the smaller particles are liquid. The particle size at which the cut-off occurs is determined by the solid volume fraction. The particle size distribution was log-normal, as defined in section 2.1. The peak of the distribution was at a particle diameter of 1 μm, and the width of the size distribution was determined by the value of σ_w. The quantity of interest is the error in applying equation 5.37 to determine solid volume fraction, as a function of the degree of polydispersity.

The difference between the actual solid volume fraction and the value calculated from the first term of equation 5.37 was first calculated as a function of solid volume fraction for the most polydisperse system. It was found that the maximum difference still occurred when half of the dispersed phase was solid (equation 5.39), although the difference is now skewed. Further calculations were therefore carried out under this

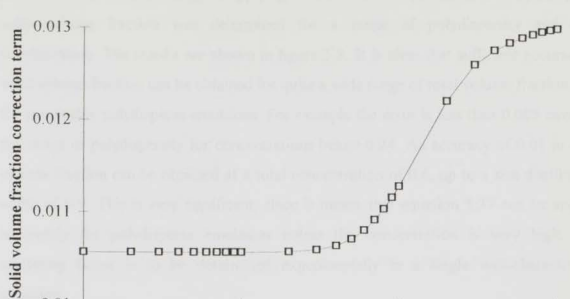

Figure 5.7 Variation of the scattering correction for solid fat content with particle size for a monodisperse hexadecane in water emulsion at 8 °C, and 1 MHz.

The total volume fraction was 0.5 (when all solid), and the solid volume fraction 0.25.

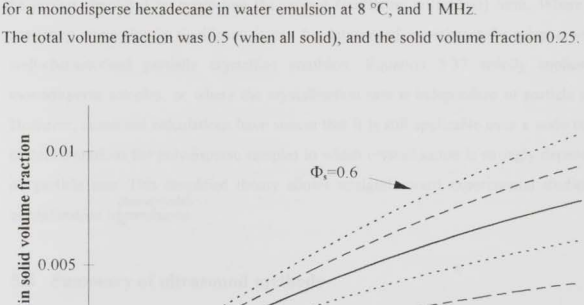

Figure 5.8 Error in determination of solid fat content as a function of polydispersity in the worst case for a hexadecane in water emulsion at 8 °C.

The solid volume fraction is half the total. The curves are for different total solid volume fraction from 0.1 to 0.6.

condition. The maximum error in applying the full form of equation 5.37 to calculate the solid volume fraction was determined for a range of polydispersity and total concentration. The results are shown in figure 5.8. It is clear that sufficient accuracy in solid volume fraction can be obtained for quite a wide range of total volume fraction, and for reasonably polydisperse emulsions. For example the error is less than 0.005 over the full range of polydispersity for concentrations below 0.24. An accuracy of 0.01 in solid volume fraction can be obtained at a total concentration of 0.6, up to a size distribution width of 0.9. This is very significant, since it means that equation 5.37 can be applied accurately for polydisperse emulsions unless the concentration is very high. The scattering factor is to be determined experimentally in a single well-characterised emulsion.

The results of this section have shown that the solid fat content of an emulsion can be determined from ultrasound velocity measurements, using equation 5.37. In many cases, especially where the constituent phases have similar densities, the relationship can be further simplified by neglecting the second (scattering correction) term. Where the scattering correction is significant, it can be determined experimentally using a single well-characterised partially crystalline emulsion. Equation 5.37 strictly applies to monodisperse samples, or where the crystallisation rate is independent of particle size. However, numerical calculations have shown that it is still applicable over a wide range of concentrations for polydisperse samples in which crystallisation is strongly dependent on particle size. This simplified theory allows straightforward experimental studies of crystallisation in some model emulsions.

5.8 Summary of ultrasound methods

The approaches explored in this chapter are designed as practical methods of interpreting ultrasound measurements in emulsions. Multiple scattering theory has been used as the theoretical basis for the development of alternative techniques of ultrasound interpretation which are more suited to routine experimental use. Scattering theory results require complex numerical calculation, and the knowledge of many physical properties of the emulsion, which are often difficult to determine. The results presented in this chapter have to some extent overcome these difficulties. The essential points of the chapter are as follows:

- The theoretical formulation of scattering theory may be applied to emulsions, but with experimental determination of the scattering properties of the system being measured.
- Simplified techniques of ultrasound measurement interpretation are applicable only in the absence of particle size or frequency effects on the scattering properties.
- Standard calibration techniques to determine the relationship between ultrasound velocity and oil concentration are essentially measurements of the scattering characteristics of the sample.
- The renormalisation method can be applied to creaming studies of emulsions to obtain the velocity–concentration relationship directly from the measured ultrasound velocity profiles.
- The ultrasound velocity and attenuation in a multiple phase system can be related to the properties of the corresponding single phase systems. Measurements of both ultrasound parameters can be used to determine the concentration of two phases.
- A simple relationship can be used to calculate the solid fat content in an emulsion which contains both solid and liquid particles. A scattering correction term has been shown to be small in many circumstances.

The techniques described in this chapter are particularly applicable to creaming and crystallisation measurements in emulsions. Although closely related to scattering theory, the methods do not rely on numerical calculations, nor on a knowledge of many physical properties of the component phases. They are more widely applicable than the theoretical results of scattering theory, since they are based on the actual properties of the experimental systems being used, rather than on theoretical assumptions. The developments discussed in this chapter allow the continued and increased use of ultrasound as a probe of emulsion stability. However, the influence of flocculation on ultrasound measurements is not understood, and the techniques presented here may or may not be applicable in such cases. Experimental results indicate that the methods are valid in the concentrated cream layer.

Chapter 6 : Conclusions

In the introduction to this thesis, the main purpose of the work was stated to be the acquisition of increased understanding of the interdependent processes of creaming, flocculation and crystallisation, and the development of improved ways to interpret the ultrasound measurements which are currently used to study these processes. The first of these general aims has been addressed through the use of computer modelling of the dynamic evolution of emulsions. The results of the models, in conjunction with an investigation of the theory of ultrasound propagation in dispersions, have been used to address the second aim. The purpose of this final chapter is briefly to draw together the specific conclusions of the different parts of the study, and to present recommendations based on the results of the whole work. Suggestions for areas of future work are also made.

The phenomenological model of creaming in idealised emulsions was shown to be a good representation of real emulsions in the absence of particle interactions. The concentration profiles predicted by the model were compared with the results from an experimental system which was thought not to include flocculation or other interactions (chapter 2). Good agreement was found except in the cream, in which the hydrodynamic description used in the model was too simplified to represent the true complexity of particle flow. The correspondence between model and experiment is evidence that the results of the model can be used as representative data of real emulsions which are studied experimentally using the ultrasound technique. Thus the application to creaming experiments of various theories for the interpretation of ultrasound measurements can be investigated using these results.

The model of creaming demonstrated that a significant degree of particle size fractionation occurs, especially in the cream region at the top of the sample. Although the predicted variation may not be exact, it is a clear indication that particle size distribution changes may occur in a creaming emulsion. The results of ultrasound scattering theory and experimental observations have shown that the ultrasound velocity in an emulsion varies with particle size, in some circumstances. The Urick equation,

which is commonly used to interpret ultrasound measurements, does not include any influence of particle size on the sound speed. The phenomenological creaming model showed that the variation of ultrasound velocity with height in the cream (according to scattering theory) could be the reverse of that expected if the effect of particle size variation were neglected (for example, using the Urick equation). Thus, an interpretation of ultrasound measurements based solely on the concentration dependence of sound speed is incorrect.

The results indicate that the use of ultrasound velocity measurements to determine concentration profiles should only be considered under conditions in which the sound speed is insensitive to particle size. A guide to the range of particle size and frequency for which this is the case can be obtained from scattering theory calculations (chapter 4). A determination of the apparent total oil concentration in the emulsion can be used to check whether particle size variation does have an influence on the interpretation of measurements in a particular creaming experiment (see chapter 5). The difference in ultrasound velocity predicted by the Urick equation and scattering theory is very large in the system modelled. These results indicate that the Urick equation should not be applied "blind" to any emulsion, since it may be inapplicable in the system of interest.

Multiple scattering theory has a sound theoretical basis for ultrasound propagation in emulsions systems. Measurements are usually made in the long wavelength limit, in which the analysis is simplified, and only the lowest order scattering modes need be considered. Although multiple scattering theory has been used as the benchmark in this study, the predictions of scattering theory have been shown to be inexact for a number of experimental systems (Holmes et al., 1993, 1994). In addition, a substantial amount of physical data is required for the calculations, and these data are often difficult to obtain. Hence, the direct application of scattering theory to interpret ultrasound measurements is impractical. Some simpler limiting solutions are available (the Urick equation being one of these) which are applicable under certain strictly specified conditions (chapter 4). In this study, new methods of interpreting ultrasound measurements have been developed. These adopt the theoretical basis of scattering theory, but the scattering characteristics of a particular system are determined experimentally (see chapter 5). Thus, instead of a reliance on a number of different theoretical formulations for the scattering properties of a system, these properties are determined directly. The difficulty of applying the scattering theory formulation to the interpretation of ultrasound measurements have,

therefore, largely been overcome. The limits of the applicability of these techniques are closely related to the effects of particle size variation seen in the creaming model.

The experimental determination of the scattering properties of an emulsion can be carried out through calibration, which is relevant to many applications of ultrasound measurements. The relationship between ultrasound velocity and oil concentration is found from measurements on a number of emulsions for which the oil concentration is already known. For creaming experiments, the renormalisation method is proposed for the determination of the sound speed–concentration relationship. The renormalisation technique uses the knowledge of the total volume of oil in the whole emulsion to calculate the unknown scattering parameters.

The use of the theoretical basis of scattering theory, but with experimental determination of the scattering properties, is also applicable to two-phase systems such as oil in water emulsions with polymer in the aqueous phase. Crystallisation experiments in emulsions with a mixture of solid and liquid droplets also fall into this category. The relationship between the ultrasound velocity in the mixed system and the concentrations of the individual components is derived from scattering theory. This relationship can, however, be written in terms of the measured ultrasound properties in the single component systems (for example an oil in water emulsion in the absence of polymer, or a polymer solution). Hence, the properties of the combined system can be determined experimentally. In crystallisation experiments, the additional knowledge of the total oil concentration when it is all liquid is applied to obtain a simplified relationship which can be used to determine solid fat content.

The application of ultrasound theory to these two-phase systems has indicated that a measurement of two ultrasound parameters, for example velocity and attenuation, could be used to obtain two properties of the emulsion. This is relevant for the determination of the concentration of both of the phases in the mixed system as described. It may be particularly applicable to the creaming of emulsions containing polymer in solution, in which the oil tends to float to the top, but the polymer becomes more concentrated at the bottom of the emulsion. Similarly, in creaming experiments of crystallising emulsions, both the solid fat and liquid oil content are varying with height. The proposed relationships for this technique have not been tested, however, and the influences of flocculation may undermine the theoretical basis in these systems.

The study of the interpretation of ultrasound measurements has shown that an awareness must exist of the restrictions of the technique. For example, in creaming experiments, the dependence of ultrasound velocity on particle size must be avoided for successful determination of concentration profiles. Within the restrictions which have been detailed, a number of techniques have been presented, each with a sound theoretical basis. These techniques are practical methods for using and interpreting ultrasound measurements in a variety of systems. An important conclusion is that the application of the Urick equation, or of scattering theory, without proper consideration of the particular system being studied, is unwise.

Having modelled creaming behaviour in emulsions in the absence of particle interactions, the effects of flocculation and crystallisation on the creaming process were investigated. The inclusion of crystallisation in the creaming model illustrated the effect of a heterogeneous crystallisation process on the 'ideal' creaming behaviour. The predominant effect on the creaming rate was found to be the density change which occurred when particles crystallised. Since the crystallisation rate in the idealised emulsion was much more rapid than creaming, the creaming process was dominated by solid droplets. Experimentally, no dramatic effect of crystallisation on creaming rate has been observed (Ma, 1995). The rates of crystallisation and creaming may become comparable when flocculation is significant, since flocculation has been shown to cause rapid creaming in some cases. The combined effects of flocculation, crystallisation and creaming have not yet been modelled, but the experimental results have not indicated a significant effect either on crystallisation rate or on creaming and flocculation behaviour.

Flocculation by non-adsorbing polymer has been seen experimentally to cause dramatic changes in the creaming behaviour of some emulsions. One particularly noticeable feature has been the large increase in creaming rate in the early stages, and the development of a sharp serum layer interface. Attempts to include the effect of flocculation in the phenomenological model of creaming were unsuccessful (chapter 2). The limited description of floc formation and their dynamic properties was unable to reproduce the characteristic features observed in practice. The small-scale lattice model of flocculation and creaming is also a very simplified model of particle behaviour, but it was able qualitatively to demonstrate some of the experimentally observed features (chapter 3). A sharp serum interface was produced in the model, and creaming was

prevented after formation of a network structure. The position of the serum interface was shown to be an indicator of the height of the energy barrier against flocculation, a relationship which may be applicable in practice. Nevertheless, the increase in creaming rate observed in the lattice model due to flocs does not appear to be sufficient to explain the dramatic serum separation observed in some experimental systems. The modelling of creaming has therefore shown good agreement with experimental results in the absence of flocculation. The effects of flocculation on creaming behaviour can to some extent be described by a very simplified model of floc formation. However, this simplified model is insufficient to explain the dramatic increase in creaming rate observed in some systems, and the richness and complexity of creaming behaviour in flocculating emulsions.

The computer modelling of creaming in emulsions has been successful in the absence of particle interactions. A phenomenological model of flocculation, and its effect on creaming behaviour, was unable to reproduce the features observed in experimental systems. A simplified model of flocculation at the level of individual particles achieved some success in demonstrating the effects of flocculation on concentration profiles. However, this model is unable to predict creaming behaviour on the scale of experimental systems. Modelling of emulsion behaviour in direct correspondence to experimental observation in the presence of particle interactions is therefore not fully developed. Some conclusions may be drawn from particle simulations such as the lattice model, but, as yet, such simulations cannot make predictions of macroscopic features or parameters characterising emulsion creaming behaviour.

The interpretation of ultrasound measurements can be carried out using multiple scattering theory techniques. The application of the theoretical results requires numerical calculations and the knowledge of a large number of physical properties of the system. However, these difficulties may largely be overcome by the use of simplified limiting forms of the theory, or through the techniques developed for the experimental determination of the scattering properties of the system. The scattering theory analysis assumes randomly distributed particles, and that there are no particle interactions. Hence, the reliability of applying these methods to systems of interacting particles, or to non-random distributions of particles (e.g. in flocs), is uncertain. The general theoretical problem of sound wave propagation through a flocculated emulsion, or conversely, the

issue of how to interpret ultrasound measurements made on such a system, is, as yet, unsolved.

The two aspects of the present work, namely computer modelling of emulsion behaviour, and the interpretation of ultrasound measurements on emulsions, are therefore limited by the current understanding of the effect of particle interactions, in particular flocculation, in emulsions. The computer models have in part accounted for the effect of flocculation on creaming behaviour. However, future development may require the use of small-scale models to predict macroscopic properties of the emulsion, which can be used in understanding experimentally observed behaviour. Predictions from small-scale models may be used in a phenomenological model to improve the simulation of flocculation and creaming behaviour. Such simulation is required to improve the understanding of the, as yet, unexplained creaming behaviour in flocculating systems. Similarly, the effect of flocculation on ultrasound propagation is unquantified. Further work is required to develop techniques for interpreting ultrasound measurements in such systems.

Bibliography

Abel, J. S., Stangle, G. C., Schilling, C. H. and Aksay, I. A. (1994). Sedimentation in flocculating colloidal suspensions. *Journal of Materials Research*, **9**, 451-461.

Ahuja, A. S. (1972). Formulation of wave equation for calculating velocity of sound in suspensions. *Journal of the Acoustical Society of America*, **51**, 916-919.

Ahuja, A. S. (1973). Wave equation and propagation parameters for sound propagation in suspensions. *Journal of Applied Physics*, **44**, 4863-4868.

Allegra, J. R. and Hawley, S. A. (1972). Attenuation of sound in suspensions and emulsions: theory and experiments. *Journal of the Acoustical Society of America*, **51**, 1545-1564.

Allen, M. P. and Tildesley, D. J. (1989). *Computer Simulation of Liquids*, Clarendon Press, Oxford.

Ansell, G. C. and Dickinson, E. (1986). Sediment formation by Brownian dynamics simulation: effect of colloidal and hydrodynamic interactions on the sediment structure. *Journal of Chemical Physics*, **85**, 4079-4086.

Anson, L. W. and Chivers, R. C. (1989). Ultrasonic propagation in suspensions – a comparison of a multiple scattering and an effective medium approach. *Journal of the Acoustical Society of America*, **85**, 535-540.

Anson, L. W. and Chivers, R. C. (1993). Ultrasonic scattering from spherical shells including viscous and thermal effects. *Journal of the Acoustical Society of America*, **93**, 1687-1699.

Asakura, S. and Oosawa, F. (1954). On the interaction between two bodies immersed in a solution of macromolecules. *Journal of Chemical Physics*, **22**, 1255-1256.

Asakura, S. and Oosawa, F. (1958). On interaction between particles suspended in solutions of macromolecules. *Journal of Polymer Science*, **33**, 183-192.

Auzerais, F. M., Jackson, R. and Russel, W. B. (1988). The resolution of shocks and the effects of compressible sediments in transient settling. *Journal of Fluid Mechanics*, **195**, 437-462.

Barnea, E. and Mizrahi, J. (1973). A generalized approach to the fluid dynamics of particulate systems. Part I. General correlation for fluidization and sedimentation in solid multiparticle systems. *Chemical Engineering Journal*, **5**, 171-189.

Batchelor, G. K. (1972). Sedimentation in a dilute dispersion of spheres. *Journal of Fluid Mechanics*, **52**, 245-268.

Batchelor, G. K. (1976). Brownian diffusion of particles with hydrodynamic interaction. *Journal of Fluid Mechanics*, **74**, 1-29.

Batchelor, G. K. (1982). Sedimentation in a dilute polydisperse system of interacting spheres. Part I. General theory. *Journal of Fluid Mechanics*, **119**, 379-408.

Batchelor, G. K. and Wen, C.-S. (1982). Sedimentation in a dilute polydisperse system of interacting spheres. Part 2. Numerical results. *Journal of Fluid Mechanics*, **124**, 495-528.

Batchelor, G. K. (1983). Diffusion in a dilute polydisperse system of interacting spheres. *Journal of Fluid Mechanics*, **131**, 155-175.

Batchelor, G. K., and Wen, C.-S. (1983). Corrigendum. *Journal of Fluid Mechanics*, **137**, 467-469.

Bedenko, V. G., Chernin, V. N., Chistyakov, B. E. and Pertsov, A. V. (1983). Sedimentation and structure of flocculated inverted emulsions. 1. Sedimentation curves and sections of the sedimentation surface. 2. Sedimentation model. *Colloid Journal of the U.S.S.R.*, **45**, 263-268, 470-474.

Bennema, P., Vogels, L. J. P. and de Jong, S. (1992). Morphology of beta-phase monoacid triacylglycerol crystals: theory and observations. *Journal of Crystal Growth*, **123**, 141-162.

Bennema, P. (1993). Morphology of crystals determined by alpha-factors, roughening temperature, F faces and connected nets. *Journal of Physics D: Applied Physics*, **26**, B1-B6.

Bijsterbosch, B. H., Bos, M. T. A., Dickinson, E., van Opheusden, J. H. J. and Walstra, P. (1995). Brownian dynamics simulation of particle gel formation: from argon to yoghurt. *Faraday Discussions*, **101**, in press.

Bonnet, J. C. and Tavlarides, L. L. (1987). Ultrasonic technique for dispersed phase hold-up measurements. *Industrial and Engineering Chemistry Research*, **26**, 811-815.

Boode, K., Bisperink, C. and Walstra, P. (1991). Destabilization of O/W emulsions containing fat crystals by temperature cycling. *Colloids and Surfaces*, **61**, 55-74.

Brady, J. (1992). Stokesian dynamics simulation of particulate flows. pp. 912-950. In *Particulate Two-Phase Flow*, ed. M. Roco, Butterworth-Heinemann, Boston.

Burgers, J. M. (1941). On the influence of the concentration of a suspension on the sedimentation velocity. *Proceedings, Koninklijke Nederlandse Akademie van Wetenschappen te Amsterdam*, **44**, 1045-1051, 1177-1184.

Burgers, J. M. (1942). On the influence of the concentration of a suspension on the sedimentation velocity. *Proceedings, Koninklijke Nederlandse Akademie van Wetenschappen te Amsterdam*, **45**, 9-16, 126-128.

Buscall, R. and White, L. R. (1987). The consolidation of concentrated suspensions. *Journal of the Chemical Society Faraday Transactions 1*, **83**, 873-891.

Buscall, R. (1990). The sedimentation of concentrated colloidal suspensions. *Colloids and Surfaces*, **43**, 33-53.

Cao, Y., Dickinson, E. and Wedlock, D. J. (1990). Creaming and flocculation in emulsions containing polysaccharide. *Food Hydrocolloids*, **4**, 185-195.

Cao, Y., Dickinson, E. and Wedlock, D. J. (1991). Influence of polysaccharides on the creaming of casein-stabilized emulsions. *Food Hydrocolloids*, **5**, 443-454.

Chhabra, R. P. and Prasad, D. (1991). A fluid-mechanic based model for the sedimentation of flocculated suspensions. *Separation Science and Technology*, **26**, 223-241.

Chow, J. C. F. (1964). Attenuation of acoustical waves in dilute emulsions and suspensions. *Journal of the Acoustical Society of America*, **36**, 2395-2401.

Colbeck, I. (1994). Aerosol formation. pp. 137-158. In *Controlled Particle, Droplet and Bubble Formation*, ed. D. J. Wedlock, Butterworth-Heinemann, Oxford.

Coupland, J., Dickinson, E., McClements, D. J., Povey, M. J. W. and de Rancourt de Mimmerand, C. (1993). A comparison of crystallisation in simple paraffins and in monoacid saturated triacylglycerols dispersed in water. pp. 243-249. In *Food Colloids*

and Polymers: Stability and Mechanical Properties, ed. E. Dickinson and P. Walstra, Royal Society of Chemistry, Cambridge.

Darling, D. F. and Birkett, R. J. (1987). Food colloids in practice. pp. 1-29. In *Food Emulsions and Foams*, ed. E. Dickinson, Royal Society of Chemistry, London.

Davis, R. H. (1993). Microhydrodynamics of particulate suspensions. *Advances in Colloid and Interface Science*, **43**, 17-50.

Davis, R. H. and Grecol, H. (1994). Hindered settling function with no empirical parameters for polydisperse suspensions. *AIChE Journal*, **40**, 570-575.

Dickinson, E. (1983). Dispersions of interacting colloidal particles. *Annual Reports on the Progress of Chemistry C*, **80**, 3-37.

Dickinson, E. (1985). Brownian dynamics with hydrodynamic interactions: the application to protein diffusional problems. *Chemical Society Reviews*, **14**, 421-455.

Dickinson, E., McClements, D. J. and Povey, M. J. W. (1991). Ultrasonic investigation of the particle size dependence of crystallisation in *n*-hexadecane-in-water emulsions. *Journal of Colloid and Interface Science*, **142**, 103-110.

Dickinson, E. (1992a). *An Introduction to Food Colloids*, Oxford University Press, Oxford.

Dickinson, E. (1992b). Structure and composition of adsorbed protein layers and the relationship to emulsion stability. *Journal of the Chemical Society Faraday Transactions*, **88**, 2973-2983.

Dickinson, E. and Euston, S. R. (1992). Short-range structure of simulated flocs of particles with bridging polymer. *Colloids and Surfaces*, **62**, 231-242.

Dickinson, E., Goller, M. I. and Wedlock, D. J. (1993a). Creaming and rheology of emulsions containing polysaccharide and non-ionic or anionic surfactants. *Colloids and Surfaces A: Physicochemical and Engineering Aspects*, **75**, 195-201.

Dickinson, E., Kruizenga, F-J., Povey, M. J. W. and van der Molen, M. (1993b). Crystallisation in oil-in-water emulsions containing liquid and solid droplets. *Colloids and Surfaces A: Physicochemical and Engineering Aspects*, **81**, 273-279.

Dickinson, E., Ma, J. and Povey, M. J. W. (1994). Creaming of concentrated oil-in-water emulsions containing xanthan. *Food Hydrocolloids*, **8**, 481-497.

Dickinson, E., Goller, M. I. and Wedlock, D. J. (1995). Osmotic pressure, creaming and rheology of emulsions containing nonionic polysaccharide. *Journal of Colloid and Interface Science*, **172**, 192-202.

Dickinson, E., Ma, J. and Povey, M. J. W. (1996). Crystallization kinetics in oil-in-water emulsions containing a mixture of solid and liquid droplets. Submitted (as a Short Communication) to *Faraday Transactions*.

Epstein, P. S. and Carhart, R. R. (1953). The absorption of sound in suspensions and emulsions. I. Water fog in air. *Journal of the Acoustical Society of America*, **25**, 553-565.

Fikioris, J. G. and Waterman, P. C. (1964). Multiple scattering of waves. II. "Hole corrections" in the scalar case. *Journal of Mathematical Physics*, **5**, 1413-1420.

Fillery-Travis, A. J., Clark, D. and Robins, M. (1990). Emulsion stability – how oil and water mix. *Food Science and Technology Today*, **4**, 89-93.

Fillery-Travis, A. J., Gunning, P. A., Hibberd, D. J. and Robins, M. M. (1993). Coexistent phases in concentrated polydisperse emulsions flocculated by non-adsorbing polymer. *Journal of Colloid and Interface Science*, **159**, 189-197.

Fligner, K. L., Fligner, M. A. and Mangino, M. E. (1991). Accelerated tests for predicting long-term creaming stability of infant formula emulsion systems. *Food Hydrocolloids*, **5**, 269-280.

Foldy, L. L. (1945). *Physics Review*, **67**, 107. Cited in Waterman and Truell (1961).

Garside, J. and Al-Dibouni, M. R. (1977). Velocity-voidage relationships for fluidisation and sedimentation in solid-liquid systems. *Industrial and Engineering Chemistry: Process Design and Development*, **16**, 206-214.

Gaunaurd, G. C. and Überall, H. (1982). Resonance theory of the effective properties of perforated solids. *Journal of the Acoustical Society of America*, **71**, 282-295. Errata: **73**, 372.

Gaunaurd, G. C. and Überall, H. (1983). Resonance effects and the ultrasonic effective properties of particulate composites. *Journal of the Acoustical Society of America*, **74**, 305-313.

Gaunaurd, G. C. and Wertman, W. (1989). Comparison of effective medium theories for inhomogeneous media. *Journal of the Acoustical Society of America*, **85**, 541-554.

Gaunaurd, G. C. and Wertman, W. (1990). Comparison of effective medium and multiple-scattering theories of predicting the ultrasonic properties of dispersions: a reexamination of results. *Journal of the Acoustical Society of America*, **87**, 2246-2248.

Gidaspow, D. (1994). *Multiphase Flow and Fluidisation*, Academic Press, London.

Glendinning, A. B. and Russel, W. B. (1982). A pairwise additive description of sedimentation and diffusion in concentrated suspensions of hard spheres. *Journal of Colloid and Interface Science*, **89**, 124-143.

Gouldby, S. J., Gunning, P. A., Hibberd, D. J. and Robins, M. M. (1991). Creaming in flocculated oil-in-water emulsions. pp. 244-261. In *Food Polymers, Gels and Colloids*, ed. E. Dickinson, Royal Society of Chemistry, Cambridge.

Gunstone, F. D., Harwood, J. L. and Padley, F. B. (eds.) (1994). *The Lipid Handbook*, 2nd ed., Chapman and Hall, London.

Happel, J. and Brenner, H. (1965). *Low Reynolds Number Hydrodynamics*, 1st ed., Prentice-Hall, London.

Harker, A. H. and Temple, J. A. G. (1988). Velocity and attenuation of ultrasound in suspensions of particles in fluids. *Journal of Physics D: Applied Physics*, **21**, 1576-1588.

Haw, M. D., Sievwright, M., Poon, W. C. K. and Pusey, P. N. (1995). Cluster-cluster gelation with finite bond energy. *Advances in Colloid and Interface Science*, **62**, 1-16.

Holmes, A. K. and Challis, R. E. (1993). Ultrasonic scattering in concentrated colloidal suspensions. *Colloids and Surfaces A: Physicochemical and Engineering Aspects*, **77**, 65-74.

Holmes, A. K., Challis, R. E. and Wedlock, D. J. (1993). A wide bandwidth study of ultrasound velocity and attenuation in suspensions: comparison of theory with experimental measurements. *Journal of Colloid and Interface Science*, **156**, 261-268.

Holmes, A. K., Challis, R. E. and Wedlock, D. J. (1994). A wide bandwidth ultrasonic study of suspensions: the variation of velocity and attenuation with particle size. *Journal of Colloid and Interface Science*, **168**, 339-348.

Hsu, J-P. and Tsao, H-K. (1992). Dynamic simulation of floc breakage with a random breakage distribution. *Colloids and Surfaces*, **62**, 23-30.

Huang, Y-B. and Somasundaran, P. (1988). Discrete modeling of sedimentation. *Physical Review A*, **38**, 6373-6376.

Jullien, R. (1990). The application of fractals to investigations of colloidal aggregation and random deposition. *New Journal of Chemistry*, **14**, 239-253.

Kauten, R. J., Maneval, J. E. and McCarthy, M. J. (1991). Fast determination of spatially localized volume fractions in emulsions. *Journal of Food Science*, **56**, 799-801.

Kaye, G. W. C. and Laby, T. H. (1986). *Tables of Physical and Chemical Constants and Some Mathematical Functions*, 15th ed., Longman, London.

Kynch, G. J. (1952). A theory of sedimentation. *Transactions of the Faraday Society*, **48**, 166-176.

Kytomaa, H. K. (1995). Theory of sound propagation in suspensions: a guide to particle size and concentration characterization. *Power Technology*, **82**, 115-121.

Ladd, A. J. C. (1993). Short-time motion of colloidal particles: numerical simulation via a fluctuating lattice-Boltzmann equation. *Physical Review Letters*, **70**, 1339-1342.

Lamb, H. (1932). *Hydrodynamics*, 6th ed., Cambridge University Press, Cambridge.

Lawler, D. F. (1993). Physical aspects of flocculation: from microscale to macroscale. *Water Science and Technology*, **27**, 165-180.

Lax, M. (1951). *Reviews in Modern Physics*, **23**, 287. Cited in Waterman and Truell (1961).

Lax, M. (1952). *Physics Review*, **85**, 621. Cited in Waterman and Truell (1961).

Liang, W., Tadros, Th. F. and Luckham, P. F. (1993). Effect of volume fraction and particle size on depletion flocculation of a sterically stabilised latex dispersion induced by addition of poly(ethylene oxide). *Journal of Colloid and Interface Science*, **155**, 156-164.

Lloyd, P. (1967a). Wave propagation through an assembly of spheres II. The density of single-particle eigenstates. *Proceedings of the Physical Society*, **90**, 207-216.

Lloyd, P. (1967b). Wave propagation through an assembly of spheres III. The density of states in a liquid. *Proceedings of the Physical Society*, **90**, 217-231.

Lloyd, P. and Berry, M. V. (1967). Wave propagation through an assembly of spheres IV. Relations between different multiple scattering theories. *Proceedings of the Physical Society*, **91**, 678-688.

Luyten, H., Jonkman, M., Kloek, W. and van Vliet, T. (1993). Creaming behaviour of dispersed particles in dilute xanthan solutions. pp. 224-234. In *Food Colloids and Polymers: Stability and Mechanical Properties*, ed. E. Dickinson and P. Walstra, Royal Society of Chemistry, Cambridge.

Ma, J. (1995). *Creaming and Crystallisation in O/W Emulsions containing Xanthan*, Ph.D. Thesis, University of Leeds.

Ma, Y., Varadan, V. V. and Varadan, V. K. (1984). Multiple scattering theory for wave propagation in discrete random media. *International Journal of Engineering Science*, **22**, 1139-1148.

Ma, Y., Varadan, V. K. and Varadan, V. V. (1990). Comments on ultrasonic propagation in suspensions. *Journal of the Acoustical Society of America*, **87**, 2779-2782.

Mandelbrot, B. B. (1975). *Les Objets Fractals: Forme, Hasard et Dimension*, Flammarion, Paris. Cited in Mandelbrot (1982).

Mandelbrot, B. B. (1982). *The Fractal Geometry of Nature*, W. H. Freeman and Company, New York.

Margulies, T. S. and Schwarz, W. H. (1994). A multiphase continuum theory for sound wave propagation through dilute suspensions of particles. *Journal of the Acoustical Society of America*, **96**, 319-331.

McClements, D. J. (1988). *The Use of Ultrasonics for Characterising Fats and Oils*, Ph.D. Thesis, University of Leeds.

McClements, D. J. and Povey, M. J. W. (1989). Scattering of ultrasound by emulsions. *Journal of Physics D: Applied Physics*, **22**, 39-47.

McClements, D. J., Dickinson, E. and Povey, M. J. W. (1990a). Crystallization in hydrocarbon-in-water emulsions containing a mixture of solid and liquid droplets. *Chemical Physics Letters*, **172**, 449-452.

McClements, D. J., Fairley, P. and Povey, M. J. W. (1990b). Comparison of effective medium and multiple-scattering theories of predicting the ultrasonic properties of dispersions. *Journal of the Acoustical Society of America*, **87**, 2244-2246.

McClements, D. J. (1992). Comparison of multiple scattering theories with experimental measurements in emulsions. *Journal of the Acoustical Society of America*, **91**, 849-853.

McClements, D. J., Dickinson, E., Dungan, S. R., Kinsella, J. E., Ma, J. G. and Povey, M. J. W. (1993). Effect of emulsifier type on the crystallization kinetics of oil-in-water emulsions containing a mixture of solid and liquid droplets. *Journal of Colloid and Interface Science*, **160**, 293-297.

McClements, D. J. (1994). Ultrasonic determination of depletion flocculation in oil-in-water emulsions containing a non-ionic surfactant. *Colloids and Surfaces A: Physicochemical and Engineering Aspects*, **90**, 25-35.

McNamara, G. and Alder, B. (1993). Analysis of the lattice Boltzmann treatment of hydrodynamics. *Physica A*, **194**, 218-228.

Meakin, P. (1988). Fractal aggregates. *Advances in Colloid and Interface Science*, **28**, 249-331.

Melik, D. H. and Fogler, H. S. (1984). Gravity-induced flocculation. *Journal of Colloid and Interface Science*, **101**, 72-83.

Mertes, T. S. and Rhodes, H. B. (1955). Liquid-particle behaviour. *Chemical Engineering Progress*, **51**, 429-432, 517-522.

Michaels, A. S. and Bolger, J. C. (1962). Settling rates and sediment volumes of flocculated kaolin suspensions. *Industrial and Engineering Chemistry Fundamentals*, **1**, 24-33.

Mirza, S. and Richardson, J. F. (1979). Sedimentation of suspensions of particles of two or more sizes. *Chemical Engineering Science*, **34**, 447-454.

Mulder, H. and Walstra, P. (1974). *The Milk Fat Globule: Emulsion Science as Applied to Milk Products and Comparable Foods*, Commonwealth Agricultural Bureaux,

Farnham Royal and Centre for Agricultural Publishing and Documentation, Wageningen, The Netherlands.

Ozilgen, S., Simoneau, C., German, J. B., McCarthy, M. J. and Reid, D. S. (1993). Crystallization kinetics of emulsified triglycerides. *Journal of the Science of Food and Agriculture*, **61**, 101-108.

Pal, R. (1994). Techniques for measuring the composition (oil and water content) of emulsions – state of the art review. *Colloids and Surfaces A: Physicochemical and Engineering Aspects*, **84**, 141-193.

Pierce, A. D. (1981). *Acoustics: An Introduction to its Physical Principles and Applications*, McGraw-Hill, New York.

Pilhofer, G. M., McCarthy, M. J., Kauten, R. J. and German, J. B. (1993). Phase separation in optically opaque emulsions. *Journal of Food Engineering*, **20**, 369-380.

Pinfield, V. J., Povey, M. J. W. and Dickinson, E. (1995). The application of modified forms of the Urick equation to the interpretation of ultrasound velocity in scattering systems. *Ultrasonics*, **33**, 243-251.

Povey, M. J. W. and McClements, D. J. (1989). Ultrasonics in food engineering. Part I: Introduction and experimental methods. *Journal of Food Engineering*, **8**, 217-245.

Reed, C. C. and Anderson, J. L. (1976). Analysis of sedimentation velocity in terms of binary particle interactions. pp. 501-512. In *Colloid and Interface Science, vol. IV, Hydrosols and Rheology*, ed. M. Kerker, Academic Press, New York.

Reed, C. C. and Anderson, J. L. (1980). Hindered settling of a suspension at low Reynolds number. *AIChE Journal*, **26**, 816-827.

Richardson, J. F. and Zaki, W. N. (1954). Sedimentation and fluidisation: Part I. *Transactions of the Institution of Chemical Engineers*, **32**, 35-53.

Roco, M. (1992). *Particulate Two-Phase Flow*, Butterworth-Heinemann, Boston.

Sami-Selim, M., Al-Naafa, A. and Jones, M. C. (1993). Brownian diffusion of hard spheres at finite concentrations. *AIChE Journal*, **39**, 3-16.

Sarvazyan, A. P. (1991). Ultrasonic velocimetry of biological compounds. *Annual Review of Biophysics and Biophysical Chemistry*, **20**, 321-42.

Selim, M. S., Kothari, A. C. and Turian, R. M. (1983). Sedimentation of multisized particles in concentrated suspensions. *AIChE Journal*, **28**, 1029-1038.

Shih, Y. T., Gidaspow, D. and Wasan, D. T. (1986). Sedimentation of fine particles in non-aqueous media: Part I–Experimental, Part II–Modeling. *Colloids and Surfaces*, **21**, 393-429.

Shih, Y. T., Gidaspow, D. and Wasan, D. T. (1987). Hydrodynamics of sedimentation of multisized particles. *Powder Technology*, **50**, 201-215.

Simoneau, C., McCarthy, M. J., Reid, D. S. and German, J. B. (1993). Influence of triglyceride composition on crystallization kinetics of model emulsions. *Journal of Food Engineering*, **19**, 365-387.

Smoluchowski, M. S. (1913). On the applicability of Stokes' law of resistance, and the modifications of it required in certain cases. pp. 192-201. In *Proceedings of the Fifth International Congress of Mathematicians, vol. 2*, Cambridge University Press, Cambridge.

Stamatakis, K. and Chi Tien (1988). Dynamics of batch sedimentation of polydispersed suspensions. *Powder Technology*, **56**, 105-117.

Stamatakis, K. and Chi Tien (1992). Batch sedimentation calculations - the effect of compressible sediment. *Powder Technology*, **72**, 227-240.

Strutt, J. W. (1872). Investigation of the disturbance produced by a spherical obstacle on the waves of sound. *Proceedings of the London Mathematical Society*, **4**, 253-283.

Strutt, J. W., Baron Rayleigh (1896). *The Theory of Sound*, 2nd ed., Macmillan, London.

Turnbull, D. and Cormia, R. L. (1961). Kinetics of crystal nucleation in some normal alkane liquids. *Journal of Chemical Physics*, **34**, 820-831.

Urick, R. J. (1947). A sound velocity method for determining the compressibility of finely divided substances. *Journal of Applied Physics*, **18**, 983-987.

Urick, R. J. and Ament, W. S. (1949). The propagation of sound in composite media. *Journal of the Acoustical Society of America*, **21**, 115-119.

van Boekel, M. A. J. S. and Walstra, P. (1981). Stability of oil in water emulsions with crystals in the disperse phase. *Colloids and Surfaces*, **3**, 109-118.

van der Knaap, E., Vreeker, R. and Hoekstra, L. L. (1994). Effect of sedimentation on the formation of particle gels. A computer simulation study. *Colloids and Surfaces A: Physicochemical and Engineering Aspects*, **85**, 265-270.

van Duijneveldt, J. S., Heinen, A. W. and Lekkerkerker, H. N. W. (1993). Phase separation in bimodal dispersions of sterically stabilized silica particles. *Europhysics Letters*, **21**, 369-374.

van Garderen, H. F., Dokter, W. H., Beelen, T. P. M., van Santen, R. A., Pantos, E., Michels, M. A. J. and Hilbers, P. A. J. (1995). Volume fraction dependence and reorganization in cluster-cluster aggregation processes. *Journal of Chemical Physics*, **102**, 480-495.

Vicsek, T. (1989). *Fractal Growth Phenomena*, World Scientific, Singapore.

Walstra, P. and Oortwijn, H. (1975). Effect of globule size and concentration on creaming in pasteurized milk. *Netherlands Milk and Dairy Journal*, **29**, 263-278.

Walstra, P. (1987a). Fat crystallization. pp. 67-85. In *Food Structure and Behaviour*, ed. J. M. V. Blanshard and P. Lillford, Academic Press, London.

Walstra, P. (1987b). Physical principles of emulsion science. pp. 87-106. In *Food Structure and Behaviour*, ed. J. M. V. Blanshard and P. Lillford, Academic Press, London.

Waterman, P. C. and Truell, R. (1961). Multiple scattering of waves. *Journal of Mathematical Physics*, **2**, 512-537.

Williams, R. A. and Amarasinghe, W. P. K. (1989). Measurement and simulation of sedimentation behaviour of concentrated polydisperse suspensions. *Transactions of the Institution of Mining and Metallurgy C*, **98**, 68-82.

Williams, R. A., Amarasinghe, W. P. K., Simons, S. J. R. and Xie, C. G. (1991). Sedimentation behaviour of complex polydisperse suspensions. *Powder Technology*, **65**, 411-432.

Wood, A. B. (1941). *A Textbook of Sound*, 2nd ed., Bell and Sons, London.

Wood, A. B. (1964). *A Textbook of Sound*, 3rd ed., Bell and Sons, London.

Yuan, X. F., Ball, R. C. and Edwards, S. F. (1993). A new approach to modelling visco-elastic flow. *Journal of Non-Newtonian Fluid Mechanics*, **46**, 331-350.

Ziman, J. M. (1966). Wave propagation through an assembly of spheres. I. The Greenian method of the theory of metals. *Proceedings of the Physical Society*, **88**, 387-405.

Zimmels, Y. (1983). Theory of hindered sedimentation of polydisperse mixtures. *AIChE Journal*, **29**, 669-676.

Zimmels, Y. (1988). Simulation of nonsteady sedimentation of polydisperse particle mixtures. *Powder Technology*, **56**, 227-250.

Zimmels, Y. (1992). Effect of self-induced structural instabilities in sedimentation and fluidization systems. *Powder Technology*, **70**, 109-129.

List of Symbols

English symbols

$\mathbf{A}$	vector potential of shear wave mode
A	azimuthal component of shear wave potential
A_n	coefficient of n'th order scattered propagational mode
A_{01}, A_{02}	two terms of the zero order scattering coefficient (equation 4.53)
a	$= kr$
a_n	modified n'th order scattering coefficient (equation 4.46)
a_ϕ	coefficient in creaming speed (equation 2.39)
B_n	coefficient of n'th order scattered thermal mode
b	$= k_t r$
C_n	coefficient of n'th order scattered shear mode
C_p	specific heat capacity at constant pressure
c	$= k_s r$
D	diffusion coefficient
D	factor in first order scattering coefficient (equations 4.55-4.58)
D_0	diffusion coefficient at infinite dilution (Stokes-Einstein coefficient)
d_f	fractal dimension
d_{32}	volume–surface average particle diameter
E_n	spatially varying coefficient of n'th order of exciting field at particle
E_n^0	coefficient of n'th order of exciting field at particle (equation 4.36)
E	energy

e_k	parameter in wavenumber (equation 4.6)
F	factor in zero order scattering coefficient (equations 4.51-4.52)
F_d	viscous drag force
F_g	gravitational force
$\boldsymbol{F}$	force applied to particle
f	frequency
f_k	parameter in wavenumber (equation 4.6)
G	coefficient of temperature variation of sound wave (equations 4.19-4.20)
$G(R_n)$	number of particles in the spherical shell denoted by R_n
g	acceleration due to gravity
$h(\phi)$	hydrodynamic hindrance factor
h_n	spherical Hankel function of order n
h_{serum}	the final height of the serum interface relative to the bottom of the sample
I	acoustic intensity
i	$\sqrt{-1}$
$\boldsymbol{J}$	particle flux
j_n	spherical Bessel function of order n
K	wavenumber of dispersion (chapter 4)
K	crystallisation rate constant (chapter 2)
$\mathbf{k}$	wavevector
k	wavenumber
k_B	Boltzmann constant
L	size of an object (chapter 2)
L	factor in first order scattering coefficient (equations 4.55-4.58)
l_N	step length moved by floc of N particles

l_{walk}	step length in a random walk
M	mobility
m	number of steps taken in a random walk
$N(R)$	number of particles within a distance R
N	number of particles in floc
$Nbonds$	number of bonds connecting a particle to its neighbours
n	scattering mode (integer)
$n(\mathbf{r})$ or n	particle number density
n_L	number of measuring units needed to cover an object of size L
P	probability of bond formation or breakage in any time step
P_{ij}	components of stress tensor
P_n	Legendre polynomial of order n
P_n^1	associated Legendre polynomial of order n
$P_{particle}$	probability of a particle breaking off from a floc in any time step
p	pressure
p_N	probability of a floc of N particles moving in any time step
Q	factor in first order scattering coefficient (equations 4.55-4.58)
q	parameter in hydrodynamic hindrance factor (equation 2.42)
R,θ,ψ	spherical polar co-ordinates
R_n	denotes a spherical shell at a given distance
$\mathbf{r}$	position vector
r	particle radius
r_f	floc radius
S	scattering parameter of dispersion (equation 5.9)
s	average interparticle spacing

T	absolute temperature
T	deviation of temperature from ambient due to sound wave (chapter 4)
T_0	ambient temperature (ultrasound theory)
$T(\mathbf{r})$	scattering operator
t	time
$\boldsymbol{U}$	velocity of a particle under a steady force
u	creaming speed
u_0	creaming speed at infinite dilution (Stokes velocity)
$\mathbf{v}$	fluid velocity
v	ultrasound velocity (usually of propagational mode)
w	natural logarithm of diameter in micrometres
x,y,z	rectilinear co-ordinates
Z	reduced variable (equation 2.18)

Greek symbols

α	ultrasound attenuation (imaginary part of wavenumber)
α	arbitrary fraction of concentration or time interval (chapter 2)
α_s	volume proportion of dispersed phase particles which are solid
β	thermal expansivity
$\beta_{i,j}$	coefficient in binary collision rate between species i and j
$\Gamma_{i,j}$	cross-scattering coefficient in velocity (equations 5.19-5.20)
γ	ratio of specific heat capacities
γ_f	parameter defining the volume of oil in a floc (equation 2.66)
δ	coefficient of velocity–concentration relationship (equation 5.1)
δ_v	coefficient of concentration–velocity relationship (equation 5.4)

ε	coefficient of velocity–concentration relationship (equation 5.1)
ε	proportion of collisions causing crystallisation or flocculation (chapter 2)
ε_v	coefficient of concentration–velocity relationship (equation 5.4)
$\zeta_{i,j}$	cross-scattering coefficient in attenuation (equation 5.22)
η	shear viscosity
θ	polar angle
κ	compressibility (usually adiabatic)
κ_0	volume averaged compressibility
λ	ultrasound wavelength (propagational mode)
μ	coefficient of compressional viscosity (liquid)
μ	bulk modulus (solid)
μ	chemical potential per particle (chapter 2)
Ξ	renormalisation parameter (equations 5.15-5.17)
ξ	scattering factor in solid volume fraction (equations 5.37-5.38)
Π	osmotic pressure
ρ	density
ρ_0	volume averaged density
σ	thermometric conductivity, $= \tau/\rho C_p$
σ_w	width of particle size distribution (log-normal)
ς	coefficient of attenuation–concentration relationship (equation 5.22)
τ	thermal conductivity
τ	volume (in spatial integration, equation 4.33)
Φ_L	dispersed phase volume fraction when all dispersed phase is liquid
Φ_S	dispersed phase volume fraction when all dispersed phase is solid
ϕ	volume fraction of dispersed phase

ϕ_L volume fraction of liquid dispersed phase

ϕ_{pack} maximum packing fraction

ϕ_S volume fraction of solid dispersed phase

φ scalar potential for compressional acoustic modes

φ_0 scalar potential for incident ultrasound wave

χ coefficient of attenuation–concentration relationship (equation 5.22)

ψ azimuthal angle

ω angular frequency $= 2\pi f$

Miscellaneous symbols

Δh layer thickness in phenomenological computer model

Δt time step in computer models

Δv_{exp} experimental error in ultrasound velocity measurement

$\Delta\left(1/v^2\right)$ $= \dfrac{1}{v^2} - \dfrac{1}{v_1^2}$

Δz difference in a quantity z between dispersed and continuous phases

$= z' - z = z_2 - z_1$

$\Delta\phi$ change in volume fraction in one time step

$\langle z \rangle_{h,t}$ average of the quantity z over the height of the sample at time t

Subscripts and superscripts

Where a symbol with its subscript or superscript does not appear in the preceding sections, the subscript or superscript has the meaning given in the following list:

0 value at zero time

0,1,2 scattering mode

1,2,3	continuous phase, liquid and solid dispersed phase respectively
bond	bond formation
break	bond breakage
crm, diff	creaming or diffusion respectively
E	exciting acoustic field at a particle
eff	effective value
f	relating to a floc
h_+, h_-	value just above or just below the height h respectively
i,j	different species or size fractions of dispersed phase
L,S	emulsion when all dispersed phase is liquid, or all solid respectively
max	maximum value
N	floc of N particles
n	scattering mode
oil	relating to oil
pol	relating to polymer
p	propagational ultrasound wave modes
R	scattered propagational mode
r,θ	components in R and θ co-ordinate directions
s	shear ultrasound wave modes
t	thermal ultrasound wave modes
Ur	relating to the Urick equation
well	potential well for flocculation
z	component in the z-coordinate direction
ϕ	relative to continuous phase
'	derivative
'	dispersed phase (scattering theory); no prime represents continuous phase

Appendix A1 : Computer Program for Phenomenological Model of Creaming and Crystallisation

```
C   Phenomenological model of creaming and crystallisation
C   of oil in water emulsions
C   by Valerie Pinfield.   1993-1995
C   Crystallisation rate equations using binary collision mechanism
C ***************************************************************
      PROGRAM CRMCRS
C ***************************************************************
      INTEGER ND,NH
      DOUBLE PRECISION DELH,G,TOTPHI,PHILIM,MEANZ,SIGMAZ,SOLPHI,COLEFF
      LOGICAL CRYST
C z=ln(diameter), totphi=volume fraction, solphi=proportion solid, coleff=collision efficiency
      PARAMETER ( ND=101,MEANZ=-0.868D0,SIGMAZ=0.5D0,
     &    NH=500,DELH=0.5D-3,G=9.81D0,
     &    TOTPHI=0.2D0,PHILIM=1.0D0,
     &    SOLPHI=0.0D0,CRYST=.FALSE.,COLEFF=8.0D-8)
      INTEGER JTOP2(1:ND),JTOP3(1:ND),JBOT2(1:ND),JBOT3(1:ND)
      CHARACTER*50 FLNAME,DFNAME
      DOUBLE PRECISION RADIUS(1:ND),STOKV2(1:ND),STOKV3(1:ND),
     &    DIFF2(1:ND),DIFF3(1:ND),DIFFR(ND,ND),DELVR(ND,ND),
     &    Q(3),RHO(3),ETA(3),MU(3),TOR(3),CP(3),GAMMA(3),
     &    BETA(3),ALPHA(3),SIGMA(3),TEMP,ANGFREQ,
     &    PHITOT(1:NH),PHI2(1:ND,1:NH),PHI3(1:ND,1:NH),
     &    HTOP2(1:ND),HBOT2(1:ND),HTOP3(1:ND),HBOT3(1:ND),DELT,RECORD,MAXT
      DELT=600.0D0
      RECORD=216000.0D0
      MAXT=2.592D6
      ANGFREQ=1.6D6*6.283185307D0
      FLNAME="crm09a.xls"
      DFNAME="hex8"
      OPEN(UNIT=20,ACCESS="SEQUENTIAL",FILE=FLNAME)
      WRITE(20,300)FLNAME,DFNAME
300   FORMAT("Creaming_profile_results ",A12," Data_file ",A12)
      WRITE(20,301)
301   FORMAT("CRMCRS.F")
      WRITE(20,302)ANGFREQ
302   FORMAT("Angular_frequency ",E15.5E3)
C *** Read material properties from data file
      CALL MTDATA(Q,RHO,ETA,MU,TOR,CP,GAMMA,BETA,ALPHA,SIGMA,
     &                    ANGFREQ,TEMP,DFNAME)
C *** Set up particle size distribution, creaming and diffusion rates
      CALL INITIALISE(ND,NH,RADIUS,STOKV2,STOKV3,DIFF2,DIFF3,
     &    DIFFR,DELVR,RHO,ETA,TEMP,G,MEANZ,SIGMAZ,
     &    CRYST,SOLPHI,TOTPHI,PHILIM,PHI2,PHI3,PHITOT,
     &    JTOP2,JBOT2,JTOP3,JBOT3,HTOP2,HBOT2,HTOP3,HBOT3,DELT,DELH)
C *** Calculate creaming process
      CALL SEQUENCE(ND,NH,RADIUS,STOKV2,STOKV3,DIFF2,DIFF3,DIFFR,DELVR,
     &    Q,RHO,ETA,MU,TOR,GAMMA,BETA,SIGMA,ANGFREQ,
     &    CRYST,COLEFF,PHILIM,PHI2,PHI3,PHITOT,
     &    JTOP2,JBOT2,JTOP3,JBOT3,HTOP2,HBOT2,HTOP3,HBOT3,
     &    RECORD,MAXT,DELT,DELH)
      END
```

```
C ***************************************************************
      SUBROUTINE INITIALISE(ND,NH,RADIUS,STOKV2,STOKV3,DIFF2,DIFF3,
     &    DIFFR,DELVR,RHO,ETA,TEMP,G,MEANZ,SIGMAZ,
     &    CRYST,SOLPHI,TOTPHI,PHILIM,PHI2,PHI3,PHITOT,
     &    JTOP2,JBOT2,JTOP3,JBOT3,HTOP2,HBOT2,HTOP3,HBOT3,DELT,DELH)
C ***************************************************************
C *** Initialise the particle size distribtion and concn profiles
C *** Initialise creaming and diffusion rates
      INTEGER ND,NH,JTOP2(1:ND),JBOT2(1:ND),JTOP3(1:ND),JBOT3(1:ND)
      DOUBLE PRECISION RADIUS(1:ND),STOKV2(1:ND),STOKV3(1:ND),
     &    DIFF2(1:ND),DIFF3(1:ND),DIFFR(ND,ND),DELVR(ND,ND),
     &    RHO(3),ETA(3),TEMP,G,SOLPHI,SOLRAD,
     &    TOTPHI,PHILIM,PHI2(1:ND,1:NH),PHI3(1:ND,1:NH),PHITOT(1:NH),
     &    HTOP2(1:ND),HBOT2(1:ND),HTOP3(1:ND),HBOT3(1:ND),
     &    RATIO,SUM,DEL,FRACT(1:101),MEANZ,SIGMAZ,DZ,DENOM,SHIFTZ,
     &    DELT,DELH,K,PI
      LOGICAL CRYST
      PARAMETER(K=1.3807D-23, PI=3.141592654D0)
      INTEGER I,J

      SUM=0.0D0
      DEL=RHO(2)/RHO(3)
      IF (ND.EQ.1) THEN
C *** Monodisperse emulsion
        RADIUS(1)=0.5D-6*DEXP(MEANZ)
        SOLRAD=RADIUS(1)*(DEL**0.3333333333D0)
C *** Stokes creaming speed, Stokes-Einstein diffusion coefficient
        STOKV2(1)=2.0D0*DABS(RHO(2)-RHO(1))*G*RADIUS(1)*RADIUS(1)
     &                  /(9.0D0*ETA(1))
        STOKV3(1)=2.0D0*DABS(RHO(3)-RHO(1))*G*RADIUS(1)*RADIUS(1)*
     &                  (DEL**(0.666666666667D0))/(9.0D0*ETA(1))
        DIFF2(1)=K*TEMP/(6.0D0*PI*ETA(1)*RADIUS(1))
        DIFF3(1)=K*TEMP/(6.0D0*PI*ETA(1)*RADIUS(1)*(DEL**0.3333333D0))
C *** Binary collision rates for crystallisation
        DIFFR(1,1)=1.5D0*(DIFF2(1)+DIFF3(1))*(RADIUS(1)+SOLRAD)/
     *      (SOLRAD**3.0D0)
        DELVR(1,1)=0.75D0*DABS(STOKV2(1)-STOKV3(1))*(RADIUS(1)+SOLRAD)
     &      *(RADIUS(1)+SOLRAD)/(SOLRAD**3.0D0)
        JTOP2(1)=NH
        JBOT2(1)=1
        HTOP2(1)=1.0D0
        HBOT2(1)=0.0D0
        JTOP3(1)=NH
        JBOT3(1)=1
        HTOP3(1)=1.0D0
        HBOT3(1)=0.0D0
        DO 104 J=1,NH
C *** Uniform emulsion. Initial proportion of oil is solid
          PHI2(1,J)=(1.0D0-SOLPHI)*TOTPHI
          PHI3(1,J)=SOLPHI*TOTPHI*DEL
          PHITOT(J)=PHI2(1,J)+PHI3(1,J)
  104   CONTINUE
      ELSE
C *** Polydisperse, log-normal distribution when plotting volume/size
C *** Z = LN (D/microns)  Natural logarithm of diameter
        DZ=6.0D0*SIGMAZ/(DBLE(ND)-1.0D0)
        DENOM=2.0D0*SIGMAZ*SIGMAZ
        DO 101 I=1,ND
          SHIFTZ = (-3.0D0*SIGMAZ)+DBLE(I-1)*DZ
```

```
                RADIUS(I)=0.5D0*1.0D-6*DEXP(MEANZ+SHIFTZ)
                FRACT(I)=DEXP(-(SHIFTZ*SHIFTZ)/DENOM)
                SUM=SUM+FRACT(I)
C *** Stokes creaming speed, Stokes-Einstein diffusion coefficient
                STOKV2(I)=2.0D0*DABS(RHO(2)-RHO(1))*G*RADIUS(I)*RADIUS(I)
     &                  /(9.0D0*ETA(1))
                STOKV3(I)=2.0D0*DABS(RHO(3)-RHO(1))*G*RADIUS(I)*RADIUS(I)*
     &                  (DEL**(0.666666666667D0))/(9.0D0*ETA(1))
                DIFF2(I)=K*TEMP/(6.0D0*PI*ETA(1)*RADIUS(I))
                DIFF3(I)=K*TEMP/(6.0D0*PI*ETA(1)*RADIUS(I)*
     &                  (DEL**0.3333333D0))
                JTOP2(I)=NH
                JBOT2(I)=1
                HTOP2(I)=1.0D0
                HBOT2(I)=0.0D0
                JTOP3(I)=NH
                JBOT3(I)=1
                HTOP3(I)=1.0D0
                HBOT3(I)=0.0D0
 101          CONTINUE
C *** Binary collision rates for crystallisation
              DO 102 I=1,ND
                DO 103 J=1,ND
                  DIFFR(I,J)=1.5D0*(DIFF2(I)+DIFF3(J))*(RADIUS(I)+
     &                    RADIUS(J)*(DEL**0.333333333D0))/
     &                    (DEL*(RADIUS(J)**3.0D0))
                  DELVR(I,J)=0.75D0*DABS(STOKV2(I)-STOKV3(J))*
     &                    (RADIUS(I)+(RADIUS(J)*(DEL**0.3333333333D0)))*
     &                    (RADIUS(I)+(RADIUS(J)*(DEL**0.3333333333D0)))/
     &                    (DEL*(RADIUS(J)**3.0D0))
 103            CONTINUE
 102          CONTINUE
              RATIO=TOTPHI/SUM
              DO 110 J=1,NH
                PHITOT(J)=0.0D0
                DO 111 I=1,ND
C *** Uniform emulsion. Initial proportion of oil is solid
                  PHI2(I,J)=(1.0D0-SOLPHI)*RATIO*FRACT(I)
                  PHI3(I,J)=SOLPHI*RATIO*FRACT(I)*DEL
                  PHITOT(J)=PHITOT(J)+PHI2(I,J)+PHI3(I,J)
 111            CONTINUE
 110          CONTINUE
            END IF

C *** Set time interval according to creaming speed
            IF (DELT.GT.(0.5D0*DELH/STOKV2(ND))) THEN
              DELT=0.5D0*DELH/STOKV2(ND)
            END IF
            IF (CRYST.AND.DELT.GT.(0.5D0*DELH/STOKV3(ND))) THEN
              DELT=0.5D0*DELH/STOKV3(ND)
            END IF
            WRITE(20,300)DELT
 300        FORMAT("Time interval ",E15.5E3)

            WRITE(20,301) NH,DELH,TOTPHI,PHILIM
 301        FORMAT(I4," layers of",E9.2,"m ; inital volume fraction ",F5.2
     &        " packing fraction ",F5.2)
            IF(CRYST)THEN
              WRITE(20,302)SOLPHI
```

```
302         FORMAT("Proportion of volume which is solid",F5.2)
          ENDIF
          WRITE(20,303)
303       FORMAT("Initial distribution, radius, volume fraction")
          DO 112 I=1,ND
            IF(CRYST)THEN
              WRITE(20,305)RADIUS(I),PHI2(I,NH),PHI3(I,NH)
305           FORMAT(3E14.6)
            ELSE
              WRITE(20,304)RADIUS(I),PHI2(I,NH)
304           FORMAT(2E14.6)
            ENDIF
 112      CONTINUE
          WRITE(20,306)TOTPHI,(1.0D0-SOLPHI)*TOTPHI,SOLPHI*DEL*TOTPHI
306       FORMAT("Total_vol_fracts",3F8.4)
          END


C ***************************************************************
          SUBROUTINE SEQUENCE(ND,NH,RADIUS,STOKV2,STOKV3,DIFF2,DIFF3,
     &      DIFFR,DELVR,Q,RHO,ETA,MU,TOR,GAMMA,BETA,SIGMA,ANGFREQ,
     &      CRYST,COLEFF,PHILIM,PHI2,PHI3,PHITOT,
     &      JTOP2,JBOT2,JTOP3,JBOT3,HTOP2,HBOT2,HTOP3,HBOT3,
     &      RECORD,MAXT,DELT,DELH)
C ***************************************************************
C     Control the sequence of time steps for the calculation of the
C     development of concentration profiles
          INTEGER ND,NH,I,J,T,
     &      JTOP2(1:ND),JBOT2(1:ND),JTOP3(1:ND),JBOT3(1:ND),
     &      JPTOP2(1:101),JPBOT2(1:101),JPTOP3(1:101),JPBOT3(1:101)

          DOUBLE PRECISION RADIUS(1:ND),STOKV2(1:ND),STOKV3(1:ND),
     &      DIFF2(1:ND),DIFF3(1:ND),DIFFR(ND,ND),DELVR(ND,ND),
     &      Q(3),RHO(3),ETA(3),MU(3),TOR(3),
     &      GAMMA(3),BETA(3),SIGMA(3),DEL23,ANGFREQ,PHILIM,COLEFF,
     &      PHI2(1:ND,1:NH),PHI3(1:ND,1:NH),PHITOT(1:NH),
     &      HTOP2(1:ND),HBOT2(1:ND),HTOP3(1:ND),HBOT3(1:ND),
     &      MAXT,RECORD,DELT,DELH

          DOUBLE PRECISION MEANV2(1:101),MEANV3(1:101),
     &      VTOP2(1:101),VBOT2(1:101),VTOP3(1:101),VBOT3(1:101),
     &      DIFHIN,CRMHIN,PHIUP2(1:101),PHIUP3(1:101),PHITUP,
     &      TMPHI2(1:101),TMPHI3(1:101),PHIT2,PHIT3,
     &      HPTOP2(1:101),HPBOT2(1:101),HPTOP3(1:101),HPBOT3(1:101),
     &      TDIVH,TDIVH2,TIME,N,DEL,
     &      SSVTH,SSVVI,SSVEL,SSATT,MSVEL,MSATT,ATTL,URICK2
          LOGICAL CRYST

          DEL=RHO(1)/RHO(2)
          DEL23=RHO(2)/RHO(3)
          TDIVH=DELT/DELH
          TDIVH2=TDIVH/DELH

          DO 101 I=1,ND
            HPTOP2(I)=HTOP2(I)
            HPBOT2(I)=HBOT2(I)
            HPTOP3(I)=HTOP3(I)
            HPBOT3(I)=HBOT3(I)
 101      CONTINUE
```

```
      T=0
 201  IF(TIME.LE.MAXT) THEN
C *** Increment time by one step
        T=T+1
        TIME=DELT*DBLE(T)

C *** Initialise arrays at top of sample
        DO 102 I=1,ND
          IF(JBOT2(I).EQ.NH)THEN
            PHIUP2(I)=PHI2(I,NH)*(1.0D0-HBOT2(I))
          ELSEIF (JTOP2(I).EQ.NH)THEN
            PHIUP2(I)=PHI2(I,NH)*HTOP2(I)
          ELSE
            PHIUP2(I)=PHI2(I,NH)
          END IF
          IF(CRYST)THEN
            IF(JBOT3(I).EQ.NH)THEN
              PHIUP3(I)=PHI3(I,NH)*(1.0D0-HBOT3(I))
            ELSEIF (JTOP3(I).EQ.NH)THEN
              PHIUP3(I)=PHI3(I,NH)*HTOP3(I)
            ELSE
              PHIUP3(I)=PHI3(I,NH)
            END IF
          ENDIF
 102    CONTINUE
        PHITUP=PHITOT(NH)

C *** Calculate velocity of upper and lower boundaries of each size
        CALL BDRYVEL(ND,NH,STOKV2,STOKV3,VTOP2,VBOT2,VTOP3,VBOT3,
     &             DIFF2,DIFF3,PHILIM,PHI2,PHI3,PHITOT,
     &             JTOP2,JBOT2,JTOP3,JBOT3,HTOP2,HBOT2,HTOP3,HBOT3,
     &             TIME,DELT,CRYST)
C *** Start with top layer and work downwards.
        DO 103 J=NH-1,1,-1
C *** Calculate the velocity of each size fraction at J/J+1 interface
          CALL CALVEL(J,ND,NH,STOKV2,STOKV3,MEANV2,MEANV3,
     &                DIFHIN,CRMHIN,PHILIM,PHI2,PHI3,
     &                JTOP2,JBOT2,JTOP3,JBOT3,HTOP2,HBOT2,HTOP3,HBOT3,CRYST)
C *** Calculate the oil volume moving across the J/J+1 layer interface
          CALL FLUX(J,ND,NH,STOKV2,STOKV3,MEANV2,MEANV3,
     &              VTOP2,VBOT2,VTOP3,VBOT3,DIFF2,DIFF3,
     &              DIFFR,DELVR,DIFHIN,CRMHIN,COLEFF,DEL23,
     &              PHILIM,PHI2,PHI3,PHITOT,PHITUP,PHIUP2,PHIUP3,
     &              JTOP2,JBOT2,JTOP3,JBOT3,HTOP2,HBOT2,HTOP3,HBOT3,
     &              JPTOP2,JPBOT2,JPTOP3,JPBOT3,
     &              HPTOP2,HPBOT2,HPTOP3,HPBOT3,
     &              DELT,TDIVH,TDIVH2,CRYST)
 103    CONTINUE
C *** Reset the arrays and variables
        PHITOT(1)=PHITUP
        DO 104 I=1,ND
          JTOP2(I)=JPTOP2(I)
          JBOT2(I)=JPBOT2(I)
          HTOP2(I)=HPTOP2(I)
          HBOT2(I)=HPBOT2(I)
          JTOP3(I)=JPTOP3(I)
          JBOT3(I)=JPBOT3(I)
          HTOP3(I)=HPTOP3(I)
          HBOT3(I)=HPBOT3(I)
```

```
C *** Check for problems and underflow
                IF(HBOT2(1).GT.1.0D0)THEN
                   WRITE(20,321)HBOT2(1)
 321               FORMAT("HBOT.GT.1",E15.5E3)
                   GOTO 202
                END IF
                IF(HBOT3(1).GT.1.0D0)THEN
                   WRITE(20,322)HBOT3(1),TIME,JBOT3(1),HBOT3(1)
 322               FORMAT("HBOT.GT.1",2E15.5E3,I5,E15.5E3)
                   GOTO 202
                END IF
                DO 105 J=1,NH
                   IF(PHI2(I,J).LT.1.0D-15)THEN
                      PHI2(I,J)=0.0D0
                   END IF
                   IF(PHI3(I,J).LT.1.0D-15)THEN
                      PHI3(I,J)=0.0D0
                   END IF
                   IF(PHITOT(J).LT.1.0D-15)THEN
                      PHITOT(J)=0.0D0
                   END IF
 105            CONTINUE
 104         CONTINUE
C *** If this is a recording step, write out results
             N=TIME/RECORD
             IF(N.GT.0.5D0.AND.DABS(TIME-(RECORD*DNINT(N))).LE.
      &                DELT/2.0D0)THEN
                WRITE(20,301)TIME/86400.0D0
 301            FORMAT("time",F8.2," days")
                WRITE(20,302)
 302            FORMAT("Height   Tot vol fract  phi(liquid)
      &         Urick vel    S.S. vel  M.S. vel  S.S Atten  M.S
      &         atten")
C *** Generate and write out concentration and velocity profiles
                DO 106 J=1,NH,1
                   PHIT2=0.0D0
                   PHIT3=0.0D0
                   DO 107 I=1,ND
C *** Calculate the local concentration at the layer interface
                      IF(J.NE.JBOT2(I).OR.(HBOT2(I).LE.0.01D0))THEN
                         PHIT2=PHIT2+PHI2(I,J)
                         TMPHI2(I)=PHI2(I,J)
                      ELSE
                         TMPHI2(I)=0.0D0
                      ENDIF
                      IF(J.NE.JBOT3(I).OR.(HBOT3(I).LE.0.01D0))THEN
                         PHIT3=PHIT3+PHI3(I,J)
                         TMPHI3(I)=PHI3(I,J)
                      ELSE
                         TMPHI3(I)=0.0D0
                      ENDIF
 107                CONTINUE
C *** Calculate ultrasound velocity
                   CALL USVELS(2,ND,RADIUS,TMPHI2,TMPHI3,ANGFREQ,
      &                  SSVTH,SSVVI,SSVEL,SSATT,MSVEL,MSATT,ATTL,
      &                  Q,RHO,ETA,MU,TOR,GAMMA,BETA,SIGMA)
                   URICK2=1.0D0/((PHIT2*(DEL+PHIT2*(1.0D0-DEL))/
      &                  (Q(2)*Q(2)))+((1.0D0-PHIT2)*(1.0D0-PHIT2*
      &                  (1.0D0-1.0D0/DEL))/(Q(1)*Q(1))))
```

```
C *** Output results
                  IF(CRYST)THEN
                     WRITE(20,303) 1.0E3*J*DELH,PHIT2,PHIT3,PHITOT(J),
     &                              (PHI2(I,J),PHI3(I,J),I=1,ND,20)
     &                              ,DSQRT(URICK2),SSVEL,MSVEL,SSATT,MSATT
303                  FORMAT (F7.2,15E11.4E2,3F8.2,2E12.4E2)
                  ELSE
                     WRITE(20,304) 1.0E3*J*DELH,PHIT2,PHITOT(J),
     &                              (PHI2(I,J),I=1,ND,10)
     &                              ,DSQRT(URICK2),SSVEL,MSVEL,SSATT,MSATT
304                  FORMAT (F7.2,13E11.4E2,3F8.2,2E12.4E2)
                  ENDIF
 106              CONTINUE
                  WRITE(20,305)(JTOP2(I),I=1,ND,10)
                  WRITE(20,306)(HTOP2(I),I=1,ND,10)
                  WRITE(20,307)(JBOT2(I),I=1,ND,10)
                  WRITE(20,308)(HBOT2(I),I=1,ND,10)
                  IF(CRYST)THEN
                     WRITE(20,305)(JTOP3(I),I=1,ND,10)
                     WRITE(20,306)(HTOP3(I),I=1,ND,10)
                     WRITE(20,307)(JBOT3(I),I=1,ND,10)
                     WRITE(20,308)(HBOT3(I),I=1,ND,10)
                  ENDIF
305               FORMAT("JTOP",I30,10I15)
306               FORMAT("JBOT",I30,10I15)
307               FORMAT("HTOP",E30.5E3,10E15.5E3)
308               FORMAT("HBOT",E30.5E3,10E15.5E3)

C *** Write out the particle size distribution
                  IF(DABS((N)-(5.0D0*DNINT(N/5.0D0))).LT.0.01D0)THEN
                     DO 108 I=1,ND,2
                        WRITE(20,309)RADIUS(I),PHI2(I,1),
     &                              (PHI2(I,J),J=50,350,50),(PHI2(I,J),J=400,500,10)
309                  FORMAT(E12.6E2,19E11.4E2)
 108                 CONTINUE
                  END IF
               END IF
C     *** Next time step
               GOTO 201
            END IF
202         END

C ***************************************************************
            SUBROUTINE CALVEL(J,ND,NH,STOKV2,STOKV3,MEANV2,MEANV3,
     &         DIFHIN,CRMHIN,PHILIM,PHI2,PHI3,
     &         JTOP2,JBOT2,JTOP3,JBOT3,HTOP2,HBOT2,HTOP3,HBOT3,CRYST)
C ***************************************************************
C *** Calculate velocity for each size fraction at J/J+1 interface.
C *** Barnea-Mizrahi (1973) hindrance factor. Zimmels (1988) polydisper
C *** Carnahan-Starling equation for thermodynamic factor of diffusion
            INTEGER I,J,ND,NH,
     &         JTOP2(1:ND),JBOT2(1:ND),JTOP3(1:ND),JBOT3(1:ND)
            DOUBLE PRECISION BARNEA
            DOUBLE PRECISION STOKV2(1:ND),STOKV3(1:ND),
     &         MEANV2(1:101),MEANV3(1:101),DIFHIN,CRMHIN,
     &         PHILIM,PHI2(1:ND,1:NH),PHI3(1:ND,1:NH),
     &         HTOP2(1:ND),HBOT2(1:ND),HTOP3(1:ND),HBOT3(1:ND),
     &         PHIABV,PHIBEL,SUMABV,SUMBEL,PHI,SUM,FAC
               LOGICAL CRYST
```

```
C *** Calculate total concn just above and just below layer interface
          PHIABV=0.0D0
          PHIBEL=0.0D0
          SUMABV=0.0D0
          SUMBEL=0.0D0
          DO 101 I=1,ND
            IF ((J.NE.JTOP2(I)).OR.((1.0D0-HTOP2(I)).LE.0.01D0)) THEN
              PHIBEL=PHIBEL+PHI2(I,J)
              SUMBEL=SUMBEL+PHI2(I,J)*STOKV2(I)
            END IF
            IF (((J+1).NE.JBOT2(I)).OR. (HBOT2(I).LE.0.01D0)) THEN
              PHIABV=PHIABV+PHI2(I,J+1)
              SUMABV=SUMABV+PHI2(I,J+1)*STOKV2(I)
            END IF
            IF(CRYST)THEN
              IF ((J.NE.JTOP3(I)).OR.((1.0D0-HTOP3(I)).LE.0.01D0)) THEN
                PHIBEL=PHIBEL+PHI3(I,J)
                SUMBEL=SUMBEL+PHI3(I,J)*STOKV3(I)
              END IF
              IF (((J+1).NE.JBOT3(I)).OR. (HBOT3(I).LE.0.01D0)) THEN
                PHIABV=PHIABV+PHI3(I,J+1)
                SUMABV=SUMABV+PHI3(I,J+1)*STOKV3(I)
              END IF
            ENDIF
  101     CONTINUE

C ** Average concn used in hindrance factor for creaming and diffusion
          PHI=0.5D0*(PHIABV+PHIBEL)
          FAC=BARNEA(PHI)
          SUM=0.5D0*(SUMABV+SUMBEL)
          DIFHIN=FAC*((1.0D0+2.0D0*PHI)*(1.0D0+2.0D0*PHI)+((PHI**3)*
         &     (PHI-4.0D0)))/((1.0D0-PHI)**3)
          CRMHIN=FAC

C *** Calculate creaming velocity of each size fraction
          DO 102 I=1,ND
            MEANV2(I)=FAC*(STOKV2(I)-SUM)
            MEANV3(I)=FAC*(STOKV3(I)-SUM)
  102     CONTINUE
          END


C ***************************************************************
          SUBROUTINE FLUX(J,ND,NH,STOKV2,STOKV3,MEANV2,MEANV3,
         &     VTOP2,VBOT2,VTOP3,VBOT3,DIFF2,DIFF3,
         &     DIFFR,DELVR,DIFHIN,CRMHIN,COLEFF,DEL23,
         &     PHILIM,PHI2,PHI3,PHITOT,PHITUP,PHIUP2,PHIUP3,
         &     JTOP2,JBOT2,JTOP3,JBOT3,HTOP2,HBOT2,HTOP3,HBOT3,
         &     JPTOP2,JPBOT2,JPTOP3,JPBOT3,HPTOP2,HPBOT2,HPTOP3,HPBOT3,
         &     DELT,TDIVH,TDIVH2,CRYST)
C ***************************************************************
C *** Calculate volume of oil which moves across the layer interface
          INTEGER I,J,II,ND,NH,
         &     JTOP2(1:ND),JBOT2(1:ND),JTOP3(1:ND),JBOT3(1:ND),
         &     JPTOP2(1:101),JPBOT2(1:101),JPTOP3(1:101),JPBOT3(1:101)
          DOUBLE PRECISION STOKV2(1:ND),STOKV3(1:ND),
         &     VTOP2(1:101),VBOT2(1:101),VTOP3(1:101),VBOT3(1:101),
         &     MEANV2(1:101),MEANV3(1:101),DIFF2(1:ND),DIFF3(1:ND),
         &     DIFF,DIFFR(ND,ND),DELVR(ND,ND),DIFHIN,CRMHIN,DEL23,COLEFF,
```

```
     &     PHILIM,PHI2(1:ND,1:NH),PHI3(1:ND,1:NH),PHITOT(1:NH),
     &     PHITUP,PHIUP2(1:101),PHIUP3(1:101),
     &     PHIJ3(1:101),PHIJ2(1:101),PHIJ12(1:101),PHIJ13(1:101),
     &     HTOP2(1:ND),HBOT2(1:ND),HTOP3(1:ND),HBOT3(1:ND),
     &     HPTOP2(1:101),HPBOT2(1:101),HPTOP3(1:101),HPBOT3(1:101),
     &     DELT,TDIVH,TDIVH2,PHIMOV,PHISUM,
     &     DVOL2I,DPHI2(101),DPHI21(101),DPHI3(101),DPHI31(101),OVRLAP
      LOGICAL CRYST

      IF (PHITOT(J+1).LT.PHILIM)THEN
         PHISUM=0.0D0
         DO 101 I=1,ND
            PHIJ12(I)=PHI2(I,J+1)
            PHIJ2(I)=PHI2(I,J)
            PHIJ13(I)=PHI3(I,J+1)
            PHIJ3(I)=PHI3(I,J)
            DIFF=DIFF2(I)*DIFHIN
C *** Calculate amount of (liquid) oil of this size crossing interface
            CALL FLOW(J,NH,MEANV2(I),VTOP2(I),VBOT2(I),DIFF,
     &                PHI2(I,J),PHI2(I,J+1),PHIJ12(I),PHIUP2(I),PHIJ2(I),
     &                PHIMOV,JTOP2(I),JBOT2(I),HTOP2(I),HBOT2(I),
     &                JPTOP2(I),JPBOT2(I),HPTOP2(I),HPBOT2(I),
     &                TDIVH,TDIVH2)
            PHISUM=PHISUM+PHIMOV
            IF(CRYST)THEN
               DIFF=DIFF3(I)*DIFHIN
C *** Calculate amount of (solid) fat of this size crossing interface
               CALL FLOW(J,NH,MEANV3(I),VTOP3(I),VBOT3(I),DIFF,
     &                   PHI3(I,J),PHI3(I,J+1),PHIJ13(I),PHIUP3(I),PHIJ3(I),
     &                   PHIMOV,JTOP3(I),JBOT3(I),HTOP3(I),HBOT3(I),
     &                   JPTOP3(I),JPBOT3(I),HPTOP3(I),HPBOT3(I),
     &                   TDIVH,TDIVH2)
               PHISUM=PHISUM+PHIMOV
            ENDIF
  101       CONTINUE
            PHITOT(J+1)=PHITUP+PHISUM
            PHITUP=PHITOT(J)-PHISUM
         ELSE
C *** No movement if layer is full. Reset arrays.
            DO 102 I=1,ND
               PHIJ12(I)=PHI2(I,J+1)
               PHIJ13(I)=PHI3(I,J+1)
               PHIJ2(I)=PHI2(I,J)
               PHIJ3(I)=PHI3(I,J)
               IF(J.EQ.JBOT2(I))THEN
                  PHIUP2(I)=PHI2(I,J)*(1.0D0-HBOT2(I))
               ELSEIF (J.EQ.JTOP2(I))THEN
                  PHIUP2(I)=PHI2(I,J)*HTOP2(I)
               ELSE
                  PHIUP2(I)=PHI2(I,J)
               END IF
               IF(CRYST)THEN
                  IF(J.EQ.JBOT3(I))THEN
                     PHIUP3(I)=PHI3(I,J)*(1.0D0-HBOT3(I))
                  ELSEIF (J.EQ.JTOP3(I))THEN
                     PHIUP3(I)=PHI3(I,J)*HTOP3(I)
                  ELSE
                     PHIUP3(I)=PHI3(I,J)
                  END IF
```

```
            ENDIF
  102     CONTINUE
          PHITUP=PHITOT(J)
        END IF
C *** Calculate the amount of oil (liquid) converted to fat (solid)
        IF(CRYST)THEN
          DO 103 I=1,ND
            IF(J+1.EQ.JPTOP2(I))THEN
              DVOL2I=0.0D0
              DO 104 II=1,ND
                IF(J+1.EQ.JPTOP3(II))THEN
                  OVRLAP=DMIN1(HPTOP2(I),HPTOP3(II))
                ELSE
                  OVRLAP=HPTOP2(I)
                ENDIF
                DVOL2I=DVOL2I+PHIJ13(II)*OVRLAP
     &                  *(DIFHIN*DIFFR(I,II)+CRMHIN*DELVR(I,II))
  104           CONTINUE
              DVOL2I=DELT*COLEFF*PHIJ12(I)*DVOL2I
              DPHI2(I)=-DVOL2I/HPTOP2(I)
C *** Protect against crystallising more liquid than is available
              IF(DABS(DPHI2(I)).GT.PHIJ12(I))THEN
                DPHI2(I)=-PHIJ12(I)
                DVOL2I=-DPHI2(I)*HPTOP2(I)
              ENDIF
            ELSEIF(J+1.EQ.JPBOT2(I))THEN
              DVOL2I=0.0D0
              DO 105 II=1,ND
                IF(J+1.EQ.JPBOT3(II))THEN
                  OVRLAP=DMIN1(1.0D0-HPBOT2(I),1.0D0-HPBOT3(II))
                ELSE
                  OVRLAP=1.0D0-HPBOT2(I)
                ENDIF
                DVOL2I=DVOL2I+PHIJ13(II)*OVRLAP
     &                  *(DIFHIN*DIFFR(I,II)+CRMHIN*DELVR(I,II))
  105           CONTINUE
              DVOL2I=DELT*COLEFF*PHIJ12(I)*DVOL2I
              DPHI2(I)=-DVOL2I/(1.0D0-HPBOT2(I))
              IF(DABS(DPHI2(I)).GT.PHIJ12(I))THEN
                DPHI2(I)=-PHIJ12(I)
                DVOL2I=-DPHI2(I)*(1.0D0-HPBOT2(I))
              ENDIF
            ELSE
              DVOL2I=0.0D0
              DO 106 II=1,ND
                IF(J+1.EQ.JPTOP3(II))THEN
                  OVRLAP=HPTOP3(II)
                ELSEIF(J+1.EQ.JPBOT3(II))THEN
                  OVRLAP=1.0D0-HPBOT3(II)
                ELSE
                  OVRLAP=1.0D0
                ENDIF
                DVOL2I=DVOL2I+PHIJ13(II)*OVRLAP
     &                  *(DIFHIN*DIFFR(I,II)+CRMHIN*DELVR(I,II))
  106           CONTINUE
              DVOL2I=DELT*COLEFF*PHIJ12(I)*DVOL2I
              DPHI2(I)=-DVOL2I
              IF(DABS(DPHI2(I)).GT.PHIJ12(I))THEN
                DVOL2I=-DPHI2(I)
```

```
                ENDIF
              ENDIF
              IF(J+1.EQ.JPTOP3(I))THEN
                DPHI3(I)=DEL23*DVOL2I/HPTOP3(I)
              ELSEIF(J+1.EQ.JPBOT3(I))THEN
                DPHI3(I)=DEL23*DVOL2I/(1.0D0-HPBOT3(I))
              ELSE
                DPHI3(I)=DEL23*DVOL2I
              ENDIF
              PHITOT(J+1)=PHITOT(J+1)-DVOL2I*(1.0D0-DEL23)
  103       CONTINUE
C *** Same crystallisation for layer J=1
            IF(J.EQ.1)THEN
              DO 107 I=1,ND
                IF(JPBOT2(I).EQ.1)THEN
                  DVOL2I=0.0D0
                  DO 108 II=1,ND
                    IF(JPBOT3(II).EQ.1)THEN
                      OVRLAP=DMIN1(1.0D0-HPBOT2(I),1.0D0-HPBOT3(II))
                    ELSE
                      OVRLAP=1.0D0-HPBOT2(I)
                    ENDIF
                    DVOL2I=DVOL2I+PHIJ3(II)*OVRLAP
     &                          *(DIFHIN*DIFFR(I,II)+CRMHIN*DELVR(I,II))
  108               CONTINUE
                  DVOL2I=DELT*COLEFF*PHIJ2(I)*DVOL2I
                  DPHI21(I)=-DVOL2I/(1.0D0-HPBOT2(I))
C *** Protect against crystallising more liquid than is available
                  IF(DABS(DPHI2(I)).GT.PHIJ2(I))THEN
                    DPHI21(I)=-PHIJ2(I)
                    DVOL2I=-DPHI21(I)*(1.0D0-HPBOT2(I))
                  ENDIF
                ELSE
                  DVOL2I=0.0D0
                  DO 109 II=1,ND
                    IF(JPBOT3(II).EQ.1)THEN
                      OVRLAP=1.0D0-HPBOT3(II)
                    ELSE
                      OVRLAP=1.0D0
                    ENDIF
                    DVOL2I=DVOL2I+PHIJ3(II)*OVRLAP
     &                          *(DIFHIN*DIFFR(I,II)+CRMHIN*DELVR(I,II))
  109               CONTINUE
                  DVOL2I=DELT*COLEFF*PHIJ2(I)*DVOL2I
                  DPHI21(I)=-DVOL2I
                  IF(DABS(DPHI21(I)).GT.PHIJ2(I))THEN
                    DPHI21(I)=-PHIJ2(I)
                    DVOL2I=-DPHI21(I)
                  ENDIF
                ENDIF
                IF(JPBOT3(I).EQ.1)THEN
                  DPHI31(I)=DEL23*DVOL2I/(1.0D0-HPBOT3(I))
                ELSE
                  DPHI31(I)=DEL23*DVOL2I
                ENDIF
                PHITOT(1)=PHITOT(1)-DVOL2I*(1.0D0-DEL23)
  107           CONTINUE
              ENDIF
```

```
C *** Set the new values of concentration in the layer
            DO 110 I=1,ND
               PHI2(I,J+1)=PHIJ12(I)+DPHI2(I)
               PHI3(I,J+1)=PHIJ13(I)+DPHI3(I)
               IF(J.EQ.1)THEN
                  PHI2(I,J)=PHIJ2(I)+DPHI21(I)
                  PHI3(I,J)=PHIJ3(I)+DPHI31(I)
               ELSE
                  PHI2(I,J)=PHIJ2(I)
                  PHI3(I,J)=PHIJ3(I)
               ENDIF
  110       CONTINUE
         ELSE
            DO 111 I=1,ND
               PHI2(I,J+1)=PHIJ12(I)
               PHI2(I,J)=PHIJ2(I)
               PHI3(I,J)=PHIJ3(I)
  111       CONTINUE
         ENDIF
         END

C ***********************************************************************
         SUBROUTINE FLOW(J,NH,MEANV,VTOP,VBOT,DIFF,
        &    PHIJ,PHIJ1,PHIJ1,PHIUP,PHIJ,PHIMOV,
        &    JTOP,JBOT,HTOP,HBOT,JPTOP,JPBOT,HPTOP,HPBOT,
        &    TDIVH,TDIVH2)
C ***********************************************************************
C *** Calculate the amount of oil of given size fraction and speed
C *** which crosses between the layers
         INTEGER J,NH,JTOP,JBOT,JPTOP,JPBOT
         DOUBLE PRECISION MEANV,VTOP,VBOT,DIFF,
        &    PHIJ,PHIJ1,PHIJ1,PHIJ,PHIUP,PHIMOV,
        &    HTOP,HBOT,HPTOP,HPBOT,
        &    CREAM,DIFFUS,TDIVH,TDIVH2

C *** Special cases near lower and upper boundaries
         IF (J .LT.(JBOT-1))THEN
            IF(J.EQ.(JBOT-2))THEN
               PHIJ1=PHIUP/(1.0D0-HPBOT)
               PHIUP=0.0D0
            END IF
            PHIMOV=0.0D0
         ELSE IF (J.GT.JTOP)THEN
            PHIUP=0.0D0
            PHIMOV=0.0D0
         ELSE
            IF (J.EQ.JBOT) THEN
               IF(VBOT.LT.0.0D0)THEN
C *** Lower boundary moves downwards (case 1)
                  IF(MEANV.GT.0.0D0) THEN
                     CREAM=PHIJ*MEANV*TDIVH
                  ELSE
                     CREAM=PHIJ1*MEANV*TDIVH
                  END IF
                  DIFFUS=DIFF*(PHIJ-PHIJ1)*TDIVH2/
        &                    (1.0D0-0.5D0*HBOT)
                  PHIMOV=CREAM+DIFFUS
                  PHIJ1=PHIUP+PHIMOV
                  PHIUP=PHIJ*(1.0D0-HBOT)-PHIMOV
```

```
                    IF(J.EQ.1)THEN
                      HPBOT=HBOT+VBOT*TDIVH
                      JPBOT=1
                      IF(HPBOT.LT.0.0D0)THEN
                        HPBOT=0.0D0
                      END IF
                      PHIJ=PHIUP/(1.0D0-HPBOT)
                    END IF
                  ELSE
C *** Lower boundary moves upwards
                    IF(VBOT*TDIVH.GE.(0.99D0-HBOT))THEN
C *** Lower boundary crosses layer interface (Case 2)
                      HPBOT=HBOT+VBOT*TDIVH-1.0D0
                      IF(HPBOT.LT.0.0D0)THEN
                        HPBOT=0.0D0
                      END IF
                      JPBOT=J+1
                      PHIMOV=(1.0D0-HBOT)*PHIIJ
                      PHIJ1=(PHIUP+PHIMOV)/(1.0D0-HPBOT)
                      PHIUP=0.0D0
                      IF(J.EQ.1)THEN
                        PHIJ=0.0D0
                      END IF
                    ELSE
C *** Lower boundary does not cross interface (Case 3)
                      IF(MEANV.GT.0.0D0) THEN
                        CREAM=PHIIJ*MEANV*TDIVH
                      ELSE
                        CREAM=PHIIJ1*MEANV*TDIVH
                      END IF
                      DIFFUS=DIFF*(PHIIJ-PHIIJ1)*TDIVH2/
     &                             (1.0D0-0.5D0*HBOT)
                      PHIMOV=CREAM+DIFFUS
                      PHIJ1=PHIUP+PHIMOV
                      PHIUP=PHIIJ*(1.0D0-HBOT)-PHIMOV
                      HPBOT=HBOT+VBOT*TDIVH
                      JPBOT=J
                      IF(J.EQ.1)THEN
                        PHIJ=PHIUP/(1.0D0-HPBOT)
                      END IF
                    END IF
                  END IF
                ELSE IF (J.EQ.JTOP) THEN
                  IF(VTOP.LT.0.0D0)THEN
C *** Upper boundary moves downwards (case 4)
                    PHIJ1=0.0D0
                    PHIUP=PHIIJ*HTOP
                    PHIMOV=0.0D0
                    IF(J.EQ.1)THEN
                      HPBOT=HBOT+VTOP*TDIVH
                      JPBOT=1
                      IF(HPBOT.LT.0.0D0)THEN
                        HPBOT=0.0D0
                      END IF
                      PHIJ=PHIUP/HPTOP
                    END IF
                  ELSE
C *** Upper boundary moves upwards
```

```
                    IF(VTOP*TDIVH.GE.(1.01D0-HTOP))THEN
C *** Upper boundary crosses layer interface (Case 5)
                      HPTOP=HTOP+VTOP*TDIVH-1.0D0
                      JPTOP=J+1
                      PHIJ1=PHIJ
                      PHIUP=PHIJ*(HTOP-HPTOP)
                      IF(J.EQ.1)THEN
                        PHIJ=PHIUP/HPBOT
                      END IF
                      PHIMOV=PHIJ*HPTOP
                    ELSE
C *** Upper boundary does not cross layer interface (Case 6)
                      PHIJ1=0.0D0
                      PHIMOV=0.0D0
                      HPTOP=HTOP+VTOP*TDIVH
                      IF(HPTOP.GT.1.0D0)THEN
                        HPTOP=1.0D0
                      END IF
                      JPTOP=J
                      PHIUP=PHIJ*HTOP
                      IF(J.EQ.1)THEN
                        PHIJ=PHIUP/HPTOP
                      END IF
                    END IF
                  END IF
                ELSEIF ((J+1).EQ.JBOT)THEN
                  IF(VBOT.GT.0.0D0)THEN
C *** Lower boundary moves upwards (Case 7)
                    IF (J.EQ.NH-1)THEN
                      HPBOT=HBOT+VBOT*TDIVH
                      JPBOT=NH
                      IF(HPBOT.GT.1.0D0)THEN
                        HPBOT=1.0D0
                      END IF
                    END IF
                    PHIJ1=PHIUP/(1.0D0-HPBOT)
                    PHIUP=0.0D0
                    IF(J.EQ.1)THEN
                      PHIJ=0.0D0
                    END IF
                    PHIMOV=0.0D0
                  ELSE
C *** Lower boundary moves downwards
                    IF((HBOT+VBOT*TDIVH).LE.-0.01D0)THEN
C *** Lower boundary crosses layer interface (Case 8)
                      HPBOT=1.0D0+HBOT+VBOT*TDIVH
                      JPBOT=J
                      PHIMOV=-PHIJ1*(1.0D0-HPBOT)
                      PHIJ1=PHIUP+PHIMOV
                      PHIUP=-PHIMOV
                      IF(J.EQ.1)THEN
                        PHIJ=PHIUP/(1.0D0-HPBOT)
                      END IF
                    ELSE
C Lower boundary does not cross layer interface (Case 9)
                      HPBOT=HBOT+VBOT*TDIVH
                      IF(HPBOT.LT.0.0D0)THEN
                        HPBOT=0.0D0
                      END IF
```

```
                        JPBOT=J+1
                        PHIMOV=0.0D0
                        PHIJ1=PHIUP/(1.0D0-HPBOT)
                        PHIUP=0.0D0
                        IF(J.EQ.1)THEN
                          PHIJ=0.0D0
                        END IF
                      END IF
                    END IF
                  ELSEIF((J+1).EQ.JTOP)THEN
                    IF(VTOP.GT.0.0D0)THEN
C *** Upper boundary moves upwards (Case 10)
                      IF (J.EQ.NH-1)THEN
                        HPTOP=HTOP+VTOP*TDIVH
                        JPTOP=NH
                        IF(HPTOP.GT.1.0D0)THEN
                          HPTOP=1.0D0
                        END IF
                      END IF
                      IF(MEANV.GT.0.0D0) THEN
                        CREAM=PHIIJ*MEANV*TDIVH
                      ELSE
                        CREAM=PHIIJ1*MEANV*TDIVH
                      END IF
                      DIFFUS=DIFF*(PHIIJ-PHIIJ1)*TDIVH2/
     &                          (0.5D0*(1.0D0+HTOP))
                      PHIMOV=CREAM+DIFFUS
                      PHIJ1=(PHIIJ1*HTOP+PHIMOV)/HPTOP
                      PHIUP=PHIIJ-PHIMOV
                      IF(J.EQ.1)THEN
                        PHIJ=PHIUP
                      END IF
                    ELSE
C *** Upper boundary moves downwards
                      IF((HTOP+VTOP*TDIVH).LE.0.01D0)THEN
C *** Upper boundary crosses layer (Case 11)
                        PHIMOV=-PHIIJ1*HTOP
                        PHIJ1=0.0D0
                        PHIUP=PHIIJ-PHIMOV
                        HPTOP=HTOP+VTOP*TDIVH+1.0D0
                        IF(HPTOP.GT.1.0D0)THEN
                          HPTOP=1.0D0
                        END IF
                        JPTOP=J
                        IF(J.EQ.1)THEN
                          PHIJ=PHIUP/HPTOP
                        END IF
                      ELSE
C *** Upper boundary does not cross layer (Case 12)
                        IF(MEANV.GT.0.0D0) THEN
                          CREAM=PHIIJ*MEANV*TDIVH
                        ELSE
                          CREAM=PHIIJ1*MEANV*TDIVH
                        END IF
                        DIFFUS=(DIFF*(PHIIJ-PHIIJ1))*TDIVH2/
     &                            (0.5D0*(1.0D0+HTOP))
                        PHIMOV=CREAM+DIFFUS
                        PHIUP=PHIIJ-PHIMOV
                        HPTOP=HTOP+VTOP*TDIVH
```

```
                    JPTOP=J+1
                    PHIJ1=(PHIJ1*HTOP+PHIMOV)/HPTOP
                    IF(J.EQ.1)THEN
                      PHIJ=PHIUP
                    END IF
                  END IF
                END IF
              ELSE
C *** Normal flux calculation
                IF(MEANV.GT.0.0D0) THEN
                  CREAM=PHIIJ*MEANV*TDIVH
                ELSE
                  CREAM=PHIIJ1*MEANV*TDIVH
                END IF
                DIFFUS=DIFF*(PHIIJ-PHIIJ1)*TDIVH2
                PHIMOV=CREAM+DIFFUS
                PHIJ1=PHIUP+PHIMOV
                PHIUP=PHIIJ-PHIMOV
                IF(J.EQ.1)THEN
                  PHIJ=PHIUP
                END IF
              END IF
            END IF
            END

C ***********************************************************************
            DOUBLE PRECISION FUNCTION BARNEA(PHI)
C ***********************************************************************
C  Barnea and Mizrahi function for the relative velocity in a given
C  volume fraction.
            DOUBLE PRECISION PHI,FAC,CONTFR
            CONTFR=(1.0D0-PHI)
            FAC=CONTFR/(1.0D0+PHI**0.3333333333D0)
            IF(PHI.GE.0.999D0)THEN
              BARNEA=0.0D0
            ELSE
              BARNEA=FAC*DEXP(-1.666666667D0*PHI/CONTFR)
            ENDIF
            RETURN
            END

C ***********************************************************************
            SUBROUTINE BDRYVEL(ND,NH,STOKV2,STOKV3,VTOP2,VBOT2,VTOP3,VBOT3,
           &   DIFF2,DIFF3,PHILIM,PHI2,PHI3,PHITOT,
           &   JTOP2,JBOT2,JTOP3,JBOT3,HTOP2,HBOT2,HTOP3,HBOT3,
           &   TIME,DELT,CRYST)
C ***********************************************************************
C *** Calculate velocities of upper and lower boundaries of each size
            INTEGER ND,NH,I,JTOP2(1:ND),JBOT2(1:ND),JTOP3(1:ND),JBOT3(1:ND)
            DOUBLE PRECISION STOKV2(1:ND),STOKV3(1:ND),
           &   VTOP2(1:101),VBOT2(1:101),VTOP3(1:101),VBOT3(1:101),
           &   DIFF2(1:ND),DIFF3(1:ND),
           &   PHILIM,PHI2(1:ND,1:NH),PHI3(1:ND,1:NH),PHITOT(1:NH),
           &   HTOP2(1:ND),HBOT2(1:ND),HTOP3(1:ND),HBOT3(1:ND),
           &   TIME,DELT
            LOGICAL CRYST
```

```
      DO 101 I=1,ND
        CALL TOPVEL(ND,NH,JTOP2(I)-1,HTOP2(I),STOKV2(I),DIFF2(I),
     &            VTOP2(I),STOKV2,STOKV3,
     &            PHILIM,PHITOT(JTOP2(I)),PHI2,PHI3,
     &            JTOP2,JBOT2,JTOP3,JBOT3,HTOP2,HBOT2,HTOP3,HBOT3,
     &            TIME,DELT,CRYST)
        CALL BOTVEL(ND,NH,JBOT2(I),HBOT2(I),STOKV2(I),DIFF2(I),
     &            VBOT2(I),STOKV2,STOKV3,
     &            PHILIM,PHITOT(JBOT2(I)+1),PHI2,PHI3,
     &            JTOP2,JBOT2,JTOP3,JBOT3,HTOP2,HBOT2,HTOP3,HBOT3,
     &            TIME,DELT,CRYST)
        IF(CRYST)THEN
          CALL TOPVEL(ND,NH,JTOP3(I)-1,HTOP3(I),STOKV3(I),DIFF3(I),
     &              VTOP3(I),STOKV2,STOKV3,
     &              PHILIM,PHITOT(JTOP3(I)),PHI2,PHI3,
     &              JTOP2,JBOT2,JTOP3,JBOT3,HTOP2,HBOT2,HTOP3,HBOT3,
     &              TIME,DELT,CRYST)
          CALL BOTVEL(ND,NH,JBOT3(I),HBOT3(I),STOKV3(I),DIFF3(I),
     &              VBOT3(I),STOKV2,STOKV3,
     &              PHILIM,PHITOT(JBOT3(I)+1),PHI2,PHI3,
     &              JTOP2,JBOT2,JTOP3,JBOT3,HTOP2,HBOT2,HTOP3,HBOT3,
     &              TIME,DELT,CRYST)
        ENDIF
  101   CONTINUE
        END

C ***************************************************************
        SUBROUTINE BOTVEL(ND,NH,J,H,STOKV,DIFF,VBDRY,
     &    STOKV2,STOKV3,PHILIM,TOTPHI,PHI2,PHI3,
     &    JTOP2,JBOT2,JTOP3,JBOT3,HTOP2,HBOT2,HTOP3,HBOT3,
     &    TIME,DELT,CRYST)
C ***************************************************************
C *** Calculate the velocity of the lower boundary
        EXTERNAL BARNEA
        INTEGER I,J,ND,NH,
     &    JTOP2(1:ND),JBOT2(1:ND),JTOP3(1:ND),JBOT3(1:ND)
        DOUBLE PRECISION STOKV2(1:ND),STOKV3(1:ND),STOKV,VBDRY,
     &    DIFF,PHILIM,TOTPHI,PHI2(1:ND,1:NH),PHI3(1:ND,1:NH),
     &    HTOP2(1:ND),HBOT2(1:ND),HTOP3(1:ND),HBOT3(1:ND),H,
     &    SUMABV,PHIABV,PHIBEL,SUMBEL,PHI,SUM,FAC,HIN,
     &    TIME,DELT,MEANV,DIFFH
        DOUBLE PRECISION BARNEA
        LOGICAL CRYST

C *** Calculate concn at nearest layer interface
        PHIABV=0.0D0
        PHIBEL=0.0D0
        SUMABV=0.0D0
        SUMBEL=0.0D0
        DO 101 I=1,ND
          IF ((J.NE.JTOP2(I)).OR.((1.0D0-HTOP2(I)).LE.0.01D0)) THEN
            PHIBEL=PHIBEL+PHI2(I,J)
            SUMBEL=SUMBEL+PHI2(I,J)*STOKV2(I)
          END IF
          IF (((J+1).NE.JBOT2(I)).OR. (HBOT2(I).LE.0.01D0)) THEN
            PHIABV=PHIABV+PHI2(I,J+1)
            SUMABV=SUMABV+PHI2(I,J+1)*STOKV2(I)
          END IF
```

```
            IF(CRYST)THEN
               IF ((J.NE.JTOP3(I)).OR.((1.0D0-HTOP3(I)).LE.0.01D0)) THEN
                  PHIBEL=PHIBEL+PHI3(I,J)
                  SUMBEL=SUMBEL+PHI3(I,J)*STOKV3(I)
               END IF
               IF (((J+1).NE.JBOT3(I)).OR. (HBOT3(I).LE.0.01D0)) THEN
                  PHIABV=PHIABV+PHI3(I,J+1)
                  SUMABV=SUMABV+PHI3(I,J+1)*STOKV3(I)
               END IF
            ENDIF
 101     CONTINUE

C *** Use average concentraion in velocity and diffusion
         PHI=0.5D0*(PHIABV+PHIBEL)
         FAC=BARNEA(PHI)
         SUM=0.5D0*(SUMABV+SUMBEL)
         HIN=FAC*((1.0D0+2.0D0*PHI)*(1.0D0+2.0D0*PHI)+((PHI**3)*
     &      (PHI-4.0D0)))/((1.0D0-PHI)**3)
         DIFFH=DIFF*HIN
         MEANV=FAC*(STOKV-SUM)
C *** Velocity of boundary including creaming and diffusion
         VBDRY=MEANV-0.95D0*DSQRT(DIFFH)*(DSQRT(TIME)-DSQRT(TIME-DELT))
     &      /DELT

         IF((VBDRY.GT.0.0D0).AND.(TOTPHI.GT.PHILIM))THEN
            VBDRY=0.0D0
         END IF
         END


C ********************************************************************
         SUBROUTINE TOPVEL(ND,NH,J,H,STOKV,DIFF,VBDRY,
     &      STOKV2,STOKV3,PHILIM,TOTPHI,PHI2,PHI3,
     &      JTOP2,JBOT2,JTOP3,JBOT3,HTOP2,HBOT2,HTOP3,HBOT3,
     &      TIME,DELT,CRYST)
C ********************************************************************
C *** Calculate velocity of upper boundary
         EXTERNAL BARNEA
         INTEGER I,J,ND,NH,
     &      JTOP2(1:ND),JBOT2(1:ND),JTOP3(1:ND),JBOT3(1:ND)
         DOUBLE PRECISION STOKV2(1:ND),STOKV3(1:ND),STOKV,VBDRY,
     &      DIFF,PHILIM,TOTPHI,PHI2(1:ND,1:NH),PHI3(1:ND,1:NH),
     &      HTOP2(1:ND),HBOT2(1:ND),HTOP3(1:ND),HBOT3(1:ND),H,
     &      PHIABV,SUMABV,SUMBEL,PHIBEL,PHI,FAC,SUM,HIN,
     &      TIME,DELT,MEANV,DIFFH
         DOUBLE PRECISION BARNEA
         LOGICAL CRYST

C *** Calculate concn at nearest layer interface
         PHIABV=0.0D0
         PHIBEL=0.0D0
         SUMABV=0.0D0
         SUMBEL=0.0D0
         DO 101 I=1,ND
            IF ((J.NE.JTOP2(I)).OR.((1.0D0-HTOP2(I)).LE.0.01D0)) THEN
               PHIBEL=PHIBEL+PHI2(I,J)
               SUMBEL=SUMBEL+PHI2(I,J)*STOKV2(I)
            END IF
```

```
            IF (((J+1).NE.JBOT2(I)).OR. (HBOT2(I).LE.0.01D0)) THEN
               PHIABV=PHIABV+PHI2(I,J+1)
               SUMABV=SUMABV+PHI2(I,J+1)*STOKV2(I)
            END IF
            IF(CRYST)THEN
               IF ((J.NE.JTOP3(I)).OR.((1.0D0-HTOP3(I)).LE.0.01D0)) THEN
                  PHIBEL=PHIBEL+PHI3(I,J)
                  SUMBEL=SUMBEL+PHI3(I,J)*STOKV3(I)
               END IF
               IF (((J+1).NE.JBOT3(I)).OR. (HBOT3(I).LE.0.01D0)) THEN
                  PHIABV=PHIABV+PHI3(I,J+1)
                  SUMABV=SUMABV+PHI3(I,J+1)*STOKV3(I)
               END IF
            ENDIF
 101     CONTINUE

C *** Use average concentraion in velocity and diffusion
         PHI=0.5D0*(PHIABV+PHIBEL)
         FAC=BARNEA(PHI)
         SUM=0.5D0*(SUMABV+SUMBEL)
         HIN=FAC*((1.0D0+2.0D0*PHI)*(1.0D0+2.0D0*PHI)+((PHI**3)*
     &       (PHI-4.0D0)))/((1.0D0-PHI)**3)
         DIFFH=DIFF*HIN
         MEANV=FAC*(STOKV-SUM)
C *** Velocity of boundary including creaming and diffusion
         VBDRY=MEANV+0.95D0*DSQRT(DIFFH)*(DSQRT(TIME)-DSQRT(TIME-DELT))
     &       /DELT

         IF((VBDRY.LT.0.0D0).AND. (TOTPHI.GT.PHILIM))THEN
            VBDRY=0.0D0
         END IF

         END
```

Appendix A2 : Computer Program for Phenomenological Model of Creaming and Flocculation

```
C    Phenomenological model of creaming and flocculation
C    of oil in water emulsions
C    by Valerie Pinfield.    1993-1995
C    Hydrodynamics using total concn of flocs and particles
C ***************************************************************************
      PROGRAM FLOC
C ***************************************************************************
      INTEGER ND,NH,NFL
      DOUBLE PRECISION DELH,G,TOTPHI,PHILIM,MEANZ,SIGMAZ,FLCPHI,
     &    RFLMAX,RADGYR,FRDIM,ADCRIT,FLCPRB
C z=ln(diameter), totphi=vol fract, flcphi=prop const, rflmax=max floc radius,frdim=fractal dimension
      PARAMETER ( ND=11,MEANZ=-0.5798D0,SIGMAZ=0.42D0,
     &    NH=80,DELH=0.5D-3,G=9.81D0,
     &    TOTPHI=0.2D0,PHILIM=1.0D0,
     &    NFL=20,FLCPHI=4.2D-7,RFLMAX=10.0D-6,FRDIM=2.0D0,
     &    RADGYR=5.0D-9,ADCRIT=0.0D-4,FLCPRB=1.0D-6)
C *** Number of pair interactions determines the size of arrays
C ***  = ND(ND+1)/2+ND.NFL+NFL(NFL+1)/2
      INTEGER JTOP2(1:ND),JBOT2(1:ND),FLSIZE(11476)
      CHARACTER*50 FLNAME,DFNAME
      DOUBLE PRECISION RADIUS(ND),FRAD(NFL),STOKV2(ND),STOKFL(NFL),
     &    DIFF2(ND),DIFFLC(NFL),
     &    DIFFPR(11476),DELVPR(11476),RFLOC3(11476),
     &    Q(3),RHO(3),ETA(3),MU(3),TOR(3),CP(3),GAMMA(3),
     &    BETA(3),ALPHA(3),SIGMA(3),TEMP,ANGFREQ,
     &    PHITOT(NH),PHI2(ND,NH),PHISM2(NH),
     &    FLC2(NFL,NH),FLC(NFL,NH),ADD(NH),
     &    HTOP2(1:ND),HBOT2(1:ND),VOLP(ND),VOLF(NFL),VOLF2(NFL),
     &    DELT,RECORD,MAXT,RMIN,DELR
      DELT=120.0D0
      RECORD=1200.0D0
      MAXT=1200.0D0
      ANGFREQ=1.0D6*6.283185307D0
      FLNAME="flctst.xls"
      DFNAME="sun30"
      OPEN(UNIT=20,ACCESS="SEQUENTIAL",FILE=FLNAME)
      WRITE(20,300)FLNAME,DFNAME
  300 FORMAT("Creaming_profile_results ",A12," Data_file ",A12)
      WRITE(20,301)
  301 FORMAT("FLOCT.F")
      WRITE(20,302)ANGFREQ
  302 FORMAT("Angular frequency ",E15.5E3)
      WRITE(20,303)FLCPRB,FLCPHI,FRDIM
  303 FORMAT("Flocculation_parameters, prob, const,dimen",3E15.5E3)
C *** Read material properties from data file
      CALL MTDATA(Q,RHO,ETA,MU,TOR,CP,GAMMA,BETA,ALPHA,SIGMA,
     &                ANGFREQ,TEMP,DFNAME)
C *** Set up particle size distribution, creaming and diffusion rates
      CALL INITIALISE(ND,NFL,NH,RADIUS,FRAD,STOKV2,STOKFL,DIFF2,DIFFLC,
     &    DIFFPR,DELVPR,RFLOC3,FLSIZE,FLCPRB,
     &    RHO,ETA,TEMP,G,MEANZ,SIGMAZ,RFLMAX,RMIN,DELR,FRDIM,
```

```
     &     PHILIM,FLCPHI,TOTPHI,PHI2,FLC,FLC2,PHITOT,PHISM2,
     &     JTOP2,JBOT2,HTOP2,HBOT2,VOLP,VOLF,VOLF2,
     &     DELT,DELH,ADD)
C *** Calculate creaming process
      CALL SEQUENCE(ND,NFL,NH,RADIUS,FRAD,STOKV2,STOKFL,DIFF2,DIFFLC,
     &     DIFFPR,DELVPR,RFLOC3,FLSIZE,FLCPRB,
     &     Q,RHO,ETA,MU,TOR,GAMMA,BETA,SIGMA,ANGFREQ,ADCRIT,
     &     RFLMAX,RMIN,DELR,RADGYR,FRDIM,
     &     PHILIM,FLCPHI,PHI2,PHITOT,PHISM2,FLC,FLC2,
     &     JTOP2,JBOT2,HTOP2,HBOT2,VOLP,VOLF,VOLF2,
     &     DELT,DELH,ADD,RECORD,MAXT)

      END

C ********************************************************************
      SUBROUTINE INITIALISE(ND,NFL,NH,RADIUS,FRAD,STOKV2,STOKFL,
     &     DIFF2,DIFFLC,DIFFPR,DELVPR,RFLOC3,FLSIZE,FLCPRB,
     &     RHO,ETA,TEMP,G,MEANZ,SIGMAZ,RFLMAX,RMIN,DELR,FRDIM,
     &     PHILIM,FLCPHI,TOTPHI,PHI2,FLC,FLC2,PHITOT,PHISM2,
     &     JTOP2,JBOT2,HTOP2,HBOT2,VOLP,VOLF,VOLF2,DELT,DELH,ADD)
C ********************************************************************
C *** Initialise the particle size distribtion and concn profiles
C *** Initialise creaming and diffusion rates
      INTEGER ND,NFL,NH,NPAIRS,FLSIZE(11476),JTOP2(1:ND),JBOT2(1:ND)
      DOUBLE PRECISION RADIUS(ND),FRAD(NFL),STOKV2(ND),STOKFL(NFL),
     &     DIFF2(ND),DIFFLC(NFL),
     &     DIFFPR(11476),DELVPR(11476),RFLOC3(11476),
     &     RHO(3),ETA(3),TEMP,G,FRDIM,DIFHMX,FLCPRB,
     &     TOTPHI,PHILIM,FLCPHI,PHI2(ND,NH),PHITOT(NH),PHISM2(NH),
     &     FLC2(NFL,NH),FLC(NFL,NH),VOLP(ND),VOLF(NFL),VOLF2(NFL),
     &     HTOP2(1:ND),HBOT2(1:ND),
     &     RATIO,SUM,DEL,FRACT(101),MEANZ,SIGMAZ,DZ,DENOM,SHIFTZ,
     &     DELR,RMIN,RFLMAX,DR32,SUMP(101),SUMFLC(50),
     &     DELT,DELH,ADD(1:NH),K,PI,PI43,VOLPI,VOLPII,VLF2I,VOIL,MAX
      PARAMETER(K=1.3807D-23, PI=3.141592654D0,PI43=4.188790205D0)
      INTEGER I,J,II

      SUM=0.0D0
      DIFHMX=1.6D0
      DEL=RHO(2)/RHO(3)
      IF (ND.EQ.1) THEN
C *** Monodisperse emulsion
        RADIUS(1)=0.5D-6*DEXP(MEANZ)
        VOLP(1)=PI43*(RADIUS(1)**3)
C *** Stokes creaming speed, Stokes-Einstein diffusion coefficient
        STOKV2(1)=2.0D0*DABS(RHO(2)-RHO(1))*G*RADIUS(1)*RADIUS(1)
     &       /(9.0D0*ETA(1))
        DIFF2(1)=K*TEMP/(6.0D0*PI*ETA(1)*RADIUS(1))
        JTOP2(1)=NH
        JBOT2(1)=1
        HTOP2(1)=1.0D0
        HBOT2(1)=0.0D0
        DO 121 J=1,NH
C *** Uniform emulsion.
          PHI2(1,J)=TOTPHI
          PHITOT(J)=PHI2(1,J)
          PHISM2(J)=PHI2(1,J)
          ADD(J)=1.0D-3
 121    CONTINUE
```

```
      ELSE
C *** Polydisperse, log-normal distribution when plotting volume/size
C *** Z = LN (D/microns)  Natural logarithm of diameter
            DZ=6.0D0*SIGMAZ/(DBLE(ND)-1.0D0)
            DENOM=2.0D0*SIGMAZ*SIGMAZ
            DO 101 I=1,ND
               SHIFTZ = (-3.0D0*SIGMAZ)+DBLE(I-1)*DZ
               RADIUS(I)=0.5D0*1.0D-6*DEXP(MEANZ+SHIFTZ)
               VOLP(I)=PI43*(RADIUS(I)**3)
               FRACT(I)=DEXP(-(SHIFTZ*SHIFTZ)/DENOM)
               SUM=SUM+FRACT(I)
C *** Stokes creaming speed, Stokes-Einstein diffusion coefficient
               STOKV2(I)=2.0D0*DABS(RHO(2)-RHO(1))*G*RADIUS(I)*RADIUS(I)
     &                        /(9.0D0*ETA(1))
               DIFF2(I)=K*TEMP/(6.0D0*PI*ETA(1)*RADIUS(I))
               JTOP2(I)=NH
               JBOT2(I)=1
               HTOP2(I)=1.0D0
               HBOT2(I)=0.0D0
               SUMP(I)=0.0D0
  101       CONTINUE
            RATIO=TOTPHI/SUM
            DO 102 J=1,NH
               PHITOT(J)=0.0D0
               PHISM2(J)=0.0D0
               ADD(J)=1.0D-3
               DO 103 I=1,ND
C *** Uniform emulsion.
                  PHI2(I,J)=RATIO*FRACT(I)
                  PHITOT(J)=PHITOT(J)+PHI2(I,J)
                  PHISM2(J)=PHISM2(J)+PHI2(I,J)
  103          CONTINUE
  102       CONTINUE
         END IF
C *** Initialise the size fractions for flocs
         RMIN=DLOG(RADIUS(1))
         DELR=(DLOG(RFLMAX)-RMIN)/(DBLE(NFL-1.0D0))
         DR32=(DEXP(1.5D0*DELR))
         DO 111 I=1,NFL
            FRAD(I)=DEXP(RMIN+DBLE(I-1)*DELR)
            VOLF(I)=PI43*FRAD(I)**3
            VOLF2(I)=FLCPHI*(FRAD(I)**FRDIM)
C *** Modified Stokes creaming speed, Stokes-Einstein diffusion coeff
            STOKFL(I)=FLCPHI*DABS(RHO(2)-RHO(1))*G*
     &                     (FRAD(I)**(FRDIM-1.0D0))/(6.0D0*PI*ETA(1))
            DIFFLC(I)=K*TEMP/(6.0D0*PI*ETA(1)*FRAD(I))
            SUMFLC(I)=0.0D0
            DO 112 J=1,NH
C *** Initially unflocculated
               FLC(I,J)=0.0D0
               FLC2(I,J)=0.0D0
  112       CONTINUE
  111    CONTINUE
C *** Binary collision rates for flocculation
         NPAIRS=0
         DO 131 I=1,ND
            VOLPI=VOLP(I)
            DO 132 II=1,ND
```

```
C *** Particle-particle collision
                NPAIRS=NPAIRS+1
                VOLPII=VOLP(II)
                DIFFPR(NPAIRS)=2.0D0*PI*(DIFF2(I)+DIFF2(II))*
     &                          (RADIUS(I)+RADIUS(II))/(VOLPI*VOLPII)
                DELVPR(NPAIRS)=PI*DABS(STOKV2(I)-STOKV2(II))*
     &                          (RADIUS(I)+RADIUS(II))*(RADIUS(I)+RADIUS(II))/
     &                          (VOLPI*VOLPII)
                VOIL=VOLPI+VOLPII
                RFLOC3(NPAIRS)=(VOIL/FLCPHI)**(3.0D0/FRDIM)
                FLSIZE(NPAIRS)=INT(1.5D0+(DLOG(RFLOC3(NPAIRS))/3.0D0
     &                          -RMIN)/DELR)
                SUMP(I)=SUMP(I)+VOLP(I)*(DIFHMX*DIFFPR(NPAIRS)
     &                          +DELVPR(NPAIRS))
                SUMP(II)=SUMP(II)+VOLP(II)*(DIFHMX*DIFFPR(NPAIRS)
     &                          +DELVPR(NPAIRS))
  132         CONTINUE
              DO 133 II=1,NFL
C *** Particle-floc collision
                NPAIRS=NPAIRS+1
                DIFFPR(NPAIRS)=2.0D0*PI*(DIFF2(I)+DIFFLC(II))*(RADIUS(I)+
     &                          FRAD(II))/(VOLP(I)*VOLF(II))
                DELVPR(NPAIRS)=PI*DABS(STOKV2(I)-STOKFL(II))*
     &                          (RADIUS(I)+FRAD(II))*(RADIUS(I)+FRAD(II))/
     &                          (VOLP(I)*VOLF(II))
                VOIL=VOLPI+VOLF2(II)
                RFLOC3(NPAIRS)=(VOIL/FLCPHI)**(3.0D0/FRDIM)
                FLSIZE(NPAIRS)=INT(1.5D0+(DLOG(RFLOC3(NPAIRS))/3.0D0
     &                          -RMIN)/DELR)
                SUMP(I)=SUMP(I)+VOLP(I)*(DIFHMX*DIFFPR(NPAIRS)
     &                          +DELVPR(NPAIRS))
                SUMFLC(II)=SUMFLC(II)+VOLF(II)*(DIFHMX*DIFFPR(NPAIRS)
     &                          +DELVPR(NPAIRS))
  133         CONTINUE
  131       CONTINUE
            DO 134 I=1,NFL
              VLF2I=VOLF2(I)
              DO 135 II=I,NFL
C *** Floc-floc collision
                NPAIRS=NPAIRS+1
                DIFFPR(NPAIRS)=2.0D0*PI*(DIFFLC(I)+DIFFLC(II))*(FRAD(I)+
     &                          FRAD(II))/(VOLF(I)*VOLF(II))
                DELVPR(NPAIRS)=PI*DABS(STOKFL(I)-STOKFL(II))*
     &                          (FRAD(I)+FRAD(II))*(FRAD(I)+FRAD(II))/
     &                          (VOLF(I)*VOLF(II))
                VOIL=VLF2I+VOLF2(II)
                RFLOC3(NPAIRS)=(VOIL/FLCPHI)**(3.0D0/FRDIM)
                FLSIZE(NPAIRS)=INT(1.5D0+(DLOG(RFLOC3(NPAIRS))/3.0D0
     &                          -RMIN)/DELR)
                SUMFLC(I)=SUMFLC(I)+VOLF(I)*(DIFHMX*DIFFPR(NPAIRS)
     &                          +DELVPR(NPAIRS))
                SUMFLC(II)=SUMFLC(II)+VOLF(II)*(DIFHMX*DIFFPR(NPAIRS)
     &                          +DELVPR(NPAIRS))
  135         CONTINUE
  134       CONTINUE

C *** Calculate maximum conversion of floc volume
            MAX=0.0D0
```

```
      DO 136 I=1,ND
        IF(SUMP(I).GT.MAX)THEN
          MAX=SUMP(I)
        ENDIF
  136 CONTINUE
      DO 137 I=1,NFL
        IF(SUMFLC(I).GT.MAX)THEN
          MAX=SUMFLC(I)
        ENDIF
  137 CONTINUE

C *** Set time interval according to creaming speed and flocc. rate
      IF (DELT.GT.(0.5D0*DELH/STOKFL(NFL))) THEN
        DELT=0.5D0*DELH/STOKFL(NFL)
        WRITE(20,*)DELT
      END IF
      IF(FLCPRB.GT.0.0D0.AND.
     &   (DELT.GT.(0.5D0/(ADD(NH)*FLCPRB*MAX))))THEN
        DELT=0.5D0/(ADD(NH)*FLCPRB*MAX)
      ENDIF
      WRITE(20,300)DELT
  300 FORMAT("Time interval ",E15.5E3)

      WRITE(20,301) NH,DELH,TOTPHI,PHILIM
  301 FORMAT(I14,"layers of",1E9.2,"m ; inital volume fraction ",1F5.2
     & ," packing fraction ",1F5.2)
      WRITE(20,302)
  302 FORMAT("Initial distribution, radius, volume fraction")
      DO 202 I=1,ND
        WRITE(20,303)RADIUS(I),PHI2(I,NH),STOKV2(I)
  303   FORMAT(3E14.6)
  202 CONTINUE
      END

C ****************************************************************
      SUBROUTINE SEQUENCE(ND,NFL,NH,RADIUS,FRAD,STOKV2,STOKFL,
     &   DIFF2,DIFFLC,DIFFPR,DELVPR,RFLOC3,FLSIZE,
     &   FLCPRB,Q,RHO,ETA,MU,TOR,GAMMA,BETA,SIGMA,ANGFREQ,ADCRIT,
     &   RFLMAX,RMIN,DELR,RADGYR,FRDIM,
     &   PHILIM,FLCPHI,PHI2,PHITOT,PHISM2,FLC,FLC2,
     &   JTOP2,JBOT2,HTOP2,HBOT2,VOLP,VOLF,VOLF2,
     &   DELT,DELH,ADD,RECORD,MAXT)
C ****************************************************************
C   Control the sequence of time steps for the calculation of the
C   development of concentration profiles
      INTEGER ND,NFL,NH,I,J,T,JTOP2(1:ND),JBOT2(1:ND),
     &   JPTOP2(1:101),JPBOT2(1:101),FLSIZE(11476)

      DOUBLE PRECISION RADIUS(ND),FRAD(NFL),STOKV2(ND),STOKFL(NFL),
     &   DIFF2(ND),DIFFLC(NFL),
     &   DIFFPR(11476),DELVPR(11476),RFLOC3(11476),
     &   Q(3),RHO(3),ETA(3),MU(3),TOR(3),
     &   GAMMA(3),BETA(3),SIGMA(3),DEL23,ANGFREQ,
     &   RFLMAX,RMIN,DELR,RADGYR,ADCRIT,PHILIM,FLCPHI,FRDIM,FLCPRB,
     &   PHI2(ND,NH),FLC(NFL,NH),FLC2(NFL,NH),PHITOT(NH),PHISM2(NH),
     &   HTOP2(ND),HBOT2(ND),VOLP(ND),VOLF(NFL),VOLF2(NFL),
     &   MAXT,RECORD,DELT,DELH,ADD(NH)
```

```
      DOUBLE PRECISION MEANV2(101),VELFLC(50),VTOP2(101),VBOT2(101),
     &   DIFHIN,CRMHIN,PHIUP2(101),FLUP(50),FLC2UP(50),
     &   PHITUP,PHS2UP,PHIT2,TMPHI2(101),
     &   HPTOP2(101),HPBOT2(101),
     &   TDIVH,TDIVH2,TIME,N,
     &   TOTAL,TOT,TOTA,TOTB,ADDUP,DEL

      DEL=RHO(1)/RHO(2)
      DEL23=RHO(2)/RHO(3)
      TDIVH=DELT/DELH
      TDIVH2=TDIVH/DELH
      DO 101 I=1,ND
        HPTOP2(I)=HTOP2(I)
        HPBOT2(I)=HBOT2(I)
  101 CONTINUE
      T=0
  201 IF(TIME.LE.MAXT) THEN
C *** Increment time by one step
      T=T+1
      TIME=DELT*DBLE(T)

C *** Initialise arrays at top of sample
        DO 102 I=1,ND
          IF(JBOT2(I).EQ.NH)THEN
            PHIUP2(I)=PHI2(I,NH)*(1.0D0-HBOT2(I))
          ELSEIF (JTOP2(I).EQ.NH)THEN
            PHIUP2(I)=PHI2(I,NH)*HTOP2(I)
          ELSE
            PHIUP2(I)=PHI2(I,NH)
          END IF
  102   CONTINUE
        DO 103 I=1,NFL
          FLUP(I)=FLC(I,NH)
          FLC2UP(I)=FLC2(I,NH)
  103   CONTINUE
        PHITUP=PHITOT(NH)
        PHS2UP=PHISM2(NH)
        ADDUP=ADD(NH)
C *** Calculate velocity of upper and lower boundaries of each size
        CALL BDRYVEL(ND,NFL,NH,STOKV2,STOKFL,VTOP2,VBOT2,
     &          DIFF2,DIFFLC,PHILIM,FLCPHI,PHI2,PHITOT,FLC,
     &          JTOP2,JBOT2,HTOP2,HBOT2,TIME,DELT)
C *** Start with top layer and work downwards.
        DO 104 J=NH-1,1,-1
C **** Calculate the velocity of each size fraction at J/J+1 interface
          CALL CALVEL(J,ND,NFL,NH,STOKV2,MEANV2,STOKFL,VELFLC,
     &          DIFHIN,CRMHIN,PHILIM,FLCPHI,PHI2,FLC,
     &          JTOP2,JBOT2,HTOP2,HBOT2)
C *** Calculate the oil volume moving across the J/J+1 layer interface
          CALL FLUX(J,ND,NFL,NH,RADIUS,FRAD,STOKV2,MEANV2,
     &          STOKFL,VELFLC,VTOP2,VBOT2,DIFF2,DIFFLC,
     &          DIFFPR,DELVPR,RFLOC3,FLSIZE,
     &          FLCPRB,DIFHIN,CRMHIN,FRDIM,
     &          DEL23,RFLMAX,RMIN,DELR,RADGYR,ADCRIT,
     &          PHILIM,FLCPHI,PHI2,FLC,FLC2,PHITOT,PHISM2,
     &          PHIUP2,FLUP,FLC2UP,PHITUP,PHS2UP,
     &          JTOP2,JBOT2,HTOP2,HBOT2,JPTOP2,JPBOT2,HPTOP2,HPBOT2,
     &          VOLP,VOLF,VOLF2,TIME,DELT,TDIVH,TDIVH2,ADD,ADDUP)
  104   CONTINUE
```

```
C *** Reset the arrays and variables
            PHITOT(1)=PHITUP
            PHISM2(1)=PHS2UP
            ADD(1)=ADDUP
            DO 105 I=1,ND
               JTOP2(I)=JPTOP2(I)
               JBOT2(I)=JPBOT2(I)
               HTOP2(I)=HPTOP2(I)
               HBOT2(I)=HPBOT2(I)
C *** Check for problems and underflow
               IF(HBOT2(1).GT.1.0D0)THEN
                  WRITE(20,321)HBOT2(1)
 321               FORMAT("HBOT.GT.1",E15.5E3)
                  GOTO 202
               END IF
               DO 106 J=1,NH
                  IF(PHI2(I,J).LT.1.0E-15)THEN
                     PHI2(I,J)=0.0D0
                  END IF
                  IF(PHITOT(J).LT.1.0E-15)THEN
                     PHITOT(J)=0.0D0
                  END IF
 106              CONTINUE
 105           CONTINUE

               DO 107 I=1,NFL
                  DO 108 J=1,NH
                     IF(FLC(I,J).LT.1.0E-15)THEN
                        FLC(I,J)=0.0D0
                     END IF
                     IF(FLC2(I,J).LT.1.0D-15)THEN
                        FLC2(I,J)=0.0D0
                     ENDIF
                     IF(PHISM2(J).LT.1.0E-15)THEN
                        PHISM2(J)=0.0D0
                     END IF
 108              CONTINUE
 107           CONTINUE
C *** If this is a recording step, write out results
               N=TIME/RECORD
               IF(N.GT.0.5 .AND. ABS(TIME-(RECORD*DNINT(N))).LE.
     &                  DELT/2.0)THEN
                  WRITE(20,301)TIME/86400.0D0
 301              FORMAT("time",F8.2," days")
                  WRITE(20,302)
 302              FORMAT("Height   Tot vol fract  phi(liquid)
     &  Urick vel   S.S. vel     M.S. vel  S.S Atten  M.S
     &  atten")
C *** Check conservation of oil volume
                  TOTB=0.0D0
                  TOTAL=0.0D0
                  TOTA=0.0D0
                  TOT=0.0D0
                  DO 109 J=1,NH
                     TOTAL=TOTAL+PHITOT(J)/NH
                     TOTB=TOTB+ADD(J)*(1.0D0-PHITOT(J))/NH
 109              CONTINUE
                  WRITE(20,303)TOTAL,TOTB,PHITOT(50),ADD(50)
 303              FORMAT("Total",4E15.5E3)
```

```
C *** Generate and write out concentration and velocity profiles
                DO 110 J=1,NH,1
                  PHIT2=0.0D0
                  TOT=0.0D0
                  DO 111 I=1,ND
C *** Calculate the local concentration at the layer interface
                    IF(J.EQ.JBOT2(I))THEN
                      TOT=TOT+PHI2(I,J)*(1.0D0-HBOT2(I))
                      TOTA=TOTA+PHI2(I,J)*(1.0D0-HBOT2(I))
                    ELSEIF(J.EQ.JTOP2(I))THEN
                      TOT=TOT+PHI2(I,J)*HTOP2(I)
                      TOTA=TOTA+PHI2(I,J)*HTOP2(I)
                    ELSE
                      TOT=TOT+PHI2(I,J)
                      TOTA=TOTA+PHI2(I,J)
                    ENDIF

                    IF (J.EQ.JBOT2(I))THEN
                      TMPHI2(I)=PHI2(I,J)*(1.0D0-HBOT2(I))
                    ELSEIF(J.EQ.JTOP2(I))THEN
                      TMPHI2(I)=PHI2(I,J)*HTOP2(I)
                    ELSE
                      TMPHI2(I)=PHI2(I,J)
                    END IF
                    PHIT2=PHIT2+TMPHI2(I)
111               CONTINUE
                  DO 112 I=1,NFL
                    TOT=TOT+FLC2(I,J)
                    TOTA=TOTA+FLC2(I,J)
112               CONTINUE

C *** Output results
                  WRITE(20,304)1.0E3*J*DELH,PHITOT(J),TOT,ADD(J),
     &                (PHI2(I,J),I=1,ND,20),(FLC(I,J),I=4,NFL-6,8)
304               FORMAT(F5.1,15E12.5E2)
110             CONTINUE

                WRITE(20,306)TOTA/NH
306             FORMAT("TOTAL",F12.6)

                WRITE(20,307)(JTOP2(I),I=1,ND,10)
                WRITE(20,308)(HTOP2(I),I=1,ND,10)
                WRITE(20,309)(JBOT2(I),I=1,ND,10)
                WRITE(20,310)(HBOT2(I),I=1,ND,10)
307             FORMAT("JTOP",I30,10I15)
308             FORMAT("JBOT",I30,10I15)
309             FORMAT("HTOP",E30.5E3,10E15.5E3)
310             FORMAT("HBOT",E30.5E3,10E15.5E3)

C *** Write out the particle size distribution
                IF (DABS(DBLE(N)-(5.0D0*DNINT(N/5.0D0))).LT.0.01D0)THEN
                  DO 113 I=1,ND,1
                    WRITE(20,311)RADIUS(I),PHI2(I,1)
311                 FORMAT(2E12.4E3)
113               CONTINUE
                  DO 114 I=1,NFL,1
                    WRITE(20,311)FRAD(I),FLC(I,1)
114               CONTINUE
                END IF
```

```
            END IF
            GOTO 201
          END IF
  202     END


C ********************************************************************
          SUBROUTINE CALVEL(J,ND,NFL,NH,STOKV2,MEANV2,STOKFL,VELFLC,
         &     DIFHIN,CRMHIN,PHILIM,FLCPHI,PHI2,FLC,
         &     JTOP2,JBOT2,HTOP2,HBOT2)
C ********************************************************************
C *** Calculate velocity for each size fraction at J/J+1 interface.
C *** Barnea-Mizrahi (1973) hindrance factor. Zimmels (1988) polydisper
C *** Carnahan-Starling equation for thermodynamic factor of diffusion
          INTEGER I,J,J1,ND,NFL,NH,JTOP2(ND),JBOT2(ND)
          DOUBLE PRECISION BARNEA
          DOUBLE PRECISION STOKV2(ND),STOKFL(NFL),
         &     MEANV2(ND),VELFLC(NFL),DIFHIN,CRMHIN,
         &     PHILIM,FLCPHI,PHI2(ND,NH),FLC(NFL,NH),
         &     HTOP2(ND),HBOT2(ND),
         &     PHIABV,PHIBEL,SUMABV,SUMBEL,PHI,SUM,FAC
C *** Calculate total concn just above and just below layer interface
          J1=J+1
          PHIABV=0.0D0
          PHIBEL=0.0D0
          SUMABV=0.0D0
          SUMBEL=0.0D0
          DO 101 I=1,ND
            IF ((J.NE.JTOP2(I)).OR.((1.0D0-HTOP2(I)).LE.0.01D0)) THEN
              PHIBEL=PHIBEL+PHI2(I,J)
              SUMBEL=SUMBEL+PHI2(I,J)*STOKV2(I)
            END IF
            IF (((J1).NE.JBOT2(I)).OR. (HBOT2(I).LE.0.01D0)) THEN
              PHIABV=PHIABV+PHI2(I,J1)
              SUMABV=SUMABV+PHI2(I,J1)*STOKV2(I)
            END IF
  101     CONTINUE
C *** Include contribution of flocs to hydrodynamic hindrance
          DO 102 I=1,NFL
            PHIBEL=PHIBEL+FLC(I,J)
            SUMBEL=SUMBEL+FLC(I,J)*STOKFL(I)
            PHIABV=PHIABV+FLC(I,J1)
            SUMABV=SUMABV+FLC(I,J1)*STOKFL(I)
  102     CONTINUE
C ** Average concn used in hindrance factor for creaming and diffusion
          PHI=0.5D0*(PHIABV+PHIBEL)
          FAC=BARNEA(PHI)
          SUM=0.5D0*(SUMABV+SUMBEL)
          DIFHIN=FAC*((1.0D0+2.0D0*PHI)*(1.0D0+2.0D0*PHI)+((PHI**3)*
         &     (PHI-4.0D0)))/((1.0D0-PHI)**3)
          CRMHIN=FAC
C *** Calculate creaming velocity of each size fraction
          DO 103 I=1,ND
            MEANV2(I)=FAC*(STOKV2(I)-SUM)
  103     CONTINUE
          DO 104 I=1,NFL
            VELFLC(I)=FAC*(STOKFL(I)-SUM)
  104     CONTINUE
          END
```

```
C ****************************************************************
      SUBROUTINE FLUX(J,ND,NFL,NH,RADIUS,FRAD,STOKV2,MEANV2,
     &     STOKFL,VELFLC,VTOP2,VBOT2,DIFF2,DIFFLC,
     &     DIFFPR,DELVPR,RFLOC3,FLSIZE,FLCPRB,
     &     DIFHIN,CRMHIN,FRDIM,DEL23,RFLMAX,RMIN,DELR,RADGYR,ADCRIT,
     &     PHILIM,FLCPHI,PHI2,FLC,FLC2,PHITOT,PHISM2,
     &     PHIUP2,FLUP,FLC2UP,PHITUP,PHS2UP,
     &     JTOP2,JBOT2,HTOP2,HBOT2,JPTOP2,JPBOT2,HPTOP2,HPBOT2,
     &     VOLP,VOLF,VOLF2,TIME,DELT,TDIVH,TDIVH2,ADD,ADDUP)
C ****************************************************************
C *** Calculate volume of oil which moves across the layer interface
      INTEGER J,ND,NFL,NH,JTOP2(ND),JBOT2(ND),JPTOP2(ND),JPBOT2(ND),
     &     I,J1,FLSIZE(11476)
      DOUBLE PRECISION RADIUS(ND),FRAD(NFL),STOKV2(ND),STOKFL(NFL),
     &     VTOP2(ND),VBOT2(ND),MEANV2(ND),VELFLC(NFL),
     &     DIFF2(ND),DIFFLC(NFL),DIFHIN,CRMHIN,FRDIM,
     &     DIFFPR(11476),DELVPR(11476),RFLOC3(11476),
     &     RFLMAX,RMIN,DELR,RADGYR,ADCRIT,DEL23,FLCPRB,
     &     PHILIM,FLCPHI,PHI2(ND,NH),PHITOT(NH),PHISM2(NH),
     &     FLC2(NFL,NH),FLC(NFL,NH),ADD(NH),
     &     PHIUP2(ND),FLUP(NFL),FLC2UP(NFL),PHITUP,PHS2UP,ADDUP,
     &     VOLP(ND),VOLF(NFL),VOLF2(NFL),
     &     HTOP2(ND),HBOT2(ND),HPTOP2(ND),HPBOT2(ND)

      DOUBLE PRECISION PHIUPT,SUMUP2,ADDUPT,PHIMOV,PHI2MV,PHISUM,PHIS2,
     &     PHITMP,PHITM2,ADDTMP,MOVADD,MASMOV,DELPHI,DELJPH,DIFF,
     &     PHIJ2(101),PHIJ12(101),FAC2(101),
     &     FLCJ1(50),FLCJ(50),FLC2J1(50),FLC2J(50),
     &     DELTA2(101),DELTAF(50),DELTF2(50),
     &     DELTJ2(101),DELTJF(50),DELJF2(50),
     &     TDIVH,TDIVH2,TIME,DELT,COLEFF

      J1=J+1
      DO 101 I=1,ND
         DELTA2(I)=0.0D0
         DELTJ2(I)=0.0D0
  101 CONTINUE
      DO 102 I=1,NFL
         DELTAF(I)=0.0D0
         DELTJF(I)=0.0D0
         DELTF2(I)=0.0D0
         DELJF2(I)=0.0D0
  102 CONTINUE

      IF (PHITOT(J1).LT.PHILIM)THEN
C *** Determine creaming and flocculation in layer J+1
         PHISUM=0.0D0
         PHIS2=0.0D0
         DELPHI=0.0D0
         DELJPH=0.0D0
         DO 103 I=1,ND
            PHIJ12(I)=PHI2(I,J1)
            PHIJ2(I)=PHI2(I,J)
            DIFF=DIFF2(I)*DIFHIN
C *** Calculate amount of oil of this size crossing interface
            CALL FLOW(J,NH,MEANV2(I),VTOP2(I),VBOT2(I),DIFF,
     &                PHI2(I,J),PHI2(I,J1),PHIJ12(I),PHIUP2(I),PHIJ2(I),
     &                PHIMOV,ADD(J),ADD(J1),
     &                JTOP2(I),JBOT2(I),HTOP2(I),HBOT2(I),
```

```
     &                    JPTOP2(I),JPBOT2(I),HPTOP2(I),HPBOT2(I),TDIVH,TDIVH2)
                PHISUM=PHISUM+PHIMOV
                PHIS2=PHIS2+PHIMOV
  103       CONTINUE

            DO 104 I=1,NFL
               FLCJ1(I)=FLC(I,J1)
               FLCJ(I)=FLC(I,J)
               FLC2J1(I)=FLC2(I,J1)
               FLC2J(I)=FLC2(I,J)
               DIFF=DIFFLC(I)*DIFHIN
C *** Calculate amount of flocs of this size crossing interface
               CALL FLOCFLOW(J,VEL,FLC(I),DIFF,
     &                    FLC(I,J),FLC(I,J1),FLCJ1(I),FLUP(I),FLCJ(I),
     &                    FLC2(I,J),FLC2(I,J1),FLC2J1(I),FLC2UP(I),FLC2J(I),
     &                    PHIMOV,PHI2MV,TDIVH,TDIVH2)
               PHISUM=PHISUM+PHIMOV
               PHIS2=PHIS2+PHI2MV
  104       CONTINUE

C *** Calculate the amount of polymer (additive) crossing interface
            IF (PHISUM.GT.0.0D0)THEN
C              MASMOV=-PHISUM*ADD(J1)
               MASMOV=-PHIS2*ADD(J1)
            ELSE
C              MASMOV=-PHISUM*ADD(J)
               MASMOV=-PHIS2*ADD(J)
            END IF
C *** Additive can be excluded from the continuous phase within flocs
            MOVADD=MASMOV
            PHITMP=PHITUP+PHISUM
C     ADDTMP=(ADDUP*(1.0D0-PHITUP)+MOVADD)/(1.0D0-PHITMP)
            PHIUPT=PHITOT(J)-PHISUM
C     ADDUPT=(ADD(J)*(1.0D0-PHITOT(J))-MOVADD)/(1.0D0-PHIUPT)
            PHITM2=PHS2UP+PHIS2
            ADDTMP=(ADDUP*(1.0D0-PHS2UP)+MOVADD)/(1.0D0-PHITM2)
            SUMUP2=PHISM2(J)-PHIS2
            ADDUPT=(ADD(J)*(1.0D0-PHISM2(J))-MOVADD)/(1.0D0-SUMUP2)

            DO 105 I=1,ND
C *** Calculate the proportion of the layer occupied by particles
               IF((J1).EQ.JPTOP2(I))THEN
                  FAC2(I)=HPTOP2(I)
               ELSEIF((J1).EQ.JPBOT2(I))THEN
                  FAC2(I)=1.0D0-HPBOT2(I)
               ELSE
                  FAC2(I)=1.0D0
               ENDIF
  105       CONTINUE
C *** Calculate the flocculation in layer J+1
            COLEFF=FLCPRB*(ADDTMP-ADCRIT)*DELT
            CALL FLOCFLOC(ND,NFL,J1,
     &                 DIFFPR,DELVPR,RFLOC3,FLSIZE,
     &                 DIFHIN,CRMHIN,FRDIM,RMIN,DELR,FLCPHI,COLEFF,
     &                 JPTOP2,JPBOT2,VOLP,VOLF,VOLF2,FAC2,
     &                 PHIJ12,FLCJ1,FLC2J1,DELTA2,DELTAF,DELTF2,DELPHI)
```

```
            IF(J.EQ.1)THEN
C *** At the bottom of the sample - calculate concn changes in J=1
               COLEFF=FLCPRB*(ADDUPT-ADCRIT)*DELT
               DO 106 I=1,ND
                  IF(JPTOP2(I).EQ.1)THEN
                     FAC2(I)=HPTOP2(I)
                  ELSEIF(JPBOT2(I).EQ.1)THEN
                     FAC2(I)=1.0D0-HPBOT2(I)
                  ELSE
                     FAC2(I)=1.0D0
                  ENDIF
  106          CONTINUE
C *** Calculate flocculation in layer J=1
               CALL FLOCFLOC(ND,NFL,1,
     &                    DIFFPR,DELVPR,RFLOC3,FLSIZE,
     &                    DIFHIN,CRMHIN,FRDIM,RMIN,DELR,FLCPHI,COLEFF,
     &                    JPTOP2,JPBOT2,VOLP,VOLF,VOLF2,FAC2,
     &                    PHIJ2,FLCJ,FLC2J,DELTJ2,DELTJF,DELJF2,DELJPH)
            END IF

C *** Reset parameters for layer J+1
C           ADD(J1)=(ADDTMP*(1.0D0-PHITMP))/(1.0D0-PHITMP-DELPHI)
C           ADDUP=(ADDUPT*(1.0D0-PHIUPT))/(1.0D0-PHIUPT-DELJPH)
            ADD(J1)=ADDTMP
            ADDUP=ADDUPT
            PHITOT(J1)=PHITMP+DELPHI
            PHISM2(J1)=PHITM2
            PHITUP=PHIUPT+DELJPH
            PHS2UP=SUMUP2
         ELSE
C *** Layer J+1 is full, no movement, no flocculation
C *** Reset parameters
            DO 107 I=1,ND
               PHIJ12(I)=PHI2(I,J1)
               PHIJ2(I)=PHI2(I,J)
               IF(J.EQ.JBOT2(I))THEN
                  PHIUP2(I)=PHI2(I,J)*(1.0D0-HBOT2(I))
               ELSEIF (J.EQ.JTOP2(I))THEN
                  PHIUP2(I)=PHI2(I,J)*HTOP2(I)
               ELSE
                  PHIUP2(I)=PHI2(I,J)
               END IF
  107       CONTINUE
            DO 108 I=1,NFL
               FLCJ1(I)=FLC(I,J1)
               FLCJ(I)=FLC(I,J)
               FLUP(I)=FLC(I,J)
               FLC2J1(I)=FLC2(I,J1)
               FLC2J(I)=FLC2(I,J)
               FLC2UP(I)=FLC2(I,J)
  108       CONTINUE
            PHITUP=PHITOT(J)
            PHS2UP=PHISM2(J)
            ADDUP=ADD(J)
         END IF
C *** Modify concentration of each size according to flocculation
         DO 109 I=1,ND
            PHI2(I,J1)=PHIJ12(I)+DELTA2(I)
            PHI2(I,J)=PHIJ2(I)+DELTJ2(I)
```

```
            IF(PHI2(I,J1).LT.0.0D0)THEN
               WRITE(20,301)TIME,I,J1,PHIJ12(I),PHI2(I,J1),DELTA2(I)
               PHI2(I,J1)=0.0D0
301               FORMAT("PHI2 negative",E15.5E2,2I4,3E15.5E3)
            ENDIF
109      CONTINUE

         DO 110 I=1,NFL
            FLC(I,J1)=FLCJ1(I)+DELTAF(I)
            FLC2(I,J1)=FLC2J1(I)+DELTF2(I)
            FLC(I,J)=FLCJ(I)+DELTJF(I)
            FLC2(I,J)=FLC2J(I)+DELJF2(I)

            IF(FLC(I,J1).LT.0.0D0)THEN
               WRITE(20,302)I,J1,FLC(I,J1),DELTAF(I)
               FLC(I,J1)=0.0D0
302               FORMAT("FLC negative",2I4,2E15.5E3)
            ENDIF
110      CONTINUE

         END

C ***************************************************************
         SUBROUTINE FLOW(J,NH,MEANV,VTOP,VBOT,DIFF,
     &      PHIIJ,PHIIJ1,PHIJ1,PHIUP,PHIJ,PHIMOV,ADDJ,ADDJ1,
     &      JTOP,JBOT,HTOP,HBOT,JPTOP,JPBOT,HPTOP,HPBOT,TDIVH,TDIVH2)
C ***************************************************************
C *** Calculate the amount of oil of given size fraction and speed
C *** which crosses between the layers
         INTEGER J,JTOP,JBOT,JPTOP,JPBOT,NH
         DOUBLE PRECISION HTOP,HBOT,HPTOP,HPBOT,VTOP,VBOT,MEANV,DIFF,
     &      PHIIJ,PHIIJ1,PHIJ1,PHIJ,PHIUP,PHIMOV,ADDJ,ADDJ1,
     &      CREAM,DIFFUS,TDIVH,TDIVH2

C *** Special cases near lower and upper boundaries
         IF (J .LT.(JBOT-1))THEN
            IF(J.EQ.(JBOT-2))THEN
               PHIJ1=PHIUP/(1.0D0-HPBOT)
               PHIUP=0.0D0
            END IF
            PHIMOV=0.0D0
         ELSE IF (J.GT.JTOP)THEN
            PHIUP=0.0D0
             PHIMOV=0.0D0
         ELSE
            IF (J.EQ.JBOT) THEN
               IF(VBOT.LT.0.0D0)THEN
C *** Lower boundary moves downwards (case 1)
                  IF(MEANV.GT.0.0D0) THEN
                     CREAM=PHIIJ*MEANV*TDIVH
                  ELSE
                     CREAM=PHIIJ1*MEANV*TDIVH
                  END IF
                  DIFFUS=DIFF*(PHIIJ-PHIIJ1)*TDIVH2/(1.0D0-0.5D0*HBOT)
                  PHIMOV=CREAM+DIFFUS
                  PHIJ1=PHIUP+PHIMOV
                  PHIUP=PHIJ*(1.0D0-HBOT)-PHIMOV
                  IF(J.EQ.1)THEN
                     HPBOT=HBOT+VBOT*TDIVH
```

```
                        JPBOT=1
                        IF(HPBOT.LT.0.0D0)THEN
                            HPBOT=0.0D0
                        END IF
                        PHIJ=PHIUP/(1.0D0-HPBOT)
                    END IF
                ELSE
C *** Lower boundary moves upwards
                    IF(VBOT*TDIVH.GE.(0.99D0-HBOT))THEN
C *** Lower boundary crosses layer interface (Case 2)
                        HPBOT=HBOT+VBOT*TDIVH-1.0D0

                        IF(HPBOT.LT.0.0D0)THEN
                            HPBOT=0.0D0
                        END IF
                        JPBOT=J+1
                        PHIMOV=(1.0D0-HBOT)*PHIJ
                        PHIJ1=(PHIUP+PHIMOV)/(1.0D0-HPBOT)
                        PHIUP=0.0D0
                        IF(J.EQ.1)THEN
                            PHIJ=0.0D0
                        END IF
                    ELSE
C *** Lower boundary does not cross interface (Case 3)
                        IF(MEANV.GT.0.0D0) THEN
                            CREAM=PHIJ*MEANV*TDIVH
                        ELSE
                            CREAM=PHIJ1*MEANV*TDIVH
                        END IF
                        DIFFUS=DIFF*(PHIJ-PHIJ1)*TDIVH2/(1.0D0-0.5D0*HBOT)
                        PHIMOV=CREAM+DIFFUS
                        PHIJ1=PHIUP+PHIMOV
                        PHIUP=PHIJ*(1.0D0-HBOT)-PHIMOV
                        HPBOT=HBOT+VBOT*TDIVH
                        JPBOT=J
                        IF(J.EQ.1)THEN
                            PHIJ=PHIUP/(1.0D0-HPBOT)
                        END IF
                    END IF
                END IF
            ELSE IF (J.EQ.JTOP) THEN
                IF(VTOP.LT.0.0D0)THEN
C *** Upper boundary moves downwards (case 4)
                    PHIJ1=0.0D0
                    PHIUP=PHIJ*HTOP
                    PHIMOV=0.0D0
                    IF(J.EQ.1)THEN
                        HPBOT=HBOT+VTOP*TDIVH
                        JPBOT=1
                        IF(HPBOT.LT.0.0D0)THEN
                            HPBOT=0.0D0
                        END IF
                        PHIJ=PHIUP/HPTOP
                    END IF
                ELSE
C *** Upper boundary moves upwards
                    IF(VTOP*TDIVH.GE.(1.01D0-HTOP))THEN
C *** Upper boundary crosses layer interface (Case 5)
                        HPTOP=HTOP+VTOP*TDIVH-1.0D0
```

```
                    JPTOP=J+1
                    PHIJ1=PHIIJ
                    PHIUP=PHIIJ*(HTOP-HPTOP)
                    IF(J.EQ.1)THEN
                      PHIJ=PHIUP/HPBOT
                    END IF
                    PHIMOV=PHIIJ*HPTOP
                  ELSE
C *** Upper boundary does not cross layer interface (Case 6)
                    PHIJ1=0.0D0
                    PHIMOV=0.0D0
                    HPTOP=HTOP+VTOP*TDIVH
                    IF(HPTOP.GT.1.0D0)THEN
                      HPTOP=1.0D0
                    END IF
                    JPTOP=J
                    PHIUP=PHIIJ*HTOP
                    IF(J.EQ.1)THEN
                      PHIJ=PHIUP/HPTOP
                    END IF
                  END IF
                END IF
              ELSEIF ((J+1).EQ.JBOT)THEN
                IF(VBOT.GT.0.0D0)THEN
C *** Lower boundary moves upwards (Case 7)
                  IF (J.EQ.NH-1)THEN
                    HPBOT=HBOT+VBOT*TDIVH
                    JPBOT=NH
                    IF(HPBOT.GT.1.0D0)THEN
                      HPBOT=1.0D0
                    END IF
                  END IF
                  PHIJ1=PHIUP/(1.0D0-HPBOT)
                  PHIUP=0.0D0
                  IF(J.EQ.1)THEN
                    PHIJ=0.0D0
                  END IF
                  PHIMOV=0.0D0
                ELSE
C *** Lower boundary moves downwards
                  IF((HBOT+VBOT*TDIVH).LE.-0.01D0)THEN
C *** Lower boundary crosses layer interface (Case 8)
                    HPBOT=1.0D0+HBOT+VBOT*TDIVH
                    JPBOT=J
                    PHIMOV=-PHIIJ1*(1.0D0-HPBOT)
                    PHIJ1=PHIUP+PHIMOV
                    PHIUP=-PHIMOV
                    IF(J.EQ.1)THEN
                      PHIJ=PHIUP/(1.0D0-HPBOT)
                    END IF
                  ELSE
C Lower boundary does not cross layer interface (Case 9)
                    HPBOT=HBOT+VBOT*TDIVH
                    IF(HPBOT.LT.0.0D0)THEN
                      HPBOT=0.0D0
                    END IF
                    JPBOT=J+1
                    PHIMOV=0.0D0
                    PHIJ1=PHIUP/(1.0D0-HPBOT)
```

```
                        PHIUP=0.0D0
                        IF(J.EQ.1)THEN
                          PHIJ=0.0D0
                        END IF
                      END IF
                    END IF
                  ELSEIF((J+1).EQ.JTOP)THEN
                    IF(VTOP.GT.0.0D0)THEN
C *** Upper boundary moves upwards (Case 10)
                      IF (J.EQ.NH-1)THEN
                        HPTOP=HTOP+VTOP*TDIVH
                        JPTOP=NH
                        IF(HPTOP.GT.1.0D0)THEN
                          HPTOP=1.0D0
                        END IF
                      END IF
                      IF(MEANV.GT.0.0D0) THEN
                        CREAM=PHIIJ*MEANV*TDIVH
                      ELSE
                        CREAM=PHIIJ1*MEANV*TDIVH
                      END IF
                      DIFFUS=DIFF*(PHIIJ-PHIIJ1)*TDIVH2/
     &                                (0.5D0*(1.0D0+HTOP))
                      PHIMOV=CREAM+DIFFUS
                      PHIJ1=(PHIIJ1*HTOP+PHIMOV)/HPTOP
                      PHIUP=PHIIJ-PHIMOV
                      IF(J.EQ.1)THEN
                        PHIJ=PHIUP
                      END IF
                    ELSE
C *** Upper boundary moves downwards
                      IF((HTOP+VTOP*TDIVH).LE.0.01D0)THEN
C *** Upper boundary crosses layer (Case 11)
                        PHIMOV=-PHIIJ1*HTOP
                        PHIJ1=0.0D0
                        PHIUP=PHIIJ-PHIMOV
                        HPTOP=HTOP+VTOP*TDIVH+1.0D0
                        IF(HPTOP.GT.1.0D0)THEN
                          HPTOP=1.0D0
                        END IF
                        JPTOP=J
                        IF(J.EQ.1)THEN
                          PHIJ=PHIUP/HPTOP
                        END IF
                      ELSE
C *** Upper boundary does not cross layer (Case 12)
                        IF(MEANV.GT.0.0D0) THEN
                          CREAM=PHIIJ*MEANV*TDIVH
                        ELSE
                          CREAM=PHIIJ1*MEANV*TDIVH
                        END IF
                        DIFFUS=DIFF*(PHIIJ-PHIIJ1)*TDIVH2/
     &                                (0.5D0*(1.0D0+HTOP))
                        PHIMOV=CREAM+DIFFUS
                        PHIUP=PHIIJ-PHIMOV
                        HPTOP=HTOP+VTOP*TDIVH
                        JPTOP=J+1
                        PHIJ1=(PHIIJ1*HTOP+PHIMOV)/HPTOP
```

```
                    IF(J.EQ.1)THEN
                      PHIJ=PHIUP
                    END IF
                  END IF
                END IF
              ELSE
C *** Normal flux calculation
                IF(MEANV.GT.0.0D0) THEN
                  CREAM=PHIIJ*MEANV*TDIVH
                ELSE
                  CREAM=PHIIJ1*MEANV*TDIVH
                END IF
                DIFFUS=DIFF*(PHIIJ-PHIIJ1)*TDIVH2
                PHIMOV=CREAM+DIFFUS
                PHIJ1=PHIUP+PHIMOV
                PHIUP=PHIIJ-PHIMOV
                IF(J.EQ.1)THEN
                  PHIJ=PHIUP
                END IF
              END IF
            END IF
            END

C ****************************************************************
            SUBROUTINE FLOCFLOW(J,MEANV,DIFF,FLCIJ,FLCIJ1,FLCJ1,FLCUP,FLCJ,
           &    FLC2IJ,FL2IJ1,FLC2J1,FLC2UP,FLC2J,PHIMOV,PHI2MV,
           &    TDIVH,TDIVH2)
C   ************************************************************
C *** Calculate the amount of oil in flocs which crosses between layers
C *** No upper/lower boundaries for flocs
            INTEGER J
            DOUBLE PRECISION MEANV,DIFF,
           &    FLCIJ,FLCIJ1,FLCJ1,FLCUP,FLCJ,
           &    FLC2IJ,FL2IJ1,FLC2J1,FLC2UP,FLC2J,
           &    PHIMOV,PHI2MV,TDIVH,TDIVH2,CRMFLC,CRMFL2,DIFFLC,DIFFL2

            IF(MEANV.GT.0.0D0) THEN
              CRMFLC=FLCIJ*MEANV*TDIVH
              CRMFL2=FLC2IJ*MEANV*TDIVH
            ELSE
              CRMFLC=FLCIJ1*MEANV*TDIVH
              CRMFL2=FL2IJ1*MEANV*TDIVH
            END IF
            DIFFLC=DIFF*(FLCIJ-FLCIJ1)*TDIVH2
            DIFFL2=DIFF*(FLC2IJ-FL2IJ1)*TDIVH2
            PHIMOV=CRMFLC+DIFFLC
            PHI2MV=CRMFL2+DIFFL2
            FLCJ1=FLCUP+PHIMOV
            FLCUP=FLCIJ-PHIMOV
            FLC2J1=FLC2UP+PHI2MV
            FLC2UP=FLC2IJ-PHI2MV
            IF(J.EQ.1)THEN
              FLCJ=FLCUP
              FLC2J=FLC2UP
            END IF
            END
```

```
C ***********************************************************************
      SUBROUTINE FLOCFLOC(ND,NFL,JJ,DIFFPR,DELVPR,RFLOC3,FLSIZE,
     &    DIFHIN,CRMHIN,FRDIM,RMIN,DELR,FLCPHI,COLEFF,
     &    JTOP,JBOT,VOLP,VOLF,VOLF2,FAC2,
     &    PHIJ2,FLCJ,FLC2J,DELTA2,DELTAF,DELTF2,DELPHI)
C ***********************************************************************
C *** Calculate the flocculation due to binary collisions
      INTEGER I,II,JJ,ND,NFL,JTOP(ND),JBOT(ND),NPAIRS,
     &    MSIZE,FLSIZE(11476)
      DOUBLE PRECISION DIFFPR(11476),DELVPR(11476),
     &    RFLOC3(11476),
     &    DIFHIN,CRMHIN,FRDIM,RMIN,DELR,FLCPHI,COLEFF,
     &    PHIJ2(ND),FLCJ(NFL),FLC2J(NFL),
     &    VOLP(ND),VOLF(NFL),VOLF2(NFL),FAC2(ND),
     &    DELTA2(ND),DELTAF(NFL),DELTF2(NFL),DELPHI,
     &    VOLPI,VOLFI,VLF2I,JTOPI,JBOTI,FAC2I,PHIJI,
     &    VOLPII,VLF2II,VOLFII,PI,PI43,OVRLAP,
     &    DELTAA,DF2I,VOIL,DVOL
      PARAMETER(PI43=4.0D0*3.141592654D0/3.0D0,PI=3.141592654D0)

      DELPHI=0.0D0
      DO 101 I=1,ND
        DELTA2(I)=0.0D0
  101 CONTINUE
      DO 102 I=1,NFL
        DELTAF(I)=0.0D0
        DELTF2(I)=0.0D0
  102 CONTINUE
      NPAIRS=0
      DO 103 I=1,ND
C *** Each size fraction interacts with all others
        VOLPI=VOLP(I)
        JTOPI=JTOP(I)
        JBOTI=JBOT(I)
        FAC2I=FAC2(I)
        PHIJI=PHIJ2(I)
        DELTAA=0.0D0
        DO 104 II=1,ND
C *** Particle-particle flocculation
          NPAIRS=NPAIRS+1
          MSIZE=FLSIZE(NPAIRS)
          IF(MSIZE.GT.NFL)THEN
            GOTO 104
          ENDIF
          VOLPII=VOLP(II)
          VOIL=VOLPI+VOLPII
C *** Shared layer volume between the two species
          IF(((JJ.EQ.JTOPI).AND.(JJ.EQ.JBOT(II))).OR.
     &          ((JJ.EQ.JBOTI).AND.(JJ.EQ.JTOP(II))))THEN
            OVRLAP=DDIM(FAC2I+FAC2(II),1.0D0)
          ELSE
            OVRLAP=DMIN1(FAC2I,FAC2(II))
          ENDIF
C *** Volume changes of two species due to flocculation
          DVOL=(DIFHIN*DIFFPR(NPAIRS)+CRMHIN*DELVPR(NPAIRS))*
     &          OVRLAP*PHIJI*PHIJ2(II)*COLEFF
          DELTAA=DELTAA-DVOL*VOLPI
          DELTA2(II)=DELTA2(II)-DVOL*VOLPII/FAC2(II)
          DELTAF(MSIZE)=DELTAF(MSIZE)+DVOL*PI43*RFLOC3(NPAIRS)
```

```
                DELTF2(MSIZE)=DELTF2(MSIZE)+DVOL*VOIL
                DELPHI=DELPHI+DVOL*(PI43*RFLOC3(NPAIRS)-VOIL)
  104         CONTINUE
              OVRLAP=FAC2I
              DO 105 II=1,NFL
C *** Particle-floc flocculation
                NPAIRS=NPAIRS+1
                MSIZE=FLSIZE(NPAIRS)
                IF(MSIZE.GT.NFL)THEN
                  GOTO 105
                ENDIF
                VOLFII=VOLF(II)
                VLF2II=VOLF2(II)
                VOIL=VOLPI+VLF2II
C *** Volume changes of two species due to flocculation
                DVOL=(DIFHIN*DIFFPR(NPAIRS)+CRMHIN*DELVPR(NPAIRS))*
     &                    OVRLAP*PHIJI*FLCJ(II)*COLEFF
                DELTAA=DELTAA-DVOL*VOLPI
                DELTAF(II)=DELTAF(II)-DVOL*VOLFII
                DELTF2(II)=DELTF2(II)-DVOL*VLF2II
                DELTAF(MSIZE)=DELTAF(MSIZE)+DVOL*PI43*RFLOC3(NPAIRS)
                DELTF2(MSIZE)=DELTF2(MSIZE)+DVOL*VOIL
                DELPHI=DELPHI+DVOL*(PI43*RFLOC3(NPAIRS)-VOLPI-VOLFII)
  105         CONTINUE
              DELTA2(I)=DELTA2(I)+DELTAA/FAC2I
  103       CONTINUE
            OVRLAP=1.0D0
            DO 106 I=1,NFL
C *** Each size of floc interacts with all other species
              VOLFI=VOLF(I)
              VLF2I=VOLF2(I)
              PHIJI=FLCJ(I)
              DELTAA=0.0D0
              DF2I=0.0D0
              DO 107 II=I,NFL
C *** Floc-floc flocculation
                NPAIRS=NPAIRS+1
                MSIZE=FLSIZE(NPAIRS)
                IF(MSIZE.GT.NFL)THEN
                  GOTO 107
                ENDIF
                VOLFII=VOLF(II)
                VLF2II=VOLF2(II)
                VOIL=VLF2I+VLF2II
C *** Volume changes of two species
                DVOL=(DIFHIN*DIFFPR(NPAIRS)+CRMHIN*DELVPR(NPAIRS))*
     &                    OVRLAP*PHIJI*FLCJ(II)*COLEFF
                DELTAA=DELTAA-DVOL*VOLFI
                DF2I=DF2I-DVOL*VLF2I
                DELTAF(II)=DELTAF(II)-DVOL*VOLFII
                DELTF2(II)=DELTF2(II)-DVOL*VLF2II
                DELTAF(MSIZE)=DELTAF(MSIZE)+DVOL*PI43*RFLOC3(NPAIRS)
                DELTF2(MSIZE)=DELTF2(MSIZE)+DVOL*VOIL
                DELPHI=DELPHI+DVOL*(PI43*RFLOC3(NPAIRS)-VOLFI-VOLFII)
  107         CONTINUE
              DELTAF(I)=DELTAF(I)+DELTAA
              DELTF2(I)=DELTF2(I)+DF2I
  106       CONTINUE
            END
```

```
C ***********************************************************************
      DOUBLE PRECISION FUNCTION BARNEA(PHI)
C ***********************************************************************
C  Barnea and Mizrahi function for the relative velocity (hydrodyn)
      DOUBLE PRECISION PHI,FAC,CONTFR
      CONTFR=(1.0D0-PHI)
      FAC=CONTFR/(1.0D0+PHI**0.3333333333D0)
      IF(PHI.GE.0.999D0)THEN
        BARNEA=0.0D0
      ELSE
        BARNEA=FAC*DEXP(-1.666666667D0*PHI/CONTFR)
      ENDIF
      RETURN
      END

C ***********************************************************************
      SUBROUTINE BDRYVEL(ND,NFL,NH,STOKV2,STOKFL,VTOP2,VBOT2,
     &    DIFF2,DIFFLC,PHILIM,FLCPHI,PHI2,TOTPHI,FLC,
     &    JTOP2,JBOT2,HTOP2,HBOT2,TIME,DELT)
C ***********************************************************************
C *** Calculate velocities of upper and lower boundaries of each size
      INTEGER ND,NFL,NH,I,JTOP2(ND),JBOT2(ND)
      DOUBLE PRECISION STOKV2(ND),VTOP2(ND),VBOT2(ND),STOKFL(NFL),
     &    DIFF2(ND),DIFFLC(NFL),
     &    PHILIM,FLCPHI,PHI2(ND,NH),TOTPHI(NH),FLC(NFL,NH),
     &    TIME,DELT,HTOP2(ND),HBOT2(ND)

      DO 101 I=1,ND
        CALL TOPVEL(ND,NFL,NH,JTOP2(I)-1,STOKV2(I),DIFF2(I),
     &          VTOP2(I),STOKV2,STOKFL,
     &          PHILIM,FLCPHI,TOTPHI(JTOP2(I)),PHI2,FLC,
     &          JTOP2,JBOT2,HTOP2,HBOT2,TIME,DELT)
        CALL BOTVEL(ND,NFL,NH,JBOT2(I),STOKV2(I),DIFF2(I),
     &          VBOT2(I),STOKV2,STOKFL,
     &          PHILIM,FLCPHI,TOTPHI(JBOT2(I)+1),PHI2,FLC,
     &          JTOP2,JBOT2,HTOP2,HBOT2,TIME,DELT)
 101  CONTINUE
      END

C ***********************************************************************
      SUBROUTINE BOTVEL(ND,NFL,NH,J,STOKV,DIFF,VBDRY,STOKV2,STOKFL,
     &    PHILIM,FLCPHI,TOTPHI,PHI2,FLC,
     &    JTOP2,JBOT2,HTOP2,HBOT2,TIME,DELT)
C ***********************************************************************
C *** Calculate the velocity of the lower boundary
      EXTERNAL BARNEA
      INTEGER ND,NFL,NH,I,J,JTOP2(ND),JBOT2(ND)
      DOUBLE PRECISION STOKV2(ND),STOKFL(NFL),STOKV,VBDRY,DIFF,
     &    PHILIM,TOTPHI,FLCPHI,PHI2(ND,NH),FLC(NFL,NH),
     &    HTOP2(ND),HBOT2(ND),PHIABV,PHIBEL,SUMABV,SUMBEL,
     &    PHI,SUM,FAC,HIN,DIFFH,MEANV,TIME,DELT
      DOUBLE PRECISION BARNEA

C *** Calculate concn at nearest layer interface
      PHIABV=0.0D0
      PHIBEL=0.0D0
      SUMABV=0.0D0
      SUMBEL=0.0D0
```

```
      DO 101 I=1,ND
        IF ((J.NE.JTOP2(I)).OR.((1.0D0-HTOP2(I)).LE.0.01D0)) THEN
          PHIBEL=PHIBEL+PHI2(I,J)
          SUMBEL=SUMBEL+PHI2(I,J)*STOKV2(I)
        END IF
        IF (((J+1).NE.JBOT2(I)).OR. (HBOT2(I).LE.0.01D0)) THEN
          PHIABV=PHIABV+PHI2(I,J+1)
          SUMABV=SUMABV+PHI2(I,J+1)*STOKV2(I)
        END IF
101   CONTINUE
      DO 102 I=1,NFL
        PHIBEL=PHIBEL+FLC(I,J)
        SUMBEL=SUMBEL+FLC(I,J)*STOKFL(I)
        PHIABV=PHIABV+FLC(I,J+1)
        SUMABV=SUMABV+FLC(I,J+1)*STOKFL(I)
102   CONTINUE

C *** Use average concentraion in velocity and diffusion
      PHI=0.5D0*(PHIABV+PHIBEL)
      FAC=BARNEA(PHI)
      SUM=0.5D0*(SUMABV+SUMBEL)
      HIN=FAC*((1.0D0+2.0D0*PHI)*(1.0D0+2.0D0*PHI)+((PHI**3)*
     &    (PHI-4.0D0)))/((1.0D0-PHI)**3)
      DIFFH=DIFF*HIN
      MEANV=FAC*(STOKV-SUM)
C *** Velocity of boundary including creaming and diffusion
      VBDRY=MEANV-0.95D0*DSQRT(DIFFH)*(DSQRT(TIME)-DSQRT(TIME-DELT))
     &    /DELT

      IF((VBDRY.GT.0.0D0).AND.(TOTPHI.GT.PHILIM))THEN
        VBDRY=0.0D0
      END IF
      END

C *********************************************************************
      SUBROUTINE TOPVEL(ND,NFL,NH,J,STOKV,DIFF,VBDRY,STOKV2,STOKFL,
     &    PHILIM,FLCPHI,TOTPHI,PHI2,FLC,
     &    JTOP2,JBOT2,HTOP2,HBOT2,TIME,DELT)
C *********************************************************************
C *** Calculate velocity of upper boundary
      EXTERNAL BARNEA
      INTEGER ND,NFL,NH,I,J,JTOP2(ND),JBOT2(ND)
      DOUBLE PRECISION STOKV2(ND),STOKFL(NFL),STOKV,VBDRY,DIFF,
     &    PHILIM,TOTPHI,FLCPHI,PHI2(ND,NH),FLC(NFL,NH),
     &    HTOP2(ND),HBOT2(ND),PHIABV,PHIBEL,SUMABV,SUMBEL,
     &    PHI,SUM,FAC,HIN,DIFFH,MEANV,TIME,DELT
      DOUBLE PRECISION BARNEA

C *** Calculate concn at nearest layer interface
      PHIABV=0.0D0
      PHIBEL=0.0D0
      SUMABV=0.0D0
      SUMBEL=0.0D0
      DO 101 I=1,ND
        IF ((J.NE.JTOP2(I)).OR.((1.0D0-HTOP2(I)).LE.0.01D0)) THEN
          PHIBEL=PHIBEL+PHI2(I,J)
          SUMBEL=SUMBEL+PHI2(I,J)*STOKV2(I)
        END IF
```

```
            IF (((J+1).NE.JBOT2(I)).OR. (HBOT2(I).LE.0.01D0)) THEN
               PHIABV=PHIABV+PHI2(I,J+1)
               SUMABV=SUMABV+PHI2(I,J+1)*STOKV2(I)
            END IF
  101       CONTINUE

            DO 102 I=1,NFL
               PHIBEL=PHIBEL+FLC(I,J)
               SUMBEL=SUMBEL+FLC(I,J)*STOKFL(I)
               PHIABV=PHIABV+FLC(I,J+1)
               SUMABV=SUMABV+FLC(I,J+1)*STOKFL(I)
  102       CONTINUE

C *** Use average concentraion in velocity and diffusion
            PHI=0.5D0*(PHIABV+PHIBEL)
            FAC=BARNEA(PHI)
            SUM=0.5D0*(SUMABV+SUMBEL)
            HIN=FAC*((1.0D0+2.0D0*PHI)*(1.0D0+2.0D0*PHI)+((PHI**3)*
           &     (PHI-4.0D0)))/((1.0D0-PHI)**3)
            DIFFH=DIFF*HIN
            MEANV=FAC*(STOKV-SUM)
C *** Velocity of boundary including creaming and diffusion
            VBDRY=MEANV+0.95D0*DSQRT(DIFFH)*(DSQRT(TIME)-DSQRT(TIME-DELT))
           &     /DELT

            IF((VBDRY.LT.0.0D0).AND. (TOTPHI.GT.PHILIM))THEN
               VBDRY=0.0D0
            END IF
            END
```

Appendix A3 : Computer Program for Lattice Model of Creaming and Flocculation

```
C   Lattice model of creaming and flocculation of emulsions
C   by Valerie Pinfield.   1993-1995
C ***********************************************************************
      PROGRAM LATTICE
      INTEGER NX,NY,NZ,NYZ,NXYZ,MAXPTS,MAXCL,MAXORD,CLPTS,
     &    NPARTS,NLOST,NSTEPS,NZ2,NLAYS,INSTEP,RECSTP,WR3D
      CHARACTER*50 FILGEN,FILPHI,FILEGR,FILE2D,FILE3D
      DOUBLE PRECISION PHI,RSTEP,BONDPR,BREAK,DELT
      LOGICAL TOPCRM
C *** X,Y,Z dimensions, bonding and breaking probabilities
      PARAMETER ( NX=70,NY=70,NZ=200,NXYZ=980000,
     &    MAXPTS=99000,MAXCL=28000,PHI=0.1D0,
     &    RSTEP=0.1D0, NSTEPS=11,NZ2=121,NLAYS=0,
     &    INSTEP=2400,RECSTP=480,DELT=0.25D0,WR3D=0,
     &    BONDPR=0.005D0,BREAK=0.002D0,
     &    TOPCRM=.TRUE.)
      INTEGER XCOORD(NXYZ),YCOORD(NXYZ),ZCOORD(NXYZ),
     &        OCCUPY(NXYZ),LOCATE(MAXPTS),CPARTS(MAXPTS),CLUSTR(MAXPTS),
     &        SIZE(MAXCL),POINTR(MAXCL),CORDER(MAXCL),CNUM(MAXCL),
     &        DFSTEP(MAXPTS),CRSTEP(MAXPTS),MMIN(NZ2),MMAX(NZ2),
     &        VOL(NZ),INVPOS(6)
      LOGICAL BONDED(MAXPTS,6),INIT
      DOUBLE PRECISION DIFFCL(MAXPTS),CRMCL(MAXPTS),GG(NZ2,NSTEPS)

      FILGEN="/home/cif1_a/prc6vp/lattice/results/rl111c.gen"
      FILPHI="/home/cif1_a/prc6vp/lattice/results/rl111c.phi"
      FILEGR="/home/cif1_a/prc6vp/lattice/results/rl111c.gR"
      FILE2D="/home/cif1_a/prc6vp/lattice/results/rl111c.2D"
      OPEN(UNIT=20,ACCESS="SEQUENTIAL",FILE=FILGEN)
      OPEN(UNIT=30,ACCESS="SEQUENTIAL",FILE=FILPHI)
      OPEN(UNIT=40,ACCESS="SEQUENTIAL",FILE=FILEGR)
      OPEN(UNIT=50,ACCESS="SEQUENTIAL",FILE=FILE2D)
      IF(WR3D.EQ.1)THEN
        FILE3D="/home/cif1_a/prc6vp/lattice/results/rl111c.3D"
        OPEN(UNIT=60,ACCESS="SEQUENTIAL",FILE=FILE3D)
      ENDIF
C *** Recorded run parameters in output files
      INIT=.TRUE.
      NPARTS=NINT(DINT(PHI*DBLE(NXYZ)))
      WRITE(20,301)NPARTS,PHI
      WRITE(30,301)NPARTS,PHI
      WRITE(40,301)NPARTS,PHI
      WRITE(50,301)NPARTS,PHI
301   FORMAT("No parts ",I10," phi          ",F15.4)
      WRITE(20,302)BONDPR,BREAK
      WRITE(30,302)BONDPR,BREAK
      WRITE(40,302)BONDPR,BREAK
      WRITE(50,302)BONDPR,BREAK
302   FORMAT("Bond prob ",F10.4," Break prb",F15.4)
      WRITE(20,303)2*NLAYS+1,INSTEP
      WRITE(30,303)2*NLAYS+1,INSTEP
```

```
      WRITE(40,303)2*NLAYS+1,INSTEP
      WRITE(50,303)2*NLAYS+1,INSTEP
303   FORMAT("NLayers av",I10," NSteps  ",I15)
      IF(WR3D.EQ.1)THEN
        WRITE(60,301)NPARTS,PHI
        WRITE(60,302)BONDPR,BREAK
        WRITE(60,303)2*NLAYS+1,INSTEP
      ENDIF
C *** Initialise random number generator. NAG library, Mark 15
      CALL G05CCF
C *** Initialise variables
      CALL INITARRAYS(NY,NZ,NYZ,NXYZ,MAXPTS,MAXCL,
     &   MAXORD,NLOST,CLPTS,
     &   OCCUPY,CLUSTR,SIZE,POINTR,CORDER,CNUM,
     &   VOL,BONDED,INVPOS)
C *** Set up lattice and assign particles at random
      CALL LATCOORDS(NX,NY,NZ,NXYZ,XCOORD,YCOORD,ZCOORD)
      CALL INITPARTICLES(NXYZ,MAXPTS,NPARTS,OCCUPY,LOCATE)
C *** Flocculate initial neighbouring particles
      CALL INITCLUSTERS(NX,NY,NZ,NYZ,NXYZ,MAXPTS,MAXCL,
     &   NPARTS,XCOORD,YCOORD,ZCOORD,LOCATE,OCCUPY,
     &   MAXORD,CLPTS,CLUSTR,CPARTS,SIZE,POINTR,CORDER,CNUM,
     &   BONDPR,BONDED,INVPOS)
C *** Calculate creaming and diffusion rates of all floc sizes
      CALL INITRATES(MAXPTS,DIFFCL,DFSTEP,CRMCL,CRSTEP,DELT)
C *** Execute creaming and flocculation sequence
      CALL STEPS(NX,NY,NZ,NYZ,NXYZ,NZ2,NSTEPS,MAXPTS,NPARTS,OCCUPY,
     &   LOCATE,XCOORD,YCOORD,ZCOORD,MAXORD,MAXCL,CPARTS,CLUSTR,
     &   SIZE,CLPTS,POINTR,CORDER,CNUM,NLOST,
     &   DIFFCL,DFSTEP,CRMCL,CRSTEP,PHI,BONDPR,BREAK,VOL,RSTEP,
     &   MMIN,MMAX,GG,NLAYS,INSTEP,RECSTP,WR3D,BONDED,INVPOS,TOPCRM)
      END

C ********************************************************************
      SUBROUTINE STEPS(NX,NY,NZ,NYZ,NXYZ,NZ2,NSTEPS,MAXPTS,NPARTS,
     &   OCCUPY,LOCATE,XCOORD,YCOORD,ZCOORD,MAXORD,MAXCL,CPARTS,
     &   CLUSTR,SIZE,CLPTS,POINTR,CORDER,CNUM,NLOST,DIFFCL,
     &   DFSTEP,CRMCL,CRSTEP,PHI,BONDPR,BREAK,VOL,RSTEP,
     &   MMIN,MMAX,GG,NLAYS,INSTEP,RECSTP,WR3D,BONDED,INVPOS,TOPCRM)
C ********************************************************************
C *** Execute creaming and flocculation sequence
      INTEGER NX,NY,NZ,NXY,NYZ,NXYZ,MAXPTS,NPARTS,
     &   MAXORD,MAXCL,CLPTS,OCCUPY(NXYZ),LOCATE(MAXPTS),
     &   XCOORD(NXYZ),YCOORD(NXYZ),ZCOORD(NXYZ),
     &   CPARTS(MAXPTS),CLUSTR(MAXPTS),SIZE(MAXCL),
     &   POINTR(MAXCL),CORDER(MAXCL),CNUM(MAXCL),
     &   DFSTEP(MAXPTS),CRSTEP(MAXPTS),VOL(NZ),
     &   ZINT,NZ2,NSTEPS,MMIN(NZ2),MMAX(NZ2),NLAYS,INVPOS(6),
     &   I,II,III,IV,IX,TLOST,TSINGL,TOTCL,NN,NLOST,CLLOST,
     &   WR3D,INSTEP,RECSTP,NSINGL,NCLUST,CL(2000),
     &   IIX,IIY,IIZ,POS,IP,J,JJ,JJJ,X(100),POINT,
     &   X01,X10,SIZEX,Y01,Y10,SIZEY,Z01,Z10,SIZEZ,Y(100),Z(200),
     &   AVEX,AVEY,AVEZ,MAXXY,NUMC,NUMR(20),SIZER
      LOGICAL BONDED(MAXPTS,6),TOPCRM,ONES
      REAL AVEN(200)
      DOUBLE PRECISION DIFFCL(MAXPTS),CRMCL(MAXPTS),PHI,BONDPR,
     &   BREAK,RSTEP,GG(NZ2,NSTEPS)
      DOUBLE PRECISION G05CAF
      EXTERNAL G05CAF
```

```
      DO 101 III=1,NZ
         VOL(III)=0
101   CONTINUE
      NXY=NX*NY
C *** Set up the parameters to calculate particle distrib function
      CALL INITDENSDISTRIB(NZ2,NSTEPS,RSTEP,MMIN,MMAX,GG)
      DO 102 IX=1,1
         DO 103 IV=1,INSTEP
C *** Increment time
            I=(IX-1)*INSTEP+IV
            CALL MOVES(NX,NY,NZ,NYZ,NXYZ,MAXPTS,NPARTS,OCCUPY,LOCATE,
     &           XCOORD,YCOORD,ZCOORD,MAXORD,MAXCL,CPARTS,CLUSTR,SIZE,
     &           CLPTS,POINTR,CORDER,CNUM,NLOST,DIFFCL,DFSTEP,CRMCL,
     &           CRSTEP,PHI,BONDPR,BREAK,BONDED,INVPOS,TOPCRM)
            DO 104 II=1,MAXORD
               IF(CRMCL(SIZE(CNUM(II))).GE.1.0D0)THEN
                  WRITE(20,301)II,CNUM(II),SIZE(CNUM(II)),
     &                 CRMCL(SIZE(CNUM(II)))
301               FORMAT("Abort, cluster too large ",3I8,E12.3E3)
                  GOTO 202
               ENDIF
104         CONTINUE
C *** Section for aggregation - run until all particles in one cluster
C     TSINGL=0
C     TOTCL=0
C     DO 105 III=1,NPARTS
C     IF(CLUSTR(III).EQ.0)THEN
C     TSINGL=TSINGL+1
C     ELSE
C     TOTCL=TOTCL+1
C     ENDIF
C     105          CONTINUE
C     IF(TSINGL.EQ.0.AND.MAXORD.EQ.1)THEN
            IF((MOD(I,RECSTP).EQ.0).OR.((I.LT.NINT(REAL(INSTEP)/3.0))
     &           .AND.(MOD(I,NINT(REAL(RECSTP)/2.0)).EQ.0)))THEN
C *** Record results every RECSTP number of steps
               WRITE(20,302)I
               WRITE(30,302)I
               WRITE(40,302)I
               WRITE(50,302)I
302            FORMAT("Step ",I15)
               NN=0
               DO 106 II=1,NXYZ
                  IF(OCCUPY(II).NE.0)THEN
                     NN=NN+1
                  ENDIF
106            CONTINUE
C *** Calculate numbers of particles lost, single or in clusters
               TLOST=0
               TSINGL=0
               TOTCL=0
               DO 107 III=1,NPARTS
                  IF(LOCATE(III).EQ.0)THEN
                     TLOST=TLOST+1
                  ELSEIF(CLUSTR(III).EQ.0)THEN
                     TSINGL=TSINGL+1
                  ELSE
                     TOTCL=TOTCL+1
                  ENDIF
```

```
 107              CONTINUE
C *** Particles in clusters which are lost
                  CLLOST=0
                  DO 108 III=1,CLPTS
                     IF(LOCATE(CPARTS(III),EQ.0)THEN
                        CLLOST=CLLOST+1
                     ENDIF
 108              CONTINUE
                  WRITE(30,303)NN
                  WRITE(20,303)NN
 303              FORMAT("Parts left",I10)
                  WRITE(30,304)NLOST,TLOST
                  WRITE(20,304)NLOST,TLOST
 304              FORMAT("Parts lost",2I10)
                  WRITE(30,305)MAXORD
                  WRITE(20,305)MAXORD
 305              FORMAT("NClusters ",I10)
                  WRITE(30,306)TSINGL
                  WRITE(20,306)TSINGL
 306              FORMAT("Sings left",I10)
                  WRITE(30,307)TOTCL
                  WRITE(20,307)TOTCL
 307              FORMAT("clpts left",I10)
                  WRITE(30,308)CLPTS
                  WRITE(20,308)CLPTS
 308              FORMAT("Clpts     ",I10)
                  WRITE(30,309)CLLOST
                  WRITE(20,309)CLLOST
 309              FORMAT("Clpts lost",I10)
C *** Calculate an average cluster size at each height
                  DO 109 IIZ=1,NZ
                     NSINGL=0
                     NCLUST=0
                     DO 110 IIY=1,NY
                        DO 111 IIX=1,NX
                           POS=IIZ+(IIY-1)*NZ+NZ*NY*(IIX-1)
                           IF(OCCUPY(POS).NE.0)THEN
                              VOL(IIZ)=VOL(IIZ)+1
                              IF(CLUSTR(OCCUPY(POS)).EQ.0)THEN
                                 NSINGL=NSINGL+1
                              ELSE
                                 DO 112 IP=1,NCLUST
                                    IF(CL(IP).EQ.CLUSTR(OCCUPY(POS)))THEN
                                       GOTO 201
                                    ENDIF
 112                             CONTINUE
                                 NCLUST=NCLUST+1
                                 CL(NCLUST)=CLUSTR(OCCUPY(POS))
 201                             CONTINUE
                              ENDIF
                           ENDIF
 111                    CONTINUE
 110                 CONTINUE
                     AVEN(IIZ)=REAL(VOL(IIZ))/REAL(NSINGL+NCLUST)
 109              CONTINUE
C *** Calculate the position of the defined serum interface
                  CALL CALCINTERFACE(NXY,NZ,VOL,PHI,ZINT)
                  WRITE(40,310)ZINT
 310              FORMAT("The          interface is at",I20)
```

```
C *** Calculate the density distribution function G(R), for fractalD
                CALL DENSITYDISTRIB(NX,NY,NZ,NYZ,NXYZ,NZ2,MAXPTS,NPARTS
     &               ,NSTEPS,OCCUPY,LOCATE,XCOORD,YCOORD,ZCOORD,
     &               CLUSTR,ZINT,GG,RSTEP,PHI,MMIN,MMAX,NLAYS)
C *** Output the concentration and cluster size as function of height
                DO 113 III=1,NZ
                  WRITE(30,311)III,DBLE(VOL(III))/DBLE(NX*NY),
     &                 AVEN(III)
                  VOL(III)=0
 113            CONTINUE
 311            FORMAT(I10,F10.5,F10.4)
C *** Output a 2D slice, scatter plot of particle position
                DO 114 II=1,NYZ
                  IF(OCCUPY(II).NE.0)THEN
                    IF(CLUSTR(OCCUPY(II)).NE.0)THEN
                      WRITE(50,312)YCOORD(II),ZCOORD(II),
     &                     OCCUPY(II),SIZE(CLUSTR(OCCUPY(II)))
                    ELSE
                      WRITE(50,312)YCOORD(II),ZCOORD(II),
     &                     OCCUPY(II),0
                    ENDIF
 312                FORMAT(3I10,I15)
                  ENDIF
 114            CONTINUE
C **** Find out the spatial extent of each cluster (is it a gel?)
                NUMC=0
                AVEX=0
                AVEY=0
                AVEZ=0
                MAXXY=0
                DO 115 J=1,20
                  NUMR(J)=0
 115            CONTINUE
                DO 116 J=1,MAXORD
                  DO 117 JJ=1,NX
                    X(JJ)=0
 117              CONTINUE
                  DO 118 JJ=1,NY
                    Y(JJ)=0
 118              CONTINUE
                  DO 119 JJ=1,NZ
                    Z(JJ)=0
 119              CONTINUE
                  POINTR=POINTR(J)
                  SIZER=1+INT(3.999999*LOG10(REAL(SIZE(CNUM(J)))))
                  NUMR(SIZER)=NUMR(SIZER)+1
                  DO 120 JJJ=0,SIZE(CNUM(J))-1
                    POS=LOCATE(CPARTS(POINTR+JJJ))
                    X(XCOORD(POS))=1
                    Y(YCOORD(POS))=1
                    Z(ZCOORD(POS))=1
 120              CONTINUE
                  X10=NX+1
                  X01=NX+1
                  Y10=NY+1
                  Y01=NY+1
                  Z10=NZ+1
                  Z01=NZ+1
```

```
      IF(X(1).EQ.1)THEN
        ONES=.TRUE.
      ELSE
        ONES=.FALSE.
      ENDIF
      DO 121 JJ=1,NX
        IF(ONES)THEN
          IF(X(JJ).EQ.0)THEN
            X10=JJ
            ONES=.FALSE.
          ENDIF
        ELSE
          IF(X(JJ).EQ.1)THEN
            X01=JJ
            ONES=.TRUE.
          ENDIF
        ENDIF
121   CONTINUE
      IF(Y(1).EQ.1)THEN
        ONES=.TRUE.
      ELSE
        ONES=.FALSE.
      ENDIF
      DO 122 JJ=1,NY
        IF(ONES)THEN
          IF(Y(JJ).EQ.0)THEN
            Y10=JJ
            ONES=.FALSE.
          ENDIF
        ELSE
          IF(Y(JJ).EQ.1)THEN
            Y01=JJ
            ONES=.TRUE.
          ENDIF
        ENDIF
122   CONTINUE
      IF(Z(1).EQ.1)THEN
        ONES=.TRUE.
      ELSE
        ONES=.FALSE.
      ENDIF
      DO 123 JJ=1,NZ
        IF(ONES)THEN
          IF(Z(JJ).EQ.0)THEN
            Z10=JJ
            ONES=.FALSE.
          ENDIF
        ELSE
          IF(Z(JJ).EQ.1)THEN
            Z01=JJ
            ONES=.TRUE.
          ENDIF
        ENDIF
123   CONTINUE
      IF(X(1).EQ.1)THEN
        SIZEX=NX-(X01-X10)
      ELSE
        SIZEX=X10-X01
      ENDIF
```

```
                    IF(Y(1).EQ.1)THEN
                      SIZEY=NY-(Y01-Y10)
                    ELSE
                      SIZEY=Y10-Y01
                    ENDIF
                    IF(Z(1).EQ.1)THEN
                      SIZEZ=NZ-(Z01-Z10)
                    ELSE
                      SIZEZ=Z10-Z01
                    ENDIF
                    IF(SIZEX.EQ.NX.OR.SIZEY.EQ.NY)THEN
C *** This cluster does span the whole box
                      WRITE(20,313)SIZE(CNUM(J)),SIZEX,SIZEY,SIZEZ
 313                  FORMAT("Cluster spans whole lattice",4I8)
                    ELSE
C *** Take an average cluster size of all others
                      NUMC=NUMC+1
                      AVEX=AVEX+SIZEX
                      AVEY=AVEY+SIZEY
                      AVEZ=AVEZ+SIZEZ
                      IF(SIZEX.GT.MAXXY)THEN
                        MAXXY=SIZEX
                      ELSEIF(SIZEY.GT.MAXXY)THEN
                        MAXXY=SIZEY
                      ENDIF
                    ENDIF
 116              CONTINUE
C *** Output cluster span, and size distribution
                  WRITE(20,314)MAXXY
                  WRITE(20,315)REAL(AVEX)/REAL(NUMC)
                  WRITE(20,316)REAL(AVEY)/REAL(NUMC)
                  WRITE(20,317)REAL(AVEZ)/REAL(NUMC)
 314              FORMAT("Max. x-y size",I7)
 315              FORMAT("ave sizeX",F11.3)
 316              FORMAT("ave sizeY",F11.3)
 317              FORMAT("ave sizeZ",F11.3)
                  NUMR(1)=TSINGL
                  DO 124 J=1,20
                    WRITE(20,318)0.125+(J-1)*0.25,NUMR(J)
 318                FORMAT(F10.3,I8)
 124              CONTINUE
                  IF(NLOST.GT.INT(2.0*REAL(NPARTS)/3.0))THEN
                    GOTO 202
C *** STOP if most particles have been lost
                  ENDIF
                ENDIF
 103          CONTINUE
C *** Initialise the random number generator every INSTEP steps
              CALL G05CCF
 102        CONTINUE
C *** Output a 3D slice of particle positions
 202        IF(WR3D.EQ.1)THEN
              WRITE(60,302)I
              DO 125 II=1,NXYZ
                IF(XCOORD(II).LE.50.AND.YCOORD(II).LE.50)THEN
                  IF(OCCUPY(II).NE.0)THEN
                    IF(CLUSTR(OCCUPY(II)).NE.0)THEN
                      WRITE(60,319)XCOORD(II),YCOORD(II),
     &                     ZCOORD(II),OCCUPY(II),CLUSTR(OCCUPY(II)),
```

```
     &                    SIZE(CLUSTR(OCCUPY(II)))
                        ELSE
                          WRITE(60,319)XCOORD(II),YCOORD(II),
     &                      ZCOORD(II),OCCUPY(II),0,0
                        ENDIF
 319                    FORMAT(6I9)
                      ENDIF
                    ENDIF
 125              CONTINUE
                ENDIF
                END

C ***************************************************************
                SUBROUTINE MOVES(NX,NY,NZ,NYZ,NXYZ,MAXPTS,NPARTS,OCCUPY,LOCATE,
     &            XCOORD,YCOORD,ZCOORD,MAXORD,MAXCL,CPARTS,CLUSTR,
     &            SIZE,CLPTS,POINTR,CORDER,CNUM,NLOST,DIFFCL,DFSTEP,
     &            CRMCL,CRSTEP,PHI,BONDPR,BREAK,BONDED,INVPOS,TOPCRM)
C ***************************************************************
C *** Execute particle movement on the lattice
                INTEGER NX,NY,NZ,NYZ,NXYZ,MAXPTS,NPARTS,MAXORD,MAXCL,CLPTS,
     &            OCCUPY(NXYZ),LOCATE(MAXPTS),
     &            XCOORD(NXYZ),YCOORD(NXYZ),ZCOORD(NXYZ),
     &            CPARTS(MAXPTS),CLUSTR(MAXPTS),SIZE(MAXCL),
     &            POINTR(MAXCL),CORDER(MAXCL),CNUM(MAXCL),
     &            DFSTEP(MAXPTS),CRSTEP(MAXPTS),
     &            PART(110000),LBL(110000),NEWPOS(110000),TEMPCL(110000),
     &            I,ITOP,NLOST,NLEFT,PICKED,LTEMP,IFOCUS,CFOCUS,POS,
     &            SIZECL,IFOC,POINT,PT_1,CORD,INVPOS(6)
                LOGICAL BONDED(MAXPTS,6),MOVE,INIT,TOPCRM
                DOUBLE PRECISION DIFFCL(MAXPTS),CRMCL(MAXPTS),PHI,BONDPR,BREAK
                DOUBLE PRECISION DRANDS,CRANDS,G05CAF,DUMM
                EXTERNAL G05CAF

                INIT=.FALSE.
                ITOP=1
                NLEFT=NPARTS
                DO 101 I=1,NPARTS
C *** Remove from the selection set particles lost over top bdry
                  IF(LOCATE(I).EQ.0)THEN
                    PART(NLEFT)=I
                    LBL(I)=NLEFT
                    NLEFT=NLEFT-1
                  ELSE
                    PART(ITOP)=I
                    LBL(I)=ITOP
                    ITOP=ITOP+1
                  ENDIF
 101              CONTINUE
                ITOP=0
                IF(NLEFT.EQ.0)THEN
                  GOTO 201
                ENDIF
 202              PICKED=1+DINT((NLEFT)*G05CAF(DUMM))
C *** Select which particle to move and random number for move or not
                IFOCUS=PART(PICKED)
                DRANDS=G05CAF(DUMM)
                CRANDS=G05CAF(DUMM)
                IF(CLUSTR(IFOCUS).NE.0)THEN
C *** Particle belongs to a cluster
```

```
            CFOCUS=CLUSTR(IFOCUS)
            CORD=CORDER(CFOCUS)
            POINT=POINTR(CORD)
            PT_1=POINT-1
            SIZECL=SIZE(CFOCUS)
            DO 102 I=1,SIZECL
C *** Remove all particles in this cluster from selection set
              IFOC=CPARTS(PT_1+I)
              TEMPCL(I)=IFOC
              LTEMP=LBL(IFOC)
              IF(LTEMP.LE.NLEFT)THEN
                PART(LTEMP)=PART(NLEFT)
                LBL(PART(LTEMP))=LTEMP
                PART(NLEFT)=IFOC
                LBL(IFOC)=NLEFT
                NLEFT=NLEFT-1
              ENDIF
  102       CONTINUE
C *** Generate the displacement for the cluster
            CALL NEWPOSITION(NX,NY,NZ,NYZ,NXYZ,MAXPTS,NPARTS,MAXORD,
     &        CLPTS,OCCUPY,LOCATE,CLUSTR,XCOORD,YCOORD,ZCOORD,
     &        DFSTEP(SIZECL),CRSTEP(SIZECL),
     &        DIFFCL(SIZECL),CRMCL(SIZECL),
     &        PHI,CFOCUS,SIZECL,TEMPCL,NEWPOS,
     &        DRANDS,CRANDS,MOVE,TOPCRM)
            IF(MOVE)THEN
C *** The cluster as a whole moves to new position.
              CALL MOVECLUSTER(NXYZ,NPARTS,MAXPTS,MAXORD,MAXCL,CLPTS,
     &          NLOST,OCCUPY,LOCATE,CPARTS,CLUSTR,SIZE,POINTR,
     &          CORDER,CNUM,NEWPOS,TEMPCL,
     &          CORD,CFOCUS,POINT,PT_1,SIZECL)
            ENDIF
C *** Bond any neighbours or break any bonds
            CALL BONDS(NX,NY,NZ,NYZ,NXYZ,NPARTS,MAXPTS,MAXORD,MAXCL,
     &        CLPTS,XCOORD,YCOORD,ZCOORD,OCCUPY,LOCATE,
     &        CPARTS,CLUSTR,SIZE,POINTR,CORDER,CNUM,
     &        BONDPR,BREAK,BONDED,INVPOS,
     &        TEMPCL,SIZECL,INIT)
C ***************************************************************
          ELSE
C ***************************************************************
C *** Just a particle. Remove it from selection set
            PART(PICKED)=PART(NLEFT)
            LBL(PART(PICKED))=PICKED
            PART(NLEFT)=IFOCUS
            LBL(IFOCUS)=NLEFT
            NLEFT=NLEFT-1
            TEMPCL(1)=IFOCUS
            POS=LOCATE(IFOCUS)
C *** Generate the displacement for the particle
            CALL NEWPOSITION(NX,NY,NZ,NYZ,NXYZ,MAXPTS,NPARTS,MAXORD,
     &        CLPTS,OCCUPY,LOCATE,CLUSTR,XCOORD,YCOORD,ZCOORD,
     &        DFSTEP(1),CRSTEP(1),DIFFCL(1),CRMCL(1),
     &        PHI,0,1,TEMPCL,NEWPOS,
     &        DRANDS,CRANDS,MOVE,TOPCRM)
            IF(MOVE)THEN
C *** The particle moves to a new position
              IF(NEWPOS(1).EQ.0)THEN
C *** Particle is lost over top boundary
```

```
                    LOCATE(IFOCUS)=0
                    OCCUPY(POS)=0
                    NLOST=NLOST+1
                  ELSE
                    LOCATE(IFOCUS)=NEWPOS(1)
                    OCCUPY(POS)=0
                    OCCUPY(NEWPOS(1))=IFOCUS
C *** Bond any neighbours or break any bonds
                    CALL BONDS(NX,NY,NZ,NYZ,NXYZ,NPARTS,MAXPTS,MAXORD,
     &                 MAXCL,CLPTS,XCOORD,YCOORD,ZCOORD,OCCUPY,LOCATE,
     &                 CPARTS,CLUSTR,SIZE,POINTR,CORDER,CNUM,
     &                 BONDPR,BREAK,BONDED,INVPOS,
     &                 TEMPCL,1,INIT)
                  ENDIF
                ELSE
C *** Bond any neighbours or break any bonds
                  CALL BONDS(NX,NY,NZ,NYZ,NXYZ,NPARTS,MAXPTS,MAXORD,
     &               MAXCL,CLPTS,XCOORD,YCOORD,ZCOORD,OCCUPY,LOCATE,
     &               CPARTS,CLUSTR,SIZE,POINTR,CORDER,CNUM,
     &               BONDPR,BREAK,BONDED,INVPOS,
     &               TEMPCL,1,INIT)
                ENDIF
              ENDIF
C *** Pick the next particle to be moved
  203         IF(NLEFT.GT.0)THEN
                GOTO 202
              ENDIF
  201         END

C ***************************************************************
            SUBROUTINE NEWPOSITION(NX,NY,NZ,NYZ,NXYZ,MAXPTS,NPARTS,
     &      MAXORD,CLPTS,OCCUPY,LOCATE,CLUSTR,XCOORD,YCOORD,ZCOORD,
     &      DFSTEP,CRSTEP,DIFFCL,CRMCL,PHI,
     &      CFOCUS,SIZECL,TEMPCL,NEWPOS,
     &      DRANDS,CRANDS,MOVE,TOPCRM)
C ***************************************************************
C *** Generate particle or cluster displacement, and is it obstructed?
            INTEGER NX,NY,NZ,NYZ,NXYZ,MAXPTS,NPARTS,MAXORD,CLPTS,
     &        OCCUPY(NXYZ),LOCATE(MAXPTS),CLUSTR(MAXPTS),
     &        XCOORD(NXYZ),YCOORD(NXYZ),ZCOORD(NXYZ),
     &        DX,DY,DZ,DDX,DDY,DDZ,DZDIFF,DZCRM,NEWX,NEWY,NEWZ,
     &        DFSTEP,CRSTEP,SIZECL,CFOCUS,
     &        TEMPCL(110000),NEWPOS(110000),
     &        IFOCUS,DNUM,POS,DESTIN,I,NMISS
            DOUBLE PRECISION DIFFCL,CRMCL,PHI,DUMM,HINFAC,PHIEFF,AVEN
            DOUBLE PRECISION G05CAF,DRANDS,CRANDS,DRAND,HINDPR
            EXTERNAL G05CAF
            LOGICAL MOVE,CRFRST,TOPCRM

C *** Hindrance for clusters part-lost over top boundary (topcrm=fal)
            HINFAC=0.55D0+0.45D0/(SIZECL**0.68D0)
            IF(SIZECL.EQ.1)THEN
              HINDPR=PHI
            ELSE
              HINDPR=HINFAC*PHI
            ENDIF
C *** Initialise zero displacement
            DX=0
            DY=0
```

```
            DZ=0
            DZDIFF=0
C *** If diffusion step, can move in any of six directions
            IF(DRANDS.LT.DIFFCL)THEN
               DNUM=1+DINT(6.0D0*DRANDS/DIFFCL)
               IF(DNUM.EQ.1)THEN
                  DX=DFSTEP
               ELSEIF(DNUM.EQ.2)THEN
                  DX=-DFSTEP
               ELSEIF(DNUM.EQ.3)THEN
                  DY=DFSTEP
               ELSEIF(DNUM.EQ.4)THEN
                  DY=-DFSTEP
               ELSEIF(DNUM.EQ.5)THEN
                  DZ=DFSTEP
                  DZDIFF=DFSTEP
               ELSE
                  DZ=-DFSTEP
                  DZDIFF=-DFSTEP
               ENDIF
            ENDIF
            DZCRM=0
C *** Creaming step - always upwards
            IF(CRANDS.LE.CRMCL)THEN
               DZ=DZ+CRSTEP
               DZCRM=CRSTEP
            ENDIF
C *** Special cases of lost over top boundary (topcrm=false)
            IF((IABS(DZDIFF)+DZCRM).GT.0.AND.
           &   G05CAF(DUMM).LE.(DZCRM/(DZCRM+IABS(DZDIFF))))THEN
C *** Cream first, then diffuse
               CRFRST=.TRUE.
            ELSE
               CRFRST=.FALSE.
            ENDIF
C *** End of special case
            MOVE=.TRUE.
            IF((DX.EQ.0).AND.(DY.EQ.0).AND.(DZ.EQ.0)
           &   .AND.(DZDIFF.EQ.0.OR.(.NOT.CRFRST)))THEN
C *** No displacement at all
               MOVE=.FALSE.
               GOTO 202
            ELSE
  201          NMISS=0
               DO 101 I=1,SIZECL
C *** Determine displacement and obstruction for each particle
                  IFOCUS=TEMPCL(I)
                  POS=LOCATE(IFOCUS)
                  IF(POS.EQ.0)THEN
                     NMISS=NMISS+1
                     IF(DZDIFF.LT.0)THEN
C *** Don't allow downwards diffusion if particles are already lost
                        DZ=DZ-DZDIFF
                        DZDIFF=0
                        GOTO 201
                     ENDIF
                     GOTO 101
                  ENDIF
C *** Generate the new position of this particle
```

```
                DDX=DX
                DDY=DY
                DDZ=DZ
                NEWZ=ZCOORD(POS)+DDZ
                IF(NEWZ.GT.NZ)THEN
C ***************************************************************
C *** Particle attempts to cross the top boundary
                  IF(TOPCRM)THEN
C *** Impenetrable top boundary - No particles leave
                    DZ=NZ-ZCOORD(POS)
                    IF(DX.EQ.0.AND.DY.EQ.0.AND.DZ.EQ.0)THEN
                      MOVE=.FALSE.
                      GOTO 202
                    ELSE
                      GOTO 201
                    ENDIF
                  ELSE
C *** Particle lost over top boundary, but with obstruction
                    DRAND=G05CAF(DUMM)
                    IF(CRFRST)THEN
C *** Cream then diffuse
                      IF(NEWZ-DZDIFF.LE.NZ)THEN
                        DZDIFF=DZDIFF+NZ-NEWZ
                        DZ=DZ+NZ-NEWZ
                        GOTO 201
                      ELSEIF(DRAND.GT.HINDPR)THEN
                        NEWPOS(I)=0
                      ELSE
C *** Movement obstructed, but try smaller displacement
                        IF(DZ.GT.1)THEN
                          DZ=DZ-1
                          GOTO 201
                        ELSEIF(DZ.LT.-1)THEN
                          DZ=DZ+1
                          GOTO 201
                        ELSEIF(DX.GT.1)THEN
                          DX=DX-1
                          GOTO 201
                        ELSEIF(DX.LT.-1)THEN
                          DX=DX+1
                          GOTO 201
                        ELSEIF(DY.GT.1)THEN
                          DY=DY-1
                          GOTO 201
                        ELSEIF(DY.LT.-1)THEN
                          DY=DY+1
                          GOTO 201
                        ENDIF
C *** No smaller displacement - cluster or particle can not move
                        MOVE=.FALSE.
                        GOTO 202
                      ENDIF
                    ELSE
C *** Diffuse then cream
                      IF(DZCRM.GT.0)THEN
                        IF(DRAND.GT.HINDPR)THEN
                          NEWPOS(I)=0
                        ELSE
C *** Movement obstructed, but try smaller displacement
```

```
                                IF(DZ.GT.1)THEN
                                   DZ=DZ-1
                                   GOTO 201
                                ELSEIF(DZ.LT.-1)THEN
                                   DZ=DZ+1
                                   GOTO 201
                                ELSEIF(DX.GT.1)THEN
                                   DX=DX-1
                                   GOTO 201
                                ELSEIF(DX.LT.-1)THEN
                                   DX=DX+1
                                   GOTO 201
                                ELSEIF(DY.GT.1)THEN
                                   DY=DY-1
                                   GOTO 201
                                ELSEIF(DY.LT.-1)THEN
                                   DY=DY+1
                                   GOTO 201
                                ENDIF
C *** No smaller displacement - cluster or particle can not move
                                MOVE=.FALSE.
                                GOTO 202
                             ENDIF
                          ELSE
                             MOVE=.FALSE.
                             GOTO 202
                          ENDIF
                       ENDIF
                    ENDIF
                 ELSE
C ***************************************************************
C *** Particle does not cross top boundary
                    IF(CRFRST.AND.(NEWZ-DZDIFF).GT.NZ)THEN
C *** Creaming makes it cross boundary, but ends inside box
                       IF(TOPCRM)THEN
C *** Top bdry - allow diffusion (downwards) only
                          DZ=DZDIFF
                          GOTO 201
                       ELSE
C *** No top bdry - if lost by creaming, can't diffuse back in
                          DZ=DZ-DZDIFF
                          DZDIFF=0
                          GOTO 201
                       ENDIF
                    ENDIF
C *** Particle tries to cross bottom boundary
                    IF(NEWZ.LT.1)THEN
                       DZ=1-ZCOORD(POS)
                       GOTO 201
                    ENDIF
C *** Special case - periodic boundaries top and bottom
C                   IF(NEWZ.LT.1)THEN
C                      DDZ=DDZ+NZ
C                   ELSEIF(NEWZ.GT.NZ)THEN
C                    DDZ=-NZ+DDZ
C                   ENDIF
C *** Apply periodic boundaries to x and y
                    NEWY=YCOORD(POS)+DDY
```

```
                    IF(NEWY.LT.1)THEN
                       DDY=NY+DDY
                    ELSEIF(NEWY.GT.NY)THEN
                       DDY=-NY+DDY
                    ENDIF
                    NEWX=XCOORD(POS)+DDX
                    IF(NEWX.LT.1)THEN
                       DDX=NX+DDX
                    ELSEIF(NEWX.GT.NX)THEN
                       DDX=-NX+DDX
                    ENDIF
                    NEWPOS(I)=POS+DDX*NYZ+DDY*NZ+DDZ
C *** Reject movement if destination site is occupied
                    DESTIN=OCCUPY(NEWPOS(I))
                    IF((DESTIN.NE.0))THEN
                       IF((CFOCUS.NE.0).AND.(CLUSTR(DESTIN).EQ.CFOCUS))THEN
C *** This position has a part from the same cluster-no obstruction
                          ELSE
                             IF(DZ.GT.1)THEN
C *** Movement obstructed, but try smaller displacement
                                DZ=DZ-1
                                GOTO 201
                             ELSEIF(DZ.LT.-1)THEN
                                DZ=DZ+1
                                GOTO 201
                             ELSEIF(DX.GT.1)THEN
                                DX=DX-1
                                GOTO 201
                             ELSEIF(DX.LT.-1)THEN
                                DX=DX+1
                                GOTO 201
                             ELSEIF(DY.GT.1)THEN
                                DY=DY-1
                                GOTO 201
                             ELSEIF(DY.LT.-1)THEN
                                DY=DY+1
                                GOTO 201
                             ENDIF
C *** No smaller displacement - cluster or particle can not move
                             MOVE=.FALSE.
                             GOTO 202
                          ENDIF
                       ENDIF
                    ENDIF
C *** Check the next particle in the cluster
  101               CONTINUE
C *** Obstruction of clusters part-lost over top boundary
                 IF(MOVE.AND.NMISS.GT.0)THEN
                    AVEN=DBLE(NPARTS)/(DBLE(MAXORD+NPARTS-CLPTS))
                    PHIEFF=(0.038D0/(SIZECL**0.92D0))+(0.068/(AVEN**
     &                    (0.65D0-(0.2D0/SIZECL))))
                    IF(G05CAF(DUMM).GT.((1.0D0-PHIEFF*HINFAC)**NMISS))THEN
                       MOVE=.FALSE.
                    ENDIF
                 ENDIF
              ENDIF
  202         END
```

```
C ***********************************************************************
      SUBROUTINE MOVECLUSTER(NXYZ,NPARTS,MAXPTS,MAXORD,MAXCL,CLPTS,
     &    NLOST,OCCUPY,LOCATE,CPARTS,CLUSTR,SIZE,POINTR,
     &    CORDER,CNUM,NEWPOS,TEMPCL,
     &    CORD,CFOCUS,POINT,PT_1,SIZECL)
C ***********************************************************************
C *** Execute displacement of cluster to new position
      INTEGER NXYZ,NPARTS,MAXPTS,MAXORD,MAXCL,CLPTS,NLOST,
     &    OCCUPY(NXYZ),LOCATE(MAXPTS),CPARTS(MAXPTS),CLUSTR(MAXPTS),
     &    SIZE(MAXCL),POINTR(MAXCL),CORDER(MAXCL),CNUM(MAXCL),
     &    NEWPOS(110000),TEMPCL(110000),
     &    I,NBROKE,IFOCUS,POS,CFOCUS,SIZECL,POINT,CORD,PT_1

      NBROKE=0
      DO 101 I=1,SIZECL
        IFOCUS=TEMPCL(I)
        POS=LOCATE(IFOCUS)
        IF(POS.NE.0)THEN
          IF(OCCUPY(POS).EQ.IFOCUS)THEN
            OCCUPY(POS)=0
          ENDIF
          IF(NEWPOS(I).EQ.0)THEN
            LOCATE(IFOCUS)=0
            NLOST=NLOST+1
          ELSE
            LOCATE(IFOCUS)=NEWPOS(I)
            OCCUPY(NEWPOS(I))=IFOCUS
          ENDIF
        ENDIF
 101  CONTINUE
      END

C ***********************************************************************
      SUBROUTINE BONDS(NX,NY,NZ,NYZ,NXYZ,NPARTS,MAXPTS,MAXORD,MAXCL,
     &    CLPTS,XCOORD,YCOORD,ZCOORD,OCCUPY,LOCATE,
     &    CPARTS,CLUSTR,SIZE,POINTR,CORDER,CNUM,
     &    BONDPR,BREAK,BONDED,INVPOS,
     &    TEMPCL,SIZECL,INIT)
C ***********************************************************************
C *** Bond formation and breakage with all neighburs
      INTEGER NX,NY,NZ,NYZ,NXYZ,MAXPTS,NPARTS,MAXORD,MAXCL,CLPTS,
     &    XCOORD(NXYZ),YCOORD(NXYZ),ZCOORD(NXYZ),
     &    OCCUPY(NXYZ),LOCATE(MAXPTS),CPARTS(MAXPTS),CLUSTR(MAXPTS),
     &    SIZE(MAXCL),POINTR(MAXCL),CORDER(MAXCL),CNUM(MAXCL),
     &    TEMPCL(110000),CFOCUS,SIZECL,
     &    I,IPOS,POS,INEIGH,IFOCUS,IMINM,IMINP,DELTA(6),INVPOS(6)
      DOUBLE PRECISION BONDPR,BREAK,G05CAF,DUMM
      LOGICAL BONDED(MAXPTS,6),INIT
      EXTERNAL G05CAF
      IFOCUS=TEMPCL(1)
      CFOCUS=CLUSTR(IFOCUS)
      POS=LOCATE(IFOCUS)
      DO 101 I=1,SIZECL
C *** Find positions of neighbours of each particle in cluster
        IFOCUS=TEMPCL(I)
        POS=LOCATE(IFOCUS)
        IF(POS.NE.0)THEN
          IF(ZCOORD(POS).EQ.NZ)THEN
C *** Miss out +z check
```

```
                  IMINP=3
                  IMINM=2
               ELSEIF(ZCOORD(POS).EQ.1)THEN
                  IMINP=1
                  IMINM=4
C *** Miss out -z check
               ELSE
                  IMINP=1
                  IMINM=2
               ENDIF
               DELTA(1)=1
               DELTA(2)=-1
C *** Periodic z-boundaries
C    IF(ZCOORD(POS).EQ.NZ)THEN
C    DELTA(1)=1-NZ
C    ELSE
C    DELTA(1)=1
C    ENDIF
C    IF(ZCOORD(POS).EQ.1)THEN
C    DELTA(2)=-1+NZ
C    ELSE
C    DELTA(2)=-1
C    ENDIF
C *** Periodic z-boundaries - end
               IF(YCOORD(POS).EQ.NY)THEN
                  DELTA(3)=NZ-NYZ
               ELSE
                  DELTA(3)=NZ
               ENDIF
               IF(YCOORD(POS).EQ.1)THEN
                  DELTA(4)=-NZ+NYZ
               ELSE
                  DELTA(4)=-NZ
               ENDIF
               IF(XCOORD(POS).EQ.NX)THEN
                  DELTA(5)=NYZ-NXYZ
               ELSE
                  DELTA(5)=NYZ
               ENDIF
               IF(XCOORD(POS).EQ.1)THEN
                  DELTA(6)=-NYZ+NXYZ
               ELSE
                  DELTA(6)=-NYZ
               ENDIF
               DO 102 IPOS=IMINP,6,2
C *** Check +z,+y,+x neighbours for form/break bonds
                  CFOCUS=CLUSTR(IFOCUS)
                  INEIGH=OCCUPY(POS+DELTA(IPOS))
                  IF(BONDED(IFOCUS,IPOS))THEN
                     IF(G05CAF(DUMM).LT.BREAK)THEN
C *** If bonded to this neighbour, break bond
                        BONDED(IFOCUS,IPOS)=.FALSE.
                        BONDED(INEIGH,INVPOS(IPOS))=.FALSE.
C *** Split the cluster if this bond held it together
                        CALL SPLITCLUSTER(NX,NY,NZ,NYZ,NXYZ,MAXPTS,
     &                     MAXORD,MAXCL,OCCUPY,LOCATE,XCOORD,YCOORD,
     &                     ZCOORD,CLPTS,CPARTS,CLUSTR,
     &                     SIZE,POINTR,CORDER,CNUM,
     &                     IFOCUS,CFOCUS,INEIGH,BONDED)
```

```
                ENDIF
              ELSE
                IF(INEIGH.NE.0)THEN
                  IF(CLUSTR(IFOCUS).NE.0 .AND.
     &                (CLUSTR(INEIGH).EQ.CLUSTR(IFOCUS)))THEN
                    IF(G05CAF(DUMM).LT.BONDPR)THEN
C *** Form a bond between particles in same cluster
                      BONDED(IFOCUS,IPOS)=.TRUE.
                      BONDED(INEIGH,INVPOS(IPOS))=.TRUE.
                    ENDIF
                  ELSE
                    IF(G05CAF(DUMM).LT.BONDPR)THEN
C *** Form a bond and merge clusters/particles
                      BONDED(IFOCUS,IPOS)=.TRUE.
                      BONDED(INEIGH,INVPOS(IPOS))=.TRUE.
                      CALL BONDNEIGHBOURS(IFOCUS,INEIGH,MAXPTS,
     &                  MAXCL,CLUSTR,CPARTS,SIZE,MAXORD,CLPTS,
     &                  POINTR,CORDER,CNUM)
                    ENDIF
                  ENDIF
                ENDIF
              ENDIF
  102       CONTINUE
            IF(.NOT.INIT)THEN
              DO 103 IPOS=IMINM,6,2
C *** Check -z,-y,-x for new neighbours only.
C *** Don't do this for initialisation - then checking ALL particles
                INEIGH=OCCUPY(POS+DELTA(IPOS))
                IF((INEIGH.NE.0).AND.(CLUSTR(INEIGH).NE.CLUSTR
     &            (IFOCUS)).AND.(G05CAF(DUMM).LT.BONDPR))THEN
C *** Form a bond and merge clusters/particles
                  BONDED(IFOCUS,IPOS)=.TRUE.
                  BONDED(INEIGH,INVPOS(IPOS))=.TRUE.
                  CALL BONDNEIGHBOURS(IFOCUS,INEIGH,MAXPTS,
     &              MAXCL,CLUSTR,CPARTS,SIZE,MAXORD,CLPTS,
     &              POINTR,CORDER,CNUM)
                ENDIF
  103         CONTINUE
              ENDIF
            ENDIF
  101     CONTINUE
          END

C *********************************************************************
          SUBROUTINE BONDNEIGHBOURS(IPART,INEIGH,MAXPTS,MAXCL,CLUSTR,
     &      CPARTS,SIZE,MAXORD,CLPTS,POINTR,CORDER,CNUM)
C *********************************************************************
C *** Make a bond between two particles - in same cluster or different
          INTEGER MAXORD,MAXPTS,MAXCL,CLPTS,
     &      CPARTS(MAXPTS),CLUSTR(MAXPTS),SIZE(MAXCL),
     &      POINTR(MAXCL),CORDER(MAXCL),CNUM(MAXCL),
     &      IPART,INEIGH,CNEIGH,CPART,CLNUM,ORDNXT,ORDNEI,ORDPT,
     &      FIRST,NPART,PPART,PTNXT,NEINXT,PNEIGH,NNEIGH,
     &      I,POINT1,TP,TEMP(0:110000)

          CNEIGH=CLUSTR(INEIGH)
          CPART=CLUSTR(IPART)
          IF(CPART.EQ.0)THEN
C *** The particle is single, not in a cluster
```

```
            IF(CNEIGH.NE.0)THEN
C *** The neighbouring particle belongs to a cluster
                ORDNXT=CORDER(CNEIGH)+1
                POINT1=POINTR(ORDNXT)
                DO 101 I=CLPTS,POINT1,-1
                   CPARTS(I+1)=CPARTS(I)
 101            CONTINUE
                DO 102 I=ORDNXT,MAXORD+1
                   POINTR(I)=POINTR(I)+1
 102            CONTINUE
                CLPTS=CLPTS+1
                CLUSTR(IPART)=CNEIGH
                CPARTS(POINT1)=IPART
                SIZE(CNEIGH)=SIZE(CNEIGH)+1
             ELSE
C *** The neighbour is a single particle
                MAXORD=MAXORD+1
                CLNUM=CNUM(MAXORD)
                SIZE(CLNUM)=2
                CPARTS(CLPTS+1)=IPART
                CPARTS(CLPTS+2)=INEIGH
                CLPTS=CLPTS+2
                POINTR(MAXORD+1)=CLPTS+1
                CLUSTR(IPART)=CLNUM
                CLUSTR(INEIGH)=CLNUM
                CORDER(CLNUM)=MAXORD
             ENDIF
          ELSE
C *** The particle is in a cluster
C *** The neighbouring particle is in a different cluster or single
             ORDPT=CORDER(CPART)
             IF(CNEIGH.NE.0)THEN
C *** The neighbour is in a cluster
                ORDNEI=CORDER(CNEIGH)
                IF(ORDPT.LT.ORDNEI)THEN
C *** The particle's cluster is higher in the array list. Sort arrays
                   PTNXT=ORDPT+1
                   FIRST=POINTR(PTNXT)
                   PNEIGH=POINTR(ORDNEI)
                   NNEIGH=SIZE(CNEIGH)
                   DO 103 I=0,NNEIGH-1
                      TEMP(I)=CPARTS(PNEIGH+I)
 103               CONTINUE
                   DO 104 I=PNEIGH-1,FIRST,-1
                      CPARTS(I+NNEIGH)=CPARTS(I)
 104               CONTINUE
                   DO 105 I=0,NNEIGH-1
                      TP=TEMP(I)
                      CPARTS(FIRST+I)=TP
                      CLUSTR(TP)=CPART
 105               CONTINUE
                   DO 106 I=PTNXT,ORDNEI-1
                      POINTR(I)=POINTR(I)+NNEIGH
 106               CONTINUE
                   MAXORD=MAXORD-1
                   DO 107 I=ORDNEI,MAXORD
                      TP=CNUM(I+1)
                      CNUM(I)=TP
                      CORDER(TP)=I
```

```
                    POINTR(I)=POINTR(I+1)
107               CONTINUE
                  POINTR(MAXORD+1)=CLPTS+1
                  CNUM(MAXORD+1)=CNEIGH
                  SIZE(CNEIGH)=0
                  SIZE(CPART)=SIZE(CPART)+NNEIGH
                ELSE
C *** The neighbours cluster is higher in the array list. Sort arrays
                  PNEIGH=POINTR(ORDNEI)
                  PPART=POINTR(ORDPT)
                  NEINXT=ORDNEI+1
                  NPART=SIZE(CPART)
                  NNEIGH=SIZE(CNEIGH)
C *** Extract the particles in the particle's cluster, then shunt down
                  DO 108 I=0,NNEIGH-1
                    CLUSTR(CPARTS(PNEIGH+I))=CPART
108               CONTINUE
                  DO 109 I=0,NPART-1
                    TEMP(I)=CPARTS(PPART+I)
109               CONTINUE
                  DO 110 I=PPART-1,PNEIGH,-1
                    CPARTS(I+NPART)=CPARTS(I)
110               CONTINUE
                  DO 111 I=0,NPART-1
                    CPARTS(PNEIGH+I)=TEMP(I)
111               CONTINUE
                  CORDER(CPART)=ORDNEI
                  CNUM(ORDNEI)=CPART
                  DO 112 I=NEINXT,ORDPT-1
                    POINTR(I)=POINTR(I)+NPART
112               CONTINUE
                  MAXORD=MAXORD-1
                  DO 113 I=ORDPT,MAXORD
                    TP=CNUM(I+1)
                    CNUM(I)=TP
                    CORDER(TP)=I
                    POINTR(I)=POINTR(I+1)
113               CONTINUE
                  POINTR(MAXORD+1)=CLPTS+1
                  CNUM(MAXORD+1)=CNEIGH
                  SIZE(CNEIGH)=0
                  SIZE(CPART)=NPART+NNEIGH
                ENDIF
              ELSE
C *** The neighbour is a single particle
                FIRST=POINTR(ORDPT+1)
                DO 114 I=CLPTS,FIRST,-1
                  CPARTS(I+1)=CPARTS(I)
114             CONTINUE
                DO 115 I=ORDPT+1,MAXORD+1
                  POINTR(I)=POINTR(I)+1
115             CONTINUE
                CLPTS=CLPTS+1
                CPARTS(FIRST)=INEIGH
                CLUSTR(INEIGH)=CPART
                SIZE(CPART)=SIZE(CPART)+1
              ENDIF
            ENDIF
            END
```

```
C ***************************************************************
      SUBROUTINE SPLITCLUSTER(NX,NY,NZ,NYZ,NXYZ,MAXPTS,MAXORD,MAXCL,
     &    OCCUPY,LOCATE,XCOORD,YCOORD,ZCOORD,CLPTS,CPARTS,CLUSTR,
     &    SIZE,POINTR,CORDER,CNUM,
     &    IFOCUS,CFOCUS,INEIGH,BONDED)
C ***************************************************************
C *** Does the cluster split when a bond has been broken?
      INTEGER NX,NY,NZ,NYZ,NXYZ,MAXORD,MAXPTS,MAXCL,CLPTS,
     &    OCCUPY(NXYZ),LOCATE(MAXPTS),
     &    XCOORD(NXYZ),YCOORD(NXYZ),ZCOORD(NXYZ),
     &    CPARTS(MAXPTS),CLUSTR(MAXPTS),SIZE(MAXCL),
     &    POINTR(MAXCL),CORDER(MAXCL),CNUM(MAXCL),
     &    IFOCUS,INEIGH,NN,NP,P(110000),NCL,PT_1,CFOCUS,
     &    II,III,CLNUM,CORD,POINT,FIRST,PPP,TEMP
      LOGICAL BONDED(MAXPTS,6),DISCON,NOLNKN,NOLNKP

      CORD=CORDER(CFOCUS)
      POINT=POINTR(CORD)
      PT_1=POINT-1
      NCL=POINTR(CORD+1)-POINTR(CORD)
      IF(NCL.EQ.2)THEN
C *** The cluster will split into two single particles
        CLPTS=CLPTS-2
        CLUSTR(CPARTS(POINT))=0
        CLUSTR(CPARTS(POINT+1))=0
        DO 101 II=POINT,CLPTS
          CPARTS(II)=CPARTS(II+2)
  101   CONTINUE
        MAXORD=MAXORD-1
        DO 102 II=CORD,MAXORD
          CNUM(II)=CNUM(II+1)
          CORDER(CNUM(II))=II
          POINTR(II)=POINTR(II+1)-2
  102   CONTINUE
        POINTR(MAXORD+1)=CLPTS+1
        CNUM(MAXORD+1)=CFOCUS
        SIZE(CFOCUS)=0
      ELSE
C *** Find out how many and which particles are connected to INEIGH
        CALL ATTACHEDPARTS(NX,NY,NZ,NYZ,NXYZ,MAXPTS,MAXCL,
     &      OCCUPY,LOCATE,XCOORD,YCOORD,ZCOORD,CLUSTR,BONDED,
     &      INEIGH,IFOCUS,P,NN,0,CFOCUS,MAXCL+1,DISCON,NOLNKN)
        IF(DISCON)THEN
C *** INEIGH is no longer connected to all the particles in cluster
C *** Unless it is by a bridge above the top boundary
          CALL ATTACHEDPARTS(NX,NY,NZ,NYZ,NXYZ,MAXPTS,MAXCL,
     &        OCCUPY,LOCATE,XCOORD,YCOORD,ZCOORD,CLUSTR,BONDED,
     &        IFOCUS,INEIGH,P,NP,NN,CFOCUS,MAXCL+2,DISCON,NOLNKP)
          IF(NOLNKN.OR.NOLNKP)THEN
C *** Exclude breakage if may be linked above top boundary
            IF(NOLNKN.AND.NN.EQ.1)THEN
C *** The single particle INEIGH breaks off
              CLUSTR(INEIGH)=0
              CLPTS=CLPTS-1
              DO 103 II=POINT,POINT+NCL-1
                IF(INEIGH.EQ.CPARTS(II))THEN
                  FIRST=II
                  GOTO 201
                ENDIF
```

```
103                 CONTINUE
201                 DO 104 II=FIRST,CLPTS
                       CPARTS(II)=CPARTS(II+1)
104                 CONTINUE
                    SIZE(CFOCUS)=SIZE(CFOCUS)-1
                    DO 105 II=1,NP
                       CLUSTR(P(NN+II))=CFOCUS
105                 CONTINUE
                    DO 106 II=CORD+1,MAXORD+1
                       POINTR(II)=POINTR(II)-1
106                 CONTINUE
                  ELSEIF(NOLNKP.AND.NP.EQ.1)THEN
C *** The single particle IPART breaks off
                    CLUSTR(IFOCUS)=0
                    CLPTS=CLPTS-1
                    DO 107 II=POINT,POINT+NCL-1
                       IF(IFOCUS.EQ.CPARTS(II))THEN
                          FIRST=II
                          GOTO 202
                       ENDIF
107                 CONTINUE
202                 DO 108 II=FIRST,CLPTS
                       CPARTS(II)=CPARTS(II+1)
108                 CONTINUE
                    SIZE(CFOCUS)=SIZE(CFOCUS)-1
                    DO 109 II=1,NN
                       CLUSTR(P(II))=CFOCUS
109                 CONTINUE
                    DO 110 II=CORD+1,MAXORD+1
                       POINTR(II)=POINTR(II)-1
110                 CONTINUE
                  ELSE
C *** The cluster breaks into two clusters
                    MAXORD=MAXORD+1
                    CLNUM=CNUM(MAXORD)
                    POINTR(MAXORD+1)=CLPTS+1
                    DO 111 II=MAXORD,CORD+2,-1
                       CNUM(II)=CNUM(II-1)
                       POINTR(II)=POINTR(II-1)
                       CORDER(CNUM(II))=II
111                 CONTINUE
                    CNUM(CORD)=CLNUM
                    CNUM(CORD+1)=CFOCUS
                    CORDER(CLNUM)=CORD
                    CORDER(CFOCUS)=CORD+1
                    IF(.NOT.NOLNKP)THEN
C *** Lost particles are attached to IFOCUS
                       FIRST=POINT
                       DO 112 II=1,NN
                          PPP=P(II)
                          CLUSTR(PPP)=CLNUM
                          DO 113 III=POINT,POINT+NCL-1
                             IF(PPP.EQ.CPARTS(III))THEN
                                TEMP=CPARTS(FIRST)
                                CPARTS(FIRST)=PPP
                                CPARTS(III)=TEMP
                                FIRST=FIRST+1
                                GOTO 112
                             ENDIF
```

```
113                     CONTINUE
112                   CONTINUE
                      DO 114 II=1,NP
                        CLUSTR(P(NN+II))=CFOCUS
114                   CONTINUE
                      SIZE(CLNUM)=NN
                      SIZE(CFOCUS)=NCL-NN
                      POINTR(CORD+1)=POINTR(CORD)+NN
                    ELSEIF(.NOT.NOLNKN)THEN
C *** Lost particles belong to INEIGH
                      FIRST=POINT
                      DO 115 II=1,NP
                        PPP=P(NN+II)
                        CLUSTR(PPP)=CLNUM
                        DO 116 III=POINT,POINT+NCL-1
                          IF(PPP.EQ.CPARTS(III))THEN
                            TEMP=CPARTS(FIRST)
                            CPARTS(FIRST)=PPP
                            CPARTS(III)=TEMP
                            FIRST=FIRST+1
                            GOTO 115
                          ENDIF
116                     CONTINUE
115                   CONTINUE
                      DO 117 II=1,NN
                        CLUSTR(P(II))=CFOCUS
117                   CONTINUE
                      SIZE(CLNUM)=NP
                      SIZE(CFOCUS)=NCL-NP
                      POINTR(CORD+1)=POINTR(CORD)+NP
                    ELSE
C *** No particles are lost in this cluster (normal, for topcrm=true)
                      DO 118 II=1,NP
                        CPARTS(PT_1+II)=P(NN+II)
                        CLUSTR(P(NN+II))=CLNUM
118                   CONTINUE
                      SIZE(CLNUM)=NP
                      DO 119 II=1,NN
                        CPARTS(PT_1+II+NP)=P(II)
                        CLUSTR(P(II))=CFOCUS
119                   CONTINUE
                      SIZE(CFOCUS)=NCL-NP
                      POINTR(CORD+1)=POINTR(CORD)+NP
                    ENDIF
                  ENDIF
                ELSE
C *** IFOCUS and INEIGH are connected above top boundary
                  DO 120 II=1,NN
                    CLUSTR(P(II))=CFOCUS
120               CONTINUE
                  DO 121 II=1,NP
                    CLUSTR(P(NN+II))=CFOCUS
121               CONTINUE
                ENDIF
              ELSE
C *** Particle and neighbour are still connected
                DO 122 II=1,NN
                  CLUSTR(P(II))=CFOCUS
122             CONTINUE
```

```
            ENDIF
          ENDIF
          END

C ***************************************************************
          SUBROUTINE ATTACHEDPARTS(NX,NY,NZ,NYZ,NXYZ,MAXPTS,MAXCL,
         &     OCCUPY,LOCATE,XCOORD,YCOORD,ZCOORD,CLUSTR,BONDED,
         &     IFOCUS,IOBJ,P,N,LASTEL,CFOCUS,CLNUM,DISCON,NOLINK)
C ***************************************************************
C *** Find all the particles which are bonded to this particle
C *** to determine whether the cluster splits when bond breaks
          INTEGER NX,NY,NZ,NYZ,NXYZ,MAXPTS,MAXCL,
         &     OCCUPY(NXYZ),LOCATE(MAXPTS),
         &     XCOORD(NXYZ),YCOORD(NXYZ),ZCOORD(NXYZ),CLUSTR(MAXPTS),
         &     IFOCUS,IOBJ,CFOCUS,P(110000),N,CLNUM,
         &     I,II,IPART,IMIN,POS,NOLD,NNEW,DELTA(6),LASTEL
          LOGICAL NEW,BONDED(MAXPTS,6),DISCON,NOLINK

          DISCON=.TRUE.
          NOLINK=.TRUE.
          NOLD=1
          NNEW=1
          P(LASTEL+1)=IFOCUS
          CLUSTR(IFOCUS)=CLNUM
          N=1
  201     NEW=.FALSE.
          DO 101 I=NOLD,NNEW
            IPART=P(LASTEL+I)
            POS=LOCATE(IPART)
C *** Periodic boundaries top and bottom - code removed
C *** Generate relative positions of neighbours
            IF(YCOORD(POS).EQ.NY)THEN
              DELTA(3)=NZ-NYZ
            ELSE
              DELTA(3)=NZ
            ENDIF
            IF(YCOORD(POS).EQ.1)THEN
              DELTA(4)=-NZ+NYZ
            ELSE
              DELTA(4)=-NZ
            ENDIF
            IF(XCOORD(POS).EQ.NX)THEN
              DELTA(5)=NYZ-NXYZ
            ELSE
              DELTA(5)=NYZ
            ENDIF
            IF(XCOORD(POS).EQ.1)THEN
              DELTA(6)=-NYZ+NXYZ
            ELSE
              DELTA(6)=-NYZ
            ENDIF
C *** Check for bonds at z boundaries
            IMIN=1
            DELTA(1)=1
            DELTA(2)=-1
            IF(ZCOORD(POS).EQ.1)THEN
              IF(BONDED(IPART,1).AND.CLUSTR(OCCUPY(POS+DELTA(1)))
         &          .NE.CLNUM)THEN
C *** The particle is bonded and hasn't been counted already
```

```
                    NEW=.TRUE.
                    N=N+1
                    CLUSTR(OCCUPY(POS+DELTA(1)))=CLNUM
                    P(LASTEL+N)=OCCUPY(POS+DELTA(1))
                    IF(P(LASTEL+N).EQ.IOBJ)THEN
C *** It is definitely connected to the other particle
                      DISCON=.FALSE.
                      GOTO 202
                    ENDIF
                  ENDIF
                  IMIN=3
                ELSEIF(ZCOORD(POS).EQ.NZ)THEN
                  IMIN=2
                  IF(BONDED(IPART,1))THEN
C *** A bond crossing the top boundary
                    NOLINK=.FALSE.
                  ENDIF
                ENDIF
                DO 102 II=IMIN,6
C *** Check each neighbour to see if it is attached
                  IF(BONDED(IPART,II).AND.CLUSTR(OCCUPY(POS+DELTA(II)))
     &                .NE.CLNUM)THEN
                    NEW=.TRUE.
                    N=N+1
                    CLUSTR(OCCUPY(POS+DELTA(II)))=CLNUM
                    P(LASTEL+N)=OCCUPY(POS+DELTA(II))
                    IF(P(LASTEL+N).EQ.IOBJ)THEN
C *** It is definitely connected to the other particle
                      DISCON=.FALSE.
                      GOTO 202
                    ENDIF
                  ENDIF
 102            CONTINUE
 101          CONTINUE
              IF(NEW)THEN
C *** The last set found new particles which are attached.
C *** Repeat to check their neighbours
                NOLD=NNEW+1
                NNEW=N
                GOTO 201
              ENDIF
 202          END

C ***************************************************************
              SUBROUTINE CALCINTERFACE(NXY,NZ,VOL,PHI,ZINT)
C ***************************************************************
C *** Calculate the serum layer interface position
C *** Based on definition of a "uniform" region of const vol fract
              INTEGER NZ,ZINT,VOL(NZ),ZZ,NXY
              DOUBLE PRECISION PHI,VV
              DO 101 ZZ=2,NZ-1
                VV=DBLE(VOL(ZZ)+VOL(ZZ-1)+VOL(ZZ+1))/(3.0D0*NXY)
                IF(VV.GT.0.9D0*PHI)THEN
                  ZINT=ZZ
                  GOTO 201
                ENDIF
 101          CONTINUE
 201          END
```

```
C ****************************************************************
      SUBROUTINE DENSITYDISTRIB(NX,NY,NZ,NYZ,NXYZ,NZ2,MAXPTS,NPARTS,
     &    NSTEPS,OCCUPY,LOCATE,XCOORD,YCOORD,ZCOORD,CLUSTR,
     &    ZINT,GG,RSTEP,PHI,MMIN,MMAX,NLAYS)
C ****************************************************************
C *** Calculate density distribution G(R) of particles in spherical
C *** shells (R)-(R+dR)
      INTEGER NX,NY,NZ,NYZ,NXYZ,MAXPTS,NPARTS,
     &    XCOORD(NXYZ),YCOORD(NXYZ),ZCOORD(NXYZ),
     &    OCCUPY(NXYZ),LOCATE(MAXPTS),CLUSTR(MAXPTS),
     &    ZINT,NZ2,NSTEPS,NLAYS,N(2500),MMIN(NZ2),MMAX(NZ2),
     &    XC,YC,ZC,DELX,DELY,DELZ,POS,POSC,XYPOS,XPOS,
     &    I,II,IMID,IZ,IG,NC,NAVE,NUM,NCOORD,NCOUNT,NL,MAXR,MAXR2,
     &    IR2,ZMID,ZMDBOT,ZMDTOP,MIN,MAX,ZMIN,ZMAX,LOW,HIGH,
     &    IP,CL(5000),NPTS,NSINGL,NCLUST,NMID,ZMD(20),NBOT,NTOP
      DOUBLE PRECISION ROUT,DD,RSTEP,RSTEP2,PHI,
     &    G(500),SUMG,GG(NZ2,NSTEPS)
      LOGICAL FRSTP

      RSTEP2=RSTEP*RSTEP
      NL=NLAYS
      DO 101 I=1,500
         G(I)=0.0D0
  101 CONTINUE
      DO 102 I=1,NZ2
         N(I)=0
  102 CONTINUE
C *** Only calc in the uniform concentration region - define limits
  205 ZMID=NINT(REAL(NZ+ZINT)/2.0)
      MAXR=11
      MAXR2=MAXR*MAXR
      MAX=1+INT(0.99999D0*DBLE(MAXR-1)/RSTEP)
      NBOT=(1+INT(0.9999*REAL(ZINT-1+(MAXR-1)+NLAYS)/5.0))
      ZMDBOT=5*NBOT
      NTOP=INT(1.00001*REAL(NZ-(MAXR-1)-NLAYS-10)/10.0)
      ZMDTOP=10*NTOP
C *** Calculate the heights to calculate distrib - in uniform region
      IF(MOD(NBOT,2).EQ.0)THEN
C *** Bottom one is a multiple of 10
         NMID=1
         ZMD(1)=ZMDBOT
         DO 103 I=2,NTOP+1
            ZMD(I)=ZMD(I-1)+10
            IF(ZMD(I).GT.ZMDTOP)THEN
               GOTO 201
            ELSE
               NMID=NMID+1
            ENDIF
  103    CONTINUE
  201    CONTINUE
      ELSE
C *** Bottom one is a multiple of 5
         NMID=1
         ZMD(1)=ZMDBOT
         ZMDBOT=ZMDBOT-5
         DO 104 I=2,NTOP+1
            ZMD(I)=ZMDBOT+(I-1)*10
            IF(ZMD(I).GT.ZMDTOP)THEN
               GOTO 202
```

```
                ELSE
                  NMID=NMID+1
                ENDIF
  104         CONTINUE
  202         CONTINUE
            ENDIF
C *** Calculate an average coordination number (100 random particles)
            NCOORD=0
            NUM=0
            NAVE=100
            DO 105 I=1,NPARTS
              POS=LOCATE(I)
              IF(POS.NE.0.AND.(ZCOORD(POS).LT.NZ).AND.
     &           (ZCOORD(POS).GT.1))THEN
                CALL COUNTNEIGHBOURS(POS,NX,NY,NZ,NYZ,
     &             NXYZ,XCOORD,YCOORD,ZCOORD,OCCUPY,NCOUNT)
                NCOORD=NCOORD+NCOUNT
                NUM=NUM+1
                IF(NUM.GE.NAVE)THEN
                  GOTO 203
                ENDIF
              ENDIF
  105         CONTINUE
  203         WRITE(40,301)NAVE,DBLE(NCOORD)/DBLE(NAVE)
  301         FORMAT("Ave coord number of ",I3," parts ",F16.3)
C *** Take averages of N(R) at 10d intervals over the height of system
            DO 106 IMID=1,NMID
              IZ=ZMD(IMID)
              NL=NLAYS
              LOW=IZ-NL
              HIGH=IZ+NL
              NC=0
              WRITE(40,302)IZ
  302         FORMAT("Height ",I13)
              FRSTP=.TRUE.
              DO 107 XC=1,NX
                XPOS=(XC-1)*NYZ
                DO 108 YC=1,NY
                  XYPOS=XPOS+NZ*(YC-1)
                  DO 109 ZC=LOW,HIGH
                    POSC=XYPOS+ZC
                    IF(OCCUPY(POSC).NE.0)THEN
C *** A particle in the central layer
                      IF(FRSTP)THEN
                        NPTS=1
                        IF(CLUSTR(OCCUPY(POSC)).EQ.0)THEN
                          NSINGL=1
                          NCLUST=0
                        ELSE
                          NSINGL=0
                          NCLUST=1
                          CL(1)=CLUSTR(OCCUPY(POSC))
                        ENDIF
                      ENDIF
                      NC=NC+1
                      ZMIN=ZC-MAXR
                      ZMAX=ZC+MAXR
                      DO 110 II=1,NPARTS
C *** For each particle in the central region, find all others in slab
```

```
                        POS=LOCATE(II)
                        IF(POS.NE.0)THEN
                          IF(ZCOORD(POS).GE.ZMIN.AND.ZCOORD(POS).LE.
     &                      ZMAX.AND.POS.NE.POSC)THEN
                        IF(FRSTP)THEN
C *** Count the particles in the section
                            NPTS=NPTS+1
                            IF(CLUSTR(II).EQ.0)THEN
                              NSINGL=NSINGL+1
                            ELSE
                              DO 111 IP=1,NCLUST
                                IF(CL(IP).EQ.CLUSTR(II))THEN
                                  GOTO 204
                                ENDIF
 111                          CONTINUE
                              NCLUST=NCLUST+1
                              CL(NCLUST)=CLUSTR(II)
 204                          CONTINUE
                            ENDIF
                          ENDIF
C *** Is this particle within the slab?
                          DELX=IABS(XCOORD(POS)-XC)
                          IF(DELX.GT.MAXR)THEN
                            DELX=DELX-NX
                          ENDIF
                          DELY=IABS(YCOORD(POS)-YC)
                          IF(DELY.GT.MAXR)THEN
                            DELY=DELY-NY
                          ENDIF
                          DELZ=IABS(ZCOORD(POS)-ZC)
                          IR2=(DELX*DELX+DELY*DELY+DELZ*DELZ)
                          IF(IR2.LE.MAXR2)THEN
                            N(IR2)=N(IR2)+1
C *** If particle is close, count it at its relative position
                          ENDIF
                        ENDIF
                      ENDIF
 110                CONTINUE
                    FRSTP=.FALSE.
                  ENDIF
 109            CONTINUE
 108          CONTINUE
 107        CONTINUE
            IF(NC.EQ.0)THEN
C *** No particles found in central layers
              NL=NL+1
              GOTO 205
            ENDIF
            DO 112 IR2=1,MAXR2
              MIN=MMIN(IR2)
              IF(MIN.LE.MAX)THEN
                DO 113 IG=MIN,MMAX(IR2)
C *** Calculate particle volumes in each shell
                  G(IG)=G(IG)+DBLE(N(IR2))*GG(IR2,IG-MIN+1)
 113            CONTINUE
              ENDIF
 112        CONTINUE
C *** Write results
            SUMG=0.0D0
```

```
            WRITE(40,303)NPTS
303         FORMAT("Particles in slice",I27)
            WRITE(40,304)NSINGL
304         FORMAT("Singles  in slice",I27)
            WRITE(40,305)NCLUST
305         FORMAT("Clusters  in slice",I27)
            WRITE(40,306)REAL(NPTS)/REAL(NSINGL+NCLUST)
306         FORMAT("Average  unit size in slice",F17.5)
            WRITE(40,307)NC,NL
307         FORMAT("No central parts for g(R) ave ",2I15)
            WRITE(40,308)
308         FORMAT("Mid-step  Rout log(Rout)  averageG
     &  averageN")
C *** Output the distribution at this height
            DO 114 I=6,MAX
               DD=(DBLE(I)-0.5D0)*RSTEP
               ROUT=DBLE(I)*RSTEP
               SUMG=SUMG+(G(I)/DBLE(NC))
               WRITE(40,309)DD,ROUT,DLOG10(ROUT),G(I)/NC,SUMG
309            FORMAT(2F13,F10.5,2F15.5)
               G(I)=0
114         CONTINUE
106      CONTINUE
         END

C ***************************************************************
         SUBROUTINE INITDENSDISTRIB(NZ2,NSTEPS,RSTEP,MMIN,MMAX,GG)
C ***************************************************************
C *** Calculate the assigment of the particle volume to the G(R)shells
C *** according to particle position
         INTEGER NZ2,NSTEPS,MMIN(NZ2),MMAX(NZ2),I,II,IG,ILAST,MAX,MIN
         DOUBLE PRECISION R,RSTEP,L1,L2,V,V0,DIST,RR2,GG(NZ2,NSTEPS)

         DO 101 I=1,NZ2
            DO 102 II=1,NSTEPS
               GG(I,II)=0.0D0
102         CONTINUE
101      CONTINUE
         MAX=NINT(DSQRT(DBLE(NZ2))/RSTEP)
         DO 103 I=1,NZ2
C *** For each relative position, minimum and maximum shells occupied
            R=DSQRT(DBLE(I))
            MMIN(I)=1+INT(1.000001D0*(R-0.5D0)/RSTEP)
            MMAX(I)=1+INT(1.000001D0*(R+0.5D0)/RSTEP)
C *** Calculate proportion of particle's volume within a distance
            MIN=MMIN(I)
            IF(MIN.LE.MAX)THEN
               V0=0.0D0
               RR2=(R-0.5D0)*(R-0.5D0)
               ILAST=MIN0(NSTEPS-1,MAX-MIN+1)
               DO 104 IG=1,ILAST
                  DIST=DBLE(MIN+IG-1)*RSTEP
                  L1=((DIST*DIST)-RR2)/(2.0D0*R)
                  L2=(0.25D0-(R-DIST)*(R-DIST))/(2.0D0*R)
                  V=2.0D0*(L1*L1*(1.5D0-L1)+L2*L2*(3.0D0*DIST-L2))
C *** V is proportion of sphere within DIST.
C *** G is proportion between DIST and the previous distance
                  GG(I,IG)=V-V0
                  V0=V
```

```
104             CONTINUE
                IF(MMAX(I).LE.MAX)THEN
                   GG(I,MMAX(I)-MMIN(I)+1)=1.0D0-V0
                ELSE
                   MMAX(I)=MAX
                ENDIF
             ENDIF
103       CONTINUE
          END

C ********************************************************************
          SUBROUTINE COUNTNEIGHBOURS(POS,NX,NY,NZ,NYZ,NXYZ,
         &     XCOORD,YCOORD,ZCOORD,OCCUPY,NCOORD)
C ********************************************************************
          INTEGER NX,NY,NZ,NYZ,NXYZ,POS,NCOORD,
         &     XCOORD(NXYZ),YCOORD(NXYZ),ZCOORD(NXYZ),OCCUPY(NXYZ),
         &     DELP(3),DELM(3),I,J,K,L,N,DEL(26)
C *** Count the number of neighbours around a particle
          DELP(1)=1
          DELM(1)=-1
C *** Find neighbouring positions
          IF(YCOORD(POS).EQ.NY)THEN
             DELP(2)=NZ-NYZ
          ELSE
             DELP(2)=NZ
          ENDIF
          IF(YCOORD(POS).EQ.1)THEN
             DELM(2)=-NZ+NYZ
          ELSE
             DELM(2)=-NZ
          ENDIF
          IF(XCOORD(POS).EQ.NX)THEN
             DELP(3)=NYZ-NXYZ
          ELSE
             DELP(3)=NYZ
          ENDIF
          IF(XCOORD(POS).EQ.1)THEN
             DELM(3)=-NYZ+NXYZ
          ELSE
             DELM(3)=-NYZ
          ENDIF
          N=0
C *** generate 26 neighbouring positions on the cube
          DO 101 I=1,3
             N=N+1
             DEL(N)=DELP(I)
             N=N+1
             DEL(N)=DELM(I)
             DO 102 J=I+1,3
                N=N+1
                DEL(N)=DELP(I)+DELP(J)
                N=N+1
                DEL(N)=DELP(I)+DELM(J)
                N=N+1
                DEL(N)=DELM(I)+DELP(J)
                N=N+1
                DEL(N)=DELM(I)+DELM(J)
                DO 103 K=J+1,3
                   DO 104 L=3,6
```

```
                    N=N+1
                    DEL(N)=DEL(L)+DELP(K)
                    N=N+1
                    DEL(N)=DEL(L)+DELM(K)
 104              CONTINUE
 103            CONTINUE
 102          CONTINUE
 101       CONTINUE
C *** Count the number of neighbours
          NCOORD=0
          DO 105 J=1,26
             IF(OCCUPY(POS+DEL(J)).NE.0)THEN
                NCOORD=NCOORD+1
             ENDIF
 105       CONTINUE
          END

C ****************************************************************
          SUBROUTINE INITARRAYS(NY,NZ,NYZ,NXYZ,MAXPTS,MAXCL,
     &       MAXORD,NLOST,CLPTS,
     &       OCCUPY,CLUSTR,SIZE,POINTR,CORDER,CNUM,
     &       VOL,BONDED,INVPOS)
C ****************************************************************
C *** Set up the arrays
          INTEGER NY,NZ,NYZ,NXYZ,MAXPTS,MAXCL,MAXORD,CLPTS,NLOST,
     &       OCCUPY(NXYZ),CLUSTR(MAXPTS),SIZE(MAXCL),
     &       POINTR(MAXCL),CORDER(MAXCL),CNUM(MAXCL),
     &       VOL(NZ),INVPOS(6),I,II
          LOGICAL BONDED(MAXPTS,6)
          NYZ=NY*NZ
          NLOST=0
          MAXORD=0
          CLPTS=0
          DO 101 I=1,NXYZ
             OCCUPY(I)=0
 101       CONTINUE
          DO 102 I=1,MAXPTS
             CLUSTR(I)=0
             DO 103 II=1,6
                BONDED(I,II)=.FALSE.
 103         CONTINUE
 102       CONTINUE
          INVPOS(1)=2
          INVPOS(2)=1
          INVPOS(3)=4
          INVPOS(4)=3
          INVPOS(5)=6
          INVPOS(6)=5
          DO 104 I=1,MAXCL
             SIZE(I)=0
             POINTR(I)=1
             CORDER(I)=0
             CNUM(I)=1
 104       CONTINUE
          DO 105 I=1,NZ
             VOL(I)=0
 105       CONTINUE
          END
```

```
C ***************************************************************
      SUBROUTINE LATCOORDS(NX,NY,NZ,NXYZ,XCOORD,YCOORD,ZCOORD)
C ***************************************************************
C *** Set up and store the x,y,z coordinates of the lattice points
      INTEGER NX,NY,NZ,NXYZ,XCOORD(NXYZ),YCOORD(NXYZ),ZCOORD(NXYZ),
     &   I,IX,IY,IZ
      I=0
      DO 101 IX=1,NX
        DO 102 IY=1,NY
          DO 103 IZ=1,NZ
            I=I+1
            XCOORD(I)=IX
            YCOORD(I)=IY
            ZCOORD(I)=IZ
 103      CONTINUE
 102    CONTINUE
 101  CONTINUE
      END
C ***************************************************************
      SUBROUTINE INITPARTICLES(NXYZ,MAXPTS,NPARTS,OCCUPY,LOCATE)
C ***************************************************************
C *** Set the initial random positions of the particles
      INTEGER NXYZ,MAXPTS,OCCUPY(NXYZ),LOCATE(MAXPTS),NPARTS,J,NJ
      DOUBLE PRECISION DUMM,G05CAF,FAC
      EXTERNAL G05CAF
      FAC=0.9999999999D0*DBLE(NXYZ)
      DO 101 J=1,NPARTS
 201    NJ=1+DINT(FAC*G05CAF(DUMM))
        IF(OCCUPY(NJ).NE.0)THEN
          GO TO 201
        ELSE
          LOCATE(J)=NJ
          OCCUPY(NJ)=J
        ENDIF
 101  CONTINUE
      END
C ***************************************************************
      SUBROUTINE INITCLUSTERS(NX,NY,NZ,NYZ,NXYZ,MAXPTS,MAXCL,
     &   NPARTS,XCOORD,YCOORD,ZCOORD,LOCATE,OCCUPY,
     &   MAXORD,CLPTS,CLUSTR,CPARTS,SIZE,POINTR,CORDER,CNUM,
     &   BONDPR,BONDED,INVPOS)
C ***************************************************************
C *** Set up the initial clusters
      INTEGER NX,NY,NZ,NYZ,NXYZ,MAXPTS,NPARTS,MAXORD,MAXCL,CLPTS,
     &   XCOORD(NXYZ),YCOORD(NXYZ),ZCOORD(NXYZ),
     &   OCCUPY(NXYZ),LOCATE(MAXPTS),
     &   CPARTS(MAXPTS),CLUSTR(MAXPTS),SIZE(MAXCL),
     &   POINTR(MAXCL),CORDER(MAXCL),CNUM(MAXCL),
     &   INVPOS(6),TEMPCL(1),I
      LOGICAL BONDED(MAXPTS,6),INIT
      DOUBLE PRECISION BONDPR
          INIT=.TRUE.
      DO 101 I=1,NPARTS
C *** Are any neighbours bonded initially?
        TEMPCL(1)=I
        CALL BONDS(NX,NY,NZ,NYZ,NXYZ,NPARTS,MAXPTS,MAXORD,MAXCL,
     &     CLPTS,XCOORD,YCOORD,ZCOORD,OCCUPY,LOCATE,
     &     CPARTS,CLUSTR,SIZE,POINTR,CORDER,CNUM,
     &     BONDPR,0.0D0,BONDED,INVPOS,
```

```
     &          TEMPCL,1,INIT)
 101    CONTINUE
        END

C ****************************************************************
       SUBROUTINE INITRATES(MAXPTS,DIFFCL,DFSTEP,CRMCL,CRSTEP,DELT)
C ****************************************************************
C *** Calculate diffusion and creaming rates for all cluster sizes
       INTEGER MAXPTS,CRSTEP(MAXPTS),DFSTEP(MAXPTS),CRSTP,DFSTP,I
       DOUBLE PRECISION DIFFCL(MAXPTS),CRMCL(MAXPTS),DFRAT,D0,C0,DELT
       CRSTP=+1
       DFSTP=1
       DFRAT=1.0D0
C *** The creaming vel and diffusion coeff in lattice and time units
       C0=0.0694579D0*DELT
       D0=0.320847D0*DELT
       WRITE(20,301)DELT
       WRITE(30,301)DELT
       WRITE(40,301)DELT
       WRITE(50,301)DELT
 301   FORMAT("Time step ",F10.2," secs          particle diam 1.2 microns")
       WRITE(20,302)C0,D0
       WRITE(30,302)C0,D0
       WRITE(40,302)C0,D0
       WRITE(50,302)C0,D0
 302   FORMAT("Cream coef",F10.5," Diff Coef",F15.5," at 30 deg C")
       WRITE(20,303)
       WRITE(30,303)
       WRITE(40,303)
       WRITE(50,303)
 303   FORMAT("Diffcl   6D0(N^-0.5 Creamcl  C0(N^0.5)/crstp")
       DO 101 I=1,MAXPTS
C *** Set movement prob and step length
         DIFFCL(I)=6.0D0*D0*(I**(-0.5D0))/(DFSTP*DFSTP)
         CRMCL(I)=C0*(I**0.5D0)/CRSTP
         IF((DIFFCL(I).LT.0.5D0*DFRAT).AND.(DFSTP.GT.1))THEN
C *** Large movement prob - take next step length
           DIFFCL(I)=DIFFCL(I)/DFRAT
           DFSTP=DFSTP-1
           DFSTEP(I)=DFSTP
           DFRAT=DBLE(DFSTP-1)*DBLE(DFSTP-1)/
     &           (DBLE(DFSTP)*DBLE(DFSTP))
         ELSE
           DFSTEP(I)=DFSTP
         ENDIF
         IF((CRMCL(I).GT.0.5D0).AND.(CRSTP.LT.5))THEN
C *** Large movement prob - take next step length
           CRMCL(I)=CRMCL(I)*CRSTP/(CRSTP+1)
           CRSTP=CRSTP+1
           CRSTEP(I)=CRSTP
         ELSEIF(CRMCL(I).GT.0.9D0)THEN
           CRMCL(I)=CRMCL(I)*CRSTP/(CRSTP+1)
           CRSTP=CRSTP+1
           CRSTEP(I)=CRSTP
         ELSE
           CRSTEP(I)=CRSTP
         ENDIF
 101   CONTINUE
       END
```

Appendix A4 : Computer Program for Multiple Scattering Theory Calculations

```
C   Calculate wavenumber, velocity and attenuation of ultrasound
C   in a dispersion (solid or liquid or mixture droplets)
C   Multiple scattering theory, long wavelength limit
C   by Valerie Pinfield.   1993-1995
C ****************************************************************
      SUBROUTINE USVELS(N,NSIZES,RADIUS,PHI,SFC,ANGFREQ,SSVTH,SSVVI,
     &    SSVEL,SSATT,
     &    MSVEL,MSATT,LBATTL,
     &    Q,RHO,ETA,MU,TOR,GAMMA,BETA,SIGMA)
C ****************************************************************
      INTEGER N,NSIZES,IZ
      DOUBLE COMPLEX I,COEFF(0:3),K(2,3),BULKK2,K11
      DOUBLE PRECISION RADIUS(NSIZES),PHI(NSIZES),SFC(NSIZES),ANGFREQ,
     &    Q(3),RHO(3),ETA(3),MU(3),TOR(3),GAMMA(3),BETA(3),SIGMA(3),
     &    SOLRAD(101),SSVEL,SSATT,SSVTH,SSVVI,
     &    MSVEL,MSATT,LBVEL,LBATT,LBATTL
      PARAMETER (I=(0.0D0,1.0D0) )

C *** Requires previous CALL to subroutine MTDATA to get mat properties
      DO 101 IZ=0,N
       COEFF(IZ)=(0.00D0,0.00D0)
  101 CONTINUE
      DO 102 IZ=1,NSIZES
        SOLRAD(IZ)=RADIUS(IZ)*(RHO(2)/RHO(3))**0.3333333333333D0
  102 CONTINUE
C *** Determine the single particle scattering coefficients for
C *** solid and liquid particles
      CALL SCATTCOEFFS(N,NSIZES,RADIUS,PHI,SFC,0,ANGFREQ,K11,COEFF,
     &    Q,RHO,ETA,MU,TOR,GAMMA,BETA,SIGMA,K)
      CALL SCATTCOEFFS(N,NSIZES,SOLRAD,PHI,SFC,1,ANGFREQ,K11,COEFF,
     &    Q,RHO,ETA,MU,TOR,GAMMA,BETA,SIGMA,K)
C *** Calculate wavenumber, velocity and atten from scatt coeffs
C *** Single scattering only
      BULKK2=K11*K11*(1.0D0-(3.0D0*I*COEFF(0)/(K11**3)))
      SSVTH=ANGFREQ/(DBLE(CDSQRT(BULKK2)))
      BULKK2=K11*K11*(1.0D0-(9.0D0*I*COEFF(1)/(K11**3)))
      SSVVI=ANGFREQ/(DBLE(CDSQRT(BULKK2)))
      BULKK2=K11*K11-((3.0D0*I/K11)*(COEFF(0)+(3.0D0*COEFF(1))+(5.0D0*
     &    COEFF(2))))
      SSVEL=ANGFREQ/(DBLE(CDSQRT(BULKK2)))
      SSATT=20.0D0*DIMAG(CDSQRT(BULKK2))*DLOG10(2.718281828D0)
C *** Multiple scattering
      IF(N.EQ.1)THEN
        BULKK2=K11*K11-((3.0D0*I/K11)*(COEFF(0)+(3.0D0*COEFF(1))))
     &        -((27.0D0/(K11**4))*((COEFF(0)*COEFF(1))
     &        +(2.0D0*COEFF(1)*COEFF(1))))
      ELSE
        BULKK2=K11*K11-((3.0D0*I/K11)*(COEFF(0)+
     &        (3.0D0*COEFF(1))+(5.0D0*COEFF(2))))
     &        -((27.0D0/(K11**4))*((COEFF(0)*COEFF(1))
     &        +(5.0D0*COEFF(1)*COEFF(2))+(2.0D0*COEFF(1)*COEFF(1))
```

```
     &          +(10.0D0*COEFF(0)*COEFF(2)/3.0D0)
     &          +(6.0D0*COEFF(1)*COEFF(2))
     &          +(230.0D0*COEFF(2)*COEFF(2)/21.0D0)))
        ENDIF

        LBVEL=ANGFREQ/(DBLE(CDSQRT(BULKK2)))
        LBATTL=(2.0D0*DIMAG(CDSQRT(BULKK2))*62.83185D0/DBLE(K11))*
     &     DLOG10(2.718281828D0)
        LBATT=20.0D0*DIMAG(CDSQRT(BULKK2))*DLOG10(2.718281828D0)

        MSVEL=LBVEL
        MSATT=LBATT
        END

C ***********************************************************************
        SUBROUTINE SCATTCOEFFS(N,NSIZES,RADIUS,PHI,SFC,SOLID,ANGFREQ,
     &     K11,COEFF,Q,RHO,ETA,MU,TOR,GAMMA,BETA,SIGMA,K)
C ***********************************************************************
C *** Calculate the single particle scattering coefficients
C *** Requires previous call to MTDATA for material parameters
        INTEGER ISIZE,IZ,N,NSIZES,SOLID
        DOUBLE PRECISION RADIUS(NSIZES),PHI(NSIZES),SFC(NSIZES),PROPN,
     &     ANGFREQ,Q(3),RHO(3),ETA(3),MU(3),TOR(3),GAMMA(3),
     &     BETA(3),SIGMA(3)
        DOUBLE COMPLEX I,K(2,3),A(2,3),G(2,2),L(2,2),
     &     JN(2,3,0:3),JNP(2,3,0:3),JNDP(2,3,0:3),
     &     HN(2,3,0:3),HNP(2,3,0:3),HNDP(2,3,0:3),
     &     ACOEFF(0:3,101),COEFF(0:3),K11
        PARAMETER (I=(0.0D0,1.0D0) )

C *** Calculate wavenumber of each mode (propl, thermal, shear)
C *** in bulk materials
        CALL WAVE(ANGFREQ,SOLID,K,G,L,Q,RHO,ETA,MU,GAMMA,BETA,SIGMA)
        K11=K(1,1)
C *** For each particle size, calculate scattering coefficients
        DO 101 ISIZE=1,NSIZES
C *** Calculate spherical Bessel functions for each parameter
           CALL SPHBES(RADIUS(ISIZE),N,K,A,JN,JNP,JNDP,HN,HNP,HNDP)
           IF (SOLID .EQ.1) THEN
              PROPN=SFC(ISIZE)
           ELSE
              PROPN=PHI(ISIZE)
           END IF
           DO 102 IZ=0,N
C *** For each scattering order, solve boundary equations at surface
              CALL SOLVEEQUATIONS(IZ,RADIUS(ISIZE),ACOEFF(IZ,ISIZE),
     &           SOLID,ANGFREQ,K,A,G,L,ETA,MU,TOR,
     &           JN,JNP,JNDP,HN,HNP,HNDP,RHO,SIGMA)
C *** Cumulative scattering coefficient (sum over sizes)
              COEFF(IZ)=COEFF(IZ)+ACOEFF(IZ,ISIZE)*PROPN/
     &           (RADIUS(ISIZE)**3)
  102      CONTINUE
  101   CONTINUE
        END
```

```
C ***************************************************************
      SUBROUTINE SOLVEEQUATIONS(ORDER,RAD,COEFF,SOLID,ANGFREQ,
     &    K,A,G,L,ETA,MU,TOR,JN,JNP,JNDP,HN,HNP,HNDP,RHO,SIGMA)
C ***************************************************************
C *** Matrix solution of six boundary equations at particle surface
C *** for the single scattering coefficients
      INTEGER ORDER,IPIV(6),INFO,II,SOLID,II,JJ
      DOUBLE PRECISION  ETA(3),MU(3),TOR(3),TOR21,ETAMU1,
     &    NFAC,N2FAC,RAD,ANGFREQ,RHO(3),SIGMA(3),
     &    FERR(1),BERR(1),RWORK(12),ANORM,RCOND
      DOUBLE COMPLEX I,MATRIX(6,6),RHS(6,1),COEFF,IWFAC,ETA2,ETA21,
     &    K(2,3),A(2,3),G(2,2),L(2,2),ETAMU2,
     &    JN(2,3,0:3),JNP(2,3,0:3),JNDP(2,3,0:3),
     &    HN(2,3,0:3),HNP(2,3,0:3),HNDP(2,3,0:3),
     &    AA(6,6),RA(6,1),WORK(12)
      PARAMETER (I=(0.0D0,1.0D0))
      EXTERNAL F06UAF
      DOUBLE PRECISION F06UAF
      NFAC=DBLE(ORDER*(ORDER+1))
      N2FAC=DBLE(ORDER*ORDER+ORDER-2)
      IF(SOLID.EQ.0)THEN
         ETA2=ETA(2)
      ELSE
         ETA2=ETA(3)/(-I*ANGFREQ)
      END IF
      TOR21=TOR(2+SOLID)/TOR(1)
      ETA21=ETA2/ETA(1)
      ETAMU1=2.0D0*(ETA(1)-MU(1))/3.0D0
      ETAMU2=2.0D0*(ETA2-MU(2+SOLID))/3.0D0
C *** Set up matrix of boundary values
C *** See Epstein and Carhart (1953) or Allegra and Hawley (1972)
C *** Equation 1 is radial velocity
      MATRIX(1,1)=A(1,1)*HNP(1,1,ORDER)
      MATRIX(1,2)=A(1,2)*HNP(1,2,ORDER)
      MATRIX(1,5)=-NFAC*HN(1,3,ORDER)
      MATRIX(1,3)=-A(2,1)*JNP(2,1,ORDER)
      MATRIX(1,4)=-A(2,2)*JNP(2,2,ORDER)
      MATRIX(1,6)=NFAC*JN(2,3,ORDER)
C *** Equation 5 is tangential velocity
      MATRIX(5,1)=HN(1,1,ORDER)
      MATRIX(5,2)=HN(1,2,ORDER)
      MATRIX(5,5)=-(HN(1,3,ORDER)+A(1,3)*HNP(1,3,ORDER))
      MATRIX(5,3)=-JN(2,1,ORDER)
      MATRIX(5,4)=-JN(2,2,ORDER)
      MATRIX(5,6)=(JN(2,3,ORDER)+A(2,3)*JNP(2,3,ORDER))
C *** Equation 2 is temperature
      MATRIX(2,1)=MATRIX(5,1)
      MATRIX(2,2)=G(1,2)*MATRIX(5,2)
      MATRIX(2,5)=0.0D0
      MATRIX(2,3)=G(2,1)*MATRIX(5,3)
      MATRIX(2,4)=G(2,2)*MATRIX(5,4)
      MATRIX(2,6)=0.0D0
C *** Equation 3 is heat flux
      MATRIX(3,1)=MATRIX(1,1)
      MATRIX(3,2)=G(1,2)*MATRIX(1,2)
      MATRIX(3,5)=0.0D0
      MATRIX(3,3)=TOR21*G(2,1)*MATRIX(1,3)
      MATRIX(3,4)=TOR21*G(2,2)*MATRIX(1,4)
      MATRIX(3,6)=0.0D0
```

```
C *** Equation 4 is radial stress Prr
      MATRIX(4,1)=HN(1,1,ORDER)-2.0D0*ETA(1)*K(1,1)*K(1,1)*
     &    (HNDP(1,1,ORDER)+HN(1,1,ORDER))/L(1,1)
      MATRIX(4,2)=(L(1,2)*HN(1,2,ORDER)-2.0D0*ETA(1)*K(1,2)*K(1,2)*
     &    (HNDP(1,2,ORDER)+HN(1,2,ORDER)))/L(1,1)
      MATRIX(4,3)=-(L(2,1)*JN(2,1,ORDER)-2.0D0*ETA2*K(2,1)*K(2,1)*
     &    (JNDP(2,1,ORDER)+JN(2,1,ORDER)))/L(1,1)
      MATRIX(4,4)=-(L(2,2)*JN(2,2,ORDER)-2.0D0*ETA2*K(2,2)*K(2,2)*
     &    (JNDP(2,2,ORDER)+JN(2,2,ORDER)))/L(1,1)
      MATRIX(4,5)=2.0D0*ETA(1)*NFAC*(A(1,3)*HNP(1,3,ORDER)-
     &      HN(1,3,ORDER))/(L(1,1)*RAD*RAD)
      MATRIX(4,6)=-2.0D0*ETA2*NFAC*(A(2,3)*JNP(2,3,ORDER)-
     &  JN(2,3,ORDER))/(L(1,1)*RAD*RAD)
C *** Alternative according to Epstein and Carhart, 1953
C     MATRIX(4,1)=ETA(1)*((A(1,3)*A(1,3)*HN(1,1,ORDER)-2.0D0*A(1,1)*
C    &    A(1,1)*HNDP(1,1,ORDER)))
C     MATRIX(4,2)=ETA(1)*(((1.0D0-(2.0D0*ETA(1)/(RHO(1)*SIGMA(1))))*
C    &    A(1,3)*A(1,3)*HN(1,2,ORDER))-(2.0D0*A(1,2)*A(1,2)*
C    &    HNDP(1,2,ORDER)))
C     MATRIX(4,3)=-ETA(2)*((A(2,3)*A(2,3)*JN(2,1,ORDER)-2.0D0*A(2,1)*
C    &    A(2,1)*JNDP(2,1,ORDER)))
C     MATRIX(4,4)=-ETA(2)*(((1.0D0-(2.0D0*ETA(2)/(RHO(2)*SIGMA(2))))*
C    &    A(2,3)*A(2,3)*JN(2,2,ORDER))-(2.0D0*A(2,2)*A(2,2)*
C    &    JNDP(2,2,ORDER)))
C     MATRIX(4,5)=2.0D0*ETA(1)*NFAC*((A(1,3)*HNP(1,3,ORDER))-
C    &    HN(1,3,ORDER))
C     MATRIX(4,6)=-2.0D0*ETA(2)*NFAC*((A(2,3)*JNP(2,3,ORDER))-
C    &    JN(2,3,ORDER))
C *** Alternative according to Allegra and Hawley, 1972
C     MATRIX(4,1)=(HN(1,1,ORDER)*(A(1,3)*A(1,3)-2.0D0*A(1,1)*A(1,1))
C    &    -2.0D0*A(1,1)*A(1,1)*HNDP(1,1,ORDER))*ETA(1)
C     MATRIX(4,2)=(HN(1,2,ORDER)*(A(1,3)*A(1,3)-2.0D0*A(1,2)*A(1,2))
C    &    -2.0D0*A(1,2)*A(1,2)*HNDP(1,2,ORDER))*ETA(1)
C     MATRIX(4,3)=(2.0D0*ETA(3)*A(2,1)*A(2,1)*JNDP(2,1,ORDER)-(ANGFREQ
C    &    *ANGFREQ*RHO(3)*RAD*RAD-2.0D0*ETA(3)*A(2,1)*A(2,1))*
C    &    JN(2,1,ORDER))/(-I*ANGFREQ)
C     MATRIX(4,4)=(2.0D0*ETA(3)*A(2,2)*A(2,2)*JNDP(2,2,ORDER)-
C    &    JN(2,2,ORDER)*(ANGFREQ*ANGFREQ*RHO(3)*RAD*RAD-2.0D0*
C    &    ETA(3)*A(2,2)*A(2,2)))/(-I*ANGFREQ)
C     MATRIX(4,5)=ETA(1)*2.0D0*NFAC*(A(1,3)*HNP(1,3,ORDER)-
C    &    HN(1,3,ORDER))
C     MATRIX(4,5)=2.0D0*ETA(1)*NFAC*(A(1,3)*HNP(1,3,ORDER)-
C    &      HN(1,3,ORDER))/(L(1,1)*RAD*RAD)
C     MATRIX(4,6)=-(ETA(3)*2.0D0*NFAC*(A(2,3)*JNP(2,3,ORDER)-
C    &    JN(2,3,ORDER)))/(-I*ANGFREQ)
C *** Equation 6 is radial stress, Pr.theta
      MATRIX(6,1)=MATRIX(1,1)-MATRIX(5,1)
      MATRIX(6,2)=MATRIX(1,2)-MATRIX(5,2)
      MATRIX(6,5)=-0.5D0*((A(1,3)*A(1,3)*HNDP(1,3,ORDER))
     &          +N2FAC*HN(1,3,ORDER))
      MATRIX(6,3)=ETA21*(MATRIX(1,3)-MATRIX(5,3))
      MATRIX(6,4)=ETA21*(MATRIX(1,4)-MATRIX(5,4))
      MATRIX(6,6)=0.5D0*ETA21*((A(2,3)*A(2,3)*JNDP(2,3,ORDER))
     &          +N2FAC*JN(2,3,ORDER))
C *** Alternative according to Allegra and Hawley, 1972
C     MATRIX(6,1)=ETA(1)*(A(1,1)*HNP(1,1,ORDER)-HN(1,1,ORDER))
C     MATRIX(6,2)=ETA(1)*(A(1,2)*HNP(1,2,ORDER)-HN(1,2,ORDER))
C     MATRIX(6,3)=-ETA(3)*(A(2,1)*JNP(2,1,ORDER)-JN(2,1,ORDER))/(-I*
C    &    ANGFREQ)
```

```
C         MATRIX(6,4)=-ETA(3)*(A(2,2)*JNP(2,2,ORDER)-JN(2,2,ORDER))/
C    *   (-I*ANGFREQ)
C         MATRIX(6,5)=-0.5D0*ETA(1)*(A(1,3)*A(1,3)*HNDP(1,3,ORDER)+N2FAC*
C     &      HN(1,3,ORDER))
C         MATRIX(6,6)=0.5D0*ETA(3)*(A(2,3)*A(2,3)*JNDP(2,3,ORDER)+N2FAC*
C     &      JN(2,3,ORDER))/(-I*ANGFREQ)
          RHS(1,1)=-A(1,1)*JNP(1,1,ORDER)
          RHS(5,1)=-JN(1,1,ORDER)
          RHS(2,1)=RHS(5,1)
          RHS(3,1)=RHS(1,1)
          RHS(4,1)=-JN(1,1,ORDER)+2.0D0*ETA(1)*K(1,1)*K(1,1)*
     &       (JNDP(1,1,ORDER)+JN(1,1,ORDER))/L(1,1)
          RHS(6,1)=RHS(1,1)-RHS(5,1)
C Alternatives E&C and A&H
C         RHS(4,1)=-ETA(1)*((A(1,3)*A(1,3)*JN(1,1,ORDER))-(2.0D0*A(1,1)
C     &      *A(1,1)*JNDP(1,1,ORDER)))
C         RHS(4,1)=-ETA(1)*(JN(1,1,ORDER)*(A(1,3)*A(1,3)-2.0D0*A(1,1)*
C     &      A(1,1))-2.0D0*A(1,1)*A(1,1)*JNDP(1,1,ORDER))
C         RHS(6,1)=-ETA(1)*(A(1,1)*JNP(1,1,ORDER)-JN(1,1,ORDER))
          IF (ORDER.NE.0) THEN
            IF (ORDER.EQ.1) THEN
C *** Convert to xFp(n)-F(n)=-xF(n+1) for n=1
              MATRIX(6,1)=-A(1,1)*HN(1,1,2)
              MATRIX(6,2)=-A(1,2)*HN(1,2,2)
              MATRIX(6,3)=A(2,1)*JN(2,1,2)*ETA21
              MATRIX(6,4)=A(2,2)*JN(2,2,2)*ETA21
              RHS(6,1)=A(1,1)*JN(1,1,2)
              MATRIX(4,5)=-2.0D0*ETA(1)*NFAC*A(1,3)*HN(1,3,2)
     &           /(L(1,1)*RAD*RAD)
              MATRIX(4,6)=2.0D0*ETA2*NFAC*A(2,3)*JN(2,3,2)
     &           /(L(1,1)*RAD*RAD)
C E&C
C             MATRIX(4,5)=-2.0D0*ETA(1)*NFAC*A(1,3)*HN(1,3,2)
C             MATRIX(4,6)=2.0D0*ETA(2)*NFAC*A(2,3)*JN(2,3,2)
C A&H
C             MATRIX(4,5)=-2.0D0*ETA(1)*NFAC*A(1,3)*HN(1,3,2)
C             MATRIX(4,6)=2.0D0*ETA(3)*NFAC*A(2,3)*JN(2,3,2)
C    &           /(-I*ANGFREQ)
C             MATRIX(6,1)=-ETA(1)*A(1,1)*HN(1,1,2)
C             MATRIX(6,2)=-ETA(1)*A(1,2)*HN(1,2,2)
C             MATRIX(6,3)=ETA(3)*A(2,1)*JN(2,1,2)/(-I*ANGFREQ)
C             MATRIX(6,4)=ETA(3)*A(2,2)*JN(2,2,2)/(-I*ANGFREQ)
C             RHS(6,1)=ETA(1)*A(1,1)*JN(1,1,2)
            END IF
            IF (SOLID .EQ.1) THEN
C *** Conversion of boundary equation for solid particles
              IWFAC=-I*ANGFREQ
              DO 101 IJ=1,6
                MATRIX(IJ,3)=IWFAC*MATRIX(IJ,3)
                MATRIX(IJ,4)=IWFAC*MATRIX(IJ,4)
                MATRIX(IJ,6)=IWFAC*MATRIX(IJ,6)
  101         CONTINUE
            END IF
C *** Set up matrices for solution
            DO 102 II=1,6
              DO 103 JJ=1,6
                AA(II,JJ)=MATRIX(II,JJ)
                RA(II,1)=RHS(II,1)
  103         CONTINUE
```

```
  102         CONTINUE
C *** Factorisation of matrix NAG library Mark 15
            CALL F07ARF(6,6,MATRIX,6,IPIV,INFO)
C *** Check for NAG errors
            IF (INFO .NE. 0) THEN
               WRITE(20,201) INFO
  201          FORMAT("ERROR IN F07ARF, INFO=",I4)
            END IF
C *** Solution of the linear simultaneous equations NAG Mark 15
            CALL F07ASF('N',6,1,MATRIX,6,IPIV,RHS,6,INFO)
C *** Check for NAG errors
            IF (INFO .NE. 0) THEN
               WRITE(20,202) INFO
  202          FORMAT("ERROR IN F07ASF, INFO=",I4)
            END IF
C *** Check matrix stability
            INFO=0
            ANORM=F06UAF('I',6,6,AA,6,RWORK)
            CALL F07AUF('I',6,MATRIX,6,ANORM,RCOND,WORK,RWORK,INFO)
            IF (INFO .NE. 0) THEN
               WRITE(20,203) INFO
  203          FORMAT("ERROR IN F07AUF, INFO=",I4)
            END IF
            INFO=0
            CALL F07AVF('N',6,1,AA,6,MATRIX,6,IPIV,RA,6,RHS,6,
     &         FERR,BERR,WORK,RWORK,INFO)
            IF (INFO .NE. 0) THEN
               WRITE(20,204) INFO
  204          FORMAT("ERROR IN F07AVF, INFO=",I4)
            END IF
          ELSE
C *** Only four boundary equations for zero order mode
            IF (SOLID .EQ.1) THEN
C *** Conversion for solid particles
               IWFAC=-I*ANGFREQ
               DO 104 IJ=1,6
                  MATRIX(IJ,3)=IWFAC*MATRIX(IJ,3)
                  MATRIX(IJ,4)=IWFAC*MATRIX(IJ,4)
                  MATRIX(IJ,6)=IWFAC*MATRIX(IJ,6)
  104          CONTINUE
            END IF
C *** Set up matrices for solution
            DO 105 II=1,6
               DO 106 JJ=1,6
                  AA(II,JJ)=MATRIX(II,JJ)
                  RA(II,1)=RHS(II,1)
  106          CONTINUE
  105       CONTINUE
C *** Factorisation of matrix NAG library Mark 15 subroutine
            CALL F07ARF(4,4,MATRIX,6,IPIV,INFO)
C *** Check for NAG errors
            IF (INFO .NE. 0) THEN
               WRITE(20,201)INFO
            END IF
C *** Solution of the linear simultaneous equations NAG Mark 15
            CALL F07ASF('N',4,1,MATRIX,6,IPIV,RHS,6,INFO)
C *** Check for NAG error
            IF (INFO .NE. 0) THEN
               WRITE(20,205)INFO
```

```
 205          FORMAT("ERROR IN F07ASF, INFO=",I4)
              END IF
C *** Check stability of matrix
              INFO=0
              ANORM=F06UAF('I',4,4,AA,6,RWORK)
              CALL F07AUF('I',4,MATRIX,6,ANORM,RCOND,WORK,RWORK,INFO)
              IF (INFO .NE. 0) THEN
                 WRITE(20,206) INFO
 206             FORMAT("ERROR IN F07AUF, INFO=",I4)
              END IF
              INFO=0
              CALL F07AVF('N',4,1,AA,6,MATRIX,6,IPIV,RA,6,RHS,6,
     &             FERR,BERR,WORK,RWORK,INFO)
              IF (INFO .NE. 0) THEN
                 WRITE(20,207) INFO
 207             FORMAT("ERROR IN F07AVF, INFO=",I4)
              END IF
           END IF
           COEFF=RHS(1,1)
C *** The single scattering coefficient is the first in the matrix
           END

C *****************************************************************
           SUBROUTINE MTDATA(Q,RHO,ETA,MU,TOR,CP,GAMMA,BETA,ALPHA,SIGMA,
     &                       ANGFREQ,TEMP,DFNAME)
C *****************************************************************
C *** Read the material parameters for the three phases from data file
           DOUBLE PRECISION Q(3),RHO(3),ETA(3),MU(3),TOR(3),CP(3),GAMMA(3),
     &                    BETA(3),ALPHA(3),SIGMA(3),ANGFREQ,TEMP
           CHARACTER*50 DFNAME
           DOUBLE COMPLEX I
           PARAMETER (I=(0.0D0,1.0D0))

           OPEN(UNIT=30,ACCESS="SEQUENTIAL",FILE=DFNAME)
           READ(30,*)
           READ(30,*)
           READ(30,*)
           READ(30,*)
           READ(30,*)TEMP
           WRITE(20,211)TEMP
 211       FORMAT("Temperature                ",E15.5E3)
           READ(30,*)Q(1),Q(2),Q(3)
           WRITE(20,212) Q(1),Q(2),Q(3)
 212       FORMAT("Sound velocity             ",E15.5E3,2E15.5E3)
           READ(30,*)RHO(1),RHO(2),RHO(3)
           WRITE(20,213) RHO(1),RHO(2),RHO(3)
 213       FORMAT("Density                    ",E15.5E3,2E15.5E3)
           READ(30,*)ETA(1),ETA(2),ETA(3)
           WRITE(20,214) ETA(1),ETA(2),ETA(3)
 214       FORMAT("Viscosity                  ",E15.5E3,2E15.5E3)
           READ(30,*)MU(1),MU(2),MU(3)
           MU(3)=0.0D0
           WRITE(20,215) MU(1),MU(2),MU(3)
 215       FORMAT("Bulk viscosity             ",E15.5E3,2E15.5E3)
           READ(30,*)TOR(1),TOR(2),TOR(3)
           WRITE(20,216) TOR(1),TOR(2),TOR(3)
 216       FORMAT("Conductivity               ",E15.5E3,2E15.5E3)
           READ(30,*)CP(1),CP(2),CP(3)
           WRITE(20,217) CP(1),CP(2),CP(3)
```

```
 217    FORMAT("Heat capacity            ",E15.5E3,2E15.5E3)
        READ(30,*)BETA(1),BETA(2),BETA(3)
        WRITE(20,218) BETA(1),BETA(2),BETA(3)
 218    FORMAT("Thermal expansivity ",E15.5E3,2E15.5E3)

        GAMMA(1)=1.0D0+(TEMP*BETA(1)*BETA(1)*Q(1)*Q(1)/CP(1))
        GAMMA(2)=1.0D0+(TEMP*BETA(2)*BETA(2)*Q(2)*Q(2)/CP(2))
        GAMMA(3)=1.0D0+(TEMP*BETA(3)*BETA(3)*Q(3)*Q(3)/CP(3))
        WRITE(20,219) GAMMA(1),GAMMA(2),GAMMA(3)
 219    FORMAT("Ratio heat capacity ",E15.5E3,2E15.5E3)
        SIGMA(1)=TOR(1)/(RHO(1)*CP(1))
        SIGMA(2)=TOR(2)/(RHO(2)*CP(2))
        SIGMA(3)=TOR(3)/(RHO(3)*CP(3))
        WRITE(20,220) SIGMA(1),SIGMA(2),SIGMA(3)
 220    FORMAT("Thermometric cond-y ",E15.5E3,2E15.5E3)
        END

C ***************************************************************
        SUBROUTINE WAVE(ANGFREQ,SOLID,K,G,L,
     &                  Q,RHO,ETA,MU,GAMMA,BETA,SIGMA)
C ***************************************************************
C *** Calculate the wavenumbers in each bulk medium
C *** Also pressure and temperature factors
        INTEGER IMAT,J,IREF,SOLID
        DOUBLE PRECISION ANGFREQ,VISCF,E,F,RQW,GWB,PI,ALPHA(3),
     &  Q(3),RHO(3),ETA(3),MU(3),GAMMA(3),BETA(3),SIGMA(3)
        DOUBLE COMPLEX I,SQUARE,FAC,COMM,K2,S2,G11,S2G,SKKW,
     &                 K(2,3),G(2,2),L(2,2)
        PARAMETER (I=(0.0D0,1.0D0) , PI=3.141592654D0)

        IREF=1
        ALPHA(1)=23.0D-13*ANGFREQ*ANGFREQ/(4.0D0*PI*PI*20.0D0*DLOG10(
     &    2.718281828D0))
        ALPHA(2)=24.0D-11*((ANGFREQ/(2.0D0*PI))**1.77)/(20.0D0*DLOG10(
     &    2.718281828D0))
        DO 101 IMAT=1,2
           VISCF=4.0D0*(1.0D0+(MU(IREF)/(2.0D0*ETA(IREF))))/3.0D0
           E=VISCF*ETA(IREF)*ANGFREQ/(RHO(IREF)*Q(IREF)*Q(IREF))
           IF (IREF.EQ.3)THEN
              E=E/(-I*ANGFREQ)
           END IF
           F=SIGMA(IREF)*ANGFREQ/(Q(IREF)*Q(IREF))
           SQUARE=(1.0D0)-(2.0D0*E*I)-(I*2.0D0*F*(GAMMA(IREF)-2.0D0))
     &          -((E-GAMMA(IREF)*F)*(E-GAMMA(IREF)*F))
           FAC=I*ANGFREQ*ANGFREQ/(2.0D0*Q(IREF)*Q(IREF)*F*
     &          (1.0D0-I*E*GAMMA(IREF)))
           COMM=1-I*E-I*GAMMA(IREF)*F
C *** Modes 1,2,3 are propagational, thermal, shear modes
           K(IMAT,1)=CDSQRT(FAC*(COMM-CDSQRT(SQUARE)))
           K(IMAT,2)=CDSQRT(FAC*(COMM+CDSQRT(SQUARE)))
           IF (IREF.NE.3)THEN
              K(IMAT,3)=(1.0D0+I)*DCMPLX(DSQRT(ANGFREQ*RHO(IREF)
     &             /(2.0D0*ETA(IREF))))
           ELSE
            K(IMAT,3)=DCMPLX(DSQRT(ANGFREQ*ANGFREQ*RHO(IREF)/ETA(IREF)))
           END IF
C *** Calculate the pressure and temperature factors - exact solutions
C *** L() for pressure, G() for temperature
           SKKW=I*SIGMA(IREF)/ANGFREQ
```

```
            RQW=RHO(IREF)*Q(IREF)*Q(IREF)/ANGFREQ
            GWB=(GAMMA(IREF)-1.0D0)/BETA(IREF)
            IF (IMAT.EQ.1) THEN
               K2=K(1,1)*K(1,1)
               G11=GWB*K2/(1.0D0+K2*SKKW*GAMMA(IREF))
            END IF
            DO 102 J=1,2
               K2=K(IMAT,J)*K(IMAT,J)
               S2=K2*SKKW
               S2G=S2*GAMMA(IREF)
C *** L is a pressure factor, G a temperature factor
               L(IMAT,J)=I*ANGFREQ*RHO(IREF)
               G(IMAT,J)=K2*GWB/((1.0D0+S2G))
               G(IMAT,J)=G(IMAT,J)/G11
C ** Take these G as factors of the material 1, propl mode
  102       CONTINUE
            G(1,1)=(1.0D0,0.0D0)
            IREF=2+SOLID
  101    CONTINUE
         END

C ***************************************************************
         SUBROUTINE SPHBES(RSIZE,N,K,A,JN,JNP,JNDP,HN,HNP,HNDP)
C ***************************************************************
C *** Calculate spherical Bessel functions for surface parameters
         DOUBLE PRECISION RSIZE,RTPI2,IM
         INTEGER IFAIL,IMAT,J,N,IZ,NZ,MAXORD
         DOUBLE COMPLEX I,SPHER,JBESS(4),HBESS(4),
     &      JN(2,3,0:3),JNP(2,3,0:3),JNDP(2,3,0:3),
     &      HN(2,3,0:3),HNP(2,3,0:3),HNDP(2,3,0:3),
     &      K(2,3),A(2,3),DEX
         PARAMETER (RTPI2=1.253314137D0, I=(0.0D0,1.0D0))

         MAXORD=N+1
         DO 101 IMAT=1,2
C *** Each material, use sound mode
            DO 102 J=1,3
               A(IMAT,J)=K(IMAT,J)*RSIZE
               SPHER=DCMPLX(RTPI2)/CDSQRT(A(IMAT,J))
               IM=DIMAG(A(IMAT,J))
               IF(IM.GT.600.0D0)THEN
C *** Calculate ordinary Bessel functions
                  JBESS(1)=CDSIN(A(IMAT,J))/(A(IMAT,J)*SPHER)
                  JBESS(2)=(CDSIN(A(IMAT,J))/A(IMAT,J)-CDCOS(
     &                  A(IMAT,J)))/(A(IMAT,J)*SPHER)
                  JBESS(3)=((3.0D0/(A(IMAT,J)*A(IMAT,J))-1.0D0)*
     &                  CDSIN(A(IMAT,J))-(3.0D0*CDCOS(A(IMAT,J))/A(IMAT,J))
     &                  )/(A(IMAT,J)*SPHER)
                  DEX=CDEXP(I*A(IMAT,J))
                  HBESS(1)=-I*(DEX)/(SPHER*A(IMAT,J))
                  HBESS(2)=-(1.0D0+(1/A(IMAT,J)))*DEX/(SPHER*A(IMAT,J))
                  HBESS(3)=(1.0D0+(3.0D0*I/A(IMAT,J))-(3.0D0/(A(IMAT,J)*
     &                  A(IMAT,J))))*I*DEX/(SPHER*A(IMAT,J))
               ELSE
C *** Out of calculable range
                  IFAIL=0
                  CALL S17DEF(0.5D0,A(IMAT,J),MAXORD+1,'U',JBESS,NZ,IFAIL)
                  IF (IFAIL.NE. 0) THEN
                     WRITE(6,201) IFAIL
```

```
                END IF
                IFAIL=0
                CALL S17DLF(1.0_5D0,A(IMAT,J),MAXORD+1,'U',HBESS,NZ,
     &               IFAIL)
                IF (IFAIL.NE. 0) THEN
                   WRITE(6,201) IFAIL
 201               FORMAT("ERROR IN BESSEL FUNCTIONS",I4)
                END IF
              END IF
              DO 103 IZ=0,MAXORD-1
C *** Calculate spherical Bessel functions and derivatives
                JN(IMAT,J,IZ)=JBESS(IZ+1)*SPHER
                JN(IMAT,J,IZ+1)=JBESS(IZ+2)*SPHER
                JNP(IMAT,J,IZ)=DBLE(IZ)*JN(IMAT,J,IZ)/A(IMAT,J)-
     &               JN(IMAT,J,IZ+1)
                JNDP(IMAT,J,IZ)=DBLE(IZ*(IZ-1))*JN(IMAT,J,IZ)/
     &               (A(IMAT,J)*A(IMAT,J))-JN(IMAT,J,IZ)+
     &               2.0D0*JN(IMAT,J,IZ+1)/A(IMAT,J)
                HN(IMAT,J,IZ)=HBESS(IZ+1)*SPHER
                HN(IMAT,J,IZ+1)=HBESS(IZ+2)*SPHER
                HNP(IMAT,J,IZ)=DBLE(IZ)*HN(IMAT,J,IZ)/A(IMAT,J)-
     &               HN(IMAT,J,IZ+1)
                HNDP(IMAT,J,IZ)=DBLE(IZ*(IZ-1))*HN(IMAT,J,IZ)/
     &               (A(IMAT,J)*A(IMAT,J))-HN(IMAT,J,IZ)+
     &               2.0D0*HN(IMAT,J,IZ+1)/A(IMAT,J)
 103          CONTINUE
 102       CONTINUE
 101    CONTINUE
        END

C ***********************************************************************
        SUBROUTINE USVEFF(N,NSIZES,RADIUS,PHI,SFC,ANGFREQ,KAPEFF,
     &     RHOEFF,THATT,VIATT,MSVEL,MSATT,LBATTL,
     &     Q,RHO,ETA,MU,TOR,GAMMA,BETA,SIGMA)
C ***********************************************************************
C *** Calculate explicit solutions for scattering coefficients
C *** Use effective density and compressibility to obtain velocity
        INTEGER N,NSIZES,IZ
        DOUBLE COMPLEX I,COEFF(0:3),K11,K(2,3),BULKK2
        DOUBLE PRECISION RADIUS(NSIZES),PHI(NSIZES),ANGFREQ,SFC(NSIZES),
     &  Q(3),RHO(3),ETA(3),MU(3),TOR(3),GAMMA(3),BETA(3),SIGMA(3),
     &  LBATTL,SOLRAD(101),VIATT,SSVTH,SSVVI,SSVEL,SSATT,
     &     MSVEL,MSATT,RHOEFF,KAPEFF,THATT
        PARAMETER (I=(0.0D0,1.0D0) )

        DO 101 IZ=0,N
           COEFF(IZ)=(0.00D0,0.00D0)
 101    CONTINUE
        DO 102 IZ=1,NSIZES
           SOLRAD(IZ)=RADIUS(IZ)*(RHO(2)/RHO(3))**0.3333333333333D0
 102    CONTINUE
C *** Determine the explicit solutions for single particle scatt coeffs
        CALL EXPLSCATTCOEFFS(N,NSIZES,RADIUS,PHI,SFC,0,ANGFREQ,K11,COEFF,
     &     Q,RHO,ETA,MU,TOR,GAMMA,BETA,SIGMA,K)
        CALL EXPLSCATTCOEFFS(N,NSIZES,SOLRAD,PHI,SFC,1,ANGFREQ,K11,COEFF,
     &     Q,RHO,ETA,MU,TOR,GAMMA,BETA,SIGMA,K)
C *** Calculate wavenumber, velocity and atten from scatt coeffs
C *** Single scattering only
        BULKK2=K11*K11*(1.0D0-(3.0D0*I*COEFF(0)/(K11**3)))
```

```
      SSVTH=ANGFREQ/(DBLE(CDSQRT(BULKK2)))
      BULKK2=K11*K11*(1.0D0-(9.0D0*I*COEFF(1)/(K11**3)))
      SSVVI=ANGFREQ/(DBLE(CDSQRT(BULKK2)))
      BULKK2=K11*K11-((3.0D0*I/K11)*(COEFF(0)+(3.0D0*COEFF(1))+(5.0D0*
     &    COEFF(2))))
      SSVEL=ANGFREQ/(DBLE(CDSQRT(BULKK2)))
      SSATT=20.0D0*DIMAG(CDSQRT(BULKK2))*DLOG10(2.718281828D0)
C *** Use effective density and compressibility
      KAPEFF=DBLE(1.0D0-(3.0D0*I*COEFF(0)/(K11**3)))/(RHO(1)*Q(1)*Q(1))
      THATT=-1.5D0*DBLE(COEFF(0))/(K11*K11)
      RHOEFF=RHO(1)*DBLE(1.0D0-(9.0D0*I*COEFF(1)/(K11**3)))
      VIATT=-4.5D0*DBLE(COEFF(1))/(K11*K11)
      MSVEL=1.0D0/(DSQRT(RHOEFF*KAPEFF))
      MSATT=THATT+VIATT
      END

C ***********************************************************************
      SUBROUTINE EXPLSCATTCOEFFS(N,NSIZES,RADIUS,PHI,SFC,SOLID,ANGFREQ,
     &    K11,COEFF,Q,RHO,ETA,MU,TOR,GAMMA,BETA,SIGMA,K)
C ***********************************************************************
C *** Calculate the single particle scattering coefficients
C *** Explicit long wavelength solutions
      INTEGER ISIZE,N,NSIZES,SOLID
      DOUBLE PRECISION RADIUS(NSIZES),PHI(NSIZES),SFC(NSIZES),PROPN,
     &    ANGFREQ,Q(3),RHO(3),ETA(3),MU(3),TOR(3),GAMMA(3),
     &    BETA(3),SIGMA(3)
      DOUBLE COMPLEX I,K(2,3),A(2,3),G(2,2),L(2,2),
     &    JN(2,3,0:3),JNP(2,3,0:3),JNDP(2,3,0:3),
     &    HN(2,3,0:3),HNP(2,3,0:3),HNDP(2,3,0:3),
     &    ACOEFF(0:3,101),COEFF(0:3),K11,QQ,TOP,BOTT,
     &    H1,H2,H3,T1,T2,T3
      PARAMETER (I=(0.0D0,1.0D0) )

C *** Calculate wavenumber of each mode (propl, thermal, shear)
C *** in bulk materials
      CALL WAVE(ANGFREQ,SOLID,K,G,L,Q,RHO,ETA,MU,GAMMA,BETA,SIGMA)
      K11=K(1,1)
C *** For each particle size, calculate scattering coefficients
      DO 101 ISIZE=1,NSIZES
C *** Calculate spherical Bessel functions for each parameter
        CALL SPHBES(RADIUS(ISIZE),N,K,A,JN,JNP,JNDP,HN,HNP,HNDP)
        IF (SOLID .EQ.1) THEN
          PROPN=SFC(ISIZE)
        ELSE
          PROPN=PHI(ISIZE)
        END IF
        IF (SOLID.EQ.0)THEN
          H1=A(1,2)*HN(1,2,1)*(1.0D0-(TOR(1)*G(1,2)/(TOR(2)*G(2,2))))
          H2=HN(1,2,0)-(TOR(1)*A(1,2)*HN(1,2,1)*JN(2,2,0)/(
     &        TOR(2)*A(2,2)*JN(2,2,1)))
          ACOEFF(0,ISIZE)=-I*A(1,1)*(A(1,1)*A(1,1)-(RHO(1)*A(2,1)*
     &        A(2,1)/RHO(2)))/3.0D0+I*A(1,1)*G(1,1)*H1*(1.0D0-
     &        (RHO(1)*G(2,1)/(RHO(2)*G(1,1))))/(G(1,2)*H2)
          QQ=A(2,3)*JN(2,3,1)-2.0D0*(1.0D0-(ETA(1)/ETA(2)))*JN(2,3,2)
          TOP=-I*(A(1,1)**3)*(RHO(1)/RHO(2)-1.0D0)
          TOP=TOP*(HN(1,3,2)*QQ-(ETA(1)*A(1,3)*HN(1,3,1)*JN(2,3,2)/
     &        ETA(2)))
          BOTT=QQ*((3.0D0*RHO(1)*HN(1,3,2)/RHO(2))+
     &        (2.0D0*(RHO(1)/RHO(2)-1.0D0)*HN(1,3,0)))
```

```
            BOTT=BOTT-ETA(1)*A(1,3)*HN(1,3,1)*JN(2,3,2)*
     &           (RHO(1)/RHO(2)+2.0D0)/ETA(2)
            BOTT=BOTT*3.0D0
            ACOEFF(1,ISIZE)=TOP/BOTT
          ELSE
            TOP=I*(A(1,1)**3)*(1.0D0-RHO(1)/RHO(3))*HN(1,3,2)
            BOTT=2.0D0*(RHO(1)/RHO(3)-1.0D0)*HN(1,3,0)+3.0D0*(RHO(1)
     &           /RHO(3))*HN(1,3,2)
            ACOEFF(1,ISIZE)=TOP/(3.0D0*BOTT)
            H1=A(1,2)*HN(1,2,1)*(1.0D0-TOR(1)*G(1,2)/(TOR(3)*G(2,2)))
            H2=HN(1,2,0)-(TOR(1)*A(1,2)*HN(1,2,1)*JN(2,2,0)/
     &           (TOR(3)*A(2,2)*JN(2,2,1)))
            H3=ETA(1)*((A(1,3)*A(1,3)-2.0D0*A(1,2)*A(1,2))*HN(1,2,0)-
     &           2.0D0*A(1,2)*A(1,2)*HNDP(1,2,0))-
     &           (TOR(1)*G(1,2)*A(1,2)*HN(1,2,1)/(TOR(3)*G(2,2)*
     &           A(2,2)*JN(2,2,1)*(-I*ANGFREQ)))*((ANGFREQ*ANGFREQ
     &           *RHO(3)*RADIUS(1)*RADIUS(1)-2.0D0*ETA(3)*A(2,2)*
     &           A(2,2))*JN(2,2,0)-2.0D0*ETA(3)*A(2,2)*A(2,2)*
     &           JNDP(2,2,0))
            T1=H1*((I*ANGFREQ*ETA(1)*G(2,1)/(ETA(3)*G(1,2)))*((4.0D0-
     &           A(1,3)*A(1,3))*I/A(1,1)+A(1,3)*A(1,3))+G(1,1)*(1.0D0-
     &           I/A(1,1))*(A(2,3)*A(2,3)-4.0D0*A(2,1)*A(2,1)/3.0D0)/
     &           G(1,2))
            T2=H2*(I*(A(2,3)*A(2,3)-4.0D0*A(2,1)*A(2,1)/3.0D0)/A(1,1)
     &           -(I*ANGFREQ*ETA(1)*A(2,1)*A(2,1)/(ETA(3)*3.0D0))*
     &           ((4.0D0-A(1,3)*A(1,3))*I/A(1,1)+A(1,3)*A(1,3)))
            T3=H3*(I*ANGFREQ/ETA(3))*(A(2,1)*A(2,1)*G(1,1)*(1.0D0-I/
     &           A(1,1))/(3.0D0*G(1,2))+G(2,1)*I/(A(1,1)*G(1,2)))
            BOTT=T1+T2+T3
            T1=H1*(G(2,1)*I*ANGFREQ*ETA(1)*A(1,3)*A(1,3)/(ETA(3)*G(1,2)
     &           )+G(1,1)*(A(2,3)*A(2,3)-4.0D0*A(2,1)*A(2,1)/3.0D0)/
     &           G(1,2))
            T2=H2*((4.0D0*A(2,1)*A(2,1)/3.0D0-A(2,3)*A(2,3))*A(1,1)*
     &           A(1,1)-I*ANGFREQ*ETA(1)*A(1,3)*A(1,3)*A(2,1)*A(2,1)
     &           /ETA(3))/3.0D0
            T3=H3*(A(2,1)*A(2,1)*G(1,1)/G(1,2)-A(1,1)*A(1,1)*G(2,1)
     &           /G(1,2))*I*ANGFREQ/(3.0D0*ETA(3))
            TOP=-(T1+T2+T3)
            ACOEFF(0,ISIZE)=TOP/BOTT
          END IF
          COEFF(0)=COEFF(0)+ACOEFF(0,ISIZE)*PROPN/
     &         (RADIUS(ISIZE)**3)
          COEFF(1)=COEFF(1)+ACOEFF(1,ISIZE)*PROPN/
     &         (RADIUS(ISIZE)**3)
101     CONTINUE
        END
```

Appendix A5 : Computer Program for Ultrasound Velocity Calculations

```
C    Front-end program for calculating ultrasound velocity
C    as a function of radius and frequency, using uscatt.f
C    by Valerie Pinfield. 1993-1995
      PROGRAM USMAIN
      INTEGER ND,MAXORD,IDEC,IRF
      CHARACTER*50 FLNAME,DFNAME
      DOUBLE PRECISION TOTPHI,PI2
      PARAMETER ( ND=1,MAXORD=2,
     &  TOTPHI=0.2D0)
      DOUBLE PRECISION RAD(ND),PHI(ND),SFC(ND),RSQRTF,FREQ,ANGFREQ,
     &    Q(3),RHO(3),ETA(3),MU(3),TOR(3),CP(3),GAMMA(3),
     &    BETA(3),ALPHA(3),SIGMA(3),FAC,
     &    TEMP,SSVEL,SSVTH,SSVVI,SSATT,MSVEL,MSATT,LBATTL
      DOUBLE COMPLEX I
      PARAMETER (I=(0.0D0,1.0D0),PI2=6.283185307D0)

      DFNAME="/home/gps_19/prc6vp/scatt/data/sun30"
      FLNAME="/home/gps_19/prc6vp/scatt/results/rrtf30.xls"
      OPEN(UNIT=20,ACCESS="SEQUENTIAL",FILE=FLNAME)
C *** Read material properties from data file
      CALL MTDATA(Q,RHO,ETA,MU,TOR,CP,GAMMA,BETA,ALPHA,SIGMA,
     &    ANGFREQ,TEMP,DFNAME)
C *** Calculate the curve of velocity against r*sqrt(f)
C *** for monodisperse system
      RAD(1)=50.0D-6
      PHI(1)=TOTPHI
      SFC(1)=0.0D0
      WRITE(20,301)RAD(1)*1.0D6,PHI(1)
 301  FORMAT("The radius used was",F6.2," microns with a volume fraction
     &    ",F6.1)
      WRITE(20,302)
 302  FORMAT("r*sqrt(f) frequency  velocity attenuation (dB/m)")
      FAC=1.0D-6
      DO 101 IDEC=1,4
        FAC=FAC*10.0D0
        DO 102 IRF=1,18
          RSQRTF=FAC*0.5D0*DBLE(IRF+1)
          FREQ=(RSQRTF*RSQRTF/(RAD(1)*RAD(1)))
          ANGFREQ=PI2*FREQ
          CALL USVELS(MAXORD,1,RAD,PHI,SFC,
     &      ANGFREQ,SSVTH,SSVVI,SSVEL,SSATT,MSVEL,MSATT,LBATTL,
     &      Q,RHO,ETA,MU,TOR,GAMMA,BETA,SIGMA)

          WRITE(20,303)RSQRTF,FREQ,MSVEL,MSATT
 303      FORMAT(2E15.5E3,F10.3,E15.5E3)
 102    CONTINUE
 101  CONTINUE
      END
```

Appendix A6 : Publications and Presentations

A number of publications and presentations have arisen from the work discussed in this thesis, and these are listed below.

Publications

Pinfield, V. J., Dickinson, E. and Povey, M. J. W. (1994). Modeling of concentration profiles and ultrasound velocity profiles in a creaming emulsion: importance of scattering effects. *Journal of Colloid and Interface Science*, **166**, 363-374.

Dickinson, E., Ma, J. G., Povey, M. J. W. and Pinfield, V. J. (1995). Ultrasonic studies of the creaming of concentrated emulsions. pp. 223-234. In *Food Macromolecules and Colloids: Proceedings of the Conference Organised by the Food Chemistry Group of the Royal Society of Chemistry*, ed. E. Dickinson and D. Lorient, Royal Society of Chemistry, Cambridge.

Pinfield, V. J., Povey, M. J. W. and Dickinson, E. (1995). The application of modified forms of the Urick equation to the interpretation of ultrasound velocity in scattering systems. *Ultrasonics*, **33**, 243-251.

Pinfield, V. J., Povey, M. J. W. and Dickinson, E. (1996). Interpretation of ultrasound velocity creaming profiles. Submitted to *Ultrasonics*.

Presentations

Oral contributions

Dickinson, E., Ma, J. G., Povey, M. J. W. and Pinfield, V. J. Ultrasonic studies of the creaming of concentrated emulsions. Presented at *Food Macromolecules and Colloids*, organised by the Food Chemistry Group of the Royal Society of Chemistry, Dijon, March 1994.

Pinfield, V. J. Simulation of creaming in concentrated polydisperse emulsions. Presented at *Theoretical Modelling and Simulation in Colloid and Interface Science*, organised by

the Colloid and Interface Science Group of the Royal Society of Chemistry, Faraday Division, Bristol, April 1994.

Pinfield, V. J., Povey, M. J. W. and Dickinson, E. The interpretation of ultrasound velocity in dispersions. Presented at *Annual Review of Progress in Physical Acoustics and Ultrasonics*, organised by the Physical Acoustics Group of the Institute of Physics, Telford, March 1995.

Pinfield, V. J. Creaming of oil-in-water emulsions. Presented at *The Third UK Colloid and Interface Science Student Meeting*, organised by the Colloid and Surface Chemistry Group of the Society of Chemical Industry and the Colloid and Interface Science Group of the Royal Society of Chemistry, Hull, July 1995.

Poster

Pinfield, V. J. Modelling of creaming in emulsions. Presented at *Chemistry Research for Britain*, sponsored by the Research Councils, London, November 1994.